

KOEBERG NUCLEAR POWER STATION: COASTAL PROCESSES TECHNICAL INFORMATION IN SUPPORT OF THE COASTAL WATERS DISCHARGE PERMIT APPLICATION

Dispersion Modelling of Thermal, Chemical, Sediment and Radionuclide Discharges

REV 05

04 September 2017



Eskom
Cape Town, South Africa


KOEBERG NUCLEAR POWER STATION: COASTAL PROCESSES TECHNICAL INFORMATION IN SUPPORT OF THE COASTAL WATERS DISCHARGE PERMIT APPLICATION

Dispersion Modelling of Thermal, Chemical, Sediment and Radionuclide Discharges

Specialist Study

S2015-RP-CE-001-R5

04 September 2017

REV.	TYPE	DATE	EXECUTED	CHECK	APPROVED	CLIENT	DESCRIPTION / COMMENTS
0	A	09/03/2016	PMH/SAL	SAL			Draft results for Lwandle
1	A	24/03/2016	PMH/SAL	SAL			Draft Final Report
2	C	31/03/2016	PMH/SAL	SAL			Addressed Eskom comments, updated screening assessment.
3	C	10/05/2016	PMH/SAL	SAL			Additional model outputs included, Reverse Osmosis Plant included.
4	A	28/08/2017	PMH	SAL			Updated discharge characterisation, Revised SWRO plant, added BWRO plant, updated screening assessment.
5	C	04/09/2017	PMH	SAL			Addressed Eskom comments.

TYPE OF ISSUE: (A) Draft (B) To bid or proposal (C) For Approval (D) Approved (E) Void



Eskom
Cape Town, South Africa





TABLE OF CONTENTS

Page N°

TABLE OF CONTENTS	III
LIST OF ACRONYMS	IX
GLOSSARY AND DEFINITIONS	XI
1. INTRODUCTION	1
1.1 Background	1
1.2 Scope	2
1.3 Report Structure	2
2. HYDRODYNAMIC AND GEOPHYSICAL FEATURES OF STUDY AREA	3
2.1 Bathymetry	3
2.2 Geology	4
2.3 Water Levels	5
2.4 Weather	6
2.5 Waves	8
2.6 Currents	10
2.7 Water Temperature	11
2.8 Salinity	13
3. DISCHARGE CHARACTERISATION	14
3.1 Discharge Locations	14
3.2 Effluent Streams Discharged at Outfall	15
3.2.1 Overview of Outfall Structure	15
3.2.1.1 Hydraulic design	15
3.2.1.2 Construction considerations	16
3.2.2 Circulating Water System (CRF)	16
3.2.3 Essential Water Service System (SEC)	17
3.2.4 Conventional Island Liquid Waste Monitoring and Discharge System (SEK)	18
3.2.5 Nuclear Island Liquid Radiological Waste Monitoring and Discharge System (KER)	20
3.2.6 Domestic Wastewater Treatment System (SEU)	21
3.2.7 Unit 2 Electrical Building Ventilation System (DEL)	22
3.2.8 Southern Stormwater System (SEO-S)	22
3.3 Effluent Streams Discharged into Intake Basin	23
3.3.1 Overview	23
3.3.2 Auxiliary Boiler Plant (XCA)	23
3.3.3 Reagent Distribution and Neutralisation System (SDX)	24
3.3.4 Demineraliser Water Production Plant (SDA)	25
3.3.5 Chlorination Plant (CTE) Effluent	25
3.3.6 Unit 1 Electrical Building Ventilation System (DEL)	26
3.3.7 Northern Stormwater System (SEO-N)	26
3.4 Proposed desalination plants	27
3.4.1 1.8 ML/d Brackish Water Reverse Osmosis (BWRO) plant	27
3.4.2 20 ML/d Seawater Reverse Osmosis (SWRO) plant	29
3.4.3 Effect of Brine Effluent on Plume Density	30
4. SCREENING OF CONSTITUENTS	32
4.1 Methodology	32
4.2 Theoretical and Minimum Dilutions in the Outfall Channel	33
4.2.1 Flow Scenarios	33
4.2.2 Dilutions	34
4.3 Background and Guideline Concentrations	37



4.4	Screening of Water Column Constituents	39
4.5	Screening of Constituents Prone to Accumulation in Sediments	42
5.	CHEMICAL DISPERSION MODELLING	44
5.1	Model Description	44
5.1.1	Hydrodynamic Modelling	44
5.1.2	Spectral Wave Modelling	44
5.1.3	ECOLab Modelling	45
5.1.3.1	ECOLab template for chlorine	45
5.1.3.2	ECOLab template for hydrazine	46
5.2	Model Setup	47
5.2.1	Mesh and Bathymetry	47
5.2.2	Water Levels	50
5.2.3	Wind	50
5.2.4	Waves	50
5.2.5	Seawater Temperature	50
5.2.6	Salinity	50
5.2.7	Atmospheric Conditions	50
5.3	Model Calibration	51
5.3.1	Waves	51
5.3.2	Currents	55
5.3.3	Temperature	58
5.3.4	Thermal Plume	59
5.4	Modelling Approach	60
5.4.1	Model Simulations	60
5.4.2	Mixing in the Outfall Channel	61
5.4.3	Post-processing of Model Results	62
5.5	Fate of Intake Basin Discharges	64
5.6	Dispersion Modelling: Temperature	66
5.6.1	Discharge Configuration	66
5.6.2	Results	66
5.7	Dispersion Modelling: Free Chlorine	72
5.7.1	Discharge Configuration	72
5.7.2	Results	72
5.8	Dispersion Modelling: Hydrazine	73
5.8.1	Discharge Configuration	73
5.8.2	Results	74
5.9	Dispersion Modelling: Phosphate	75
5.9.1	Discharge Configuration	75
5.9.2	Results	76
5.10	Summary	77
6.	RADIONUCLIDE DISPERSION MODELLING	78
6.1	Discharge Characterisation	78
6.2	Model Description	78
6.2.1	Hydrodynamics	78
6.2.2	ECOLab template for radionuclides	78
6.3	Model Setup	80
6.4	Model Calibration	81
6.4.1	Distribution of Fine Sediment on the Seabed	81
6.4.2	Suspended Sediment Concentrations	85
6.4.3	Radionuclide Activity in Bed Sediment	86
6.5	Model Results	89
6.5.1	Results for Co-60	89



6.5.2	Results for Remaining Radionuclides	97
6.6	PC CREAM Model Input Parameters	97
6.7	Summary	99
7.	SUMMARY	100
8.	REFERENCES	101
ANNEXURE A DRAWINGS OF KOEBERG NUCLEAR POWER STATION OUTFALL CHANNEL		1
ANNEXURE B RESULTS OF CHEMICAL DISPERSION MODELLING		1
ANNEXURE C ADDITIONAL RESULTS OF RADIONUCLIDE DISPERSION MODELLING		1

TABLES	Page N°
Table 2-1: Tidal characteristics for the Port of Cape Town (SANHO, 2016)	6
Table 2-2: Summary of available seawater temperature datasets	11
Table 2-3: Seasonal statistics of measured seawater stratification between depths of -10 and -30 m.	12
Table 3-1: Characterisation of CRF discharges	17
Table 3-2: Characterisation of SEC discharge	18
Table 3-3: Characterisation of SEK discharges	19
Table 3-4: Characterisation of exceptional SEK discharges: hydrazine releases associated with outages	20
Table 3-5: Characterisation of KER discharges	21
Table 3-6: Characterisation of exceptional boron releases via KER	21
Table 3-7: Characterisation of SEU discharges	22
Table 3-8: Characterisation of Unit 2 DEL discharges	22
Table 3-9: Characterisation of XCA discharges	24
Table 3-10: Characterisation of SDX discharges	25
Table 3-11: Characterisation of SDA discharges	25
Table 3-12: Characterisation of CTE discharges	26
Table 3-13: Characterisation of Unit 1 DEL discharges	26
Table 3-14: Characterisation of the brine effluent from the proposed BWRO desalination plant	28
Table 3-15: Characterisation of the pre-treatment effluent from the proposed BWRO desalination plant	28
Table 3-16: Characterisation of the discharge from the proposed SWRO desalination plant	30
Table 3-17: Calculation of the density of the combined cooling water and brine effluent	31
Table 4-1: Summary of flow scenarios	34
Table 4-2: Theoretical dilutions achieved at the end of the outfall channel for each effluent stream and flow scenario. The theoretical dilutions are calculated assuming complete mixing in the outfall channel.	35
Table 4-3: Non-uniform dilution factor at the end of the outfall channel for each effluent stream and flow scenario. The non-uniform dilution factor describes the extent to which complete mixing is achieved, where a value of 1.0 indicates complete mixing and 0.0 indicates no mixing.	36
Table 4-4: Minimum dilutions achieved at the end of the outfall channel for each effluent stream and flow scenario. The minimum dilutions assume non-uniform mixing in the outfall channel, and are calculated as the product of the theoretical dilutions (Table 4-2) and the non-uniform dilution factor (Table 4-3).	36
Table 4-5: Ecological guideline and background concentrations for constituents discharged at KNPS	38
Table 4-6: Screening of constituents	41



Table 4-7: Calculation of the sediment mass in the top 10 cm of the seabed in the KNPS intake basin	42
Table 4-8: Calculation of the number of years required before the ecological guideline for heavy metal concentration in seabed sediment is reached.	43
Table 5-1: Rate constants for chlorine demand and decay determined from laboratory testing of Hinkley Point seawater (BEEMS, 2010a)	46
Table 5-2: Rate constants for hydrazine decay determined from laboratory testing (BEEMS, 2010c)	47
Table 5-3: Rate constants for hydrazine decay interpolated from the results of laboratory testing (Table 5-2).	47
Table 5-4: Configuration of temperature releases: plant operation at full capacity	66
Table 5-5: Configuration of temperature releases: pump trip scenario	66
Table 5-6: Summary of model results for temperature presented in Annexure B	71
Table 5-7: Configuration of free chlorine releases: plant operation at full capacity	72
Table 5-8: Summary of model results for free chlorine dispersion presented in Annexure B	72
Table 5-9: Configuration of hydrazine releases: plant operation at full capacity	73
Table 5-10: Configuration of hydrazine releases: reactor outages	73
Table 5-11: Summary of model results for hydrazine dispersion presented in Annexure B	74
Table 5-12: Characterisation of phosphate leaks into all effluent streams	75
Table 5-13: Configuration of phosphate releases during outages	75
Table 5-14: Summary of model results for phosphate dispersion presented in Annexure B	76
Table 6-1: Annual load of radionuclides released at KNPS	78
Table 6-2: Input parameters used in the modelling of fine particulate matter.	80
Table 6-3: Distribution coefficients (K_d) and half-lives of radionuclides modelled	80
Table 6-4: Predicted steady state concentrations of radionuclides released from KNPS.	97
Table 6-5: PC CREAM required input parameters for local compartments.	99

FIGURES

Page N°

Figure 1-1: Aerial view of the Koeberg Nuclear Power Station (KNPS)	1
Figure 2-1: Local bathymetry at KNPS. The figure also shows the multi-beam bathymetric survey and the locations of other measurement stations discussed in Sections 2.4 to 2.7.	4
Figure 2-2: Measured sediment grain size at Duynfontein	5
Figure 2-3: Seasonal wind roses of hourly averaged wind data measured at 10 m above ground level at the KNPS Meteorological Station (X = -51 849 m, Y = -3 728 624 m, WG19). The roses are constructed from 14 years of measured data (1997-2010).	7
Figure 2-4: Seasonal exceedance of hourly averaged wind speeds recorded 10 m above ground level at the KNPS Meteorological Station (X = -51 849 m, Y = -3 728 624 m, WG19). The curves are drawn from 14 years of measured data (1997-2010).	7
Figure 2-5: Time series of air temperature recorded 10 m above ground level at the KNPS Meteorological Station (X = -51 849 m, Y = -3 728 624 m, WG19).	8
Figure 2-6: Wave roses of wave data measured at Site A (X = -54 253 m, Y = -3 727 223 m WG19, -10 m CD) from January 2008 to July 2010 and at Site B (X = -56 587 m, Y = -3 727 857 m WG19, -30 m CD) from July 2008 to January 2014.	8
Figure 2-7: Seasonal exceedance of significant wave height measured at Site A (X = -54 253 m, Y = -3 727 223 m WG19, -10 m CD).	9



Figure 2-8: Seasonal exceedance of significant wave height measured at Site B (X = -56 587 m, Y = -3 727 857 m WG19, -30 m CD).	9
Figure 2-9: Rose plots of near-surface and near-seabed currents measured by ADCPs at Site A (X = -54 253 m, Y = -3 727 223 m WG19, -10 m CD) between January 2008 and July 2010 and at Site B (X = -56 587 m, Y = -3 727 857 m WG19, -30 m CD) between July 2008 and January 2014.	10
Figure 2-10: Exceedance of near-surface and near-seabed current speeds measured by ADCPs at Site A (X = -54 253 m, Y = -3 727 223 m WG19, -10 m CD) between January 2008 and July 2010 and at Site B (X = -56 587 m, Y = -3 727 857 m WG19, -30 m CD) between July 2008 and January 2014.	11
Figure 2-11: Time series of measured seawater temperatures at Sites A to E. The coordinates and depths of the measurement locations are reported in Table 2-2.	12
Figure 3-1: Outfall channel of the KNPS. The figure also indicates the location of the discharge point.	14
Figure 3-2: Location of the KNPS intake basin discharge point.	15
Figure 3-3: Layout of effluent streams released into outfall channel	16
Figure 4-1: Flow chart describing the screening process used to identify constituents discharged at KNPS which do not pose a significant risk to the receiving environment, and can therefore be excluded from further assessment.	32
Figure 5-1: Model bathymetry	48
Figure 5-2: Model mesh	49
Figure 5-3: Time series plot of measured and modelled wave parameters at Site A (X = -54 253 m, Y = -3 727 223 m WG19, -10 m CD).	52
Figure 5-4: Time series plot of measured and modelled wave parameters at Site B (X = -56 587 m, Y = -3 727 857 m WG19, -30 m CD).	53
Figure 5-5: Scatter plot of measured and modelled H_{m0} at Site A (X = -54 253 m, Y = -3 727 223 m WG19, -10 m CD).	54
Figure 5-6: Scatter plot of measured and modelled H_{m0} at Site B (X = -56 587 m, Y = -3 727 857 m WG19, -30 m CD).	54
Figure 5-7: Time series comparison of measured and modelled currents at Site A (X = -54 253 m, Y = -3 727 223 m WG19, -10 m CD)	55
Figure 5-8: Time series comparison of measured and modelled currents at Site B (X = -56 587 m, Y = -3 727 857 m WG19, -30 m CD)	56
Figure 5-9: Current roses constructed from 1 year (2009) of measured and modelled currents at Site A (X = -54 253 m, Y = -3 727 223 m WG19, -10 m CD)	57
Figure 5-10: Current roses constructed from 1 year (2009) of measured and modelled currents at Site B (X = -56 587 m, Y = -3 727 857 m WG19, -30 m CD)	57
Figure 5-11: Time series of measured and modelled near-seabed seawater temperatures at Sites A to E. The coordinates of the locations are reported in Table 2-2 in Section 2.7.	58
Figure 5-12: Comparison of modelled and measured surface temperature on 14 October 1985.	59
Figure 5-13: Comparison of modelled and measured surface temperature on 16 October 1985.	60
Figure 5-14: Model results from previous hydrodynamic modelling of the KNPS outfall channel indicating mixing between CRF trains (PRDW, 2013). The figure presents the number of dilutions of a conservative tracer released into one CRF train, while two trains are operational.	61
Figure 5-15: Locations of sensitive receptors where time series of near-surface and near-seabed concentrations are presented for the continuous release scenarios. The time series are presented in Annexure B.	63
Figure 5-16: 95 th percentile dilutions for a tracer released into the intake basin at 60 m ³ /h: near-surface and near-seabed.	65



Figure 5-17: Instantaneous contour plot of the increase in temperature (ΔT) during a typical south-easterly wind event: near-surface, plant operation at full capacity. The vectors indicate current speed and direction.	67
Figure 5-18: Instantaneous contour plot of the increase in temperature (ΔT) during a typical south-easterly wind event: near-seabed, plant operation at full capacity. The vectors indicate current speed and direction.	68
Figure 5-19: Instantaneous contour plot of the increase in temperature (ΔT) during a typical north-westerly wind event: near-surface, plant operation at full capacity. The vectors indicate current speed and direction.	69
Figure 5-20: Instantaneous contour plot of the increase in temperature (ΔT) during a typical north-westerly wind event: near-seabed, plant operation at full capacity. The vectors indicate current speed and direction.	70
Figure 6-1: Grab sample locations offshore of KNPS (Detail A) and inside the KNPS intake basin (Detail B).	82
Figure 6-2: Grab sample locations in Murray's Harbour on Robben Island (Detail C) and in the Port of Cape Town (Detail D).	83
Figure 6-3: Percentage fines obtained from a number of sediment sampling campaigns.	84
Figure 6-4: Correlation of the percentage fines measured in grab samples of the seabed sediment and the 95 th percentile modelled bed shear stress.	85
Figure 6-5: Comparison of measured and modelled total suspended sediment (TSS) concentrations offshore of the KNPS in water depths from 3 m to 30 m.	86
Figure 6-6: Comparison of measured and modelled radionuclide activity in bed sediment. The dotted red bars represent the Minimum Detectable Activity (MDA) of the radionuclide and are shown where measured activity was not sufficient to positively identify a radionuclide. The modelled bars (blue) indicate the predicted steady state concentration at all sites except in the KNPS intake basin which is continually dredged and thus only one year of accumulation is assumed.	87
Figure 6-7: 95 th percentile concentration of dissolved Co-60 activity in the water column: near-surface.	90
Figure 6-8: 95 th percentile concentration of dissolved Co-60 activity in the water column: near-seabed.	91
Figure 6-9: 95 th percentile concentration of adsorbed Co-60 activity in the water column: near-surface.	92
Figure 6-10: 95 th percentile concentration of adsorbed Co-60 activity in the water column: near-seabed.	93
Figure 6-11: Maximum concentration of Co-60 activity in seabed sediment in one modelled year: overview.	94
Figure 6-12: Maximum concentration of Co-60 activity in seabed sediment in one modelled year: detail of depo-centres.	95
Figure 6-13: Time series of concentration of Co-60 activity in the seabed sediment at the three depo-centres. For comparative purposes, the concentration is plotted on a logarithmic scale.	96
Figure 6-14: Predicted steady state concentration of Co-60 in the KNPS intake basin.	97
Figure 6-15: Layout of Boxes 1, 2 and 3 of which the PC CREAM input data are summarised in Table 6-5.	98



LIST OF ACRONYMS

3D	Three-dimensional
AE	Alcohol Ethoxylates
AES	Alcohol Ethoxysulfates
BOD	Biochemical Oxygen Demand
BWRO	Brackish Water Reverse Osmosis
BWRO-B	BWRO Brine effluent
BWRO-PT	BWRO Pre-Treatment effluent
CD	Chart Datum
CFSR	Climate Forecast System Reanalysis
COD	Chemical Oxygen Demand
CRF	Circulating Water System
CTE	Chlorination Plant
CWDP	Coastal Waters Discharge Permit
DBNPA	Dibromonitrolopropionamide
DEL	Electrical Building Ventilation System
DHI	Danish Hydraulics Institute
DW	Dry Weight
ECMWF	European Centre for Medium-Range Weather Forecasts
EDTA	Ethylenediaminetetraacetic acid
IAEA	International Atomic Energy Agency
KER	Nuclear Island Liquid Radiological Waste Monitoring and Discharge System
KNPS	Koeberg Nuclear Power Station
LAS	Linear Alkylbenzene Sulfonate
MSL	Mean Sea Level
MW	Megawatt
NCEP	National Centers for Environmental Prediction



NNR	National Nuclear Regulator
NOAA	National Oceanic and Atmospheric Administration
PIM	Particulate Inorganic Matter
POM	Particulate Organic Matter
psu	Practical Salinity Unit. 1 psu is equivalent to 1 g/l or 1 ppt
RO	Reverse Osmosis
SDA	Demineraliser Water Production Plant
SDX	Reagent Distribution and Neutralisation System
SEC	Essential Service Water System
SEK	Conventional Island Liquid Waste Monitoring and Discharge System
SEO-N	Northern Stormwater System
SEO-S	Southern Stormwater System
SEU	Domestic Wastewater Treatment System
SWRO	Seawater Reverse Osmosis
ΔT	Change in temperature
TRO	Total Residual Oxidants
TSS	Total Suspended Sediment
XCA	Auxiliary Boiler Plant



GLOSSARY AND DEFINITIONS

Advection	The transfer of a property such as heat by the movement of water.
Bathymetry	Underwater depth of the ocean bed.
Biocide	A substance, such as a chlorine or Dibromo Nitrolopropionamide (DBNPA), that is capable of destroying living organisms if applied in sufficient doses.
Biofouling	The fouling of underwater pipes and other surfaces by organisms such as barnacles, mussels and algae.
Breakwater	A barrier built out into the sea to protect a coast or harbour from the force of waves.
Coriolis force	A force that as a result of the earth's rotation deflects moving objects.
Current	Flow of water in a specific direction.
Current direction	The direction towards which the current is flowing, measured clockwise from true north.
D ₅₀	Median grain size.
Direct (once-through) water cooling	A process of heat removal from industrial equipment using water as the heat conductor, where the water is discharged back into the original body of water after use (sea or fresh water can be used).
Dispersion	Mixing of one substance into another.
Ecological	The scientific analysis and study of interactions among organisms and their environment.
Eddy	The swirling of a fluid and the reverse current created when the fluid flows past an obstacle
Effluent	A complex waste material (e.g. liquid industrial discharge or sewage) that may be discharged into the environment.
Evaporation	The change from a liquid to a gas or vapour.
Far-field	Zone where dispersion due to ambient currents and coastal processes dominates the mixing processes.
Grading coefficient	The sediment grading coefficient describes the distribution of particle sizes and is calculated as $\sigma_g = \sqrt{d_{84}/d_{16}}$, where d_{84} is the 84 th percentile particle size and d_{16} is the 16 th percentile particle size.
Hindcast	Historical wind and wave data that provides information for the analysis of atmospheric and marine environments at specific sites.
Horizontal coordinate system	The WG19 coordinate system was used for this study. All spatial plots include x and y axes showing the x and y coordinates in metres in the WG19 system. True north is always pointing upwards.



Hydrodynamics	The movement of fluid.
Mixing zone	An administrative construct which defines a limited area or volume of the receiving water where the initial dilution of a discharge is allowed to occur, until the water quality standards are met. In practice, it may occur within the near-field or far-field of a hydrodynamic mixing process and therefore depends on source, ambient and regulatory constraints.
Near field	The zone close to the discharge point where the mixing is dominated by the momentum and buoyancy of the discharge.
Peak wave period	The wave period with maximum wave energy density in the wave energy spectrum.
Salinity	The measure of all the salts dissolved in water.
Significant wave height	The significant wave height, determined from the zeroth moment of the wave energy spectrum. It is approximately equal to the average of the highest one-third of the waves in a given sea state.
Stratification	Formation of water layers based on salinity and temperature.
Thermal discharge	The discharge of heated cooling water used in power generation into a colder body of water such as the ocean.
Thermal plume	Hot water discharged into a receiving body of water which moves as a single mass until it cools and gradually mixes with the cooler water.
Time zone	All times in this study are in South African Standard Time (Time Zone -2).
Upwelling	An oceanographic phenomenon that involves wind- and Coriolis-driven motion of dense, cooler, and usually nutrient-rich water towards the ocean surface, replacing the warmer, usually nutrient-depleted surface water.
Vertical coordinate system	Seabed levels and water levels in this study are relative the Chart Datum (CD). CD is 0.825 m below Land Levelling Datum (LLD) which is also known as Mean Sea Level (MSL).
Viscosity	A fluid's resistance to gradual deformation by shear stress or tensile stress.
Wave direction	The direction from which the wave is coming, measured clockwise from true north.
Wave transformation	Waves that propagate towards the shore interact with coastal structures and the sea bed which results in a change of wave shape and incoming direction.
Wind direction	The direction from which the wind is coming, measured clockwise from true north.
Wind setup	The vertical rise in the still water level on the leeward side of a body of water caused by wind stresses on the surface of the water.
95 th percentile	The value below which 95% of the observations are found.

KOEBERG NUCLEAR POWER STATION: COASTAL PROCESSES TECHNICAL INFORMATION IN SUPPORT OF THE COASTAL WATERS DISCHARGE PERMIT APPLICATION

Dispersion Modelling of Thermal, Chemical, Sediment and Radionuclide Discharges

Specialist Study

1. INTRODUCTION

1.1 Background

Eskom is in the process of applying for a Coastal Waters Discharge Permit (CWDP) for the Koeberg Nuclear Power Station (KNPS) in terms of Section 69 of the Integrated Coastal Management Act (ICMA). PRDW (Pty) Ltd were appointed by Eskom to undertake a specialist study to provide coastal processes information in support of this application.

This report should be read together with the report of the Marine Ecology Specialist Study (Lwandle, 2017) which provides details of the applicable marine ecological guidelines and an assessment of the impact of the discharges on the marine ecology, based on the modelling results described in this report.

The KNPS is located on Cape Farm Dynefontyn 1552, approximately 5 km north of Melkbosstrand and 25 km north of Cape Town. The power station consists of two 900 MW nuclear reactors, using a once-through cooling water system. An aerial image of the KNPS is presented in Figure 1-1, which shows the intake basin, power plant and outfall channel.



Figure 1-1: Aerial view of the Koeberg Nuclear Power Station (KNPS)



1.2 Scope

The scope of the study is to provide the necessary coastal processes information required in the CWDP application. The specific tasks outlining the scope are:

- Description of the hydrodynamic and geophysical features of the study area;
- Characterising the discharge (based on data provided by Eskom);
- Screening the constituents (based on the water quality guidelines provided by Lwandle);
- Modelling of the cooling water thermal and chemical constituents dispersion;
- Modelling of the sediment and radionuclide dispersion; and
- Reporting.

The reporting section of the scope of work includes the collation and presentation of information required in the CWDP application, as outlined in the Generic Assessment Criteria for Coastal Waters Discharge Permits published by the Department of Environmental Affairs (DEA, 2014). The list of required information is shown below, also indicating which items are covered in this report (labelled as 'PRDW' and referenced to the relevant section in this report), which items are covered in the report of the Marine Ecology Specialist Study (Lwandle, 2017) and which items are the responsibility of Eskom.

- Scope of the study area and features (hydrodynamic and geophysical): PRDW, Section 2.
- Biogeochemical processes (water column and sediment): Lwandle
- Marine ecology: Lwandle
- Microbiological factors: Lwandle
- Hydraulic design: PRDW, Section 3.2.1.
- Achievable dilution: PRDW, Section 5.6 to 5.9.
- Sedimentation/re-suspension of solid phase particles: PRDW, Section 6.4.
- Compliance with environmental quality objectives: Lwandle (relevant model outputs are provided in Sections 5.6 to 5.9 of this document, but are interpreted in the report of the Marine Ecology Specialist Study).
- Construction considerations and structural design: PRDW, Section 3.2.1.
- Monitoring programme: Lwandle
- Reporting: Eskom
- Contingency planning: Eskom
- Public participation: Eskom

1.3 Report Structure

Section 2 presents the hydrodynamic and geophysical features of the study area. The discharge from KNPS is characterised in Section 3, and includes descriptions of the outfall, the constituents discharged and the flow rates. Section 4 presents a screening process by which constituents which do not pose a significant threat to the environment are identified and excluded from further assessment. Section 5 presents the modelling of the dispersion and fate of chemical constituents which were not screened out. This section includes descriptions of the models used, calibration of the models and the results of the dispersion modelling. Section 6 presents the modelling of the dispersion and fate of radiological constituents in the KNPS discharge. A summary of the report is presented in Section 7, with a list of references used in Section 8.



2. HYDRODYNAMIC AND GEOPHYSICAL FEATURES OF STUDY AREA

2.1 Bathymetry

Regional and nearshore bathymetry have been sourced from the '*MIKE by DHI*' *CMAP Electronic Charts* (DHI, 2014a). In addition, nearshore bathymetry was available from the following surveys:

- Multi-beam bathymetric surveys by the Council for Geoscience (CGS, 2006) and Fugro Survey Africa (Fugro, 2007);
- Single beam bathymetric survey of the Koeberg intake basin and adjacent seabed by Tritan Survey cc in 2006 and 2007;
- Beach profile survey of the coastline north and south of KNPS by Tritan Survey cc (Tritan Survey cc, 2008);
- Koeberg Lidar Survey in 2007 provided by Eskom.

The local bathymetry is presented in Figure 2-1, which also shows the multi-beam bathymetric survey and the locations of other measurement stations discussed in Sections 2.4 to 2.7. More detailed plots of the bathymetry are provided in Figure 5-1 in Section 5.2.1, which also presents the offshore bathymetry.

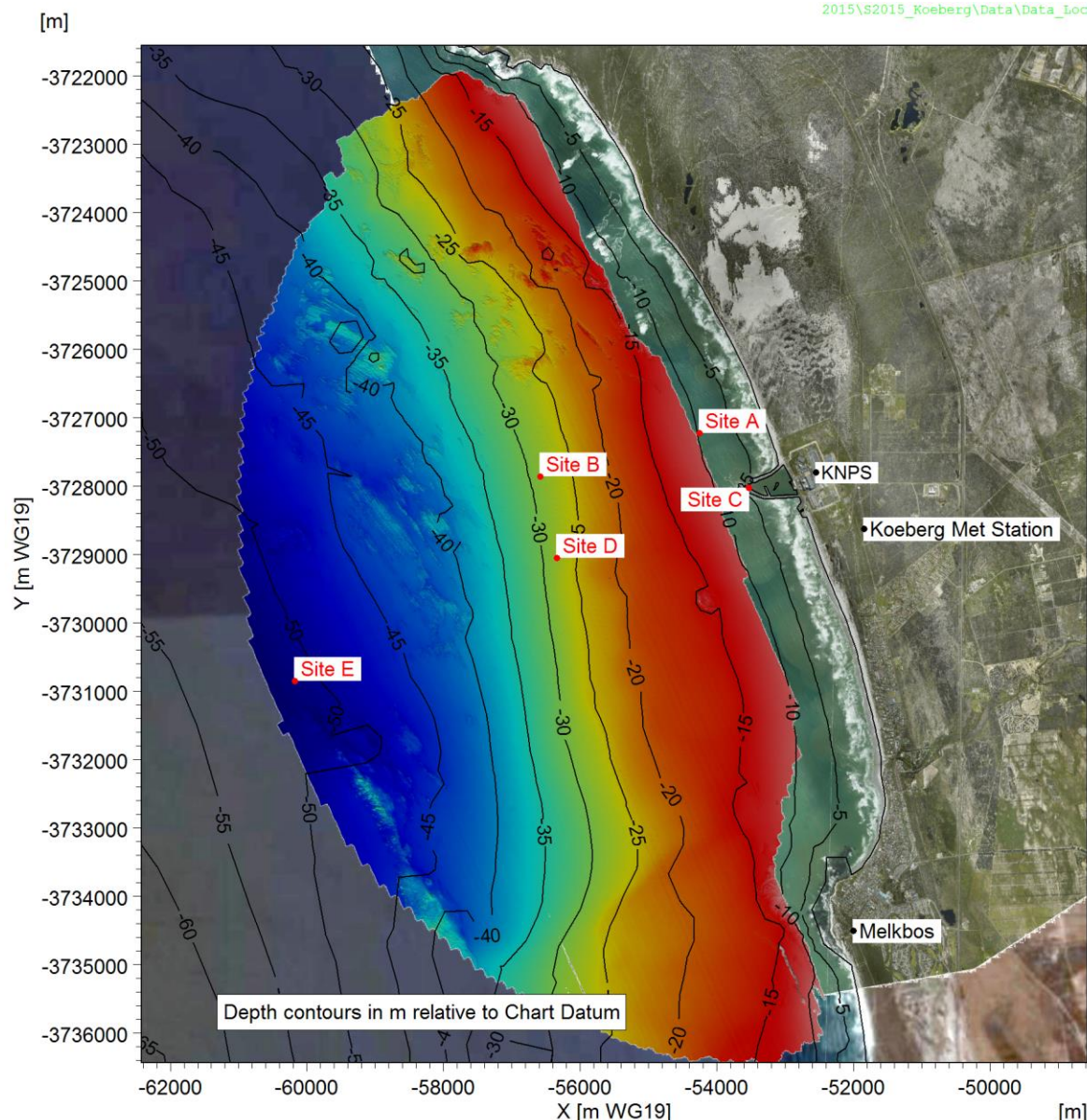


Figure 2-1: Local bathymetry at KNPS. The figure also shows the multi-beam bathymetric survey and the locations of other measurement stations discussed in Sections 2.4 to 2.7.

2.2 Geology

The Koeberg site is characterised by a shallow sloping sandy beach. The seabed slopes vary along the site, decreasing from north to south. Between +3 m CD and +13 m CD, the average beach slope ranges from 1:12 in the north to 1:60 in the south. In the breaker zone between -4 m CD and +3 m CD, the average slope ranges from 1:42 in the north to 1:60 in the south. Further offshore, between -29 m CD and -4 m CD, the average slope ranges from 1:100 in the north to 1:145 in the south.

Previous geotechnical investigations (Watermeyer, et al., 1972) indicated that rocks of the Malmesbury Series of Precambrian age occur at the site within -5 m CD to -12 m CD. Boreholes of the previous geotechnical investigations indicated that Malmesbury Shales are variably weathered to depths of about -54 m CD to -65 m CD.

Sediment samples have been collected from the nearshore (depths between -9 and -29 m CD) and from the beach at the high and low water marks (see Figure 2-2). The sand on the beach south of the KNPS has a D_{50} of approximately 0.2 mm and a grading of approximately 1.2. The sand on the beach north of the KNPS has a D_{50} of approximately 0.4 mm and a grading of approximately 1.4, reflecting the steeper beach slope and larger waves north of the KNPS. The sand offshore has a D_{50} of approximately 0.15 mm and a grading of approximately 1.2, reflecting the deposition of finer sediments in deeper water.

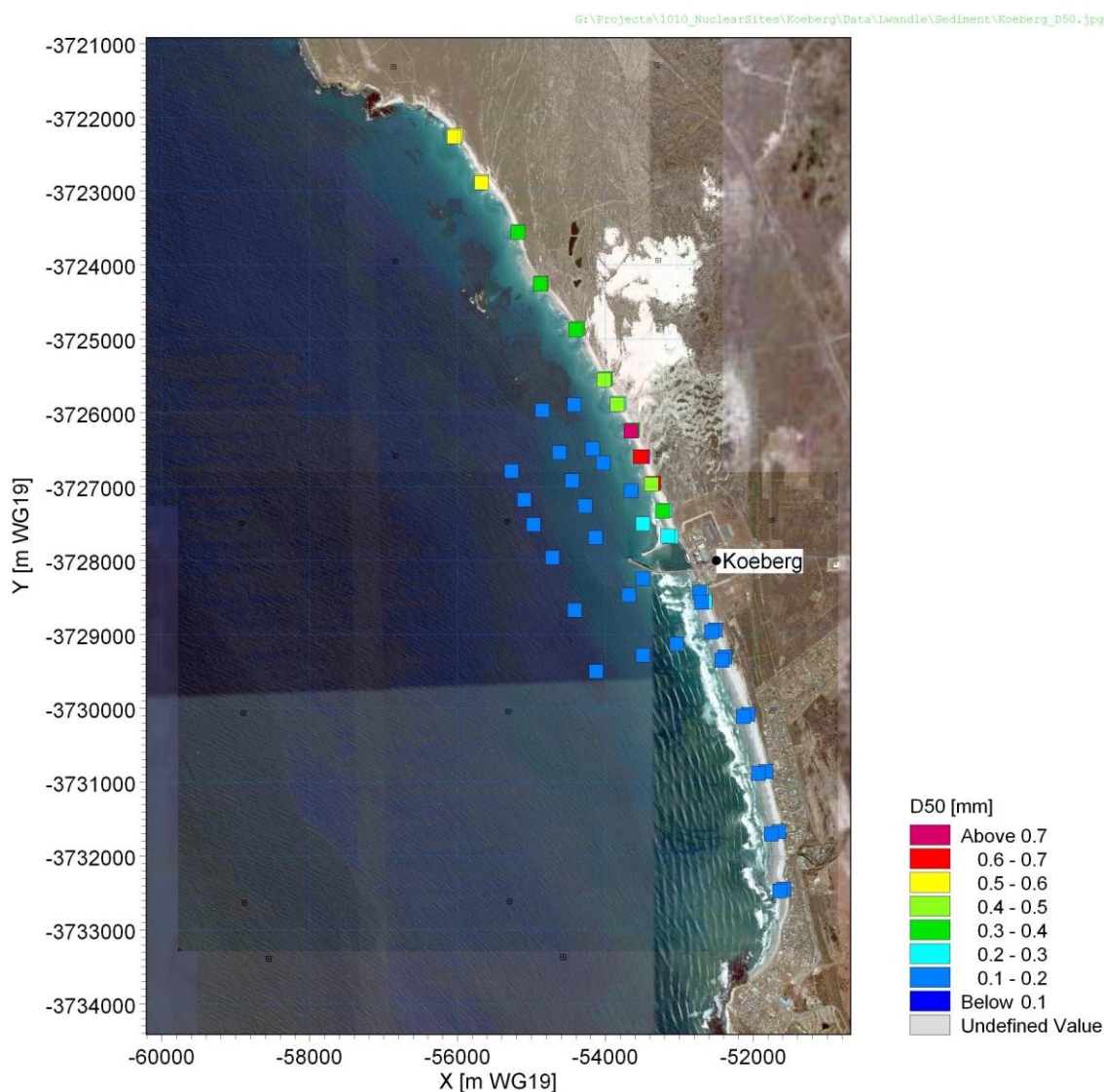


Figure 2-2: Measured sediment grain size at Duynefontein

2.3 Water Levels

The predicted tide for the Port of Cape Town was used for modelling. The tidal characteristics are presented in Table 2-1. The levels are referenced to Chart Datum (CD), defined as 0.825 m below Land Levelling Datum (LLD) also commonly referred to as Mean Sea Level (MSL).



Table 2-1: Tidal characteristics for the Port of Cape Town (SANHO, 2016)

Description	Level [m CD]
Highest Astronomical Tide (HAT)	2.02
Mean High Water Springs (MHWS)	1.74
Mean High Water Neaps (MHWN)	1.26
Mean Level (ML)	0.98
Mean Low Water Neaps (MLWN)	0.70
Mean Low Water Springs (MLWS)	0.25
Lowest Astronomical Tide (LAT)	0.00

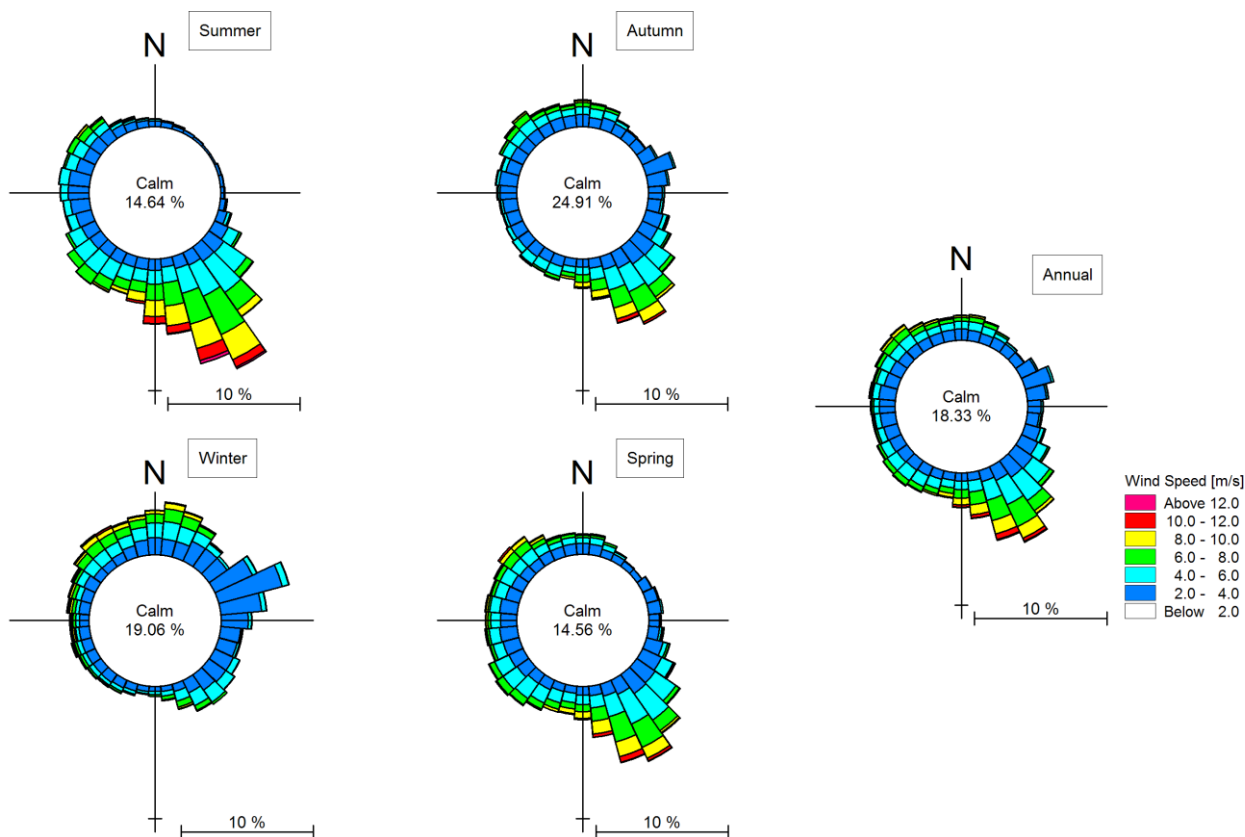
2.4 Weather

Weather data measured at the Koeberg meteorological station (see Figure 2-1) at hourly intervals for the period of October 1997 to June 2010 was used. The dataset includes a number of weather parameters collected at a range of heights. The following parameters were used in this study:

- Air temperature at 10 m above ground level; and
- Hourly averaged wind speed and direction at 10 m above ground level.

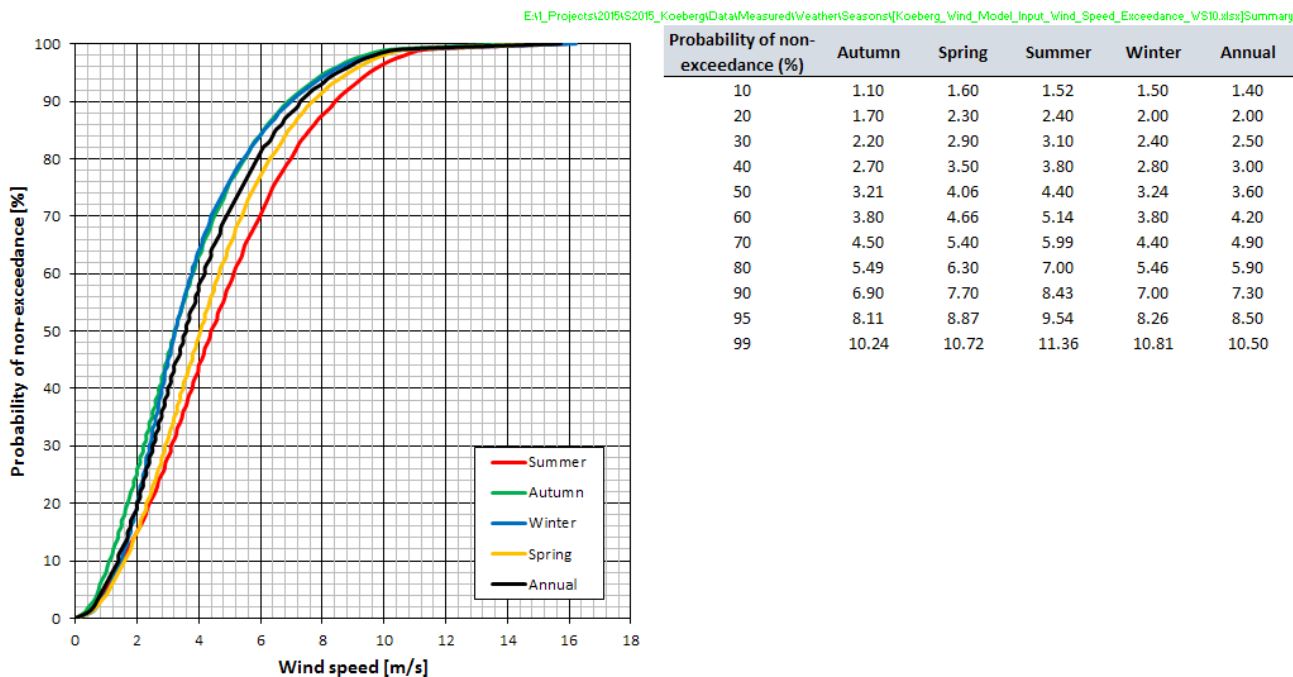
Seasonal wind rose and wind speed exceedance plots are presented in Figure 2-3 and Figure 2-4. The strongest winds occur during the summer months, which are characterised by strong, persistent south-easterly winds. The winter months are generally calmer, with the strongest winds from north-west to north-north-east.

A time series plot of measured air temperature is presented in Figure 2-5 for 2008 and 2009. At the height of summer, air temperatures typically vary between 15°C and 35°C, reducing to 5°C to 25°C in the mid-winter months.



2015\S2015_Koeberg\Data\Measured\Weather\Seasons\Koeberg_Wind_Model_Input_Roses.png

Figure 2-3: Seasonal wind roses of hourly averaged wind data measured at 10 m above ground level at the KNPS Meteorological Station (X = -51 849 m, Y = -3 728 624 m, WG19). The roses are constructed from 14 years of measured data (1997-2010).



E:\Projects\2015\S2015_Koeberg\Data\Measured\Weather\Seasons\Koeberg_Wind_Model_Input_Wind_Speed_Exceedance_WS10.xlsx)Summary

Figure 2-4: Seasonal exceedance of hourly averaged wind speeds recorded 10 m above ground level at the KNPS Meteorological Station (X = -51 849 m, Y = -3 728 624 m, WG19). The curves are drawn from 14 years of measured data (1997-2010).

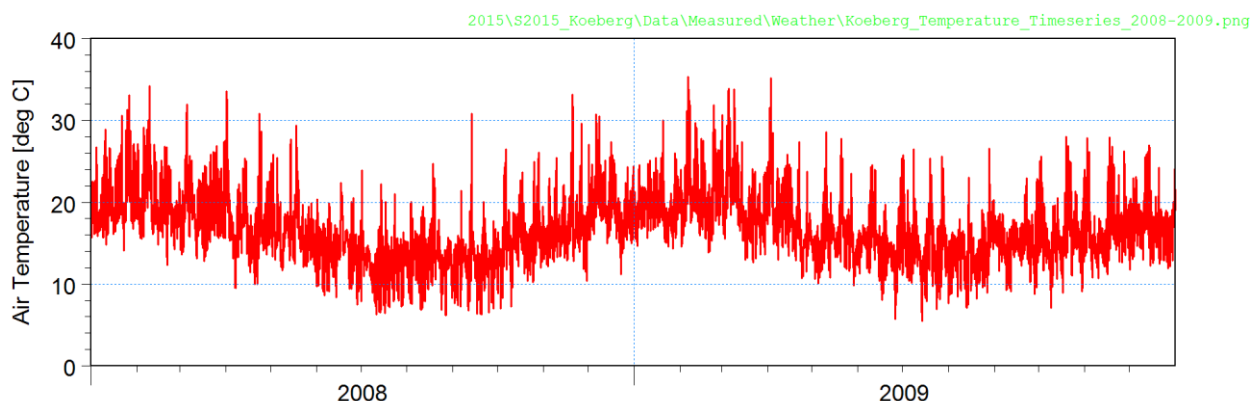


Figure 2-5: Time series of air temperature recorded 10 m above ground level at the KNPS Meteorological Station ($X = -51\ 849\text{ m}$, $Y = -3\ 728\ 624\text{ m}$, WG19).

2.5 Waves

Nearshore wave data measured by Acoustic Doppler Current Profilers (ADCPs) are available at Site A for the period of January 2008 to July 2010 and at Site B for the period of July 2008 to January 2014. The positions of the instruments are shown on Figure 2-1. The datasets comprise hourly measurements of wave spectra, from which significant wave height (H_{m0}), peak wave period (T_p) and mean wave direction (Dir_{mean}) have been calculated. Wave roses for the two sites are presented in Figure 2-6, while seasonal exceedance plots of significant wave height are presented in Figure 2-7 and Figure 2-8 for Site A and Site B, respectively. The measurements indicate an exposed wave climate with median and 99th percentile significant wave heights of 1.5 m and 4.0 m at Site A and 1.6 m and 4.5 m Site B.

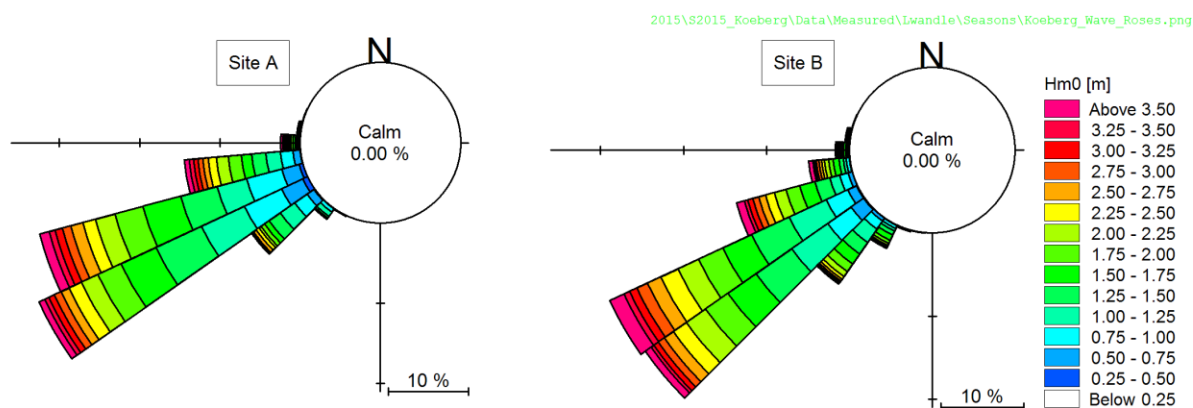
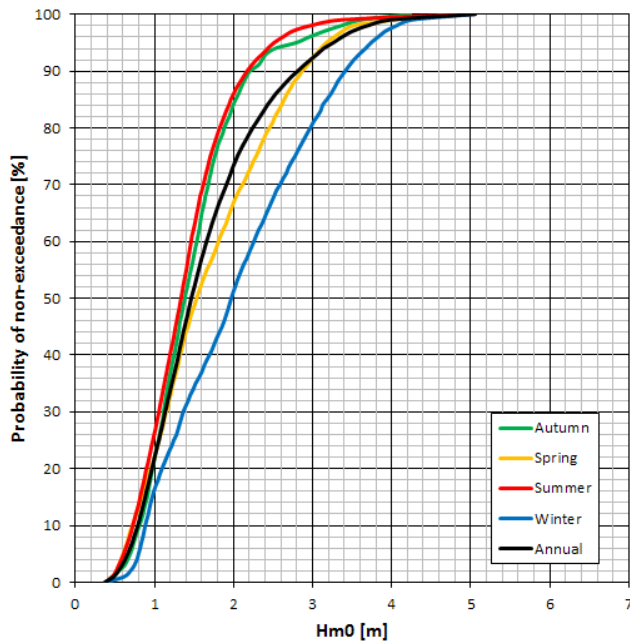


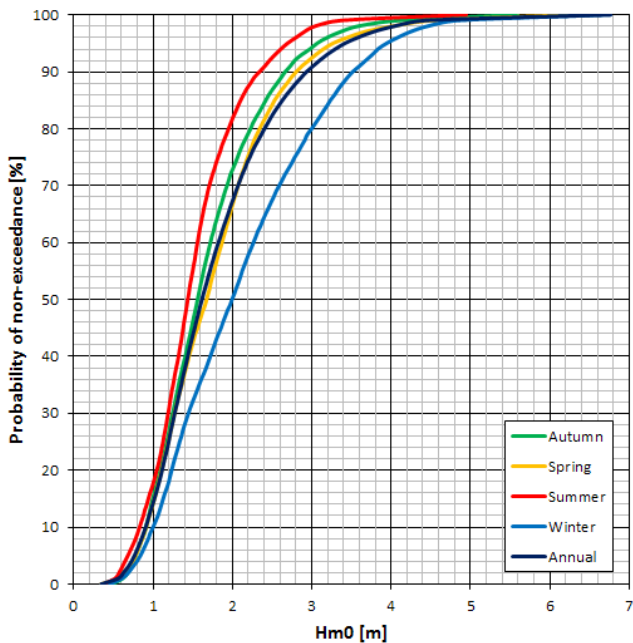
Figure 2-6: Wave roses of wave data measured at Site A ($X = -54\ 253\text{ m}$, $Y = -3\ 727\ 223\text{ m}$ WG19, -10 m CD) from January 2008 to July 2010 and at Site B ($X = -56\ 587\text{ m}$, $Y = -3\ 727\ 857\text{ m}$ WG19, -30 m CD) from July 2008 to January 2014.



E:\Projects\2015\2015_KoebergData\Measured\Wandlet\Seasons\Koeberg_A_W0_P01_25_Exceedance_Hm0.xls\Summary

Probability of non-exceedance [%]	Autumn	Spring	Summer	Winter	Annual
10	0.80	0.72	0.72	0.88	0.78
20	0.97	0.95	0.89	1.09	0.96
30	1.11	1.15	1.06	1.36	1.13
40	1.24	1.32	1.19	1.69	1.30
50	1.38	1.53	1.33	1.97	1.46
60	1.53	1.81	1.46	2.26	1.65
70	1.68	2.11	1.62	2.59	1.91
80	1.88	2.45	1.83	2.97	2.24
90	2.21	2.87	2.17	3.42	2.81
95	2.80	3.18	2.52	3.74	3.26
99	3.63	4.04	3.38	4.26	3.99
100	4.24	4.91	5.05	5.06	5.06

Figure 2-7: Seasonal exceedance of significant wave height measured at Site A (X = -54 253 m, Y = -3 727 223 m WG19, -10 m CD).



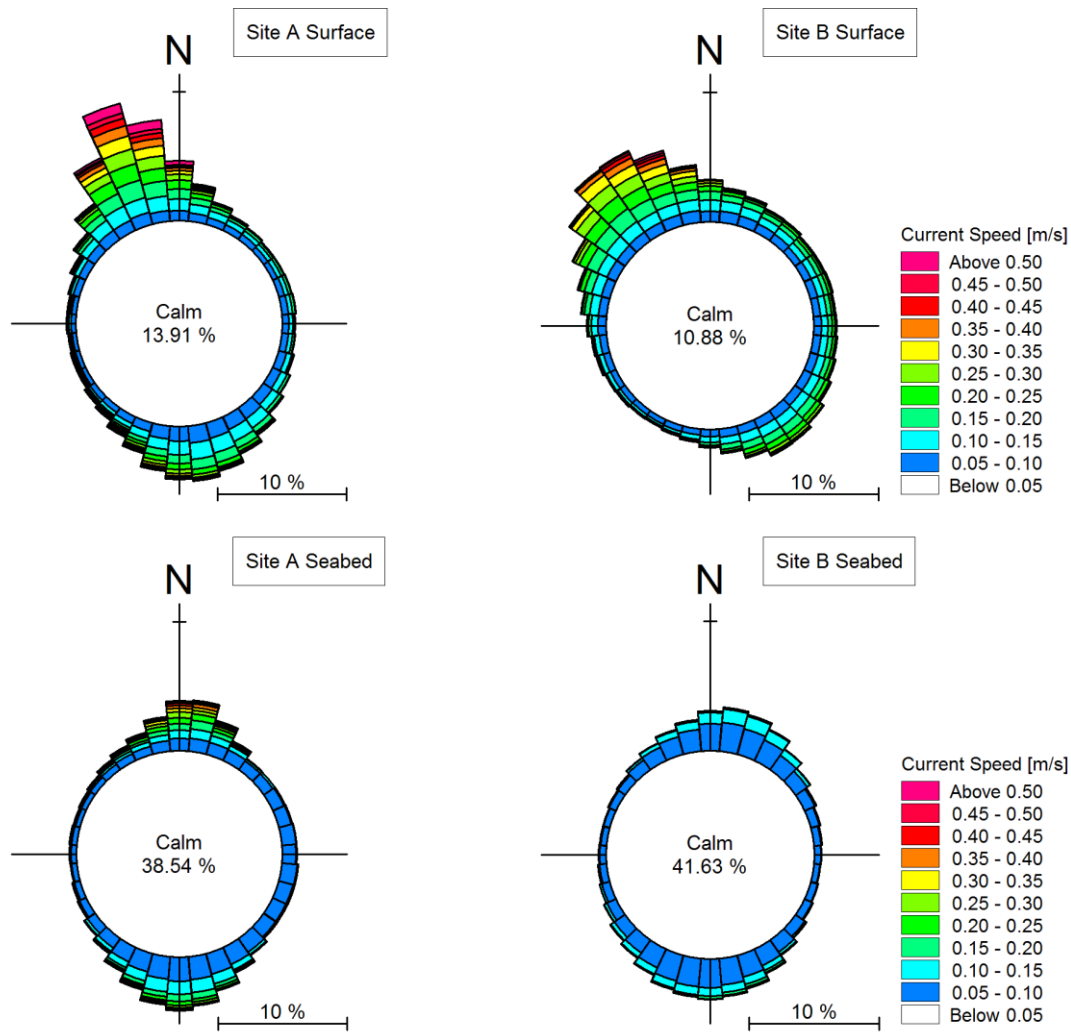
E:\Projects\2015\2015_KoebergData\Measured\Wandlet\Seasons\Koeberg_B_W0_P03_57_Exceedance_Hm0.xls\Summary

Probability of non-exceedance [%]	Autumn	Spring	Summer	Winter	Annual
10	0.92	0.92	0.83	1.00	0.91
20	1.10	1.11	1.05	1.23	1.12
30	1.25	1.28	1.19	1.44	1.28
40	1.41	1.46	1.32	1.72	1.44
50	1.57	1.68	1.44	1.99	1.62
60	1.73	1.87	1.56	2.27	1.83
70	1.94	2.08	1.71	2.59	2.08
80	2.24	2.35	1.95	3.00	2.41
90	2.67	2.81	2.34	3.52	2.94
95	3.08	3.27	2.70	3.95	3.43
99	4.11	4.54	3.38	4.86	4.46
100	5.60	6.31	4.94	6.77	6.77

Figure 2-8: Seasonal exceedance of significant wave height measured at Site B (X = -56 587 m, Y = -3 727 857 m WG19, -30 m CD).

2.6 Currents

Currents measured by the same ADCPs at Site A and Site B (see Figure 2-1) are also available for the same durations. Current speeds were measured every 10 minutes through the water column at 0.3 m intervals at Site A and at 0.5 m intervals at Site B. Rose plots of the near-surface and near-seabed currents are shown in Figure 2-9, while exceedance plots of the near-surface and near-seabed currents at both sites are shown in Figure 2-10.

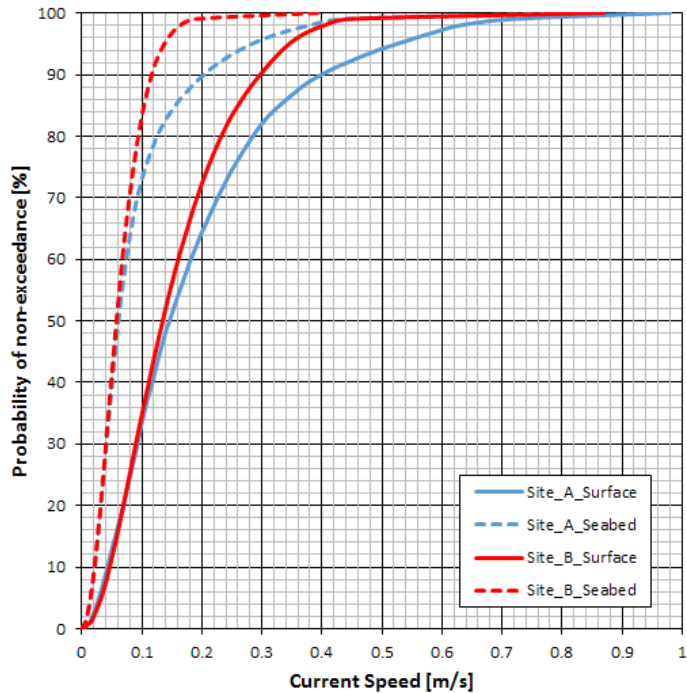


2015\S2015_Koeberg\Data\Measured\Lwandle\Seasons\Koeberg_Current_Roses.png

Figure 2-9: Rose plots of near-surface and near-seabed currents measured by ADCPs at Site A (X = -54 253 m, Y = -3 727 223 m WG19, -10 m CD) between January 2008 and July 2010 and at Site B (X = -56 587 m, Y = -3 727 857 m WG19, -30 m CD) between July 2008 and January 2014.



E:\Projects\2015\2015_KoebergData\Measured\Wandlet\Seasons\Koeberg_Currents_Exceedance.xlsx\Summary



Probability of non-exceedance [%]	Current Speed [m/s]			
	Site A Surface	Site A Seabed	Site B Surface	Site B Seabed
10	0.04	0.02	0.05	0.02
20	0.07	0.03	0.07	0.03
30	0.09	0.04	0.09	0.04
40	0.12	0.05	0.11	0.05
50	0.15	0.06	0.14	0.06
60	0.18	0.07	0.16	0.07
70	0.23	0.09	0.19	0.08
80	0.28	0.13	0.23	0.09
90	0.40	0.20	0.30	0.12
95	0.53	0.28	0.35	0.14
99	0.72	0.44	0.44	0.19

Figure 2-10: Exceedance of near-surface and near-seabed current speeds measured by ADCPs at Site A (X = -54 253 m, Y = -3 727 223 m WG19, -10 m CD) between January 2008 and July 2010 and at Site B (X = -56 587 m, Y = -3 727 857 m WG19, -30 m CD) between July 2008 and January 2014.

2.7 Water Temperature

Measurements of seawater temperatures from five datasets are available. Table 2-2 presents a summary of the measured datasets. The positions of the measurements are shown in Figure 2-1.

Table 2-2: Summary of available seawater temperature datasets

Location	Depth [m CD]	Length of dataset	Minimum Temperature [°C]	Mean Temperature [°C]	Maximum Temperature [°C]
Site A	-10	4.6 years	8.2	12.5	19.2
Site B/D	-30	4.4 years	8.1	11.4	17.9
Site C	-3	7.3 years	8.7	13.4	20.1
Site E	-50	6.7 months	9.0	11.4	15.2

Figure 2-11 presents a comparison of the measured seawater temperatures at the five sites for the years of 2008 and 2009. The measurements indicate a well-mixed water column during the winter months (May to mid-September), with relatively little variability in temperatures. During the summer months, (mid-September to April), a higher variability in temperatures is observed in all datasets. The differences between the shallower and deeper datasets are also more pronounced during the summer months, which indicates the presence of water column stratification. The stratification is the result of the influx of cold water from offshore caused by wind-driven upwelling as well as atmospheric heating of the water surface. Wind-driven upwelling occurs under strong south-easterly wind conditions which are dominant during the summer months.



Table 2-3 presents the difference in seawater temperature between the -10 m and -30 m sites. The table supports the observations of stratification, showing larger differences between shallower and deeper temperatures during summer months than during winter months.

Table 2-3: Seasonal statistics of measured seawater stratification between depths of -10 and -30 m.

Summer			Autumn			Winter			Spring		
Min. (°C)	Mean (°C)	Max. (°C)	Min. (°C)	Mean (°C)	Max. (°C)	Min. (°C)	Mean (°C)	Max. (°C)	Min. (°C)	Mean (°C)	Max. (°C)
-0.2	1.7	8.4	-0.9	1.1	6.7	-0.9	0.5	4.2	-0.9	1.4	6.5

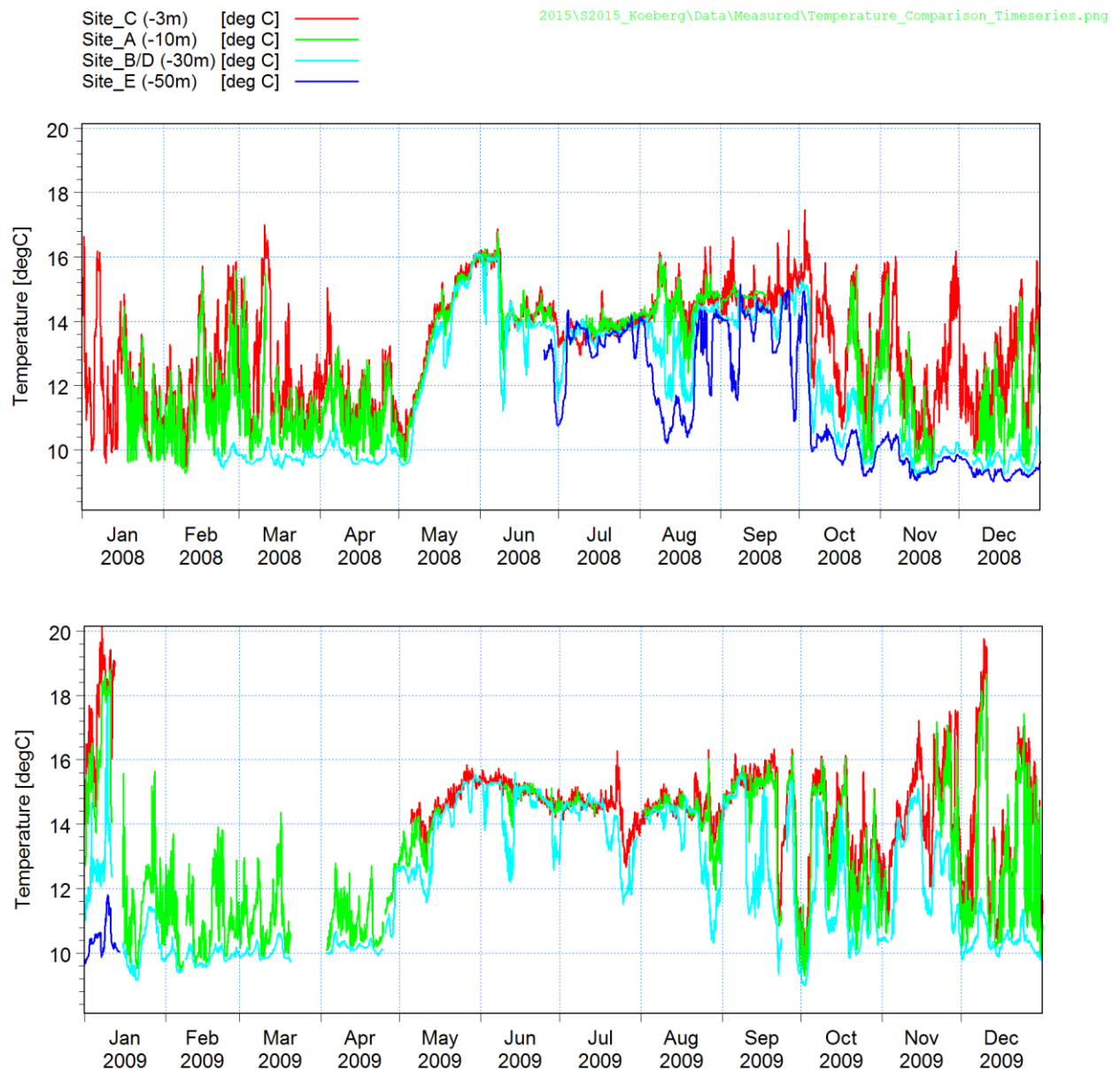


Figure 2-11: Time series of measured seawater temperatures at Sites A to E. The coordinates and depths of the measurement locations are reported in Table 2-2.



2.8 Salinity

Historical measurements at KNPS in a water depth of 30 m at depths of 10 m and 30 m below the surface have shown an average of 35 psu with little variation (<1.0 psu) (PRDW, 2012).

3. DISCHARGE CHARACTERISATION

3.1 Discharge Locations

The outfall of the KNPS is situated south of the intake basin, on the Eskom-owned land of Cape Farm Dynefontyn 1552. This position was selected on the basis that during south-easterly wind conditions when currents flow northwards, coastal upwelling of cold water occurs. This results in the efficient cooling of the northward drifting warm water plume, minimising recirculation effects. During north-westerly wind conditions and southerly currents, when ambient water temperatures are typically higher due to the absence of upwelling, the warm water plume is carried southwards away from the intake basin.

Various designs were considered in the original development of the cooling water system (WLPU, Sir William Halcrow and Partners, 1972). The most feasible option was that of a basin scheme with a concrete channel outfall in close proximity to the power station. The outfall consists of a concrete channel approximately 150 m long initiating on land and discharging into the sea at a depth of approximately -2 m CD.

The magnitude of the flow of the cooling water (discussed in Section 3.2) prevents the penetration of ambient seawater into the outfall channel. Therefore, the effective position of the discharge is the end of the outfall channel, as shown on Figure 3-1. The coordinates of the discharge location are $X = -52\ 795\text{ m}$, $Y = -3\ 728\ 381\text{ m}$ (WG19).

The individual streams discharged into the outfall channel are discussed in Section 3.2.



Figure 3-1: Outfall channel of the KNPS. The figure also indicates the location of the discharge point.

In addition to the effluent streams discharged into the outfall channel, the effluents from some processes are discharged into the intake basin via a single discharge point, as shown in Figure 3-2. Although these discharges are released into the intake basin, the streams are sucked in by the cooling water intakes, pass through the cooling water system and are effectively discharged in the outfall channel. This assumption is validated in Section 5.5. The individual streams discharged into the intake basin are discussed in Section 3.3.



Figure 3-2: Location of the KNPS intake basin discharge point.

3.2 Effluent Streams Discharged at Outfall

3.2.1 Overview of Outfall Structure

3.2.1.1 Hydraulic design

An overview of the arrangement of effluent streams discharged into the outfall channel is presented in Figure 3-3.

The outflow pipes of the Circulating Water System (CRF, discussed in Section 3.2.2) which dominates the effluent from KNPS enter the outfall channel in a concrete housing at its northern end. The cooling water for each unit is discharged into the outfall channel through two 3 m diameter pipes with invert levels at -2.2 m CD. The outlet pipes of the total of four CRF trains are equally spaced horizontally into the structure. A number of structural and flow stabilising baffles are located in front of the pipes as well as a 3 m high weir. The 150 m long channel is constructed of smooth reinforced concrete and contains a bend in order to direct the flow offshore. A detailed plan view and cross-section of the outfall channel are presented in Annexure A.



Figure 3-3: Layout of effluent streams released into outfall channel

3.2.1.2 Construction considerations

The initial concept design of the outfall was to have a low elevation sheet pile channel wall and to accept wave action in the outfall channel. However, owing to the design of the stop logs at the top of the outlet structure, it was found to be necessary to exclude wave action from the channel. The rock mound or 'Wave Energy Dissipater' located in the centre of channel was designed to eliminate wave action without incurring additional head losses and pumping costs of the cooling water system. The outlet channel is protected with a 1 to 3 tonne rubble mound revetment.

The channel is constructed of reinforced concrete and is inspected for settling on an annual basis as part of the coastal structures monitoring programme. Visual inspections of the structural integrity of the outfall structure and channel are also conducted periodically. The inspections identify areas for further investigation and remedial action is recommended where necessary.

3.2.2 Circulating Water System (CRF)

The circulating water system supplies cooling water to the main condenser, to two heat exchangers of the conventional island closed cooling water system and to the coolers for the water-sealed storage tanks of the



condenser vacuum pump system. In addition to the discharge of heat, the CRF cooling water contains residual free chlorine resulting from sodium hypochlorite dosing required to prevent biofouling.

For each of the two reactor units, cooling water is extracted from the intake basin through a system consisting of two totally independent pump trains. Each unit is also provided with a stand-by pump with the same characteristics as the main operating pumps. The mean flow rate in each pump train is 81 972 m³/h. Although variations in the tidal water level result in variable pump rates, the minimum and maximum rates vary by less than 10% of the mean flow rate.

As shown on Figure 3-3 in blue, the four CRF pump trains are discharged at the top of the outfall channel.

During plant operation at full capacity, both reactor units and therefore four CRF pump trains are operational. Scheduled outages of one reactor at a time occur for maintenance and refuelling. Each reactor unit is refuelled at approximately 18 month intervals and refuelling outages last approximately one to three months each. On average, therefore, one of the reactor units is refuelled every 9 months.

In the event of the trip of one CRF pump, the change in temperature (ΔT) in the second train of the same reactor unit may increase from the normal 11.7°C to 22.7°C. The duration of this discharge scenario is 12 hours, which is the estimated time required to bring the stand-by pump into operation. For the current study, this event is conservatively (worst case) considered to occur during a refuelling outage (i.e. only one reactor unit is operational), thereby not including any dilution of the train with elevated ΔT into the flow from other CRF trains with a normal ΔT .

Table 3-1 presents the characterisation of the CRF discharge during operation at full capacity, during refuelling outages and during a pump trip.

Table 3-1: Characterisation of CRF discharges

Parameter	Unit	Value		
		Full capacity: 2 Units CRF	Refuelling outage: 1 Unit CRF	1 Unit CRF, 1 Pump Trip
Discharge	m ³ /h	327 888	163 944	81 972
Duration	h	Continuous	Continuous	12
Frequency	-	-	-	Abnormal conditions
ΔT	°C	11.7	11.7	22.7
Free Chlorine	mg/kg	0.5	0.5	0.5
Bromoform	mg/kg	unknown ⁽¹⁾	unknown ⁽¹⁾	unknown ⁽¹⁾

Notes:

- (1) Bromoform is expected to be formed as a by-product of the chlorination of seawater. The concentration of bromoform formed at KNPS is currently unknown.

3.2.3 Essential Water Service System (SEC)

The essential water service system supplies cooling water to the nuclear island. Similar to the CRF, the SEC intake structure extracts seawater from the intake basin. However, for safety reasons the SEC is operated as an entirely independent system.

Chlorination of the SEC is also required to prevent biofouling. In addition to normal chlorination levels, the SEC experiences variability in free chlorine concentrations and is subjected to routine shock chlorination. The characterisation of the SEC discharge is presented in Table 3-2.

As shown in Figure 3-3 in red, the SEC system is discharged directly below the CRF trains, on the north-western wall of the outfall channel through a baffled anti-splash chamber.



Table 3-2: Characterisation of SEC discharge

Parameter	Unit	Value	Variability in concentrations		
			Value	Duration [h]	Frequency
Discharge	m ³ /h	12 700	-	-	-
Duration	h	Continuous	-	-	-
Frequency	-	-	-	-	-
ΔT	°C	12	-	-	-
Free Chlorine	mg/kg	1	2 ⁽¹⁾	8	Once per week
			25 ⁽²⁾	0.5	Once every two weeks
Bromoform	mg/kg	unknown ⁽³⁾	-	-	-

Notes:

- (1) Approximation of the variability in normal chlorine levels.
- (2) This characterisation of the shock chlorination is extremely conservative, since in reality only one of four SEC trains would be shock chlorinated at a time.
- (3) Bromoform is expected to be formed as a by-product of the chlorination of seawater. The concentration of bromoform formed at KNPS is currently unknown.

3.2.4 Conventional Island Liquid Waste Monitoring and Discharge System (SEK)

The SEK is designed to collect, monitor and discharge liquid effluent from the conventional island secondary system. Although the SEK system is a radiological effluent system, it also contains non-radiological effluent. The SEK is common to both reactor units and collects a number of continuous, intermittent and exceptional streams (e.g. during reactor shutdown) from a number of processes on the conventional island.

Under default operation, effluent is routed to bypass the SEK tanks via a bypass line which is fitted with volume/flow counters and activity detectors which have redundancy. In the event that the pre-determined radioactivity threshold is exceeded, release is interrupted and switched automatically to SEK collection tanks. Effluent is then monitored, measured and not released from the tanks until the cause of the abnormal condition is remedied. As shown in Figure 3-3 in green, discharges via SEK are released directly into the CRF effluent stream at the top of the outfall channel.

The loads and dispersion of radiological effluent from the SEK are described in Section 6. The radiological releases are regulated by the National Nuclear Regulator (NNR).

Depending on which pumps are used, releases from SEK tanks can occur at either 300 m³/h or 20 m³/h, while releases during SEK-bypass are variable with a maximum rate of 240 m³/h (three pumps with a capacity of 80 m³/h each). For this study, the maximum flow rate for pumping from SEK tanks (300 m³/h) has been assumed for all SEK releases. This flow rate is larger than the maximum rate expected during SEK-bypass, and is therefore conservative. The characterisation of SEK discharges is presented in Table 3-3. These releases may occur during plant operation at full capacity (2 reactor units operational) or during refuelling outages (1 reactor unit operational).

Table 3-3: Characterisation of SEK discharges

Parameter	Unit	Value	Abnormal Value
Discharge	m ³ /h	80	300
Duration	h	6	
Frequency	-	Daily	
Temperature	°C	55	
pH	-	5.0 to 11.7	
Total Suspended Sediment (TSS)	mg/kg	75	
Hydrazine	mg/kg	0.2	
Ammonia	mg/kg	20	100 ⁽¹⁾
Ethanolamine	mg/kg	6	
Phosphates	mg/kg	550 ⁽³⁾	
Nitrates	mg/kg	15	
Nitrites	mg/kg	3	
Aluminium	mg/kg	2	
Copper	mg/kg	0.04	
Chromium	mg/kg	2	
Iron	mg/kg	0.2	
Manganese	mg/kg	0.2	
Nickel	mg/kg	2	
Lead	mg/kg	1.5	
Zinc	mg/kg	1	
Sulphate	mg/kg	8 000	
Sodium	mg/kg	4 000	
Detergents – Linear Alkylbenzene Sulfonate (LAS)	mg/kg	7 ⁽²⁾	
Detergents – Alcohol Ethoxysulfates (AES)	mg/kg	280 ⁽²⁾	
Detergents – Alcohol Ethoxylates (AE)	mg/kg	35 ⁽²⁾	
Biochemical Oxygen Demand (BOD)	mg/kg	568	
Chemical Oxygen Demand (COD)	mg/kg	1410	
Oil/grease	mg/kg	154	

Notes:

- (1) The abnormal ammonia value corresponds to the upper pH limit. It has never occurred, but is possible.
- (2) Maximum allowable concentration not exceeding the relevant ecological guideline at the end of the outfall channel.
- (3) The phosphate releases occur only during outages, daily for three days.

In addition to the discharges described above, exceptional hydrazine releases occur via SEK during refuelling outages. Under default operation, the effluent is released via the SEK by-pass at a maximum flow rate of 80 m³/h. If the release is collected in SEK tanks, the effluent is either pumped at 300 m³/h or at 20 m³/h. However, the pumping system used is chosen such to not exceed the concentration of hydrazine in the CRF outfall during release via SEK by-pass. Thus, if the hydrazine concentration in the SEK tanks exceeds 50 mg/l, the effluent is pumped at the lower rate of 20 m³/h. The 80 m³/h rate has been assumed in this study. The discharge characterisation for these releases is summarised in Table 3-4.



Table 3-4: Characterisation of exceptional SEK discharges: hydrazine releases associated with outages

	Parameter	Unit	Value
Release 1	Discharge	m ³ /h	80
	Duration	h	0.5
	Frequency	-	Daily
	Hydrazine	mg/kg	187.5
Release 2	Discharge	m ³ /h	80
	Duration	h	1.67
	Frequency	-	Weekly
	Hydrazine	mg/kg	187.5

3.2.5 Nuclear Island Liquid Radiological Waste Monitoring and Discharge System (KER)

The KER system is design to collect, discharge and monitor the volume and activity of liquid radiological effluent discharged from the nuclear island. Although the KER system is a radiological effluent system it also contains non-radiological constituents in the radiological effluent. The system consists of three tanks in which activity is monitored and from which the effluent is released to the outfall once effluent standards are met. The characterisation of the KER discharges is presented in Table 3-5. These releases may occur during plant operation at full capacity (2 reactor units operational) or during refuelling outages (1 reactor unit operational). As shown on Figure 3-3 in purple, the discharges from KER are released directly into the CRF effluent stream at the top of the outfall channel.

The loads and dispersion of radiological effluent from KER are described in Section 6. The radiological releases are regulated by the National Nuclear Regulator (NNR).

Table 3-5: Characterisation of KER discharges

Parameter	Unit	Value
Discharge	m ³ /h	25
Duration	h	5
Frequency	-	Once every 2 days
Temperature	°C	55
pH	-	5.0 to 11.7
Total Suspended Sediment (TSS)	mg/kg	150
Boron	mg/kg	188
Lithium Hydroxide	mg/kg	3.5
Phosphate	mg/kg	1 250 ⁽¹⁾
Detergents – Linear Alkylbenzene Sulfonate (LAS)	mg/kg	63
Detergents – Alcohol Ethoxysulfates (AES)	mg/kg	280
Detergents – Alcohol Ethoxylates (AE)	mg/kg	250
Aluminium	mg/kg	2
Copper	mg/kg	0.2
Chromium	mg/kg	2
Iron	mg/kg	2
Manganese	mg/kg	0.2
Nickel	mg/kg	2
Lead	mg/kg	1.5
Zinc	mg/kg	1
Ethylenediaminetetraacetic acid (EDTA)	mg/kg	1 500
Citric Acid	mg/kg	3 000
Zinc Acetate as Zinc	mg/kg	0.005
Total Zinc	mg/kg	1
Chemical Oxygen Demand (COD)	mg/kg	1 410
Biochemical Oxygen Demand (BOD)	mg/kg	568
Oil/grease	mg/kg	154
Nitrates	mg/kg	15
Nitrites	mg/kg	3
Ammonia	mg/kg	18

Notes:

- (1) The phosphate releases occur only during outages and are limited to two releases, two days apart.

While this is highly unusual, if required, the KER effluent can be released via SEK. Should this be required, the concentrations in Table 3-5 will be adjusted in proportion to the SEK release rate to ensure that concentrations in the outfall channel do not exceed those estimated in Table 4-6.

In addition to normal operational discharges, an exceptional boron release occurs approximately five times per year. The exceptional release is characterised in Table 3-6.

Table 3-6: Characterisation of exceptional boron releases via KER

Parameter	Unit	Value
Discharge	m ³ /h	25
Duration	h	13.5
Frequency	-	5 times per year
Boron	mg/kg	2 700

3.2.6 Domestic Wastewater Treatment System (SEU)

The domestic wastewater treatment plant receives sewage and grey water effluent from a number of sources across KNPS, including rest rooms, laundries and rain water drainage. The plant is designed to accommodate



a peak flow of 28 m³/h. As shown in Figure 3-3 in orange, the SEU system is discharged into the southern part of the stormwater (SEO-S) system, which in turn is discharged through a grated chamber directly below the CRF trains, on the south-eastern wall of the outfall channel. The characterisation of the SEU discharge is presented in Table 3-7.

Table 3-7: Characterisation of SEU discharges

Parameter	Unit	Value
Discharge	m ³ /h	28
Duration	h	Continuous
Frequency	-	-
Temperature	°C	20
pH		4.5 to 10.5
Total Suspended Sediment (TSS)	mg/kg	90
Ammonia (NH ₃ -N)	mg/kg	60
Free Chlorine	mg/kg	5
Chemical Oxygen Demand (COD)	mg/kg	140
Biochemical Oxygen Demand (BOD)	mg/kg	65
Faecal Coliforms	counts/100ml	1000
Detergents – Linear Alkylbenzene Sulfonate (LAS)	mg/kg	20
Detergents – Alcohol Ethoxysulfates (AES)	mg/kg	95
Detergents – Alcohol Ethoxylates (AE)	mg/kg	85

3.2.7 Unit 2 Electrical Building Ventilation System (DEL)

The ventilation system in the unit 2 electrical building is used to keep electrical equipment at suitable temperatures. This system uses a refrigeration gas which is compressed and used to cool a closed water cooling system. This closed water cooling system is dosed with phosphate to prevent corrosion. Any leaks from the cooling system or drains for maintenance purposes are discharged to the SEO-S system (shown in orange in Figure 3-3), on the south-eastern wall of the outfall channel. The characterisation of Unit 2 DEL discharges is presented in Table 3-8. Draining of the DEL system for maintenance could occur outside of outages, but this is unusual.

Table 3-8: Characterisation of Unit 2 DEL discharges

Parameter	Unit	Value
Discharge	m ³ /h	20
Duration	h	2
Frequency	-	Once per year during an outage of Unit 2
Phosphate	mg/kg	1 250

3.2.8 Southern Stormwater System (SEO-S)

The southern stormwater system is mainly used for the draining of stormwater from the southern section of KNPS and from a number of buildings on site. The SEO-S system is also used for the draining of the SEU system and, on exception, for the draining of the Unit 2 DEL stream as presented in Section 3.2.7. In order to ensure limited oil and hydrocarbon pollution of the SEO-S discharge, oil traps are provided on buildings and facilities that may have some oil or hydrocarbon sources.

As shown in Figure 3-3 in orange, the SEO-S system is discharged directly below the CRF trains on the south-eastern wall of the outfall channel. During rainfall events, stormwater from the southern portion of the site is discharged via this system; however only the process effluents described in Table 3-7 and Table 3-8 have



been considered in this study. Given the type of industrial processes on site and the use of oil traps, the contamination of stormwater is not considered significant.

3.3 Effluent Streams Discharged into Intake Basin

3.3.1 Overview

Discharges into the intake basin occur via the northern stormwater system (SEO-N) which is mainly used for the draining of stormwater from the northern section of KNPS, but is also used for the draining of some specific plants. The discharges from processes which drain into SEO-N are characterised in the sections below.

Although these discharges are released into the intake basin, the streams are sucked in by the cooling water intakes, pass through the cooling water system and are effectively discharged in the outfall channel. This is validated in Section 5.5.

3.3.2 Auxiliary Boiler Plant (XCA)

The three auxiliary boilers are used to provide steam to the power station in the unusual event that both reactors are shut down and steam is required for plant start-up and de-aeration of feed water. The boilers are conventional diesel fired boilers and have three modes of operation, namely steam production, stand-by (or banked) and shutdown. The boilers are dosed with ammonia to increase pH and hydrazine for oxygen scavenging. Both the oxygen and pH control are for boiler corrosion prevention. The boilers spend most of their time in shutdown mode, but are started up periodically for testing purposes and are in stand-by mode when one or both reactors are down. A change in plant mode results in a change on boiler water level which results in an effluent release from XCA to the SEO-N. The characterisation of XCA discharges is presented in Table 3-9.

Table 3-9: Characterisation of XCA discharges

	Parameter	Unit	Value	Abnormal Value
Release 1	Discharge	m ³ /h	60	
	Duration	h	0.42	
	Frequency	-	Monthly	
	Temperature	°C	60	
	Ammonia	mg/kg	15	100 ⁽¹⁾
	Hydrazine	mg/kg	300	
	Total Suspended Sediment (TSS)	mg/kg	10	
	pH	-	7.5 to 10.5	
	Biochemical Oxygen Demand (BOD)	mg/kg	100	
	Chemical Oxygen Demand (COD)	mg/kg	800	
Release 2	Discharge	m ³ /h	60	
	Duration	h	1.17	
	Frequency	-	Once per outage	
	Temperature	°C	20	
	Ammonia	mg/kg	15	
	Hydrazine	mg/kg	300	
	Total Suspended Sediment (TSS)	mg/kg	10	
	pH	-	7.5 to 10.5	
	Biochemical Oxygen Demand (BOD)	mg/kg	100	
	Chemical Oxygen Demand (COD)	mg/kg	800	

Notes:

- (1) The abnormal ammonia corresponds to the upper pH limit. This level is not reached during normal operation, but could occur approximately once per year.

3.3.3 Reagent Distribution and Neutralisation System (SDX)

The demineraliser plant (SDA) provides demineralised water to the power station. It is important to have almost pure water in the plant to limit deposits in the plant systems which include steam generators and the reactor core. The demineraliser plant consists of carbon filters and ion exchange resins. The effluents from the SDA plant are discharged to the SDX sumps which are released into the SEO-N system. The effluent consists of filter backwashing and ion exchange regeneration. Sulphuric acid and soda hydroxide are used to regenerate the ion exchange systems which after mixing and thus neutralisation generates quantities of sulphate and sodium as an effluent stream. The characterisation of SDX discharges is presented in Table 3-10.

Table 3-10: Characterisation of SDX discharges

Parameter	Unit	Value
Discharge	m ³ /h	400
Duration	h	1
Frequency	-	Twice per week
Temperature	°C	20
pH	-	7.5 to 9.5
Total Suspended Sediment (TSS)	mg/kg	60
Sulphate	mg/kg	8 000
Sodium	mg/kg	4 000
Biochemical Oxygen Demand (BOD)	mg/kg	12
Chemical Oxygen Demand (COD)	mg/kg	90

3.3.4 Demineraliser Water Production Plant (SDA)

The demineraliser plant described in Section 3.3.3 has an active charcoal filter before the ion exchange resins. Aluminium sulphate is injected as a flocculent prior to this filter. When the filter is backwashed periodically, aluminium and solids concentrated from the potable water feed are released to the SEO-N system. The characterisation of SDA discharges is presented in Table 3-11.

Table 3-11: Characterisation of SDA discharges

Parameter	Unit	Value
Discharge	m ³ /h	100
Duration	h	1
Frequency	-	Weekly
Temperature	°C	20
Aluminium Sulphate	mg/kg	150
Total Suspended Sediment (TSS)	mg/kg	80
Biochemical Oxygen Demand (BOD)	mg/kg	30
Chemical Oxygen Demand (COD)	mg/kg	240

3.3.5 Chlorination Plant (CTE) Effluent

The chlorine production and distribution system (CTE) is used to prevent biofouling of the sea water cooling systems (CRF and SEC). The system is designed to produce sodium hypochlorite by using electrolyzers in sufficient quantities to ensure excess free chlorine in the discharge of CRF and SEC. The CTE plant effluent comes from the need to perform an acid wash of the electrolyzers on a regular (weekly) basis using hydrochloric acid. This acid is neutralised with sodium hydroxide and this produces chlorides and sodium as by-products. The neutralisation and subsequent draining occurs on a monthly basis. The characterisation of CTE discharges is presented in Table 3-12.



Table 3-12: Characterisation of CTE discharges

Parameter	Unit	Value
Discharge	m ³ /h	6
Duration	h	2
Frequency	-	Monthly
Temperature	°C	20
pH	-	7.5 to 9.5
Chloride	mg/kg	120 000
Total Suspended Sediment (TSS)	mg/kg	5
Sodium	mg/kg	80 000
Salinity	psu	200

Although the high salinity of the discharge results in a dense effluent, the abstraction rate of the CRF is sufficient to ensure a consistent near-seabed current of approximately 0.15 m/s toward the intakes. Therefore, even though the discharge is dense, it will be drawn in by the CRF flow and not accumulate on the seabed. Based on a distance of approximately 200 m between the discharge point and the CRF intakes, this should occur in approximately 20 minutes.

3.3.6 Unit 1 Electrical Building Ventilation System (DEL)

The ventilation system in the electrical building is used to keep electrical equipment at suitable temperatures. This system uses a refrigeration gas which is compressed and used to cool a closed water cooling system. This closed water cooling system is dosed with phosphate to prevent corrosion. Any leaks or draining of the cooling system for maintenance purposes is discharged to the SEO-N system. The characterisation of Unit 1 DEL discharges is presented in Table 3-13.

Table 3-13: Characterisation of Unit 1 DEL discharges

Parameter	Unit	Value
Discharge	m ³ /h	20
Duration	h	2
Frequency	-	Once per year during and outage of Unit 1
Phosphate	mg/kg	1 250

3.3.7 Northern Stormwater System (SEO-N)

The northern storm water system is used to collect storm water from the northern zone of the power station site and from a number of buildings on site. The SEO-N system is also used to collect and discharge effluent from the XCA, SDX, SDA and CTE systems described above. In order to ensure limited oil and hydrocarbon pollution of the SEO-N discharge, oil traps are provided on buildings and facilities that may have some oil or hydrocarbon sources.

During rainfall events, stormwater from the northern portion of the site is discharged via this system; however only the process effluents described in Table 3-9 to Table 3-13 have been considered in this study. Given the type of industrial processes on site and the use of oil traps, the contamination of stormwater is not considered significant.



3.4 Proposed desalination plants

In addition to the existing streams discharged at KNPS, it is proposed to install two desalination facilities in the near future. The facilities are a Brackish Water Reverse Osmosis (BWRO) plant for the provision of potable water to KNPS and a Seawater Reverse Osmosis (SWRO) plant for the provision of potable water to the City of Cape Town. The plants are discussed in more detail in the sections below.

3.4.1 1.8 ML/d Brackish Water Reverse Osmosis (BWRO) plant

KNPS is planning to install a Brackish Water Reverse Osmosis plant to produce 1.8 ML/day of potable water for use at the power station. The facility will extract brackish groundwater from the Atlantis aquifer. Prior to passing through the RO membranes, the abstracted water will be pre-treated to remove suspended solids and metals in the feed water through filtration. The pre-treatment will include oxidation of metals (Al, Fe and Mn), dosing of coagulants (e.g. ferric chloride) and filtration. The pre-treatment effluent arises from the periodic backwash of the primary filters. After pre-treatment, the feed water will pass through the membranes, producing a potable permeate stream and a brine effluent.

Due to the current drought, an emergency temporary plant will be constructed imminently. The discharge from this plant for both effluents will be into the KNPS outfall via the SEO-S stream (shown in orange in Figure 3-3). Once the permanent plant has been installed, the effluent streams may be re-routed to discharge at the top of the outfall similar to SEK (shown in green in Figure 3-3), which would improve the dilution of the effluent in the outfall (see Section 4.2.2).

The brine effluent is characterised in Table 3-14, while the pre-treatment effluent is characterised in Table 3-15. The concentrations of the dosed constituents are based on values obtained from reference seawater reverse osmosis plants. Therefore, the characterisation may differ based on local site-specific conditions and plant design. Should the concentrations, loads or substances differ from those included here, the vendor should be required to prove that the effluent meets the applicable water quality guidelines or is non-toxic after dilution into the other streams discharge at KNPS.



Table 3-14: Characterisation of the brine effluent from the proposed BWRO desalination plant

Parameter	Unit	Value
Produced freshwater	m ³ /h	75
Recovery rate	-	0.75 to 0.85
Feed water	m ³ /h	100 ⁽¹⁾
Discharge	m ³ /h	25 ⁽¹⁾
Temperature	°C	20
Salinity	psu	15 ⁽²⁾
Nitrite (NO ₂)	mg/l	7.33
Nitrate (NO ₃)	mg/l	9.33
Silica (SiO ₂)	mg/l	66
Sulphates	mg/l	2500
Phosphonate antiscalant	mg/l	31.3 ⁽³⁾
Chlorine	mg/l	0.002 – 0.1 ⁽⁴⁾
Sodium metabisulphate ⁽⁵⁾	mg/l	3
Peroxyacetic acid	mg/l	1.55
Low pH cleaner	mg/l	4.13
High pH cleaner	mg/l	4.13
Total residual dibromonitrolopropionamide (DBNPA) ⁽⁶⁾	mg/l	1.15 - 2.475 ⁽⁷⁾

Notes:

- (1) Maximum value (based on minimum recovery rate of 0.75)
- (2) Maximum salinity during discharge of Cleaning In Place (CIP) effluent.
- (3) Based on the maximum recovery rate of 0.85 and a dose rate of 4.7 mg/l into the feed water.
- (4) Usually low because of reactions with sodium bisulfate (neutralised). A maximum value of 0.1 mg/l was assumed in (Van Ballegooyen, et al., 2007).
- (5) For the neutralisation of chlorine. May lead to reduction of dissolved oxygen if overdosed.
- (6) Alternative to chlorine.
- (7) (Van Ballegooyen, et al., 2007)

Table 3-15: Characterisation of the pre-treatment effluent from the proposed BWRO desalination plant

Parameter	Unit	Value
Discharge ⁽¹⁾	m ³ /h	40
Temperature	°C	20
Aluminium	mg/l	32
Iron	mg/l	22
Manganese	mg/l	5.5
Total Suspended Solids (TSS)	mg/l	400
Total Organic Carbon (TOC)	mg/l	150
Coagulant: Ferric Chloride (as Fe) ⁽²⁾	mg/l	20.6
Ferric Chloride (as Fe(OH) ₃)	mg/l	39.4
Anionic Polymer ⁽³⁾	mg/l	3

Notes:

- (1) Discharge expected to occur for approximately 6 minutes every hour.
- (2) Ferric Chloride (FeCl₃) will precipitate into Ferric Hydroxide, which will contribute to the TSS of the discharge. The Ferric Hydroxide may cause a discolouration of the pre-treatment effluent.
- (3) Alternative to Ferric Chloride.



3.4.2 20 ML/d Seawater Reverse Osmosis (SWRO) plant

The City of Cape Town is planning to install a seawater desalination plant at KNPS for the provision of 20 ML/d of potable water for use by the City of Cape Town. The facility will extract seawater from the KNPS intake basin, while the brine effluent will be discharged at the top of the KNPS outfall, similar to the SEK stream shown in green in Figure 3-3.

The characteristics of the effluent from the desalination plant have been estimated from the characteristics of similar facilities by Lwandle Technologies as reported in the Marine Ecology Specialist Report (Lwandle, 2017). The primary sources reviewed include Environmental Impact Assessment reports of desalination plants at Volwaterbaai (Pulfrich & Steffani, 2014), Saldanha Bay (Van Ballegooyen, et al., 2007) and at Tongaat (CSIR, 2016). The discharge characterisation is shown in Table 3-16.



Table 3-16: Characterisation of the discharge from the proposed SWRO desalination plant

Parameter	Unit	Value
Produced freshwater	m ³ /h	833
Feed water	m ³ /h	2 083 ⁽¹⁾
Brine discharge	m ³ /h	1 250 ⁽²⁾
Salinity	psu	66 ⁽³⁾
Increase in temperature (ΔT)	°C	2
pH	-	7.3-8.2
Suspended Solids	mg/l	11.76
Coagulant: Ferric Chloride (as Fe) ⁽⁴⁾	mg/l	3.33
Coagulant: Ferric Chloride (as Fe(OH) ₃) ⁽⁴⁾	mg/l	6.37
Total Suspended Solids	mg/l	18.04 ⁽⁵⁾
Phosphonate antiscalant	mg/l	4.7 ⁽⁶⁾
Chlorine	mg/l	0.002 – 0.1 ⁽⁷⁾
Sodium metabisulphate ⁽⁸⁾	mg/l	3.14
Peroxyacetic acid	mg/l	1.55
Low pH cleaner ⁽⁹⁾	mg/l	4.13
High pH cleaner ⁽¹⁰⁾	mg/l	4.13
Total residual dibromonitrolopropionamide (DBNPA) ⁽¹¹⁾	mg/l	1.15 – 2.475 ⁽¹²⁾
Anionic polymer (alternative to Ferric Chloride)	mg/l	1.67

Notes:

- (1) Assuming 40% of feed water is converted to freshwater.
- (2) Assuming 60% of feed water is discharged as brine.
- (3) An intake salinity of 35 psu and a freshwater recovery of 40% results in a brine salinity of 58.3 psu. A brine salinity of 66 psu is thus conservative and takes into account variations in the intake salinity and variations in the concentration of the brine.
- (4) Ferric Chloride (FeCl₃) will precipitate into Ferric Hydroxide, which will contribute to the TSS of the discharge. The concentrations presented here assume that the pre-treatment effluent is blended with the brine. The Ferric Hydroxide may cause a discolouration of the pre-treatment effluent. Options to limit the metal discharges in the filter backwash effluent shall be considered. If found to be necessary, these options may include a Dissolved Air Floatation system or diversion of the primary filter backwash for clarification and sludge disposal.
- (5) Including Ferric Hydroxide precipitant.
- (6) Typically dosed into feed water at 3 mg/l which results in ~5 mg/l in effluent.
- (7) Usually low because of reactions with sodium bisulfate (neutralised). A maximum value of 0.1 mg/l was assumed in (Van Ballegooyen, et al., 2007).
- (8) May lead to reduction of dissolved oxygen if overdosed.
- (9) Generally sulphuric acid. Effect would be reduction in pH, therefore pH guidelines apply.
- (10) Alkaline cleaner. Effect would be on pH, therefore pH guidelines apply.
- (11) Alternative to chlorine.
- (12) (Van Ballegooyen, et al., 2007)

3.4.3 Effect of Brine Effluent on Plume Density

Since the brine effluent from the SWRO plant has a high salinity (up to 66 psu), the effluent has a higher density than that of ambient seawater. In pure brine effluent, this generally raises a concern since dense effluent plumes tend to sink to the bottom of the water column, where the effluent may accumulate depending on bathymetry and ambient conditions. However, in this case the brine is mixed with cooling water effluent, which is buoyant owing to its elevated temperature (ΔT = +11.7°C). To ensure that the combined cooling water and brine plume remains positively buoyant, the density of the combined effluent is calculated in Table 3-17, assuming an ambient seawater temperature of 13°C and salinity of 35 psu.



Table 3-17: Calculation of the density of the combined cooling water and brine effluent

Stream	Flow Rate [m ³ /h]	Salinity [g/l]	Temperature [°C]	Density ⁽¹⁾ [kg/m ³]	Buoyancy ⁽²⁾ [kg/m ³]
Ambient seawater	-	35	13	1026.377	0.000
Cooling water (1 Unit operating)	163 944	35	24.7	1023.120	3.257
Brine	1 250	66	13	1050.168	-23.791
Combined effluent	165 194	35.235	24.611	1023.324	3.053

Notes:

- (1) Calculated according to the equation presented in (El-Dessouky & Ettouny, 2002).
- (2) The buoyancy is calculated as the difference between the density of the ambient seawater and that of the released stream. A positive buoyancy indicates a buoyant plume while a negative buoyancy indicates a dense plume.

The table indicates that the addition of the SWRO brine to the cooling water effluent reduces the buoyancy of the effluent by a maximum of 0.204 kg/m³ (6.68%). The resulting effect on the dispersion of the plume is not considered to be significant.



4. SCREENING OF CONSTITUENTS

4.1 Methodology

From the characterisation of the effluent streams in Section 3, the complicated nature of the discharges at KNPS is clearly shown. Therefore, as a pragmatic approach to the CWDP application, a methodology has been developed to identify constituents discharged at KNPS which do not pose a significant threat to the receiving environment. The exclusion of these constituents from further assessment allows for the efforts of this study to be focussed on further investigation of the dispersion and fate of constituents which do not pass the screening tests.

The receiving environment is demarcated as the seaward end of the outfall channel (Figure 3-1 and Figure 3-3), since the flow down the outfall channel prevents ambient seawater from penetrating up the channel. Thus the different effluent streams are allowed to mix and dilute in the outfall channel prior to reaching the receiving environment.

The process for the screening of constituents is outlined in the flow chart presented in Figure 4-1, and is further discussed below.

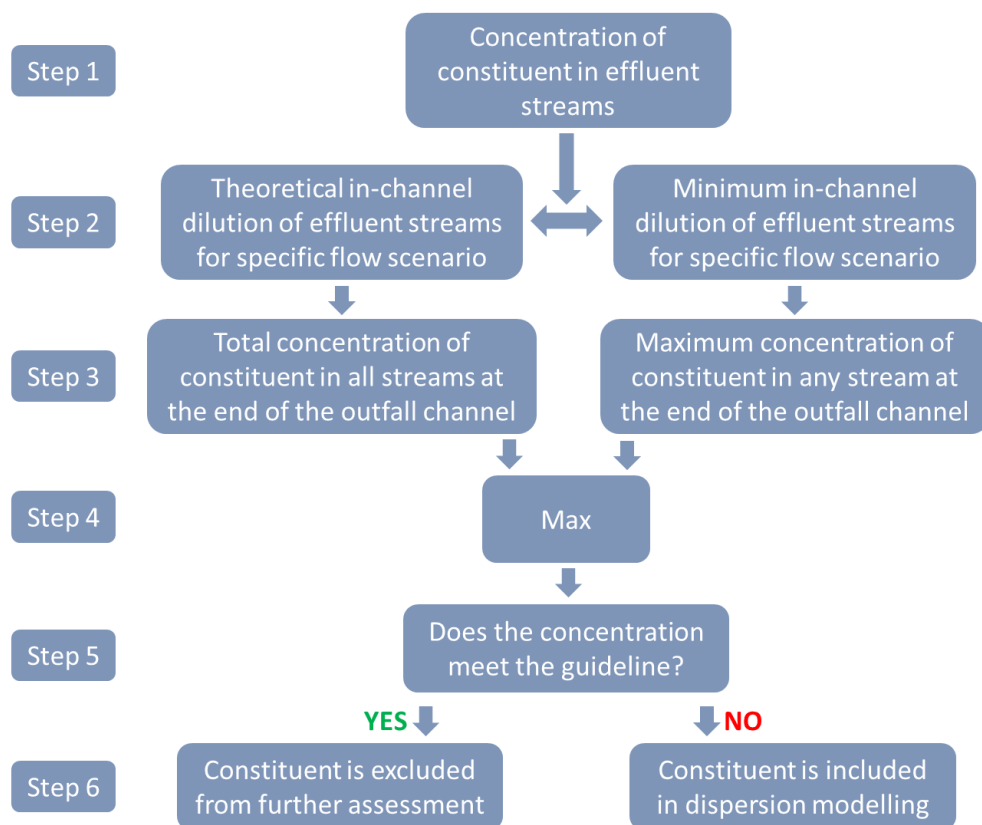


Figure 4-1: Flow chart describing the screening process used to identify constituents discharged at KNPS which do not pose a significant risk to the receiving environment, and can therefore be excluded from further assessment.

The screening process for a given constituent starts with the characterisation of its discharge in all streams. This has been presented in Section 3.

Step 2 calls for the theoretical and minimum number of dilutions in the outfall channel to be calculated. The theoretical dilution of each effluent stream is the dilution achieved by complete mixing of all streams in the



outfall. For a given flow scenario, the theoretical number of dilutions for any particular stream is calculated as the ratio of the flow rate of that stream to that of the overall discharge.

The theoretical dilution assumes that complete mixing is achieved. However, due to the structural arrangement of the various discharge points in the outfall, the mixing from a given stream into the main flow is sensitive to the specific hydrodynamics of the overall flow scenario and may not be uniform. In other words, at the end of the outfall channel, some effluent streams may not be fully mixed with the main flow. Therefore, a given stream may have achieved fewer dilutions than the theoretical number assuming complete mixing.

Detailed hydrodynamic modelling of the outfall channel is required to quantify the extent to which complete mixing is achieved. Section 4.2 presents the derivation of the theoretical and minimum number of dilutions at the end of the outfall channel from the results of a previous detailed hydrodynamic modelling study.

In step 3, the concentration at the end of the outfall is calculated in two ways. Firstly, the diluted concentration in each stream is calculated using the theoretical number of dilutions which assumes complete mixing. The total concentration at the end of the outfall channel is then calculated as the sum of the diluted contributions from all streams. This is effectively the same as the total mass discharge of the constituent divided by the total volume discharge through the outfall.

This approach is mass-conserving and is an accurate representation of the concentration averaged over the cross-section of the flow at the end of the outfall channel.

In the case of incomplete mixing, the concentration from a given stream varies over the cross-section and in some areas may be higher than the total concentration from all streams assuming complete mixing. In this case, the maximum concentration at the end of the outfall channel due to each stream is calculated separately using the minimum number of dilutions of that particular stream.

In step 4, the larger of the total concentration assuming complete mixing and the maximum concentration assuming non-uniform mixing is determined. In step 5, it is then compared to the ecological guideline for the constituent in question. If the guideline is met at the end of the outfall channel, the relevant constituent is screened out from further assessment.

The background concentrations and ecological guidelines used in the screening process are presented in Section 4.3. The calculated concentration at the end of the outfall for each constituent and the screening of constituents are presented in Section 4.4.

Some of the discharged constituents such as heavy metals have a known tendency to accumulate in sediments. The screening of these constituents is presented in Section 4.5. The risk of bioaccumulation of these constituents is generally considered to be included in the guidelines for water column concentrations and is therefore not further considered here. Nevertheless, the bioaccumulation risk is further discussed in the report of the Marine Ecology Specialist Study (Lwandle, 2017).

4.2 Theoretical and Minimum Dilutions in the Outfall Channel

4.2.1 Flow Scenarios

From the characterisation of the effluent streams in Section 3, the flow scenarios shown in Table 4-1 have been developed for use in the screening process. Scenarios 1A to 1C correspond to plant operation at full capacity, while scenarios 2A to 2C and 3A to 3C correspond to outages of Unit 1 and Unit 2, respectively. Scenario 4 corresponds to a main sea water cooling (CRF) pump trip occurring during a refuelling outage.



Table 4-1: Summary of flow scenarios

Flow Scenario	Description	Flow per effluent stream [m³/h]													
		CRF	SEK	KER	SEO-S		SEC	Proposed RO Plants			SEO-N ⁽¹⁾				
					SEU	DEL		BWRO-B ⁽²⁾	BWRO-PT ⁽³⁾	SWRO	XCA	CTE	SDX	SDA	DEL
1A	Normal operating conditions, both units, high SEK flow	327 888	300	25	28	20	12 700	25	40	1 250	60	6	400	100	20
1B	Normal operating conditions, both units, intermediate SEK flow		60												
1C	Normal operating conditions, both units, low SEK flow		20												
2A	Normal operating conditions, Unit 1 only, high SEK flow	163 944	300												
2B	Normal operating conditions, Unit 1 only, intermediate SEK flow		60												
2C	Normal operating conditions, Unit 1 only, low SEK flow		20												
3A	Normal operating conditions, Unit 2 only, high SEK flow	163 944	300												
3B	Normal operating conditions, Unit 2 only, intermediate SEK flow		60												
3C	Normal operating conditions, Unit 2 only, low SEK flow		20												
4	Unit 1 operational, one CRF pump trip ⁽⁴⁾	81 972	0	0		0			0		0	0	0	0	0

Notes:

- (1) Effluent streams released via SEO-N into intake basin and ultimately into CRF.
- (2) Brackish Water Reverse Osmosis Brine effluent.
- (3) Brackish Water Reverse Osmosis Pre-Treatment effluent.

4.2.2 Dilutions

For a given flow scenario, the theoretical number of dilutions for any particular stream is calculated as the ratio of the flow rate of that stream to that of the overall discharge. The results are shown in Table 4-2 .

The effluent streams discharged into the intake basin ultimately form part of the CRF stream (discussed in Section 5.5). Therefore, these streams were assumed to be mixed directly into the CRF stream. This is a conservative assumption, since in reality the streams will mix with ambient seawater in the intake basin before being passed through CRF. The theoretical number of dilutions at the end of the outfall channel was calculated as the ratio of the flow rate of that stream to that of the CRF, multiplied by the theoretical dilution of the CRF stream.



Table 4-2: Theoretical dilutions achieved at the end of the outfall channel for each effluent stream and flow scenario. The theoretical dilutions are calculated assuming complete mixing in the outfall channel.

Flow Scenario	Theoretical achieved dilution at end of outfall channel assuming complete mixing ⁽¹⁾													
	CRF	SEK	KER	SEO-S		SEC	Proposed RO Plants			SEO-N ⁽²⁾				
				SEU	DEL		BWRO-B	BWRO-PT	SWRO	XCA	CTE	SDX	SDA	DEL
1A	1.04	1141	13677	12210	17096	27	13676	8548	274	5698	56982	855	3419	17095
1B	1.04	4275	13677	12210	17096	27	13676	8548	274	5698	56982	855	3419	17095
1C	1.04	17096	13677	12210	17096	27	13676	8548	274	5698	56982	855	3419	17095
2A	1.09	594	7119	6355	8898	14	7118	4450	142	2966	29658	445	1779	8897
2B	1.09	2225	7119	6355	8898	14	7118	4450	142	2966	29658	445	1779	8897
2C	1.09	8898	7119	6355	8898	14	7118	4450	142	2966	29658	445	1779	8897
3A	1.09	594	7119	6355	8898	14	7118	4450	142	2966	29658	445	1779	8897
3B	1.09	2225	7119	6355	8898	14	7118	4450	142	2966	29658	445	1779	8897
3C	1.09	8898	7119	6355	8898	14	7118	4450	142	2966	29658	445	1779	8897
4	1.17	-	-	3428	-	8	3839	-	77	-	-	-	-	-

Notes:

- (1) The theoretical number of dilutions for any particular stream is calculated as the ratio of the flow rate of that stream to that of the overall discharge. The overall discharge is calculated as the sum of the continuous streams.
- (2) Theoretical dilution calculated as: (theoretical dilution into CRF) x (theoretical dilution of CRF in outfall).

As described in Section 4.1, the mixing from a given stream into the main flow is sensitive to the specific hydrodynamics of the overall flow scenario and may not be uniform. The extent to which each stream achieves complete mixing in the outfall channel has been investigated in a previous hydrodynamic modelling study of the KNPS outfall (PRDW, 2013). In the study, the outfall channel was modelled in high resolution (0.5 m) to accurately reflect the real positions of effluent streams in the outfall. This allowed the model to investigate the mixing between the streams and to account for subtleties in the structural arrangement of the effluent release points. The number of dilutions of each stream at the end of the outfall channel was determined for a number of flow scenarios. These results were used to calculate a non-uniform dilution factor, which describes the extent to which complete mixing is achieved. A value of 1.0 indicates complete mixing and 0.0 indicates no mixing. The non-uniform dilution factors are presented in Table 4-3 for each stream and flow scenario considered in this study.

Since the effluent streams released into the intake basin ultimately form part of the CRF stream, their non-uniform dilution factors were taken to be that of the CRF.



Table 4-3: Non-uniform dilution factor at the end of the outfall channel for each effluent stream and flow scenario. The non-uniform dilution factor describes the extent to which complete mixing is achieved, where a value of 1.0 indicates complete mixing and 0.0 indicates no mixing.

Flow Scenario	Non-uniform dilution factor at the end of the outfall channel													
	CRF	SEK	KER	SEO-S		SEC	Proposed RO Plants			SEO-N ⁽¹⁾				
				SEU	DEL		BWRO-B ⁽²⁾	BWRO-PT ⁽²⁾	SWRO ⁽³⁾	XCA	CTE	SDX	SDA	DEL
1A	0.96	0.87	0.83	0.36	0.36	0.43	0.36	0.36	0.87	0.96	0.96	0.96	0.96	0.96
1B	0.96	0.87	0.83	0.36	0.36	0.43	0.36	0.36	0.87	0.96	0.96	0.96	0.96	0.96
1C	0.96	0.87	0.83	0.36	0.36	0.43	0.36	0.36	0.87	0.96	0.96	0.96	0.96	0.96
2A	0.92	0.85	0.75	0.34	0.34	0.53	0.34	0.34	0.85	0.92	0.92	0.92	0.92	0.92
2B	0.92	0.85	0.75	0.34	0.34	0.53	0.34	0.34	0.85	0.92	0.92	0.92	0.92	0.92
2C	0.92	0.85	0.75	0.34	0.34	0.53	0.34	0.34	0.85	0.92	0.92	0.92	0.92	0.92
3A	0.92	0.88	0.69	0.41	0.41	0.29	0.41	0.41	0.88	0.92	0.92	0.92	0.92	0.92
3B	0.92	0.88	0.69	0.41	0.41	0.29	0.41	0.41	0.88	0.92	0.92	0.92	0.92	0.92
3C	0.92	0.88	0.69	0.41	0.41	0.29	0.41	0.41	0.88	0.92	0.92	0.92	0.92	0.92
4	0.92	0.85	0.69	0.34	0.34	0.29	0.34	0.34	0.85	0.92	0.92	0.92	0.92	0.92

Notes:

- (1) Effluents released via SEO-N into intake basin and ultimately into CRF. Therefore, these streams have the same non-uniform dilution factor as CRF.
- (2) Effluent of temporary plant to be released via SEO-S.
- (3) Effluents to be released at the top of the outfall basin - similar to SEK release.

The minimum number of dilutions in the outfall channel was calculated as the product of the theoretical number of dilutions and the non-uniform dilution factor. The minimum number of dilutions at the end of the outfall channel occurs at the point in the cross-section of the flow where the lowest mixing with the total flow occurs. This is therefore also the point where the highest concentration of constituents discharged in that stream will occur. The minimum dilutions are presented in Table 4-4.

Table 4-4: Minimum dilutions achieved at the end of the outfall channel for each effluent stream and flow scenario. The minimum dilutions assume non-uniform mixing in the outfall channel, and are calculated as the product of the theoretical dilutions (Table 4-2) and the non-uniform dilution factor (Table 4-3).

Flow Scenario	Minimum achieved dilution at end of outfall channel assuming non-uniform mixing													
	CRF	SEK	KER	SEO-S		SEC	Proposed RO Plants			SEO-N ⁽¹⁾				
				SEU	DEL		BWRO-B	BWRO-PT	SWRO	XCA	CTE	SDX	SDA	DEL
1A	1.00	989	11360	4417	6184	12	4947	3092	237	5465	54648	820	3279	16394
1B	1.00	3707	11360	4417	6184	12	4947	3092	237	5465	54648	820	3279	16394
1C	1.00	14826	11360	4417	6184	12	4947	3092	237	5465	54648	820	3279	16394
2A	1.00	504	5309	2159	3023	7	2418	1512	121	2738	27381	411	1643	8214
2B	1.00	1888	5309	2159	3023	7	2418	1512	121	2738	27381	411	1643	8214
2C	1.00	7549	5309	2159	3023	7	2418	1512	121	2738	27381	411	1643	8214
3A	1.00	521	4916	2604	3645	4	2916	1823	125	2732	27324	410	1639	8197
3B	1.00	1950	4916	2604	3645	4	2916	1823	125	2732	27324	410	1639	8197
3C	1.00	7797	4916	2604	3645	4	2916	1823	125	2732	27324	410	1639	8197
4	1.08	-	-	1164	-	2	1304	-	65	-	-	-	-	-

Notes:

- (1) Achieved dilution calculated as: (theoretical dilution into CRF) x (non-uniform dilution of CRF in outfall).



4.3 Background and Guideline Concentrations

The background and guideline concentrations shown in Table 4-5 have been developed by Lwandle Technologies for the constituents in the discharge characterisation. The sources of and commentary on the values used are included in the report of the Marine Ecology Specialist Study (Lwandle, 2017).



Table 4-5: Ecological guideline and background concentrations for constituents discharged at KNPS

Constituent	Unit	Guideline Concentration	Background Concentration
Temperature Increase (ΔT)	°C	1	0
Free Chlorine (General guideline)	mg/l	0.003	0
Free Chlorine (Site-specific guideline)	mg/l	0.01	
Bromoform	mg/l	0.01	0.00008
Total Suspended Sediment (TSS)	mg/l	7 ⁽¹⁾	4 ⁽²⁾
Hydrazine (General guideline)	mg/l	0.0002	0
Hydrazine (Site-specific guideline)	mg/l	0.0025	
Sulphate	mg/l	Non-toxic	2700
Sodium	mg/l	Non-toxic	10763
Aluminium Sulphate	mg/l	Precipitates	-
Ammonia	mg/l	0.6	0.015
Chloride	mg/l	-	19400
Boron	mg/l	7.00	4.50
Lithium Hydroxide	mg/l	-	0.17
Phosphate	mg/l	0.053	0.037
Detergents - Linear Alkylbenzene Sulfonate (LAS)	mg/l	0.033	0
Detergents – Alcohol Ethoxysulfates (AES)	mg/l	0.65	0
Detergents – Alcohol Ethoxylates (AE)	mg/l	0.14	0
Aluminium	mg/l	0.024	0.001
Copper	mg/l	0.0013	0.0008
Chromium	mg/l	0.0144	0.00008
Iron	mg/l	0.01	0.003
Manganese	mg/l	0.007	0.0007
Nickel	mg/l	0.025	0.00056
Lead	mg/l	0.012	0.00015
Zinc	mg/l	0.025	0.0012
Ethylenediaminetetraacetic acid (EDTA)	mg/l	500	0
Citric Acid	mg/l	1	0.1
Ethanolamine	mg/l	0.09	0
Nitrates	mg/l	1.28	0.67
Nitrites	mg/l	0.013	0.017
Faecal Coliforms	counts/100ml	20	0
Biochemical Oxygen Demand (BOD)	mg/l	5	-
Chemical Oxygen Demand (COD)	mg/l	25	-
Oil/Grease	mg/l	15	0
Salinity	psu	36	35
Silica	mg/l	-	0.63
Phosphonate Antiscalant	mg/l	2	0
Sodium metabisulphate	mg/l	0.032	0
Peroxyacetic acid	mg/l	0.05	0
Low pH cleaner	mg/l	-	0
High pH cleaner	mg/l	-	0
DBNPA	mg/l	0.035	0
TOC	mg/l	-	1.08
Anionic Polymer	mg/l	-	0
Ferric Chloride (as Fe)	mg/l	-	-

Notes:

- (1) 80th percentile TSS concentration from measurements taken offshore of KNPS (PRDW, 2012).
- (2) 50th percentile TSS concentration from measurements taken offshore of KNPS (PRDW, 2012).



4.4 Screening of Water Column Constituents

From the discharge characterisation presented in Section 3 and the theoretical and minimum achieved dilutions presented in Section 4.2, the concentration at the end of the outfall channel for each constituent and flow scenario has been calculated. As discussed in Section 4.1, both the total concentration assuming complete mixing and the maximum concentration assuming non-uniform mixing have been calculated. The maximum concentration between these is shown in Table 4-6, together with the flow scenario(s) in which it occurred.

Table 4-6 also presents the comparison between the concentration at the end of the outfall and the ecological guideline. The constituents which meet the relevant ecological guideline at the end of the outfall channel or which have no known marine toxicity are highlighted in green.

In the case that the guideline is exceeded at the end of the outfall, the number of required dilutions in the sea is calculated as:

$$\text{Number of required dilutions} = \frac{(\text{Effluent concentration} - \text{Background concentration})}{(\text{Guideline concentration} - \text{Background concentration})}$$

For the constituents which have normal and exceptional release scenarios (temperature, free chlorine and hydrazine), the maximum concentration due to both the normal and exceptional scenarios are shown. This serves to indicate that the large number of dilutions required for these constituents only occurs during exceptional release scenarios, and that the number of dilutions required during normal operation is significantly lower.

The following constituents could not be screened out due to a lack of available release concentrations, background concentrations or ecological guideline concentrations:

- Bromoform
- Lithium Hydroxide
- Nitrites
- BOD
- COD
- Silica
- Phosphonate antiscalant
- Sodium metabisulfate
- Peroxyacetic acid
- Low pH cleaner
- High pH cleaner
- TOC
- Anionic Polymer
- Ferric Chloride

Although these constituents could not be screened out due to a lack of information, an assessment presented in Section 3 of the Marine Ecology Specialist Study (Lwandle, 2017) has indicated that these constituents do not pose a significant threat to the environment.



The constituents which do not meet the ecological guidelines have been highlighted in orange. These constituents (listed below) were not screened out and will be included in the dispersion modelling presented in Section 5.

- Temperature increase
- Free Chlorine
- Hydrazine
- Phosphate



Table 4-6: Screening of constituents

Constituent	Unit	Maximum concentration at end of outfall	Flow scenario	Background concentration	Guideline concentration	Required dilutions ⁽¹⁾
Temperature Increase (ΔT)	°C	11.77	3A	0	1	12
Temperature Increase (ΔT): Pump Trip	°C	21.18	4	0	1	21
Free Chlorine	mg/l	0.60	3A-C	0	0.003 ⁽²⁾	199
					0.01 ⁽³⁾	60
Free Chlorine: Shock Chlorination	mg/l	6.597	3A, 3B	0	0.003 ⁽²⁾	2199
					0.01 ⁽³⁾	660
Bromoform	mg/l	unknown ⁽⁴⁾		0.00008	0.01	-
Total Suspended Sediment (TSS)	mg/l	4.704	2A	4	7	0
Hydrazine	mg/l	0.110	3A-C	0	0.0002 ⁽²⁾	549
					0.0025 ⁽³⁾	44
Hydrazine: Exceptional releases during outages	mg/l	0.200	2B	0	0.0002 ⁽²⁾	1002
					0.0025 ⁽³⁾	80
Sulphate	mg/l	2 744	2A, 3A	2 700	-	Non-toxic
Sodium	mg/l	10 829	2A, 3A	10 763	-	Non-toxic
Aluminium Sulphate	mg/l	0.09	3A-C	-	-	Precipitates
Ammonia	mg/l	0.23	2A	0.015	0.6	0
Chloride	mg/l	19489.12	2A-C,3A-C	19400	-	Non-toxic ⁽⁵⁾
Boron	mg/l	5.02	3A,3B	4.5	7	0
Lithium Hydroxide	mg/l	0.1714	3A-C	0.17	-	-
Phosphate	mg/l	0.87	2B	0.037	0.053	52
Detergents - Linear Alkylbenzene Sulfonate (LAS)	mg/l	0.030	2A	0	0.033	0
Detergents – Alcohol Ethoxysulfates (AES)	mg/l	0.610	2A	0	0.65	0
Detergents – Alcohol Ethoxylates (AE)	mg/l	0.133	2A	0	0.14	0
Aluminium	mg/l	0.0053	2A	0.001	0.024	0
Copper	mg/l	0.0009	3A	0.0008	0.0013	0
Chromium	mg/l	0.0043	2A	0.00008	0.0144	0
Iron	mg/l	0.0038	3A	0.003	0.01	0
Manganese	mg/l	0.0011	2A	0.0007	0.007	0
Nickel	mg/l	0.0048	2A	0.00056	0.025	0
Lead	mg/l	0.0033	2A	0.00015	0.012	0
Zinc	mg/l	0.0033	2A	0.0012	0.025	0
Ethylenediaminetetraacetic acid (EDTA)	mg/l	0.31	3A-C	0	500	0
Citric Acid	mg/l	0.71	3A-C	0.1	1	0
Ethanolamine	mg/l	0.0119	2A	0	0.09	0
Nitrates	mg/l	0.705	2A	0.67	1.28	0
Nitrites	mg/l	0.0256	2A	0.017	0.013	-
Faecal Coliforms	counts/100ml	0.46	2A-C	0	20	0
Biochemical Oxygen Demand (BOD)	mg/l	1.29	2A	-	5	-
Chemical Oxygen Demand (COD)	mg/l	3.62	2A	-	25	-
Oil/Grease	mg/l	0.33	2A	0	15	0
Salinity	psu	35.22	2A-C,3A-C	35	36	0
Silica	mg/l	0.66	2A-C	0.63	-	-
Phosphonate Antiscalant	mg/l	0.05	2A-C	0	2	0
Sodium metabisulphate	mg/l	0.03	2A-C	0	0.032	-
Peroxyacetic acid	mg/l	0.01	2A-C	0	0.05	-
Low pH cleaner	mg/l	0.03	2A-C	0	-	-
High pH cleaner	mg/l	0.03	2A-C	0	-	-
DBNPA	mg/l	0.02	2A-C	0	0.035	0
TOC	mg/l	1.18	2A-C	1.08	-	-
Anionic Polymer	mg/l	0.02	2A-C	0	-	-
Ferric Chloride (as Fe)	mg/l	0.04	2A-C	-	-	-

(1) Rounded to the nearest integer.

(2) General guideline.

(3) Site-specific guideline.

(4) Bromoform is expected to be formed as a by-product of the chlorination of seawater. The concentration of bromoform formed at KNPS is currently unknown.

(5) Screened out based on contribution to salinity.



4.5 Screening of Constituents Prone to Accumulation in Sediments

The discharge characterisation presented in Section 3 includes heavy metals in some of the discharge streams. These constituents have a known tendency to attach to fine sediment particles through adsorption. In calm areas (e.g. ports) where bed shear stresses are sufficiently low, fine sediment particles can settle and accumulate in seabed sediment. Therefore, heavy metals cannot be screened out based solely on meeting the ecological thresholds for water column concentrations, but consideration should also be given to their toxicity in seabed sediment.

Since the ultimate deposition centres of the discharged heavy metals are unknown, a highly conservative assumption has been made for the purposes of this screening assessment. It has been assumed that the entire load of heavy metals discharged from the KNPS outfall channel attaches to fine sediment and then settles in the top 10 cm of the seabed in the KNPS intake basin. This is the location nearest to the discharge point where bed shear stresses are sufficiently low to allow for long-term deposition of fine particles, although in reality only a fraction of the metals will deposit here. Table 4-7 presents the calculation of the dry mass of the sediment in the assumed deposition centre.

Table 4-7: Calculation of the sediment mass in the top 10 cm of the seabed in the KNPS intake basin

Parameter	Unit	Value
Deposition area (inner sheltered part of KNPS intake basin)	m ²	130 000
Sediment layer thickness	m	0.10
Sediment volume	m ³	13 000
Sediment density	kg/m ³	2 650
Sediment porosity	-	0.50
Dry sediment mass	kg	17 225 000

The heavy metal concentrations in the effluent streams presented in Section 3 were given as conservative estimates of maximum water column concentrations. However, when considering the long-term accumulation of heavy metals it is more appropriate to use average annual loads. The annual loads of heavy metals released at KNPS were provided by Eskom and are shown in Table 4-8. The table also presents the ecological guidelines for heavy metal concentrations in seabed sediment, provided by Lwandle Technologies.

Assuming that the entire annual heavy metal load from KNPS settles in the intake basin, the total number of years required before the ecological guideline is reached can be calculated for each heavy metal as follows:

$$\text{Time until guideline is reached [years]} = \frac{\text{Guideline [mg/kg]} \times \text{Mass of dry sediment in intake basin [kg]}}{\text{Annual Load [mg/year]}}$$



Table 4-8: Calculation of the number of years required before the ecological guideline for heavy metal concentration in seabed sediment is reached.

Constituent	Annual Load [kg/year]	Guideline Sediment Concentration [mg/kg]	Comments	Time until guideline is reached [years]
Aluminium (Al) released from KNPS	208	-	No guideline. Naturally occurs in high concentrations in sediments and is associated with clay sized particles	-
Additional Al from proposed BWRO plant	1 556 ⁽¹⁾			
Total Al	1 764			
Chromium (Cr)	2	52.3	Recommended guideline value (BCLME, 2006)	450
Copper (Cu)	2	18.7	Recommended guideline value (BCLME, 2006)	163
Iron (Fe) released from KNPS	22	-	No guideline available. Naturally occurs in high concentrations in sediments	-
Additional Fe from proposed BWRO plant	1 689 ⁽²⁾			
Additional Fe from proposed SWRO plant	36 488 ⁽³⁾			
Total Fe	38 200 ⁽⁴⁾			
Manganese (Mn) released from KNPS	2	-	No guideline available. Naturally occurs in high concentrations in sediments	-
Additional Mn from proposed BWRO plant	193 ⁽⁵⁾			
Total Mn	195			
Nickel (Ni)	2	15.9	Recommended guideline value (BCLME, 2006)	141
Lead (Pb)	4	30.2	Recommended guideline value (BCLME, 2006)	136
Zinc (Zn)	14	124	Recommended guideline value (BCLME, 2006)	154

Notes:

- (1) The aluminium load from the proposed BWRO plant arises from Al in the feed water, see Table 3-15.
- (2) The iron load from the proposed BWRO plant arises from Fe in the feed water (965 kg/y) and from the dosed ferric chloride coagulant (724 kg/y), see Table 3-15.
- (3) The iron load from the proposed SWRO plant arises from the dosed ferric chloride coagulant, see Table 3-16.
- (4) Although iron naturally occurs in high concentrations in sediment, the ecological relevance of this load is discussed in the Marine Ecology Specialist Study (Lwandle, 2017).
- (5) The manganese load from the proposed BWRO plant arises from Mn in the feed water, see Table 3-15.

The calculations shown in Table 4-8 indicate durations longer than 100 years which is significantly longer than the total lifetime of KNPS, which is approximately 60 years (1984 – 2044). This also ignores the ongoing dredging in the intake basin which will further reduce the build-up of heavy metals in these sediments. On this basis, heavy metal concentrations in seabed sediment have been excluded from further assessment.

Subsequent measurements of the heavy metals in the sediments of the intake basin indicated higher concentrations than predicted by the screening assessment presented here. These results and their implications are discussed in the Marine Ecology Specialist Report (Lwandle, 2017).



5. CHEMICAL DISPERSION MODELLING

5.1 Model Description

The simulation of waves and currents was carried out through a coupling of spectral wave and hydrodynamic models. The dispersion and fate of discharged constituents was modelled using the ECOLab model. These models are described individually below.

5.1.1 Hydrodynamic Modelling

The three-dimensional *MIKE 3 Flow Flexible Mesh Model* was used for the far-field modelling. The application of the model is described in the User Manual (DHI, 2014b), while full details of the physical processes being simulated and the numerical solution techniques are described in the Scientific Documentation (DHI, 2014c).

The model is based on the numerical solution of the three-dimensional incompressible Reynolds averaged Navier-Stokes equations invoking the assumptions of Boussinesq and of hydrostatic pressure. The model consists of the continuity, momentum, temperature, salinity and density equations and is closed by a $k-\epsilon$ vertical turbulence closure scheme. Horizontal eddy viscosity is modelled with the Smagorinsky formulation.

The time integration of the shallow water equations and the transport equations is performed using a semi-implicit scheme, where the horizontal terms are treated explicitly and the vertical terms are treated implicitly. In the vertical direction a structured mesh, based on a sigma-coordinate transformation is used, while the geometrical flexibility of the unstructured flexible mesh comprising triangles or quadrangles is utilised in the horizontal plane.

MIKE 3 Flow Flexible Mesh Model includes the following physical phenomena:

- Currents due to tides;
- Currents due to wind stress on the water surface;
- Currents due to density gradients;
- Currents due to waves; the second order stresses due to breaking of short period waves are included using the radiation stresses computed in the Spectral Wave model;
- Coriolis forcing;
- Bottom friction;
- Flooding and drying;
- Sources and sinks; and
- Heat exchange.

5.1.2 Spectral Wave Modelling

The MIKE 21 Spectral Waves (SW) Flexible Mesh model was used for simulating wave transformation to the nearshore. The application of the model is described in the User Manual (DHI, 2014d), while full details of the physical processes being simulated and the numerical solution techniques are described in the Scientific Documentation (DHI, 2014e). The model simulates the growth, decay and transformation of wind-generated waves and swells in offshore and coastal areas using unstructured meshes.



In this study, the model included the following physical phenomena:

- Dissipation due to bottom friction;
- Dissipation due to depth-induced wave breaking;
- Refraction and shoaling due to depth variations; and
- The effect of time-varying water depth; the water depth at each time-step is computed in the hydrodynamic model.

For this study the model was run in the directionally decoupled parametric, quasi-stationary formulation excluding the effect of additional wave generation within the model due to wind.

5.1.3 ECOLab Modelling

The MIKE ECO Lab Model was used to simulate the dispersion of discharged constituents. The application of the model is described in the User Manual (DHI, 2014f), while full details of the physical processes being simulated and the numerical solution techniques are described in the Scientific Documentation (DHI, 2014g).

The model simulates the transport and fate of constituents in three dimensions based on advection-dispersion and non-conservative processes. The model can be used to describe chemical, biological, ecological processes and interactions between state variables and also the physical process of sedimentation of components can be described. The hydrodynamics are obtained via an online coupling to the MIKE 3 Flow Flexible Mesh Model and the same three-dimensional grid is used.

An ECOLab template is used to describe the processes relevant for each specific constituent. In this study templates were developed for chlorine (Section 5.1.3.1), hydrazine (Section 5.1.3.2) and radionuclides (Section 6.2.2).

5.1.3.1 ECOLab template for chlorine

The possible chemical reactions of chlorine in water are varied and complex, depending on chlorine dose and water characteristics (Abarnou & Miossec, 1992). In solution, chlorine produces a combination of hypochlorous acid and the hypochlorite ion. However, due to the high concentration of bromine in natural seawater, chlorine is rapidly replaced by bromine and the subsequent chemistry is predominantly bromine-based (BEEMS, 2011). Therefore, rather than modelling the concentration of free chlorine, it is more appropriate for the oxidising ability of free chlorine to be expressed as Total Residual Oxidants (TRO) due to chlorination.

To be effective, biocides are highly reactive against a wide range of organic matter. The oxidants formed by chlorination are therefore short-lived toxic compounds which do not persist in natural waters (BEEMS, 2011). Studies of the kinetics of oxidant decay indicate that it occurs in two phases; a rapid phase, followed by continuous loss at a reduced rate (Abarnou & Miossec, 1992), (Jiangning, et al., 2009), (UNEP, 1984), (Sohn, et al., 2004)). However, due to the complex nature of TRO reactions in seawater, most modelling studies assume a 1st order decay (BEEMS, 2010a).

Reports of laboratory testing and mathematical modelling of the decay of TRO in seawater conducted for the new build nuclear power station at Hinkley Point C were available by kind permission of EDF Energy (BEEMS, 2010a), (BEEMS, 2010b). The studies supported the findings of the two-stage decay of TRO. For inclusion in a dispersion modelling study for the Hinkley Point C nuclear power station, a mathematical formulation was developed to describe the demand and decay of TRO in seawater (BEEMS, 2010a). The rate equations below present the initial rapid decrease in TRO concentrations $[C, \text{mg/l}]$ as a demand by (an) unspecified reactant(s), $S [\text{mg/l}]$. Simultaneously, the slower decay of chlorine is described by a 1st order decay.



$$\frac{dC}{dt} = -k_2 C^2 S - k_1 C$$

$$\frac{dS}{dt} = -k_2 C^2 S$$

$$C(t = 0) = C_0, \quad S(t = 0) = S_0$$

In the study, the rate constants (k_1 [second⁻¹] and k_2 [second⁻¹(mg/l)⁻²]) and the concentration of the reactive compound (S , [mg/l]) were determined from laboratory experiments using Hinkley Point seawater. Both turbid (TSS = 100 to 850 mg/l) and clear (settled) samples were used. The calibrated rate constants for the two sets of water samples are presented in Table 5-1.

Table 5-1: Rate constants for chlorine demand and decay determined from laboratory testing of Hinkley Point seawater (BEEMS, 2010a)

Parameter	Units	Clear Water	Turbid Water
k_1	second ⁻¹	4.2×10^{-5}	0.0
k_2	second ⁻¹ .(mg/l) ⁻²	1.3×10^{-2}	1.3×10^{-2}

The median suspended sediment concentration at KNPS is 4 mg/l. Therefore, in the absence of laboratory studies using local seawater from KNPS, the rate constants (k_1 and k_2) corresponding to clear water from Hinkley Point were applied in this study. The concentration of the unspecified reactive compound in the ambient seawater (S_0) is a site-specific parameter. From the chlorination practiced at KNPS, it is known that the free chlorine concentration at discharge is approximately 1 mg/l lower than the dose received. This suggests that the demand for chlorine in the cooling water and hence in the ambient seawater is 1 mg/l. This value has been used in this study.

5.1.3.2 ECOLab template for hydrazine

The fate of hydrazine in natural waters depends on the relative rates of chemical and biological degradation. The main mechanisms of hydrazine degradation are biodegradation (depending on bacterial abundance) and autoxidation (depending on a number of water characteristics including oxygen content, organic matter content, pH and water temperature) (Environmental Health Canada, 2011).

Reports of laboratory testing and mathematical modelling of the decay of hydrazine in seawater conducted for the new build nuclear power station at Hinkley Point C were available by kind permission of EDF Energy (BEEMS, 2010c). Varying doses of hydrazine were added to seawater samples and concentrations were measured over time. For a given initial hydrazine concentration (C_0), the data fitted well to 1st order decay. However, the decay rate showed strong dependence on C_0 , with lower C_0 resulting in a faster decay. Therefore, as pragmatic approach, it was proposed to use linear decay with rate constants specific to the initial dose. The initial concentrations and corresponding rate constants are shown in Table 5-2. The first order decay formulation is shown below:

$$\frac{dC}{dt} = -kC$$



Table 5-2: Rate constants for hydrazine decay determined from laboratory testing (BEEMS, 2010c)

Initial hydrazine concentration [mg/l]	Decay rate constant (k) [h ⁻¹]	Half-life [hours]
0.05	0.082	8.5
0.15	0.0335	20.7
0.3	0.0116	59.8

In the absence of specific laboratory studies on hydrazine decay using local seawater from KNPS, the decay rates determined from the BEEMS study were applied here. For the two scenarios modelled in this study, the highest concentrations assuming complete mixing are 0.053 mg/l (plant operation at full capacity) and 0.187 mg/l (exceptional releases during reactor outages). Since the rate constants are dependent on initial hydrazine concentration, the rate constants for these scenarios were interpolated from the laboratory results presented in Table 5-2. The interpolated rate constants and corresponding half-lives are presented in Table 5-3. The 1st order decay of hydrazine was modelled using the ECOLab model, described in Section 5.1.3.

Table 5-3: Rate constants for hydrazine decay interpolated from the results of laboratory testing (Table 5-2).

Scenario	Initial hydrazine concentration [mg/l]	Decay rate constant (k) [h ⁻¹]	Half-life [hours]
Plant operating at full capacity	0.053	0.08	8.6
Exceptional hydrazine releases during outages	0.187	0.028	24.6

The processes described above do not account for the possible oxidation of hydrazine by the TRO in the outfall, which would further reduce the concentration of hydrazine, i.e. the model results are conservative. It is recommended that research be undertaken to quantify the interaction between hydrazine and TRO.

5.2 Model Setup

5.2.1 Mesh and Bathymetry

The WG19 horizontal coordinate system was used for this study. All spatial plots include x and y axes showing the x and y coordinates in metres in the WG19 system. True north is always pointing upwards.

Seabed levels and water levels are relative the Chart Datum (CD). CD is 0.825 m below Land Levelling Datum (LLD) which is also known as Mean Sea Level (MSL).

The model bathymetry and mesh are shown in Figure 5-1 and Figure 5-2. The data used to construct the model bathymetry have been described in Section 2.1. The mesh extends approximately 45 km offshore of the KNPS. Along the offshore boundary, the depth varies between -140 m CD in the north and -250 m CD in the south, but was truncated at -150 m CD for model stability. The horizontal mesh resolution varies between approximately 2 km at the offshore boundary to approximately 50 m at the KNPS outfall and intake basin. The vertical mesh is comprised of eight sigma layers with equal layer thicknesses.

The vertical eddy viscosity was computed using the k- ϵ vertical turbulence closure scheme, while the vertical eddy dispersion was set to 0.1 times the vertical eddy viscosity. This scaling factor was applied to compensate for additional vertical mixing caused by the use of only eight vertical layers and the associated smoothing of the vertical density gradients. A bottom roughness height of 0.05 m was used.

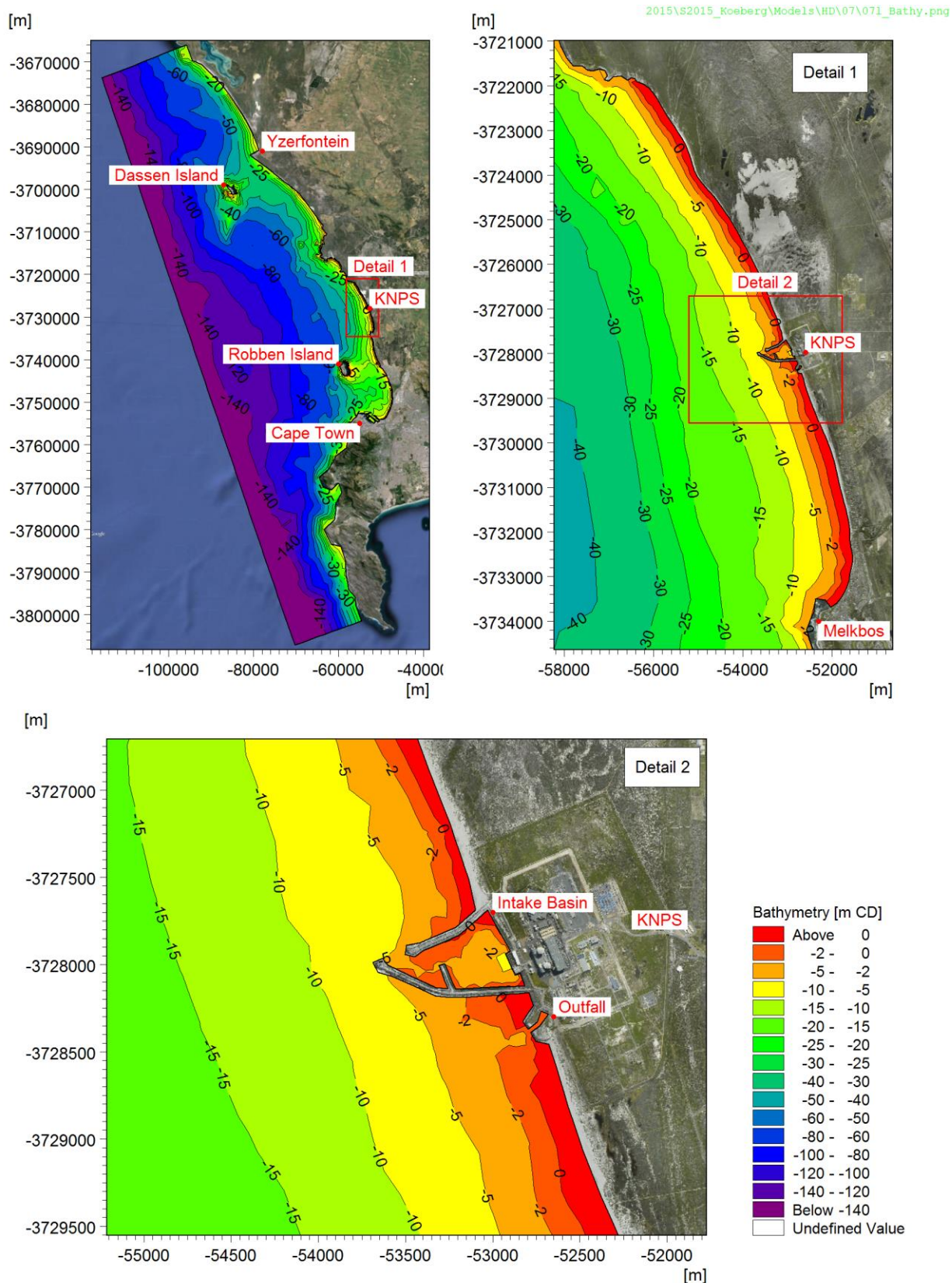


Figure 5-1: Model bathymetry

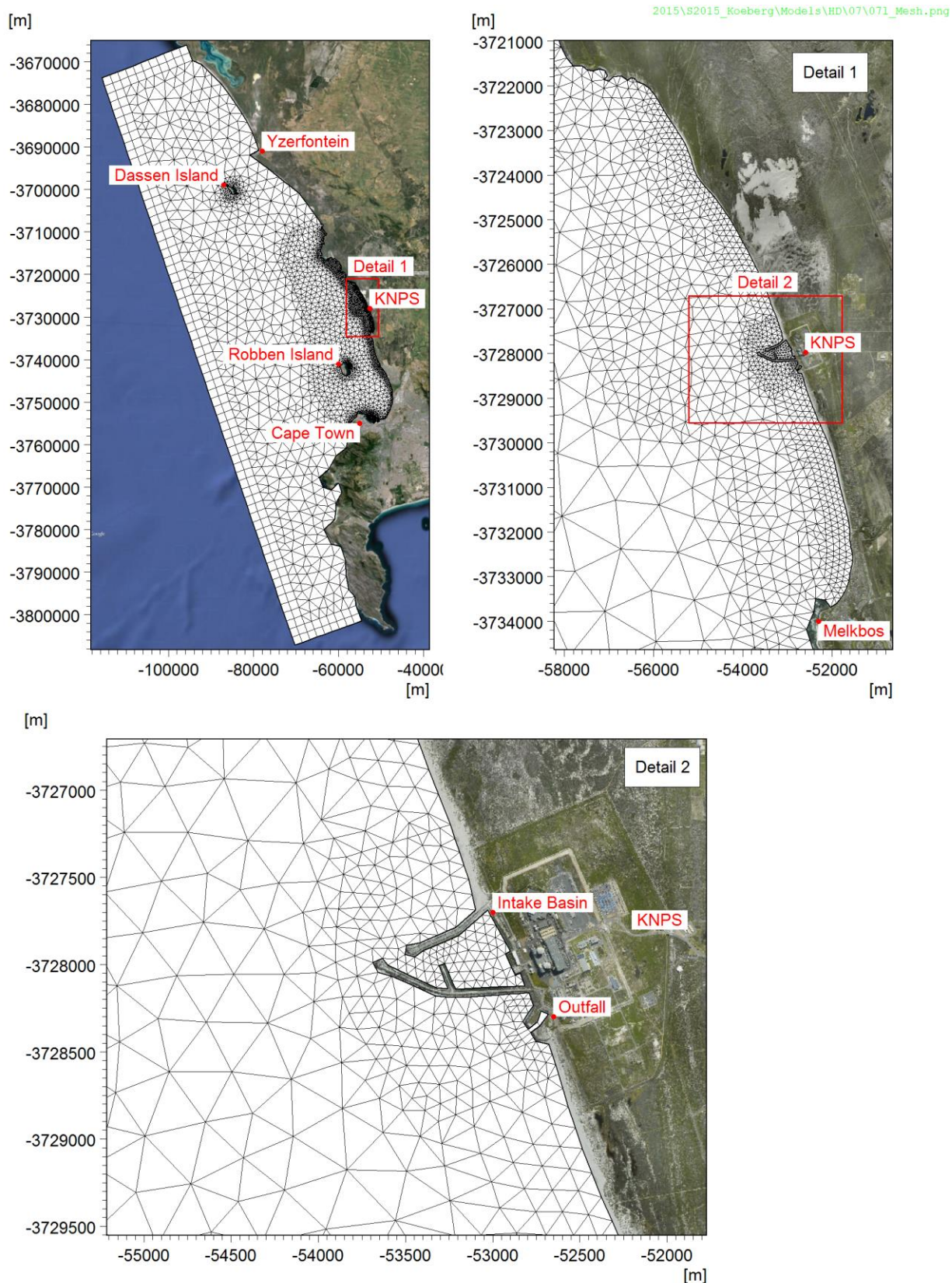


Figure 5-2: Model mesh



5.2.2 Water Levels

Predicted tidal water levels for the Port of Cape Town were applied as time-varying water levels along the model boundaries. Corrections for wind setup and Coriolis force were applied to the water levels prescribed along the lateral boundaries.

5.2.3 Wind

The dataset of wind measurements at KNPS was used for the generation of wind-driven currents and atmospheric heat exchange in the model. To account for the fact that winds are typically stronger offshore than on land, measured wind speeds were increased by a scale factor of 1.65, based on a comparison between the wind speed at the KNP and offshore wind speeds from the European Centre for Medium-Range Weather Forecasts (ECMWF) hindcast model.

5.2.4 Waves

Offshore hindcast wave data were available from the NOAA/NCEP WAVEWATCH III CFSR Reanalysis Reforecast Hindcast Dataset (NCEP, 2012). The dataset contains 31 years (1979 to 2009) of uninterrupted parametric wave data (H_{m0} , T_p , mean wave direction at T_p) recorded at 3-hourly intervals on a 0.5° longitude/latitude global grid.

For this study, wave parameters were extracted at grid point 18°E , 34°S in a depth of approximately -200 m CD. The data was calibrated to wave height measurements from available altimetry data. For application along the offshore model boundary at a depth of -150 m CD, the extracted data was transformed through the application of linear refraction.

Lateral boundaries were specified along the north-eastern and south-western model boundaries. Local wind generation was not included in the model. Bottom friction was modelled using a Nikuradse roughness with a constant value of $k_N = 0.03$ m.

5.2.5 Seawater Temperature

Seawater temperature profiles were applied along the model boundaries as spatially constant, time-varying profiles. The boundary conditions were varied over time to account for seasonal trends in water column stratification. The profiles were tuned to physically realistic values which yielded the best agreement between modelled and measured seawater temperatures.

5.2.6 Salinity

A constant background salinity of 35 psu has been assumed. This is consistent with the average from measurements reported in Section 2.8.

The increased salinity of the KNPS discharge due to the brine from the SWRO plant (discussed in Section 3.4.2) was not considered in the modelled discharges, since the plant had not yet been planned at the time of modelling. However, the calculation of the combined plume density presented in Section 3.4.3 has indicated the reduction in plume buoyancy to be small ($<7\%$). Therefore, the possible effects on the results of the dispersion modelling are not expected to be significant.

5.2.7 Atmospheric Conditions

Heat exchange between the water and the atmosphere was included in the model. Total cloud cover and relative humidity data were extracted from the ERA-Interim global atmospheric reanalysis product provided by ECMWF (ECMWF, 2015) and were applied as space and time varying input conditions to the model.



The dataset of air temperature measured at the KNPS meteorological station (presented in Section 2.4) was applied as spatially constant time-varying input to the model.

5.3 Model Calibration

5.3.1 Waves

The purpose of the spectral wave model is to provide the following:

- Input to the hydrodynamic model for the generation of wave-driven currents. These currents affect the plume dynamics and the dispersion of chemical and radiological constituents released from KNPS; and
- Input to the radionuclide model (discussed in Section 6) for the calculation of bed shear stresses required in the modelling of background suspended sediment.

The calibration of the spectral wave model was thus focussed on the provision of typical operational wave conditions, rather than extreme wave events. From initial calibration efforts of the spectral wave model, the operational wave heights at the KNPS were consistently over predicted. Therefore, the input wave heights were scaled by a factor of 0.8 to improve model calibration.

Figure 5-3 and Figure 5-4 present time series comparisons of measured and modelled wave parameters at Site A and Site B (see Figure 2-1) for the four month period between August and November 2009. Scatter plots of modelled and measured wave heights compiled from the entire year of 2009 are presented in Figure 5-5 and Figure 5-6 for Site A and Site B. The figures show that the spectral wave model is able to reproduce the measured data sufficiently well for the purpose of this study.

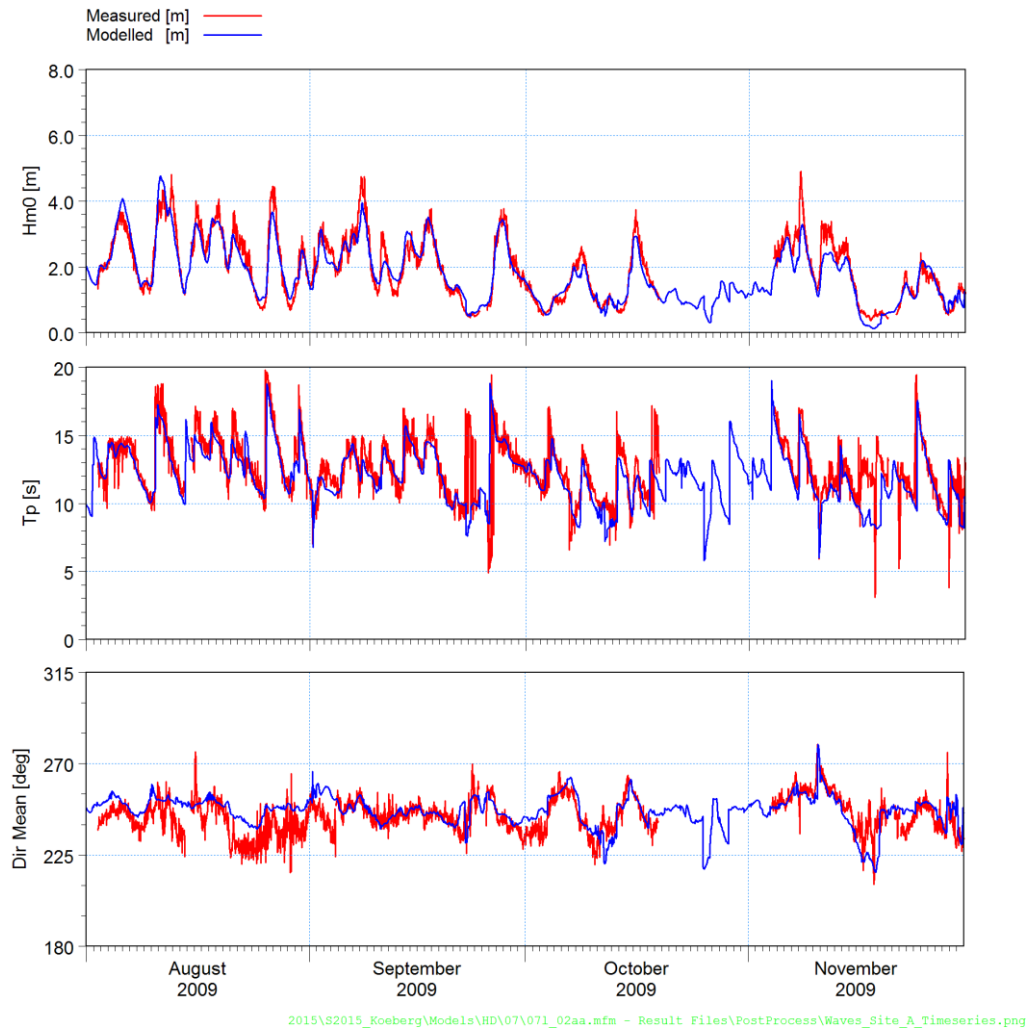


Figure 5-3: Time series plot of measured and modelled wave parameters at Site A ($X = -54\,253\text{ m}$, $Y = -3\,727\,223\text{ m WG19}$, -10 m CD).

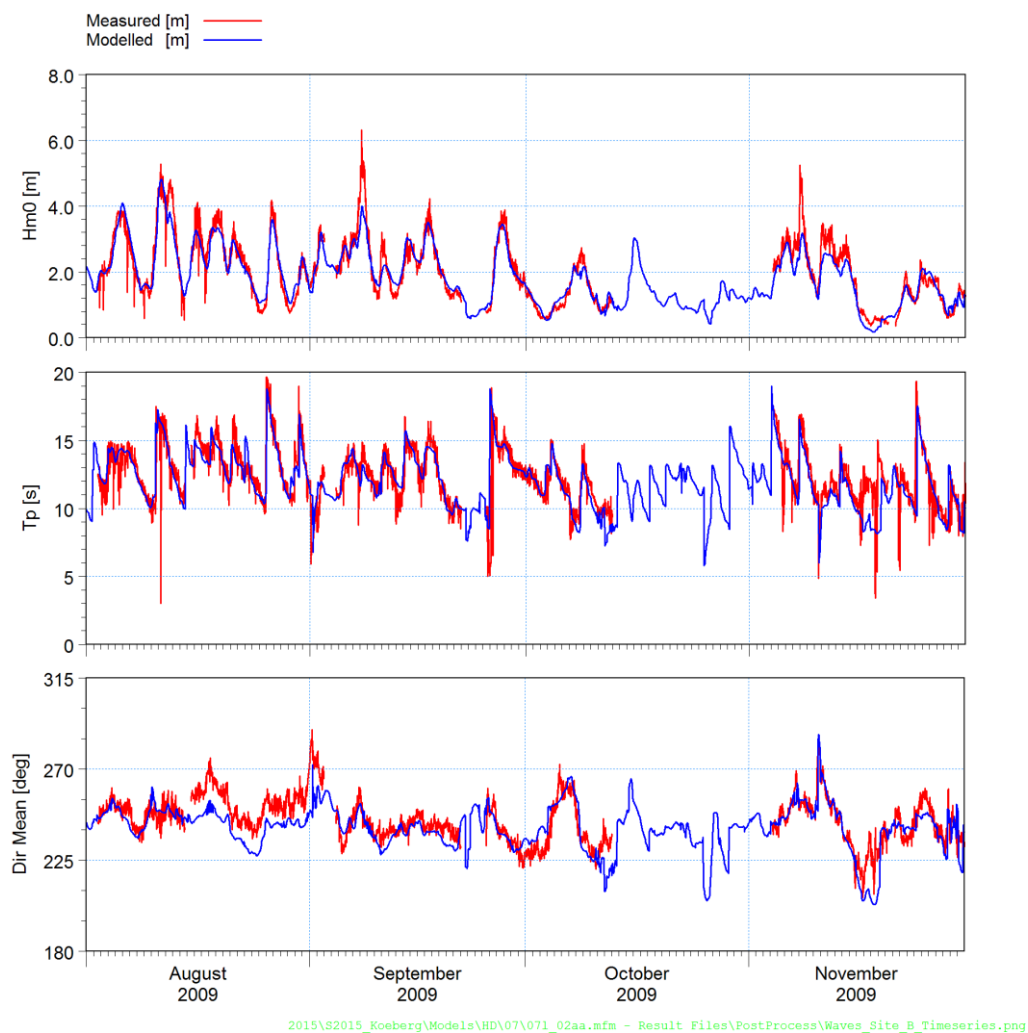


Figure 5-4: Time series plot of measured and modelled wave parameters at Site B ($X = -56\,587\text{ m}$, $Y = -3\,727\,857\text{ m WG19}$, -30 m CD).

E:\L_Projects\2015\2015_Koeberg\Modells\HD\07\07L_02sa.mfm - Result Files\PostProcess\Compare_Waves_Site_A.xlsx\Gridded_Data

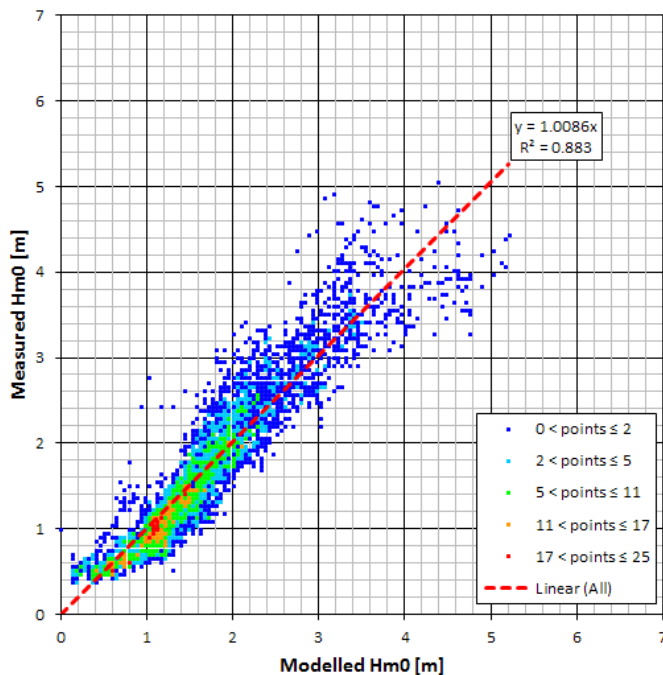


Figure 5-5: Scatter plot of measured and modelled H_{m0} at Site A ($X = -54\ 253\ m$, $Y = -3\ 727\ 223\ m$ WG19, -10 m CD).

E:\L_Projects\2015\2015_Koeberg\Modells\HD\07\07L_02sa.mfm - Result Files\PostProcess\Compare_Waves_Site_B.xlsx\Gridded_Data

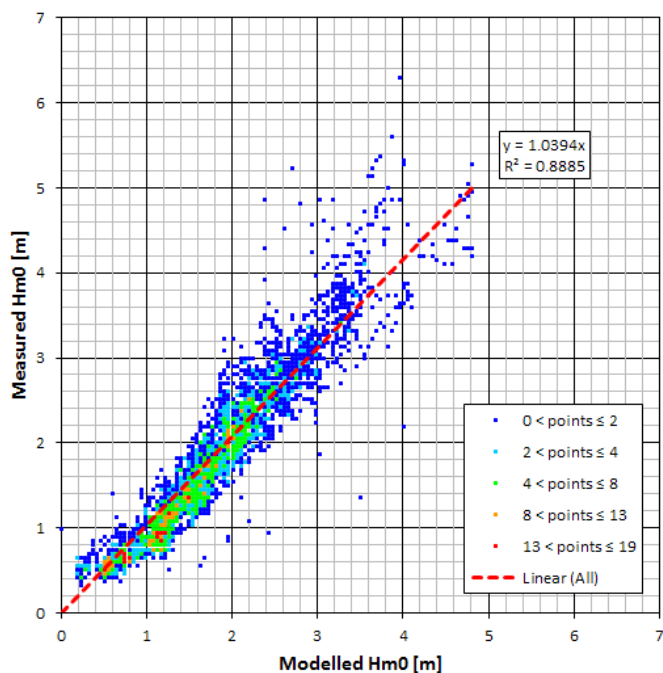


Figure 5-6: Scatter plot of measured and modelled H_{m0} at Site B ($X = -56\ 587\ m$, $Y = -3\ 727\ 857\ m$ WG19, -30 m CD).

5.3.2 Currents

Figure 5-7 and Figure 5-8 present time series comparisons of measured and modelled currents at Site A and Site B for the four month period of August to November 2009. Roses of modelled and measured currents constructed from the entire year of 2009 are shown in Figure 5-9 and Figure 5-10 for the two sites.

At both sites, the model is observed to reproduce the measured currents with reasonable accuracy. From the current roses, it can be seen that the model accurately reproduces the main current directions, although measured current directions are more variable. At both sites, the model is seen to accurately reproduce the difference in current directions at the surface and the seabed. This suggests that the model is reproducing the ambient stratification at Koeberg.

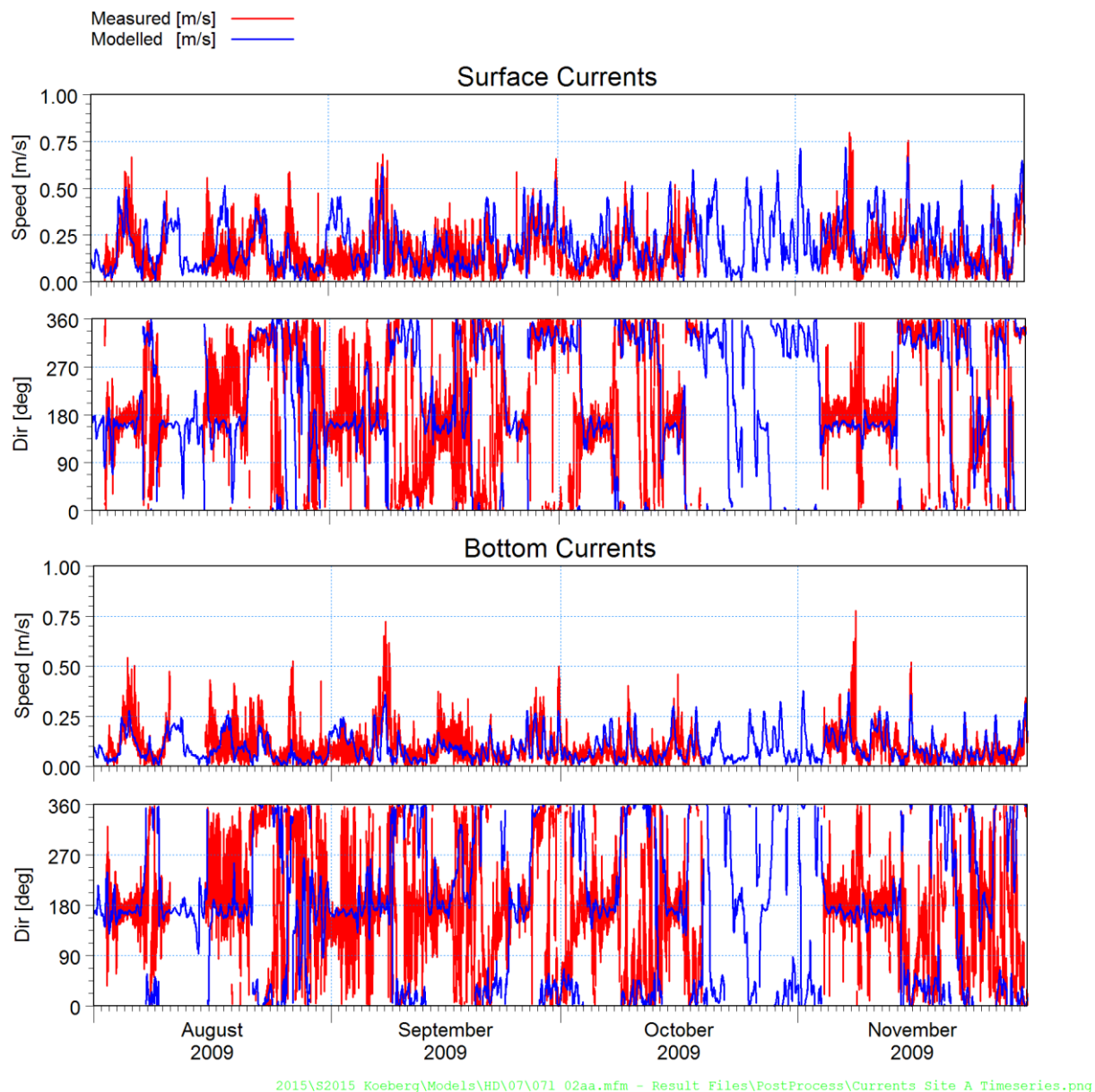
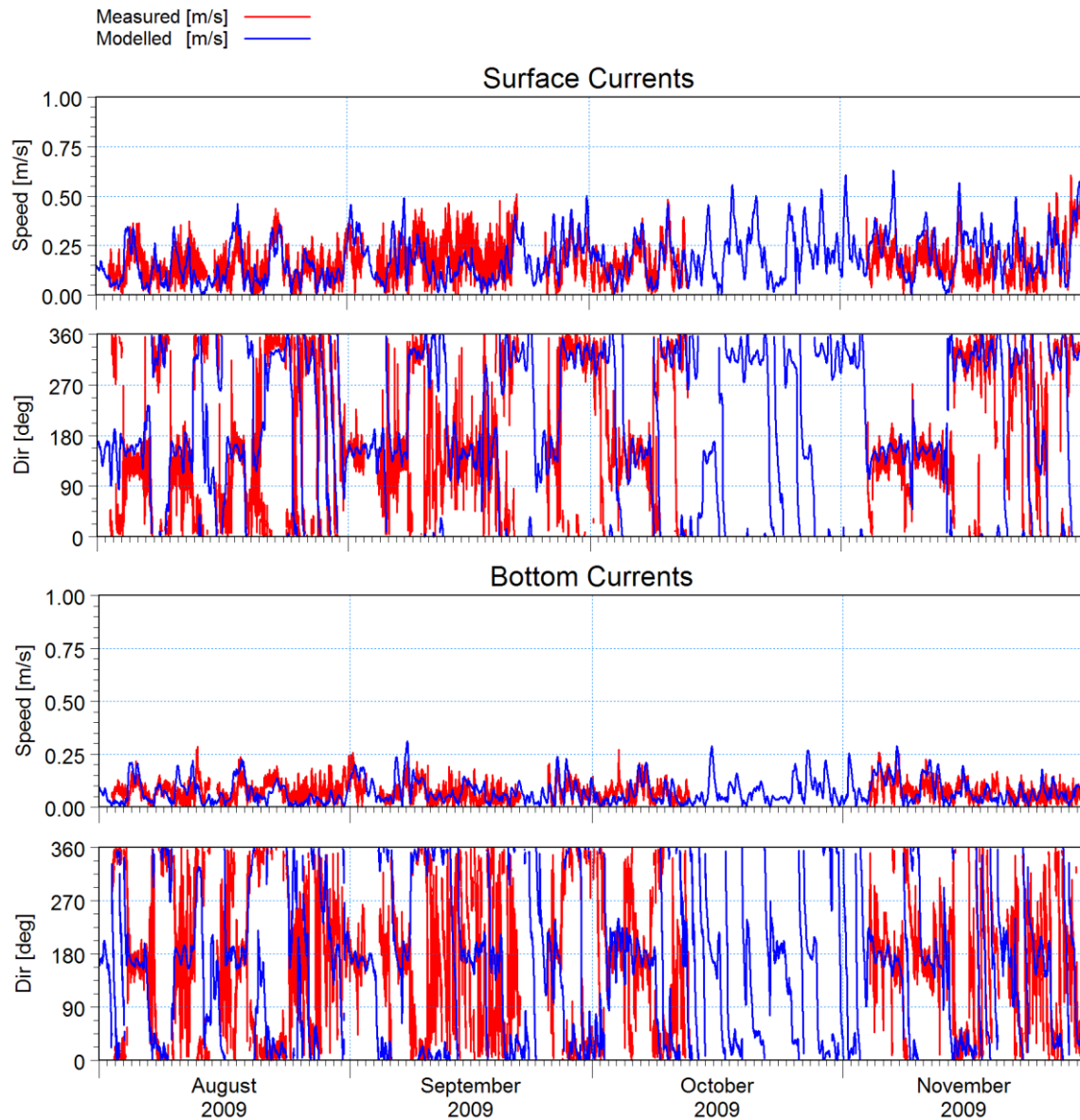
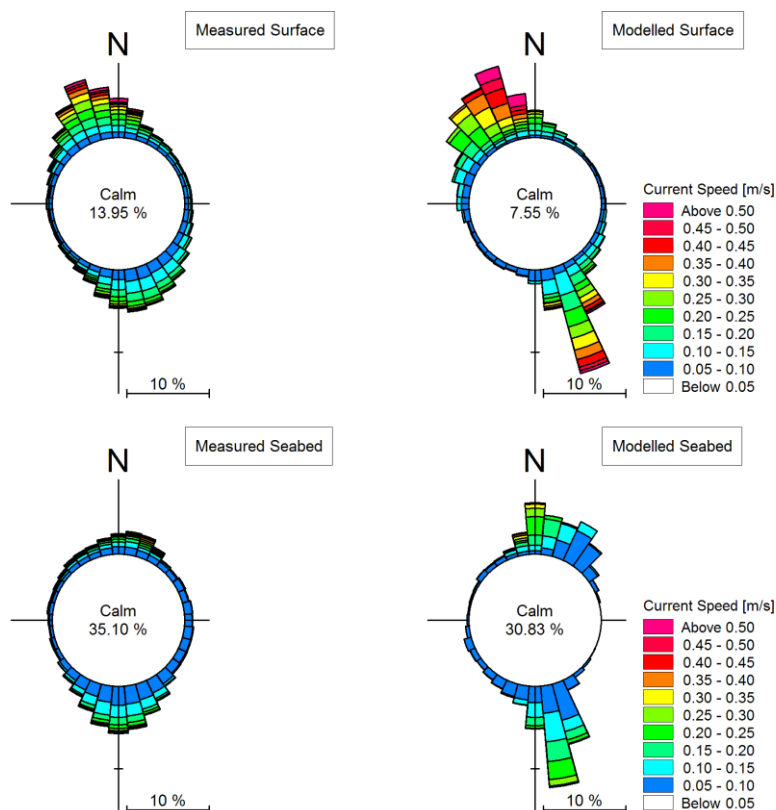


Figure 5-7: Time series comparison of measured and modelled currents at Site A ($X = -54\ 253\ m$, $Y = -3\ 727\ 223\ m\ WG19$, $-10\ m\ CD$)



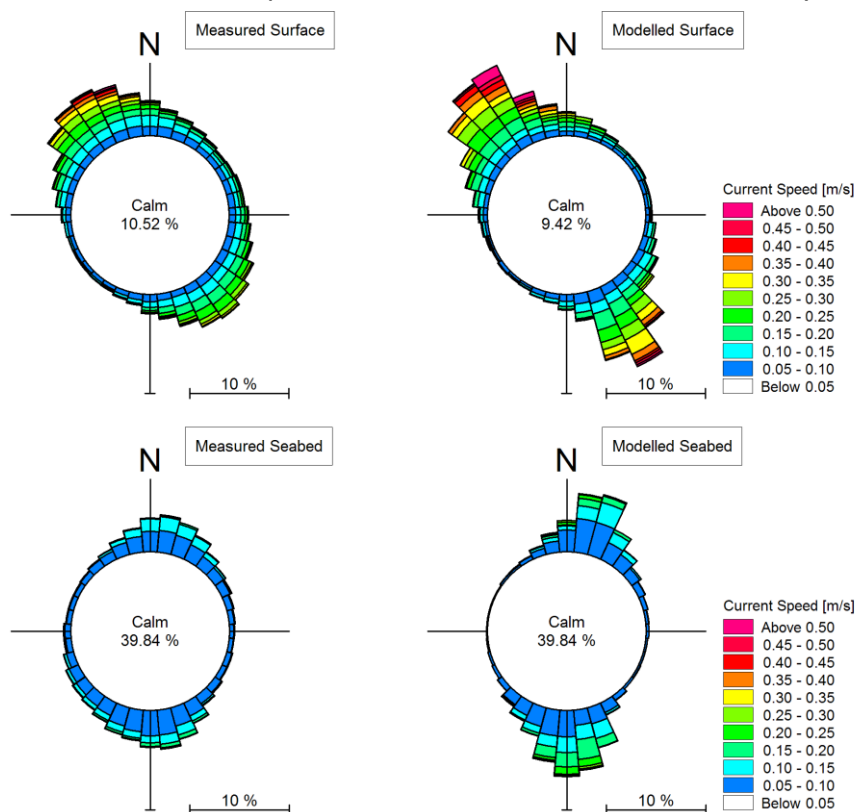
2015\S2015_Koeberg\Models\HD\07\071_02aa.mfm - Result Files\PostProcess\Currents_Site_B_Timeseries.png

Figure 5-8: Time series comparison of measured and modelled currents at Site B (X = -56 587 m, Y = -3 727 857 m WG19, -30 m CD)



2015\S2015_Koeberg\Models\HD\07\071_02aa.mfm - Result Files\PostProcess\Current_Roses\Currents_Site_A_Roses.png

Figure 5-9: Current roses constructed from 1 year (2009) of measured and modelled currents at Site A ($X = -54\ 253\ \text{m}$, $Y = -3\ 727\ 223\ \text{m}$ WG19, -10 m CD)



2015\S2015_Koeberg\Models\HD\07\071_02aa.mfm - Result Files\PostProcess\Current_Roses\Currents_Site_B_Roses.png

Figure 5-10: Current roses constructed from 1 year (2009) of measured and modelled currents at Site B ($X = -56\ 587\ \text{m}$, $Y = -3\ 727\ 857\ \text{m}$ WG19, -30 m CD)



5.3.3 Temperature

Figure 5-11 presents a time series comparison of measured and modelled near-seabed seawater temperatures at Sites A to E. The coordinates of the positions are listed in Table 2-2 in Section 2.7. The model is seen to reproduce the well-mixed conditions which dominate the winter months. The model also shows the high variability and colder temperatures associated with upwelling events which occur during summer months when south-easterly winds are dominant. The model is considered to adequately reproduce seawater temperatures for the purposes of this study.

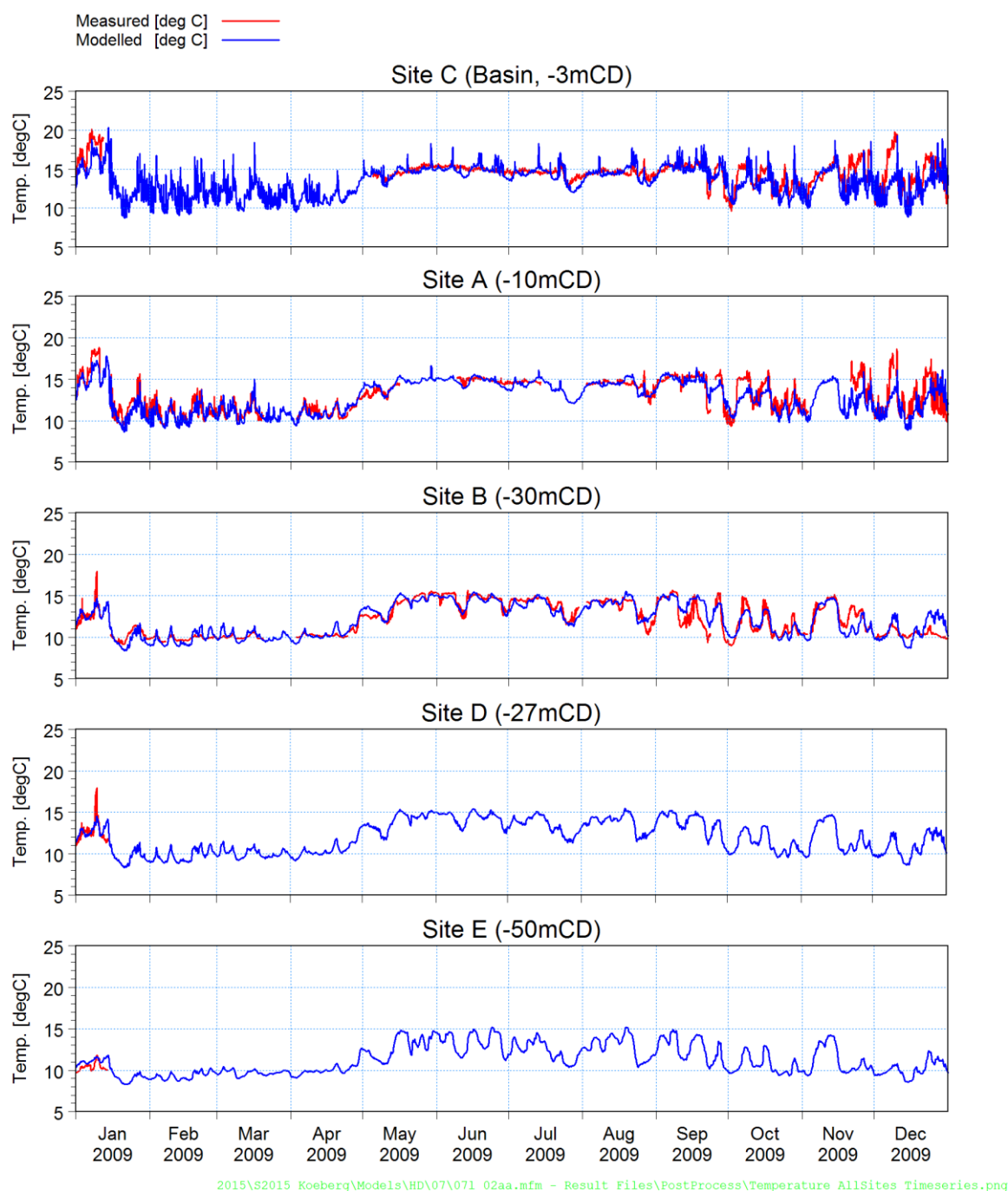


Figure 5-11: Time series of measured and modelled near-seabed seawater temperatures at Sites A to E. The coordinates of the locations are reported in Table 2-2 in Section 2.7.

5.3.4 Thermal Plume

Historical measurements of the thermal plume during October 1985 are available. The measurements were conducted using a skiboat and a helicopter. The skiboat was equipped with a temperature probe mounted 30 cm below the water surface and traversed the study area on a grid pattern in order to measure the ambient water temperature and define the surface extent of the plume. A helicopter equipped with an infrared sea surface temperature recorder took measurements on a grid pattern from a height of 100 m above the thermal plume over the survey period of approximately 1 hour.

The surveys conducted on 14 and 16 October were selected for calibration. The wind applied in the model was hourly data measured at 10 m height at Koeberg with the wind speed increased by a factor 1.65 to account for the increase in wind speeds experienced offshore. The wave height and period applied on the offshore boundary of the model were the 6-hourly values measured by a Waverider buoy in 170 m water depth approximately 15 km west of Slangkop (X = -75 951 m, Y = -3 778 017 m, WG19). Since the wave direction was not measured, a constant direction of 230° was assumed, corresponding to the average wave direction obtained from wave hindcast data in this area.

The plume calibration results are presented in Figure 5-12 and Figure 5-13. Considering the uncertainties in the measurements (e.g. due to the averaging of the plume over the hour long survey period) and the uncertainties in the model inputs, the results correspond reasonably well to the measurements and thus provide confidence in the predictive capability of the hydrodynamic model.

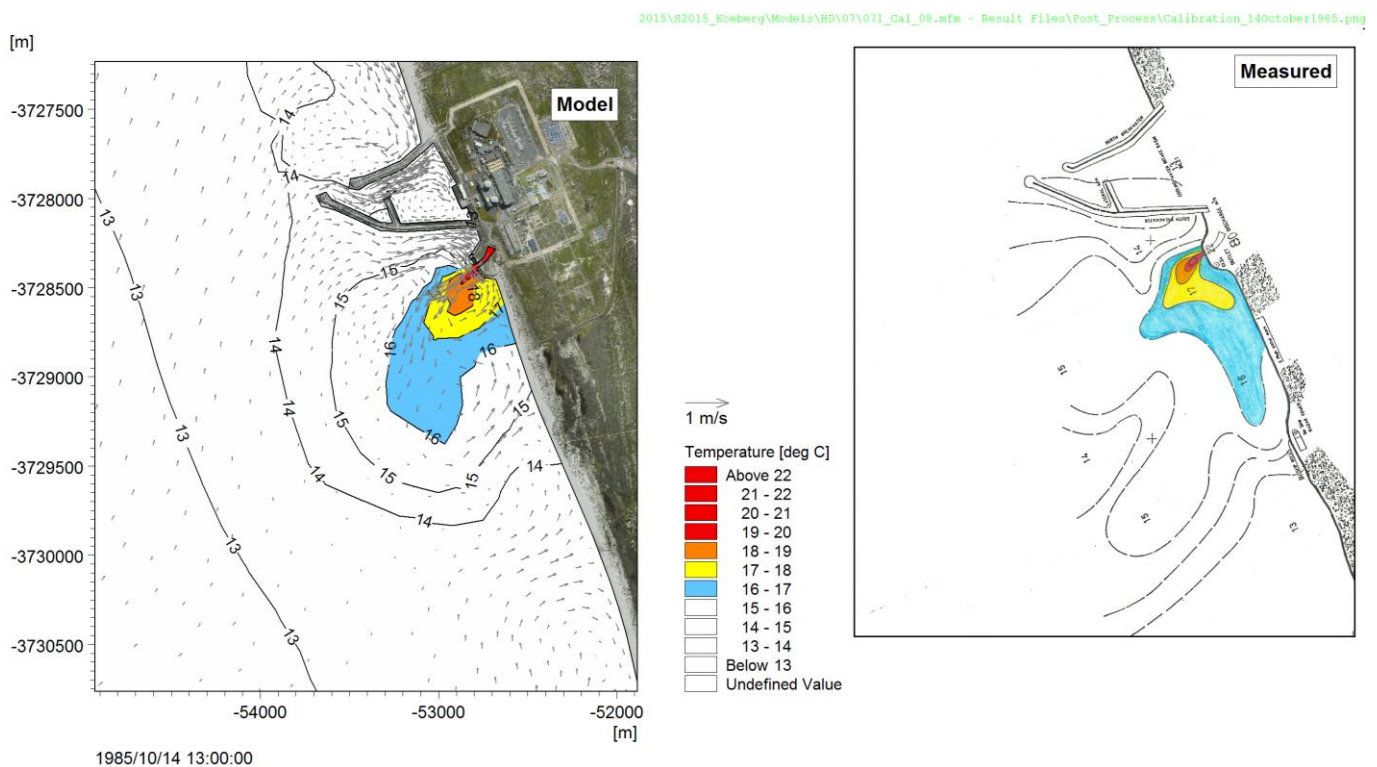


Figure 5-12: Comparison of modelled and measured surface temperature on 14 October 1985.

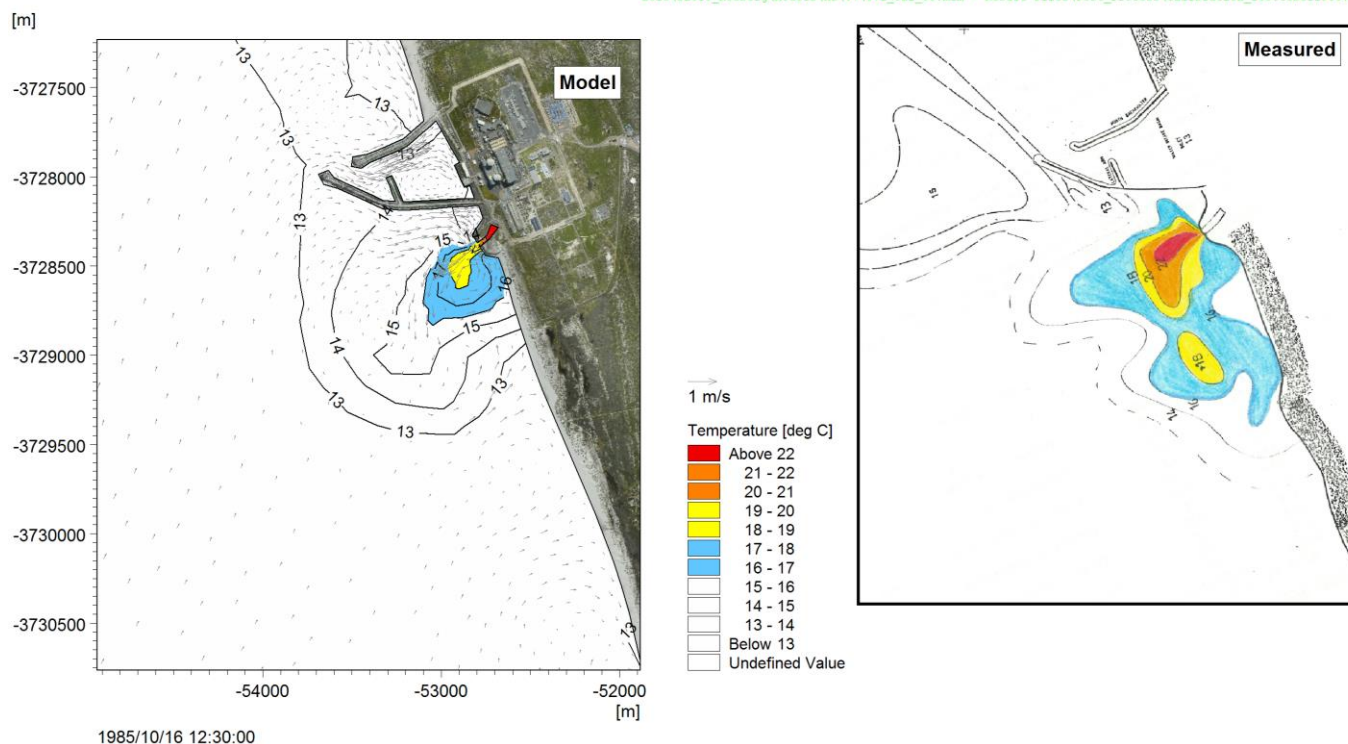


Figure 5-13: Comparison of modelled and measured surface temperature on 16 October 1985.

5.4 Modelling Approach

5.4.1 Model Simulations

In the screening of constituents presented Section 4, the following constituents did not meet the relevant ecological guidelines at the end of the outfall channel and were therefore identified to be included in the dispersion modelling:

- Temperature;
- Free Chlorine;
- Hydrazine; and
- Phosphate.

To investigate the dispersion of the constituents listed above, the model was run for a full year to capture seasonal trends in environmental conditions. The year of 2009 was selected for modelling since it was covered by all of the datasets required as model input and by those necessary for the proper calibration of the model. Furthermore, the highest seawater temperatures recorded in the 6-year dataset of measurements in the KNPS intake basin (Site C, see Figure 2-11) occurred in January 2009, thereby making this a conservative year during which to assess the impact of temperature releases.

For the constituents which behave non-conservatively (e.g. through decay), specific ECOLab models were set up to reproduce the relevant processes. These ECOLab models have been described in Sections 5.1.3.1 and 5.1.3.2. The releases of the constituents to be modelled occur either as continuous releases, batch releases or a combination between the two. The specific releases for each constituent were characterised in detail, and are presented in the subsection below for the relevant constituent.

5.4.2 Mixing in the Outfall Channel

When modelling the dispersion of these constituents in the sea, it is important that the total load of each constituent is accurately represented in the model. Therefore, the concentrations at discharge were calculated as the total load (mass/time) divided by the total flow rate (volume/time), i.e. assuming complete mixing in the outfall channel.

As discussed in Section 4, in reality complete mixing between the individual streams is not achieved by the end of the outfall channel. However, model results from a previous modelling study of the KNPS discharges (PRDW, 2013) indicate that complete mixing is achieved approximately 100 m beyond the end of the outfall channel. This can be observed in Figure 5-14 which presents the dilution of a conservative tracer released into one train of the CRF flow, while only two trains (i.e. one unit) are operational. Within the outfall channel and at the end of the outfall, the streams have not mixed and dilutions below 1.0 are observed, indicating that the tracer is still concentrated in one stream. Where the number of dilutions reaches 1.0, the tracer is no longer concentrated into one stream and complete mixing between the trains has been achieved. This is observed to occur within 100 m from the end of the outfall channel.

Therefore, when investigating the dispersion of constituents beyond the 100 m radius around the outfall, the assumption of complete mixing has little impact on the mixing zone size determined from the model results.

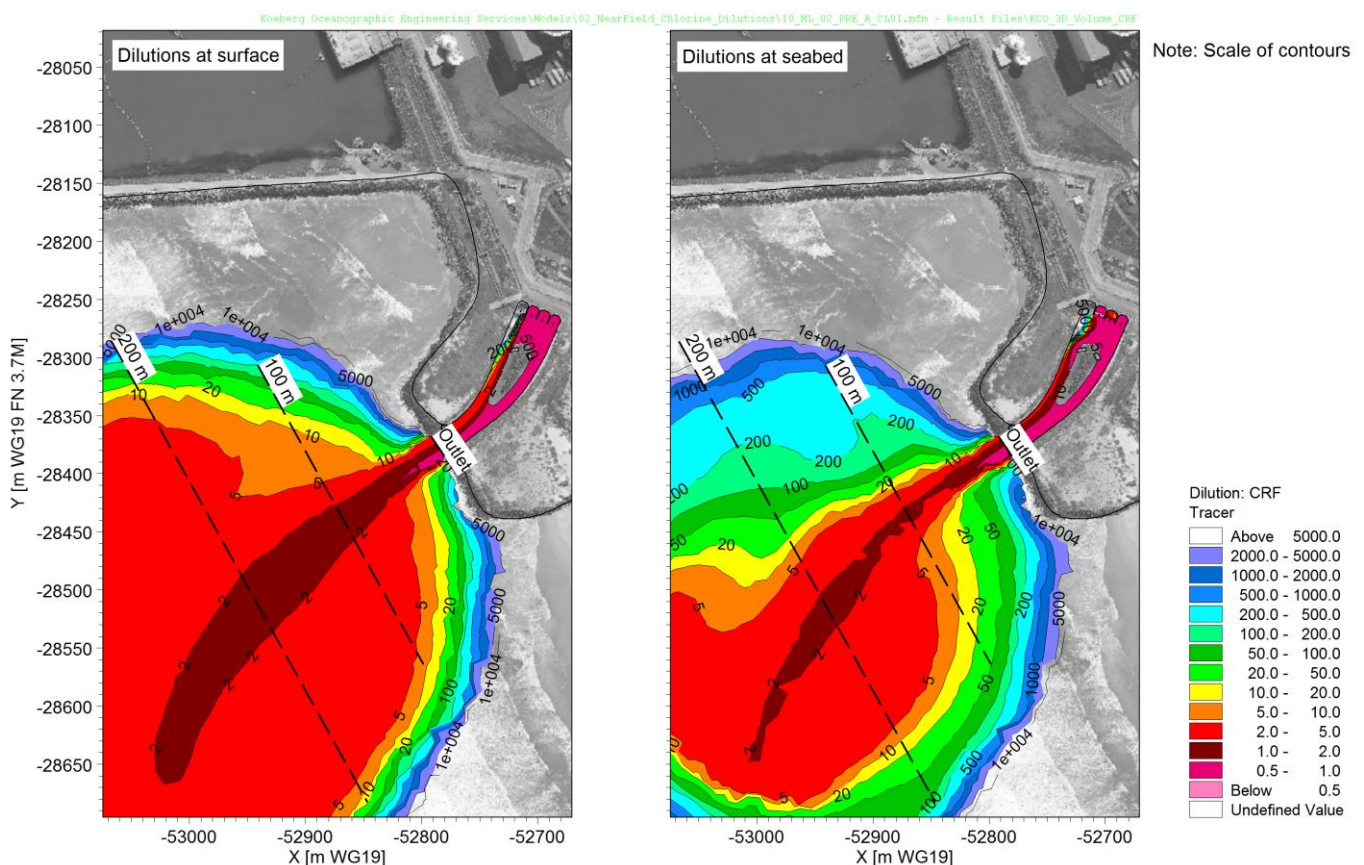


Figure 5-14: Model results from previous hydrodynamic modelling of the KNPS outfall channel indicating mixing between CRF trains (PRDW, 2013). The figure presents the number of dilutions of a conservative tracer released into one CRF train, while two trains are operational.



5.4.3 Post-processing of Model Results

For both continuous and batch releases, the model results were post-processed to calculate the duration that the ecological guideline is exceeded in the modelled year.

For continuous releases, the duration that the ecological guideline is exceeded is expressed as a percentage per year. By definition, the area enclosed by the 5% contour corresponds to that area in which concentrations are above the guideline for at least 5% of the time and therefore represents the 95th percentile mixing zone.

The modelling of batch releases is more complex since they occur infrequently (e.g. once per outage) and then only for short durations. If these releases were modelled at their true frequencies, the variability of the environmental conditions would not be sufficiently sampled to define worst case conditions with sufficient confidence. In order to increase the number of environmental conditions sampled, the modelled year (2009) was effectively repeated a number of times, while releasing the batches at different dates in each repetition. In this way the releases were modelled under a greater range of environmental conditions, thereby increasing the probability that unfavourable environmental conditions were sampled.

For a given element in the model domain, the model results were post-processed to calculate the duration that the guideline is exceeded due to each individual batch release. For a batch release which in reality occurs only n times per year, the n modelled batch releases with the longest exceedance durations (i.e. the batches released under the n worst environmental conditions) were identified. The exceedance durations from these n releases were then added, and together represent the longest duration that the guideline is exceeded per year. Since the batch releases occur infrequently and only for short durations, the total annual duration of the releases is generally well below 5% of the time. Therefore, although the post-processed results are the same for continuous and batch releases, the result for batch releases is presented in units of hours per year rather than percentage of time per year. This result is more easily interpreted than a very low percentage.

At elements along beaches, water level variations due to astronomical tide cause drying and flooding of the elements. In the post-processing of model results, if an element is dry, it is not considered to exceed the guideline. Since elements in the intertidal zone are often dry, the exceedance percentage is lower than in the deeper elements further offshore. In reality, wave run-up and perhaps groundwater seepage would expose the sandy beaches to the effluent plume. This should be kept in mind when evaluating the exceedance durations along the shoreline.

In addition to the exceedance durations, the 95th percentile concentration in each element is presented for the continuous releases and the maximum concentration in each element is presented for the batch releases.

A number of sensitive receptor locations have been identified by Lwandle, as shown in Figure 5-15. At these locations, time series of near-surface and near-seabed concentrations are presented for the continuous release scenarios only. These figures are not presented in the subsections below, but are presented in Annexure B.

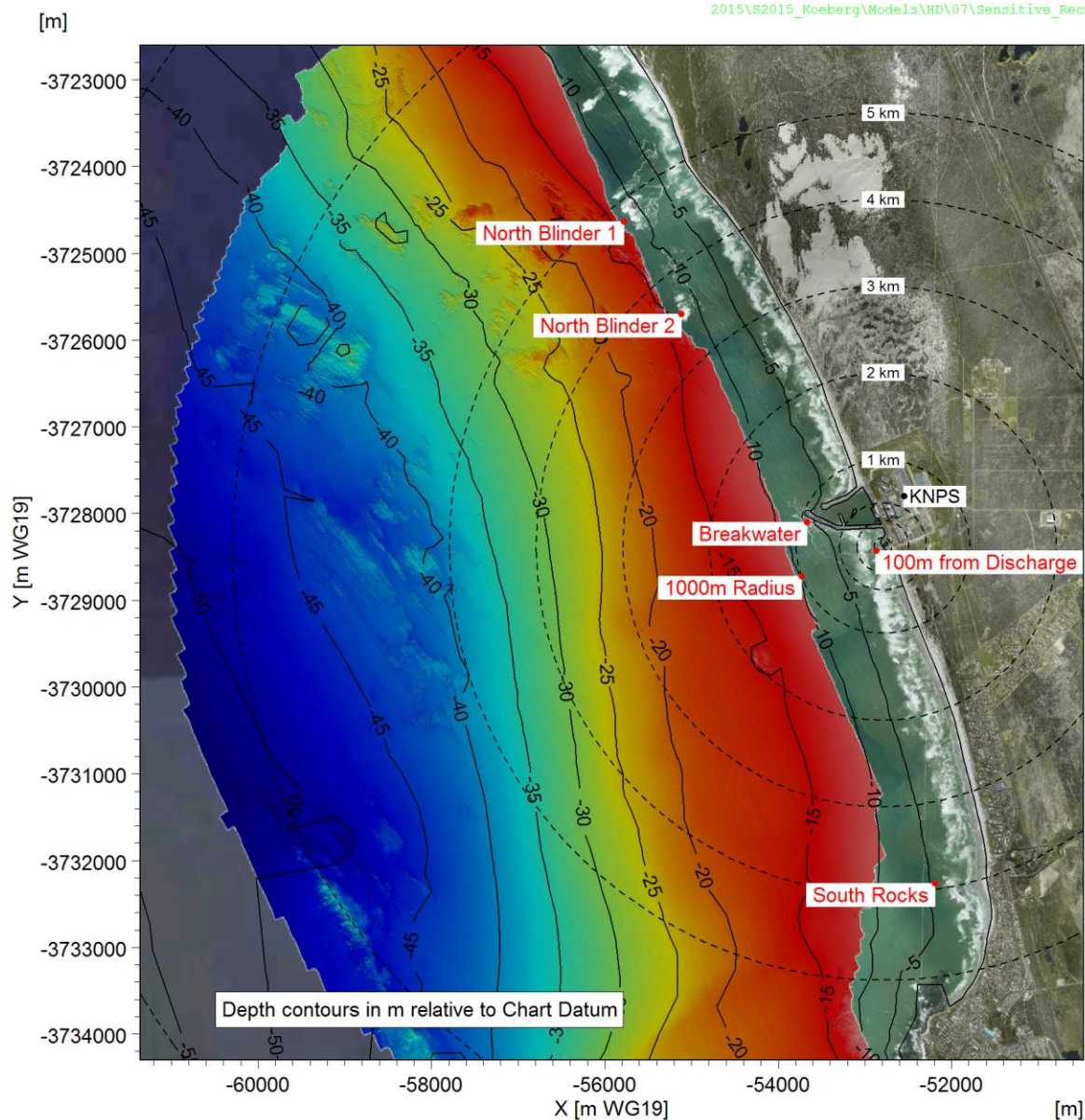


Figure 5-15: Locations of sensitive receptors where time series of near-surface and near-seabed concentrations are presented for the continuous release scenarios. The time series are presented in Annexure B.



5.5 Fate of Intake Basin Discharges

In order to validate the assumption that intake basin discharges ultimately pass through the cooling water system and are effectively discharged at the KNPS outfall channel, a simulation was run in which a conservative tracer was released into the intake basin. The flow rate was based on that of the exceptional hydrazine discharge ($60 \text{ m}^3/\text{h}$), while a unit concentration of the tracer was released.

For conservatism, it was assumed that only one CRF unit is operational. The model was configured such that the mass of the tracer sucked in by the cooling water intakes was not released at the outfall. Therefore, any tracer concentrations outside the intake basin would be due to advection or diffusion out of the basin, and not due to circulation through the cooling water. The model was run for one year with a continuous release of the tracer. The resulting 95th percentile number of dilutions at the surface and at the seabed is shown in Figure 5-16.

The figure indicates that a number of dilutions in excess of 1×10^7 occur before reaching the end of the inner part of the basin. For the exceptional hydrazine discharge of 300 mg/l at $60 \text{ m}^3/\text{h}$, the corresponding concentration at the edge of the inner part of the basin is $3 \times 10^{-5} \text{ mg/l}$ (ignoring the additional reduction in hydrazine concentration due to non-linear processes), which is well below the guideline of $2 \times 10^{-4} \text{ mg/l}$ (see Table 4-5). This validates the assumption that intake basin releases primarily pass through the cooling water system and are discharged to sea at the outfall, whilst any constituents that are advected or diffused out of the intake basin are well below ecological guidelines.

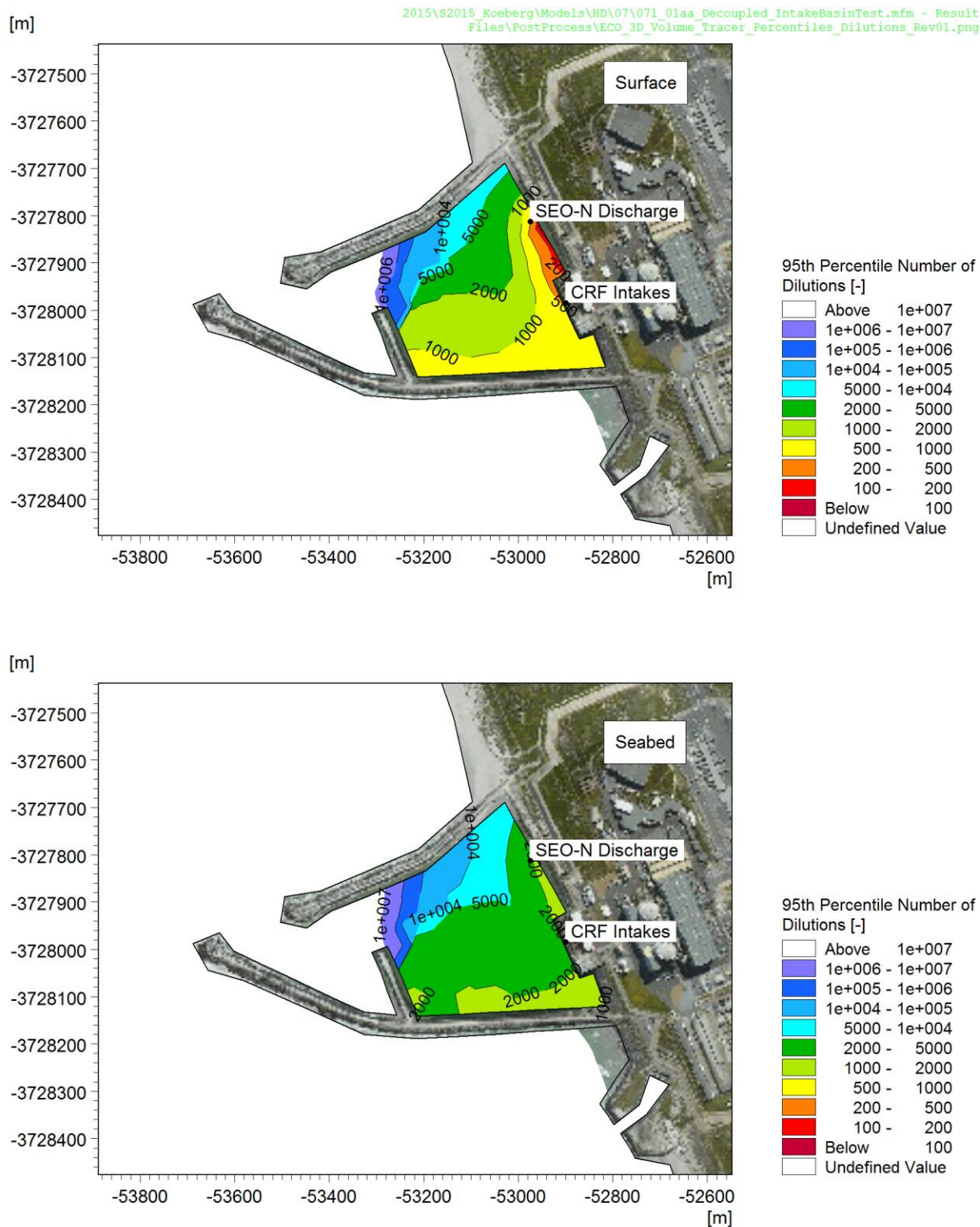


Figure 5-16: 95th percentile dilutions for a tracer released into the intake basin at 60 m³/h: near-surface and near-seabed.



5.6 Dispersion Modelling: Temperature

5.6.1 Discharge Configuration

For temperature releases, two scenarios were modelled. The first scenario corresponds to the KNPS operating at full capacity and consists of continuous releases from the CRF and SEC streams (see Table 5-4).

Table 5-4: Configuration of temperature releases: plant operation at full capacity

Stream	Discharge [m ³ /h]	ΔT [°C]	Duration [h]	Release interval [days]	Total duration per year [hrs]
CRF	327 888	11.7		continuous	
SEC	12 700	12		continuous	

The second scenario is that of one CRF pump trip. As discussed in Section 3.2.2, this is conservatively considered to occur during an outage, i.e. only one CRF unit in operation. As presented in Table 5-5, this scenario consists of continuous releases from the CRF (with one unit operational) and SEC streams. As a batch release of 12 hours duration, the CRF flow is reduced to only one train and the ΔT is increased to 22.7°C.

As discussed in Section 5.4, batch releases were repeated a number of times to increase the number of environmental conditions sampled. This batch was repeated 53 times. Since this batch release only occurs under abnormal operation, the real number of releases expected to occur per year is unknown.

Table 5-5: Configuration of temperature releases: pump trip scenario

Stream	Discharge [m ³ /h]	ΔT [°C]	Duration [h]	Release interval [days]	Total duration per year [hrs]
CRF	163 944	11.7		continuous	
	81 972	22.7	12	Abnormal	-
SEC	12 700	12		continuous	

In addition to advection and dispersion, the fate of the thermal plume is dependent on the processes of buoyancy and heat exchange between the sea surface and the atmosphere. These processes are simulated by the three-dimensional hydrodynamic model (see Section 5.1.1).

5.6.2 Results

Instantaneous plots of the dispersion of the temperature plume during a typical south-easterly wind event are presented in Figure 5-17 and Figure 5-18. The figures present contours of the increase in temperature (ΔT) at the surface and seabed. The vectors shown on the figures indicate the current speed and direction. The same plots for a typical north-westerly wind event are shown in Figure 5-19 and Figure 5-20. Both sets of figures correspond to the KNPS operating at full capacity.

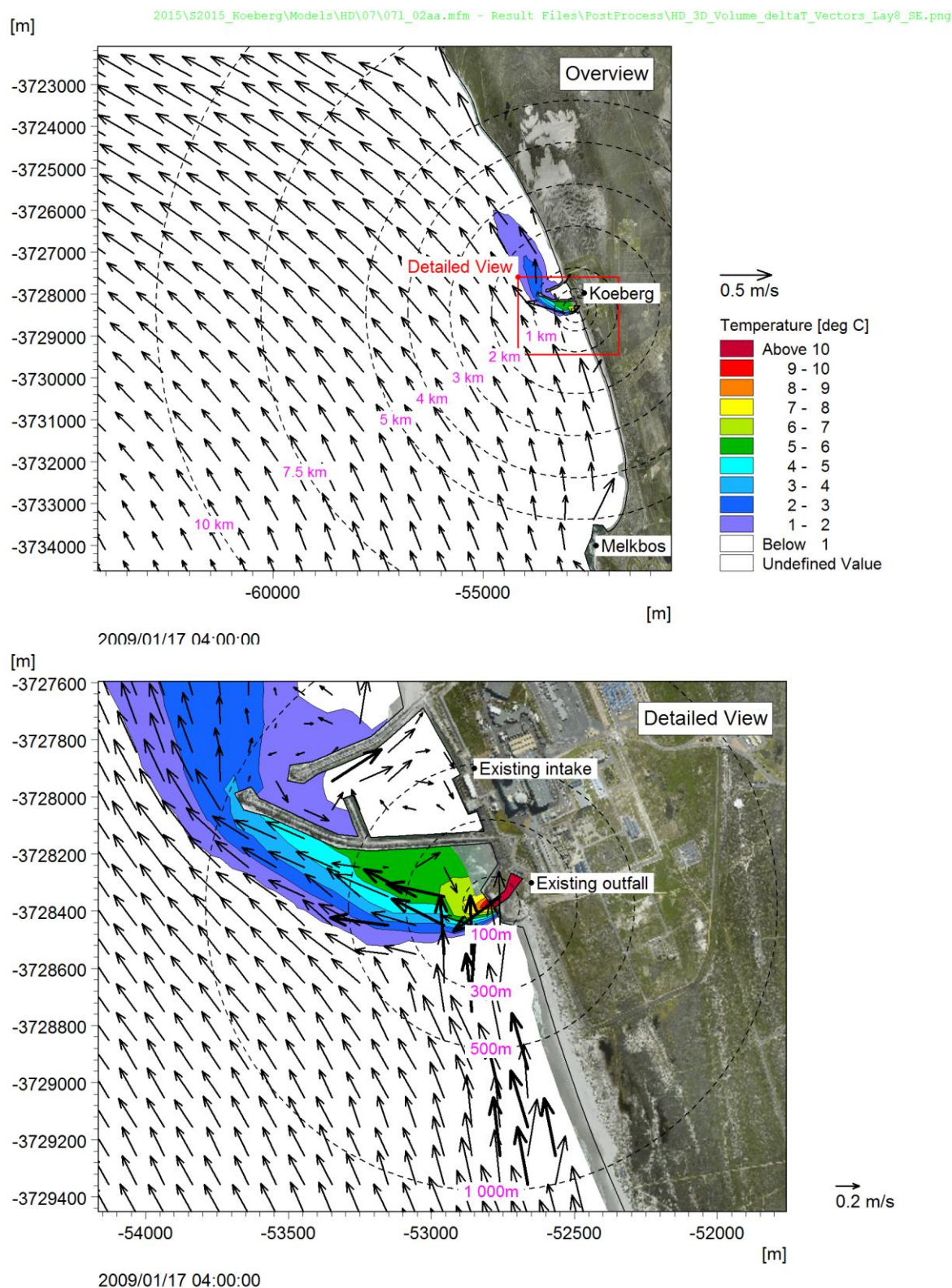


Figure 5-17: Instantaneous contour plot of the increase in temperature (ΔT) during a typical south-easterly wind event: near-surface, plant operation at full capacity. The vectors indicate current speed and direction.

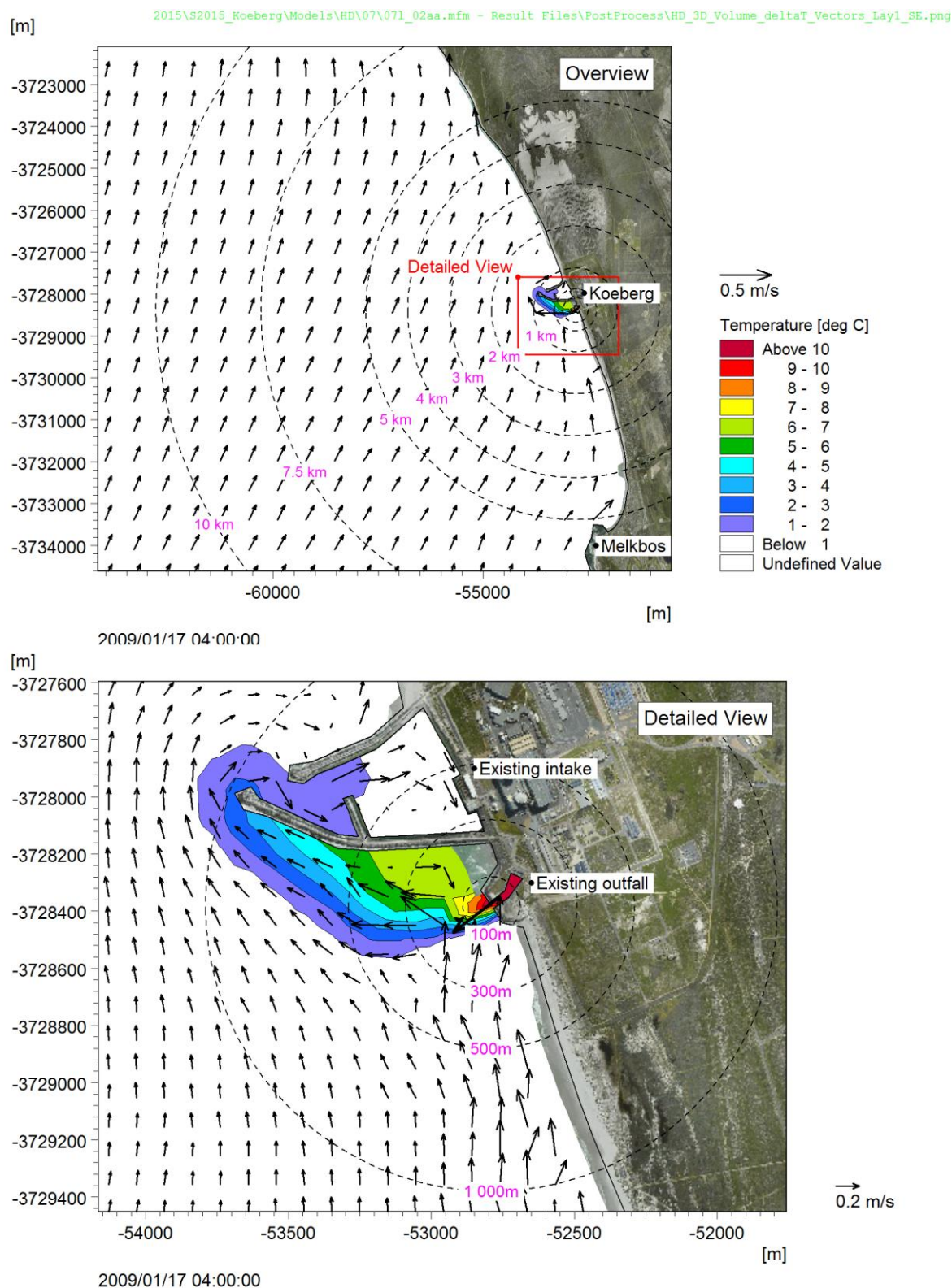


Figure 5-18: Instantaneous contour plot of the increase in temperature (ΔT) during a typical south-easterly wind event: near-seabed, plant operation at full capacity. The vectors indicate current speed and direction.

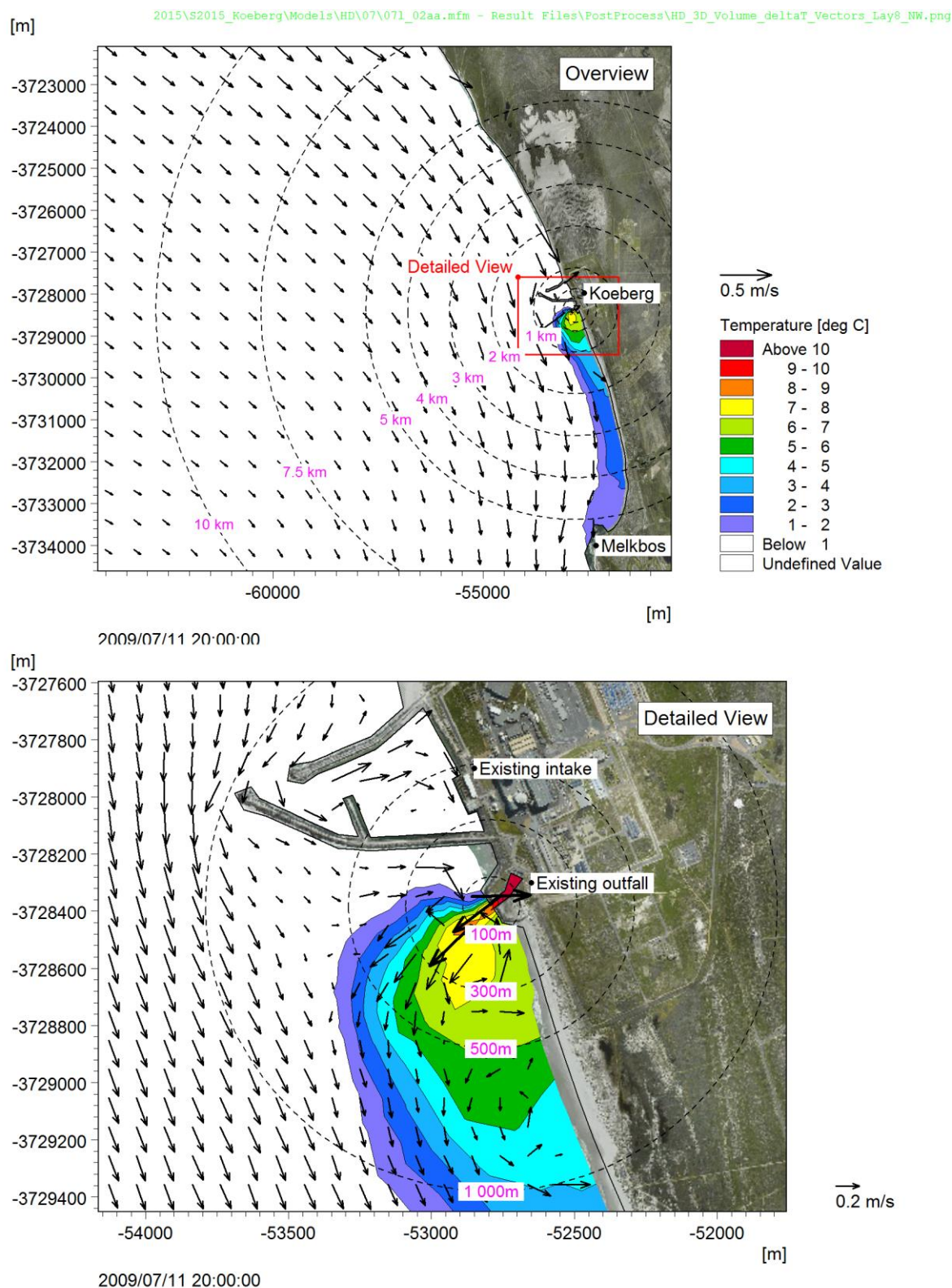


Figure 5-19: Instantaneous contour plot of the increase in temperature (ΔT) during a typical north-westerly wind event: near-surface, plant operation at full capacity. The vectors indicate current speed and direction.

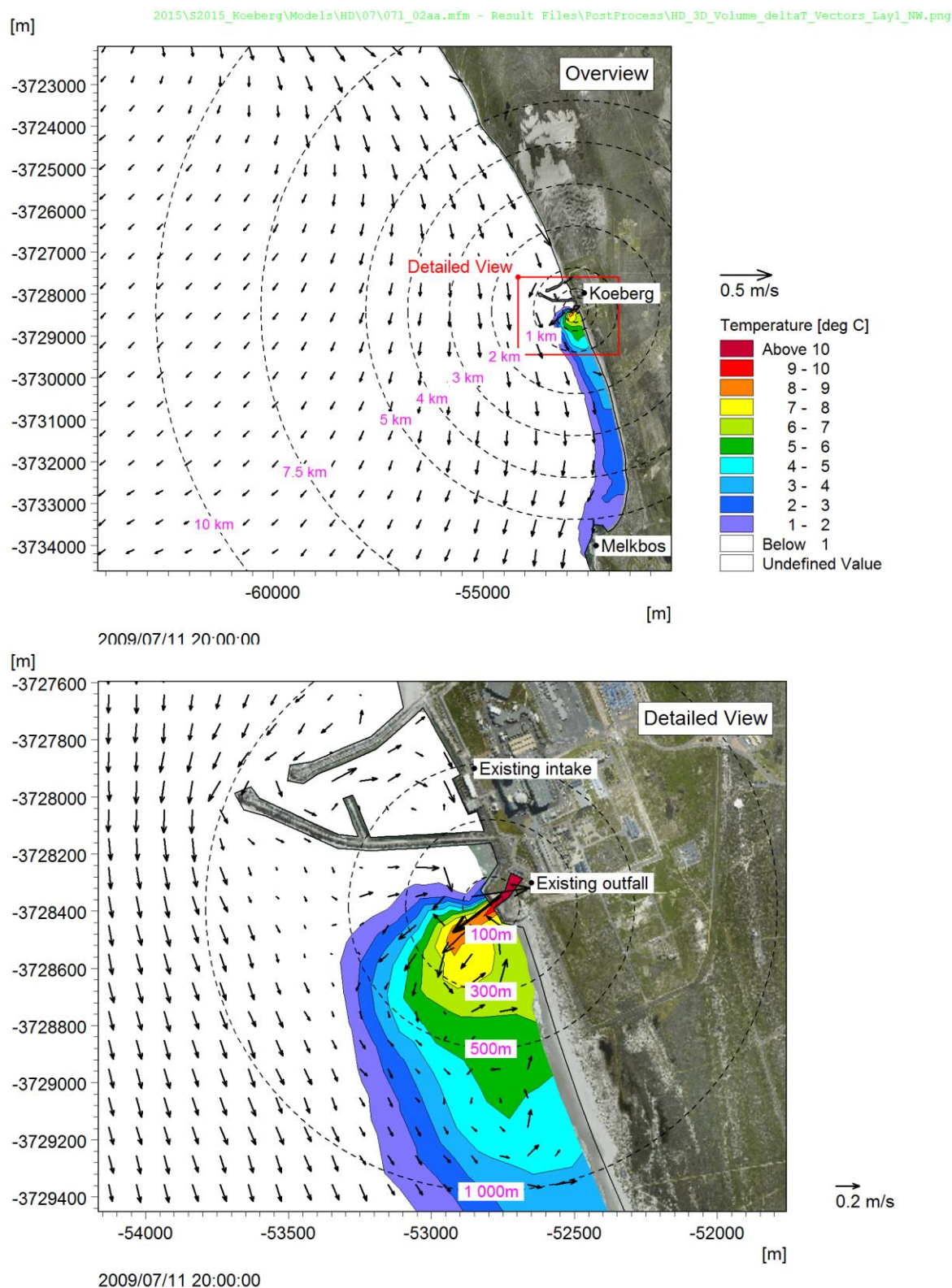


Figure 5-20: Instantaneous contour plot of the increase in temperature (ΔT) during a typical north-westerly wind event: near-seabed, plant operation at full capacity. The vectors indicate current speed and direction.



During south-easterly wind events, the plume is transported northward, deflected offshore along the southern breakwater of the KNPS intake basin and ultimately travels northward with the ambient currents. During north-westerly events, the plume is transported southward towards Melkbosstrand.

In general, the extent of the plume is larger on the surface than on the seabed due to the buoyancy induced by the elevated temperature of the effluent. This effect is enhanced during the south-easterly wind events (such as in Figure 5-17 and Figure 5-18) during which upwelling is induced and the water column becomes stratified. Conversely, during north-westerly wind events (Figure 5-19 and Figure 5-20), the upwelling is relaxed and the water column becomes well-mixed. Therefore, the extent of the plume is similar on the surface and the bottom.

The scenarios described in Section 5.6.1 were modelled and were post-processed as described in Section 5.4.3 to produce statistical outputs informing the ecological assessment (Lwandle, 2017). In addition to the ecological guidelines determined for the screening of constituents presented in Section 4.4, the results were also post-processed using other ecological thresholds of significance to further inform the ecological risk assessment. A list of the prepared outputs is presented in Table 5-6, with linked references to Annexure B in which the figures are presented.

Table 5-6: Summary of model results for temperature presented in Annexure B

Scenario	Statistic Plotted	Level	Reference
Releases during operation at full capacity	Annual duration that guideline ΔT is exceeded [% of time]	$\Delta T = 1^\circ\text{C}$ Surface	Figure B-1
		$\Delta T = 1^\circ\text{C}$ Seabed	Figure B-2
		$\Delta T = 2^\circ\text{C}$ Surface	Figure B-3
		$\Delta T = 2^\circ\text{C}$ Seabed	Figure B-4
		$\Delta T = 3^\circ\text{C}$ Surface	Figure B-5
		$\Delta T = 3^\circ\text{C}$ Seabed	Figure B-6
	95th percentile temperature [$^\circ\text{C}$]	ΔT Surface	Figure B-7
		ΔT Seabed	Figure B-8
		Absolute T Surface	Figure B-9
		Absolute T Seabed	Figure B-10
	Time series of temperature at sensitive receptors [$^\circ\text{C}$]	ΔT Surface and Seabed	Figure B-11 to Figure B-16
		Absolute T Surface and Seabed	Figure B-17 to Figure B-28
Pump Trip	Maximum temperature [$^\circ\text{C}$]	Absolute T Surface	Figure B-29
		Absolute T Seabed	Figure B-30

For the pump trip scenario, the ecological concern is the maximum temperature reached. Therefore, the model results for this scenario indicate the maximum absolute temperature in any of the modelled batch releases, rather than the duration that the guideline is exceeded. It is important to note that this is not a snapshot of the plume in time, but rather a statistical plot indicating the maximum in each cell from all of the modelled batch releases.



5.7 Dispersion Modelling: Free Chlorine

5.7.1 Discharge Configuration

The configuration of the discharge of residual free chlorine is presented in Table 5-7. The modelled scenario corresponds to the plant operating at full capacity, i.e. two units CRF are operational. The free chlorine concentration in the SEC stream was elevated above the normal concentration of 1 mg/l for the durations and frequencies shown in the table. These elevated concentrations allow for variability in the chlorination (2 mg/l) and for bi-weekly shock chlorination (25 mg/l). For the remainder of the time, the normal concentration (1 mg/l) is applied.

The contributions of the free chlorine in the effluent from the BWRO and SWRO plants have not been included, since these plants had not been planned at the time of modelling. However, due to the relatively low flow rates and chlorine concentrations, the total chlorine load from these effluent streams is approximately three orders of magnitude lower than that in CRF. Therefore, the operation of these facilities is not expected to significantly affect the ecological impact of the free chlorine released from KNPS.

Table 5-7: Configuration of free chlorine releases: plant operation at full capacity

Stream	Discharge [m³/h]	Concentration [mg/l]	Load [kg/h]	Duration [h]	Release interval [days]	Total duration per year [hrs]	Total Annual Load [kg]
CRF	327 888	0.5	164	continuous		8766	1 437 133
SEC	12 700	1	13	continuous		8336	105 861
		2	25	8	7	417	10 603
		25	318	0.5	14	13	4 142
SEU	28	5	0.14	continuous		8766	1 227
BWRO ⁽¹⁾	25	0.1	0.0025	continuous		8766	22
SWRO ⁽¹⁾	1 250	0.1	0.125	continuous		8766	1096

Notes:

- (1) The contribution of free chlorine in this stream has not been included in the modelled discharge, since the reverse osmosis plants had not been planned at the time of modelling.

In addition to advection and dispersion, the fate of the chlorine is dependent on decay processes as described in Section 5.1.3.1. As described in the same section, it is more appropriate for free chlorine to be modelled as Total Residual Oxidants (TRO). This has been adopted here.

5.7.2 Results

The scenarios described above were modelled and post-processed as described in Section 5.4.3 to produce statistical outputs informing the ecological assessment (Lwandle, 2017). In addition to the ecological guidelines determined for the screening of constituents presented in Section 4.4, the results were also post-processed using other ecological thresholds of significance to further inform the ecological risk assessment. A list of the prepared outputs is presented in Table 5-8, with linked references to Annexure B in which the figures are presented.

Table 5-8: Summary of model results for free chlorine dispersion presented in Annexure B

Scenario	Statistic Plotted	Guideline	Level	Reference
Releases during operation at full capacity	Annual duration that guideline concentration is exceeded [% of time]	0.003 mg/l	Surface	Figure B-31
			Seabed	Figure B-32
	Annual duration that guideline concentration is exceeded [% time]	0.01 mg/l	Surface	Figure B-33
			Seabed	Figure B-34
	95th percentile TRO concentration [mg/l]	-	Surface	Figure B-35
			Seabed	Figure B-36
	Time series of TRO concentration at sensitive receptors [mg/l]	-	Surface and Seabed	Figure B-37 to Figure B-42



5.8 Dispersion Modelling: Hydrazine

5.8.1 Discharge Configuration

Two scenarios for the release of hydrazine were modelled. The first scenario corresponds to the hydrazine releases which occur during plant operation at full capacity. These include the following:

- Daily releases of low concentration hydrazine via SEK;
- Monthly releases from XCA via SEO-N corresponding to partial draining of auxiliary boiler tanks; and
- Semi-annual releases from XCA via SEO-N due to complete draining of auxiliary boiler tanks.

The releases from XCA correspond to the draining of the same tanks and therefore do not co-occur. The configuration of this release scenario is presented in Table 5-9. To increase the number of environmental conditions sampled, the scenario was repeated 6 times while discharging the monthly and semi-annual releases at different times in each repetition.

Table 5-9: Configuration of hydrazine releases: plant operation at full capacity

Stream	Discharge [m ³ /h]	Concentration [mg/l]	Load [kg/h]	Duration [h]	Release interval [days]	Total duration per year [hrs]	Total Annual Load [kg]
SEK_A	300	0.2	0.06	6	1	2 192	131
XCA_A	60	300	18	0.42	Monthly	5.00	90
XCA_B	60	300	18	1.17	Twice per year	2.33	42

The second scenario corresponds to the exceptional releases of hydrazine associated with reactor outages. These releases occur over a three week period during outages and consist of the following:

- Daily releases via SEK due to partial draining of the Steam Generators;
- Weekly releases via SEK due to complete draining of the Steam Generators; and
- Releases from XCA via SEO-N occurring once per outage.

The configuration of this release scenario is presented in Table 5-10. Since outages occur at 9 month intervals on average, any given year may contain two outages. For conservatism, two outages were assumed to occur in the modelled year. To increase the number of environmental conditions sampled, this scenario was repeated 6 times while releasing the monthly and semi-annual releases at different times in each repetition.

Table 5-10: Configuration of hydrazine releases: reactor outages

Stream	Discharge [m ³ /h]	Concentration [mg/l]	Load [kg/h]	Duration [h]	Release interval during outage [days]	Total duration per year ⁽¹⁾ [hrs]	Total Annual Load [kg]
SEK_B	80	187.5	15	0.50	1	21	315
SEK_C	80	187.5	15	1.67	7	10	150
XCA_A	60	300	18	0.42	once per outage	0.83	15

Notes:

- (1) Total annual duration calculated assuming hydrazine discharges to occur for three weeks per outage, two outages per year.

In both scenarios the releases from the SEK stream were discharged into the outfall, while the releases via the SEO-N stream were discharged into the intake basin.

In addition to advection and dispersion, the fate of the hydrazine is dependent on decay processes as described in Section 5.1.3.2.



5.8.2 Results

The scenarios described above were modelled and post-processed as described in Section 5.4.3 to produce statistical outputs informing the ecological assessment (Lwandle, 2017). In addition to the ecological guidelines determined for the screening of constituents presented in Section 4.4, the results were also post-processed using other ecological thresholds of significance to further inform the ecological risk assessment. A list of the prepared outputs is presented in Table 5-11, with linked references to Annexure B in which the figures are presented.

Table 5-11: Summary of model results for hydrazine dispersion presented in Annexure B

Scenario	Statistic Plotted	Guideline	Level	Reference
Releases during operation at full capacity	Maximum annual duration that guideline is exceeded [hours]	0.0002 mg/l	Surface	Figure B-43
			Seabed	Figure B-44
	Maximum annual duration that guideline is exceeded [hours]	0.0025 mg/l	Surface	Figure B-45
			Seabed	Figure B-46
	Maximum Hydrazine concentration [mg/l]	-	Surface	Figure B-47
			Seabed	Figure B-48
Releases during outages	Maximum annual duration that guideline is exceeded [hours]	0.0002 mg/l	Surface	Figure B-49
			Seabed	Figure B-50
	Maximum annual duration that guideline is exceeded [hours]	0.0025 mg/l	Surface	Figure B-51
			Seabed	Figure B-52
	Maximum Hydrazine concentration [mg/l]	-	Surface	Figure B-53
			Seabed	Figure B-54



5.9 Dispersion Modelling: Phosphate

5.9.1 Discharge Configuration

The draining of systems containing phosphate occurs during reactor outages. These releases occur in the following streams:

- KER;
- SEK;
- DEL of Unit 1 draining via SEO-N; and
- DEL of Unit 2 draining via SEO-S.

In addition to the phosphate drains described above, leaks of phosphate at low concentrations occur continuously in all effluent streams, as shown in Table 5-12. After dilution under plant operation at full capacity, these leaks fall well below the ecological guideline for phosphates. Therefore, it is not necessary to model phosphate releases for this scenario. However, the total load from the phosphate leaks has been added to the releases described above which occur during outages. The configuration of this release scenario is presented in Table 5-13.

Table 5-12: Characterisation of phosphate leaks into all effluent streams

Stream	Discharge [m ³ /h]	Concentration [mg/l]	Load [kg/h]	Duration [h]	Release interval [days]	Total duration per year [hrs]	Total Annual Load [kg]
External leak (DEL via SEO-N)	0.024	1250	0.030	continuous		8 766	263
External leak (DEL via SEO-S)	0.024	1250	0.030	continuous		8 766	263
External leak (SRI via SEK)	0.240	550	0.132	continuous		8 766	1 157
External leak (SES via SEK)	0.008	550	0.004	continuous		8 766	39
Leak into CRF (SRI via CRF)	0.120	550	0.066	continuous		8 766	579
Leak into CRF (SES via CRF)	0.004	550	0.002	continuous		8 766	19
External leak (DEG via KER)	0.024	1250	0.030	continuous		8 766	263
External leak (RRI via KER)	0.240	550	0.132	continuous		8 766	1 157
Leak to SEC (RRI via SEC)	0.120	550	0.066	continuous		8 766	579
TOTAL LEAKS	0.804	613	0.493	continuous		8 766	4318

Table 5-13: Configuration of phosphate releases during outages

Stream	Discharge [m ³ /h]	Concentration [mg/l]	Load [kg/h]	Duration [h]	Release characterisation during outage	Total duration per year [hrs]	Total Annual Load ⁽¹⁾ [kg]
Leaks	0.804	613	0.493	continuous		8 766	4318
SEK	60	550	33	2	daily for three days	12 ⁽¹⁾	396
KER	25	1 250	31	5	two releases, two days apart	20 ⁽¹⁾	625
DEL via SEO-S	20	1 250	25	2	single release	2 ⁽¹⁾	50
DEL via SEO-N	20	1 250	25	2	single release	2 ⁽¹⁾	50

Notes:

(1) Total annual duration calculated assuming two outages per year. SEO-S and SEO-N releases do not occur during the same outage.

Since outages occur at 9 month intervals on average, any given year may contain two outages. Since the DELs are specific to a reactor unit, the draining of these systems does not occur during the same outage. For conservatism, two outages were assumed to occur in the modelled year, thus each DEL drain is assumed to occur once.



To increase the number of environmental conditions sampled, this scenario was repeated 13 times while discharging the releases at different times in each repetition. The leaks and drains via KER, SEK and SEO-S were discharged at the outfall, while drains via SEO-N were discharged into the intake basin.

Phosphate is modelled as a conservative tracer, i.e. dilution is due to mixing only. This is a conservative approach since biogeochemical reactions will tend to further reduce the concentration of phosphate after discharge.

5.9.2 Results

The scenario described above was modelled and post-processed as described in Section 5.4.3 to produce statistical outputs informing the ecological assessment (Lwandle, 2017). The guideline concentration against which the model results were evaluated is 0.053 mg/l, with a background concentration of 0.037 mg/l. A list of the prepared outputs is presented in Table 5-14, with linked references to Annexure B in which the figures are presented.

Table 5-14: Summary of model results for phosphate dispersion presented in Annexure B

Scenario	Statistic Plotted	Guideline	Level	Reference
Releases during outages	Maximum annual duration that guideline is exceeded [hours]	0.053 mg/l	Surface	Figure B-55
			Seabed	Figure B-56
	Maximum Phosphate concentration [mg/l]	-	Surface	Figure B-57
			Seabed	Figure B-58



5.10 Summary

This section presented the setup and calibration of the hydrodynamic model used for the dispersion modelling, as well as the modelling of the constituents which did not pass the screening test presented in Section 4. These include temperature, free chlorine, hydrazine and phosphate. As requested by the marine ecology specialist, the model results have been post-processed to present plots of the duration that specified guidelines are exceeded, the 95th percentile concentrations (for continuous releases) and the maximum concentrations (for batch releases). These figures are presented in Annexure B. For the continuous release scenarios, time series plots of near-surface and near-seabed concentration at the sensitive receptor locations (see Figure 5-15) are also presented in Annexure B. The interpretation of these results is presented in the report of the Marine Ecology Specialist Study (Lwandle, 2017).



6. RADIONUCLIDE DISPERSION MODELLING

6.1 Discharge Characterisation

The radiological releases from KNPS occur in the SEK and KER streams (see descriptions of the streams in Sections 3.2.4 and 3.2.5). While the dispersion of radionuclides and their accumulation in seabed sediment are modelled here, the accumulation in marine biota is modelled by Eskom using ERICA, a specialised model suited for this purpose.

The total annual load of radionuclides was used for the modelling and was released at a constant rate throughout the year. The annual loads were provided by Eskom and are presented in Table 6-1. The radionuclides highlighted in grey are considered by Eskom to be a lower priority and have thus not been modelled in this study.

Table 6-1: Annual load of radionuclides released at KNPS

Element	Radionuclide	Annual Load [Bq/y]
Silver (Ag)	Ag-110m	1.28E+09
Carbon (C)	C-14	2.05E+10
Cobalt (Co)	Co-58	5.10E+09
	Co-60	1.62E+09
Caesium (Cs)	Cs-134	5.18E+08
	Cs-137	1.26E+09
Iron (Fe)	Fe-55	1.15E+10
Hydrogen (H)	H-3	4.14E+13
Iodine (I)	I-131	1.06E+08
Manganese (Mn)	Mn-54	2.29E+08
Nickel (Ni)	Ni-63	1.54E+10
Tellurium (Te)	Te-123m	5.18E+08

6.2 Model Description

6.2.1 Hydrodynamics

To model the dispersion and fate of radionuclides released from KNPS, the same hydrodynamic and wave models described in Section 5.1.3.1 were coupled to an ECOLab model. The hydrodynamic model description and the generic ECOLab description are presented in Section 5.1. The specific ECOLab template developed for the radionuclide modelling is described below.

6.2.2 ECOLab template for radionuclides

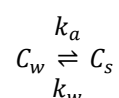
The dispersion of radionuclides in the marine environment is primarily governed by advection and dispersion due to currents and turbulence driven by wind, waves, tides and density gradients, which are represented in the 3D hydrodynamic model described in Section 5. In addition to these processes, radionuclides are subject to chemical reactions such as adsorption and desorption between water and fine particulate matter, physical processes such as the deposition and resuspension of suspended particles and first order decay. An ECOLab template was developed to describe these processes.



The modelling of fine particulate matter was based on the formulations in the MIKE by DHI Mud Transport Module which are described in the Scientific Documentation (DHI, 2014h). The model includes the following processes:

- Advection-dispersion of suspended sediment by currents;
- Settling of suspended sediment and deposition onto the seabed, dependent on the critical shear stress for deposition and the settling velocity;
- Resuspension of sediment from the seabed, dependant on the critical shear stress for resuspension and the erosion coefficient; and
- Bed shear stress due to combined currents and wave orbital velocities.

The adsorption and desorption kinetics are described by a reversible chemical reaction, which can be expressed as:



where C_w is the radionuclide activity concentration per unit volume of water [Bq/L], C_s is the activity concentration per solid mass of particulate [Bq/kg], k_a is the adsorption rate [L/kg/day] and k_w is the desorption rate in water [day^{-1}]. Bq (Becquerel) is the SI unit for radioactivity, and is directly proportional to the mass of radionuclide. The affinity of a radionuclide to be adsorbed onto particulate matter differs between elements and also depends on the nature of the particulate matter and environmental conditions.

The relationship between C_s and C_w at equilibrium is described by the distribution coefficient (K_d), which is defined as (IAEA, 2004):

$$K_d [\text{L/kg}] = \frac{\text{Concentration per unit mass of particulate } (C_s) [\text{kg/kg or Bq/kg dry weight}]}{\text{Concentration per unit volume of water } (C_w) [\text{kg/L or Bq/L}]}$$

The reaction rates for adsorption (k_a) and desorption (k_w) are related according to the distribution coefficient (K_d) as:

$$K_d = \frac{k_a}{k_w}$$

In the model, the adsorption-desorption rates are applied in the water column at each time step. In reality, sorption occurs not only in the water column, but also between bed sediment and pore water. Activity dissolved in pore water can then be transferred to the water column through diffusion. In exposed areas, the mechanism for contamination of the water column by activity in bed sediment is expected to be dominated by resuspension events rather than diffusion between pore water and the water column. The sorption kinetics in pore water and associated contamination through diffusion have not been included in the model.

Another limitation of the model is that the gradual burial of contaminated sediment over extended periods of time is not represented.

The decay of radionuclide activity follows the first order decay formulation, which is expressed as:

$$\frac{dC}{dt} = -kC$$

where C is the activity concentration [Bq/kg or Bq/L] and k is the decay coefficient [day^{-1}]. The decay coefficient differs for each radionuclide. The decay was applied to the activity dissolved in the water column,



the activity adsorbed to suspended sediment in the water column and to the activity adsorbed to sediment on the seabed.

6.3 Model Setup

The radionuclide model was coupled to the hydrodynamic and spectral wave models described in Sections 5.1 and 5.1.3.1, and was run for the year of 2009.

A suspended sediment concentration of 4 mg/l was assumed as the initial condition and was applied along the model boundaries. This is the median concentration observed in measurements through the water column offshore of the KNPS in total water depths ranging between 3 m and 30 m (PRDW, 2012). This is fine cohesive sediment (<63 micron) and comprises both particulate organic matter (POM) and particulate inorganic matter (PIM). These were modelled as one fine sediment fraction characterised by the parameters shown in Table 6-2.

Table 6-2: Input parameters used in the modelling of fine particulate matter.

Parameter	Unit	Value
Settling velocity of suspended sediment	m/s	5×10^{-5}
Critical shear stress for resuspension	N/m ²	0.2
Critical shear stress for deposition	N/m ²	0.1
Resuspension rate	kgDW/m ² /s	1×10^{-4}
Bulk density of dry sediment	kg/m ³ bulk	400

The values of the distribution coefficient (K_d) suggested by the International Atomic Energy Agency (IAEA) for use in models simulating the marine dispersion of radioactive effluent (IAEA, 2004) were used in this study. The values corresponding to the ocean margin were used, and are shown in Table 6-3 for the radionuclides considered in this study. The table also presents the half-life of each radionuclide.

Table 6-3: Distribution coefficients (K_d) and half-lives of radionuclides modelled

Radionuclide	K_d (L/kg); Ocean Margin (IAEA, 2004)	Half-life ($T_{1/2}$)
Ag-110m	1.00E+04	249.76 days
C-14	1.00E+03	5.70E3 years
Co-58	3.00E+05	70.86 days
Co-60		5.27 years
Cs-134	4.00E+03	2.06 years
Cs-137		30.17 years
H-3	1.00E+00	12.32 years
I-131	7.00E+01	8.02 days
Mn-54	2.00E+06	312.12 days

In a study of adsorption-desorption kinetics of a range of radionuclides (Nyffeler, et al., 1984), it was found that the adsorption rate constant (k_a) varied over several orders of magnitude for different radionuclides. However, the variability of the desorption rate in water (k_w) was found to be significantly lower, varying over only one order of magnitude. The k_w measured for Caesium of 1 day⁻¹ has been successfully applied in previous radionuclide dispersion modelling studies ((Periáñez, 2000), (Periáñez, 2005), (Periáñez, 2012)) as a constant for all radionuclides. This rate has therefore been applied in this study.



The initial concentrations and boundary conditions for activity were set to zero. For a given radionuclide, the activity was discharged at a constant rate and activity concentration (Bq/m^3), corresponding to the total annual load (see Table 6-1). The discharge rate corresponds to that which occurs when the plant is operating at full capacity (i.e. $94.5 \text{ m}^3/\text{s}$).

The modelled year was repeated a number of times for each radionuclide. In each successive run, the concentrations of the activity dissolved in the water column, the activity adsorbed to particles suspended in the water column and the adsorbed activity in the seabed sediment at the end of the previous run were applied as initial conditions for the next run. For radionuclides with long half-lives, the model was repeated four times, which is the minimum number of repetitions required to derive and confirm the steady state concentrations of activity accumulated in the seabed sediment. For radionuclides with sufficiently short half-lives, the steady state concentration of activity accumulated in the seabed was reached before the fourth repetition, rendering further repetitions redundant.

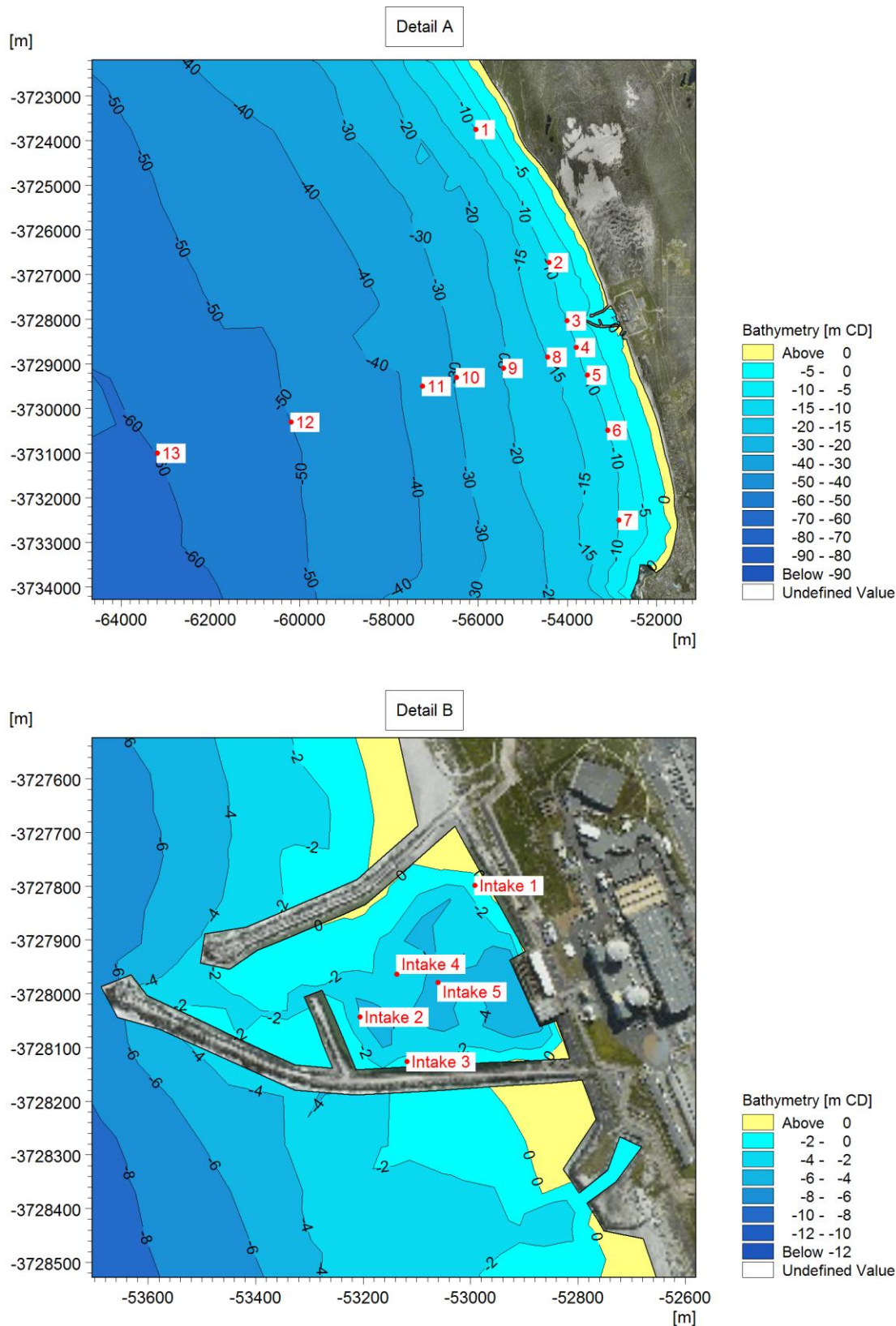
6.4 Model Calibration

6.4.1 Distribution of Fine Sediment on the Seabed

To aid the calibration of the radionuclide dispersion model, sediment grab samples were taken at the locations shown on Figure 6-1 and Figure 6-2. Sieve analyses were carried out on each of the samples to determine the percentage fines ($<75 \text{ micron}$). In addition to the grab samples taken for this study, analysed sediment samples were also available from historical studies in the following areas:

- 5 km to the west, north-west and north of Robben Island (7 Sea Geosciences, 2012);
- 7 km offshore of Mouille Point and Sea Point (Van Ballegooyen, et al., 2006); and
- 5 km north-east of Robben Island (CSIR, 2003)

The percentage fines from all the available sources are shown together in Figure 6-3.



2015\S2015_Koeberg\Models\HD\07\Sampling_Locations\Sampling_Locations_Actual_Detail1.png

Figure 6-1: Grab sample locations offshore of KNPS (Detail A) and inside the KNPS intake basin (Detail B).

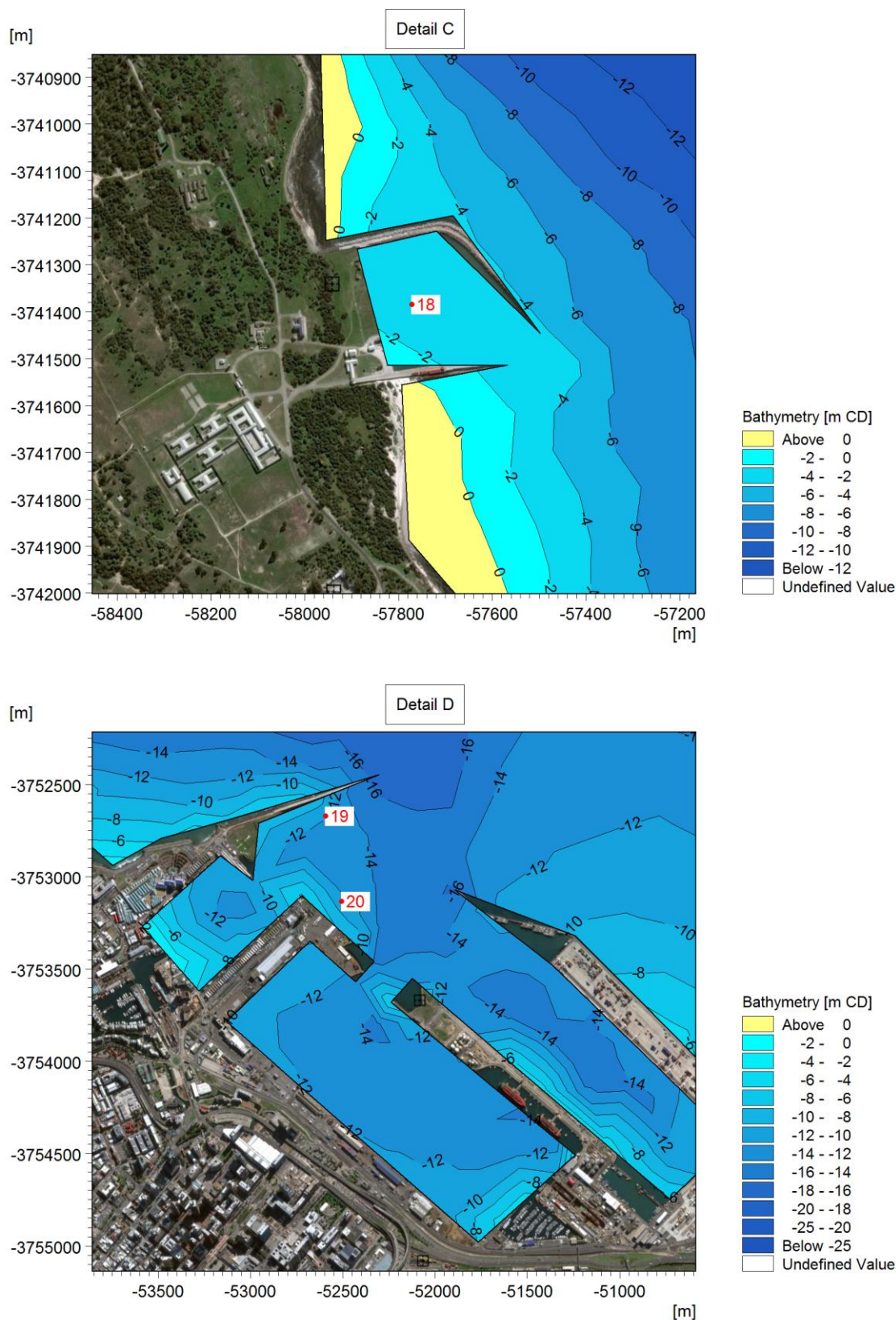


Figure 6-2: Grab sample locations in Murray's Harbour on Robben Island (Detail C) and in the Port of Cape Town (Detail D).

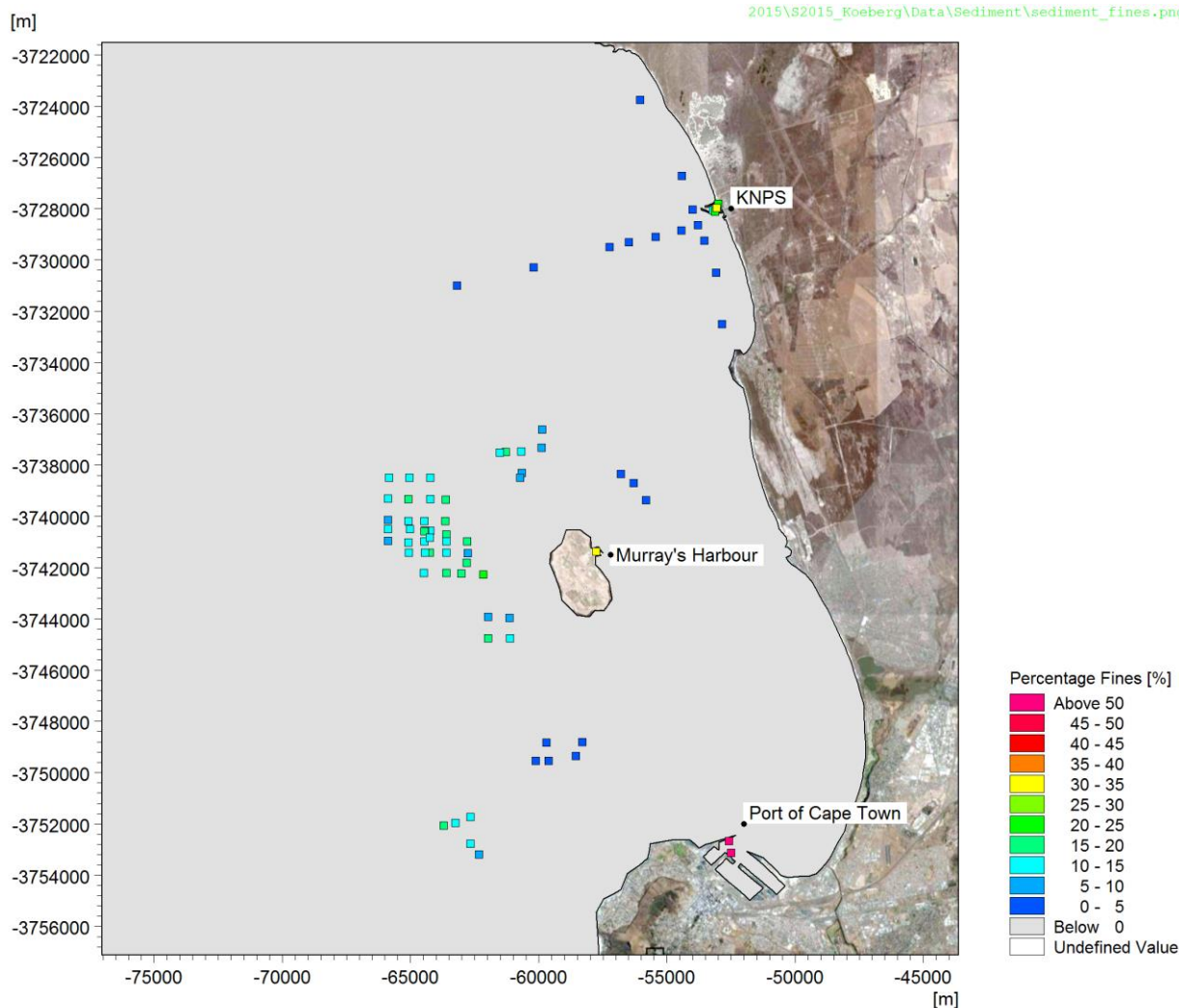


Figure 6-3: Percentage fines obtained from a number of sediment sampling campaigns.

The fines percentages at the -10 m CD contour along the Koeberg shoreline (Sites 1 to 7) and along the cross-shore transect extending to -60 m CD (Sites 8 to 13) were found to be insignificant. In deeper water offshore of Robben Island, the analyses showed fines percentages of approximately 10% to 15%. This suggests the temporary deposition of fine particulate matter, i.e. most of the time the bed shear stresses are sufficiently low for deposition to occur, but resuspension occurs during storm events with large waves. The permanent depo-centres were identified by a high percentage fines and include the KNPS intake basin, the Port of Cape Town and Murray's Harbour (on Robben Island).

To validate the bed shear stress formulation used in the dispersion model, the 95th percentile bed shear stress at each sample location was plotted against the measured fines percentage, as shown in Figure 6-4. The expected behaviour is that areas with low bed shear stresses allow for the deposition of fines and will therefore reflect a high fines percentage. As shown in the figure, this trend is supported. The distinction between permanent depo-centres and areas with temporary deposition (fines percentages of approximately 10 - 15%) occurs at a 95th percentile bed shear stress in the order of 0.2 N/m². This supports the choice of the critical bed shear stress for deposition of 0.1 N/m² and the critical bed shear stress for resuspension of 0.2 N/m².

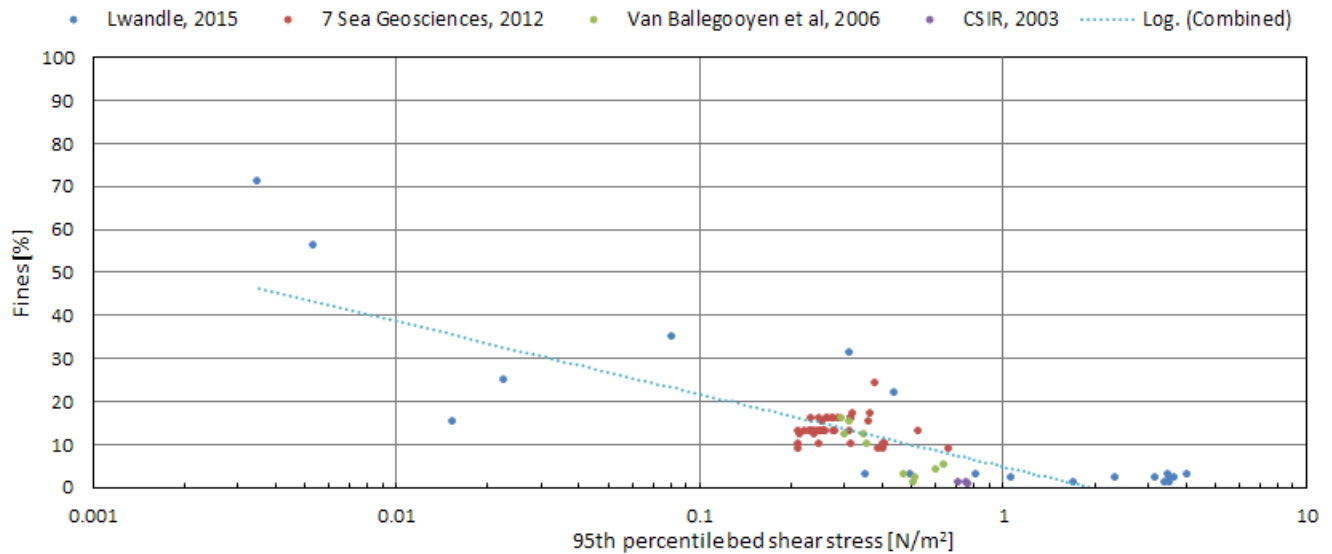
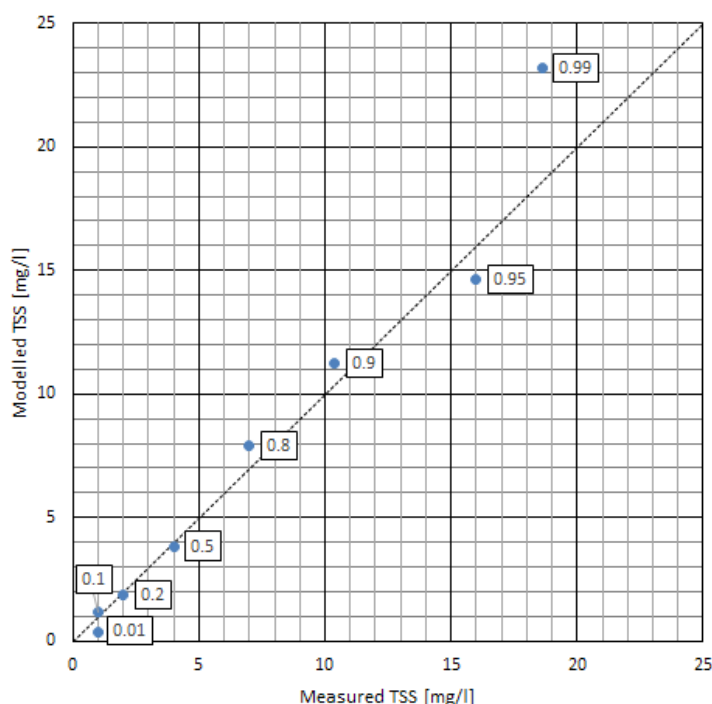


Figure 6-4: Correlation of the percentage fines measured in grab samples of the seabed sediment and the 95th percentile modelled bed shear stress.

6.4.2 Suspended Sediment Concentrations

In addition to the accurate prediction of long-term depo-centres, it is important that the background suspended sediment concentration in the model is representative of local conditions. Figure 6-5 presents a scatter plot comparing percentiles of the modelled TSS (Total Suspended Sediment) concentrations to those measured offshore of the KNPS in total water depths ranging between 3 m and 30 m (PRDW, 2012). The figure shows good agreement between the distributions of modelled and measured TSS concentrations. The modelled background suspended sediment is therefore considered to be sufficiently accurate for the purposes of this study.



Percentile	TSS Concentration [mg/l]	
	Measured	Modelled
0.01	1.0	0.4
0.1	1.0	1.2
0.2	2.0	1.9
0.5	4.0	3.9
0.8	7.0	7.9
0.9	10.4	11.2
0.95	16.0	14.6
0.99	18.6	23.2

E:\Projects\2015\2015_Koeberg\Models\HD\07\07_02aa_Decoupled_MT_c.mfm - Result Files\PostProcess\TSS_Calibration_c.xlsx\Plot

Figure 6-5: Comparison of measured and modelled total suspended sediment (TSS) concentrations offshore of the KNPS in water depths from 3 m to 30 m.

6.4.3 Radionuclide Activity in Bed Sediment

In addition to the sieve analyses, the sediment grab samples taken for this study (locations shown in Figure 6-1 and Figure 6-2) were analysed by Eskom for radioactivity by means of gamma-ray spectrometry. Measurable radioactivity originating from KNPS was found in the KNPS intake basin, the Port of Cape Town and Murray's Harbour. No measureable activity was found in any of the exposed sites (sites 1 to 13).

To compare the modelled and measured activity in each of the permanent depo-centres, the following approach was used:

- The activity concentration in the seabed sediment is modelled in units of Bq/m², while the activity is measured as Bq/kg of sediment. In order to convert the modelled activity to Bq/kg, it was assumed that the accumulated activity is mixed in the top 10 cm of the seabed sediment, which approximately corresponds to the penetration depth of a grab sample. A bulk density of 400 kg/m³ was assumed for the seabed sediment, based on the measured particle size distribution of the samples.
- The steady-state activity at each of the sample locations was forecast from model results. The derivation of the steady state is discussed in Section 6.5.1.
- Since the KNPS intake basin is continuously dredged, it cannot be guaranteed that the steady state concentration will be reached. Therefore, for this depo-centre the concentration after 1 year was extracted rather than the steady state concentration.
- Within each depo-centre, the average over all the sample locations was calculated for both the modelled and measured activity concentration.



The resulting modelled and measured activity concentrations at the three depo-centres and at the deepest exposed location (Site 13) are shown in Figure 6-6. The Minimum Detectable Activity (MDA) for each radionuclide represents a threshold below which the confidence in measured activity is lower than a predetermined level required to positively confirm its presence. In other words, activity below the MDA may be present at the measurement location, but it cannot be confirmed with certainty. Therefore, if no activity is positively measured, the MDA represents the upper limit of activity that could be present at the location. In cases where no activity was measured for a specific radionuclide, the MDA is thus shown to indicate the upper limit of the possible activity for comparison with model predictions.

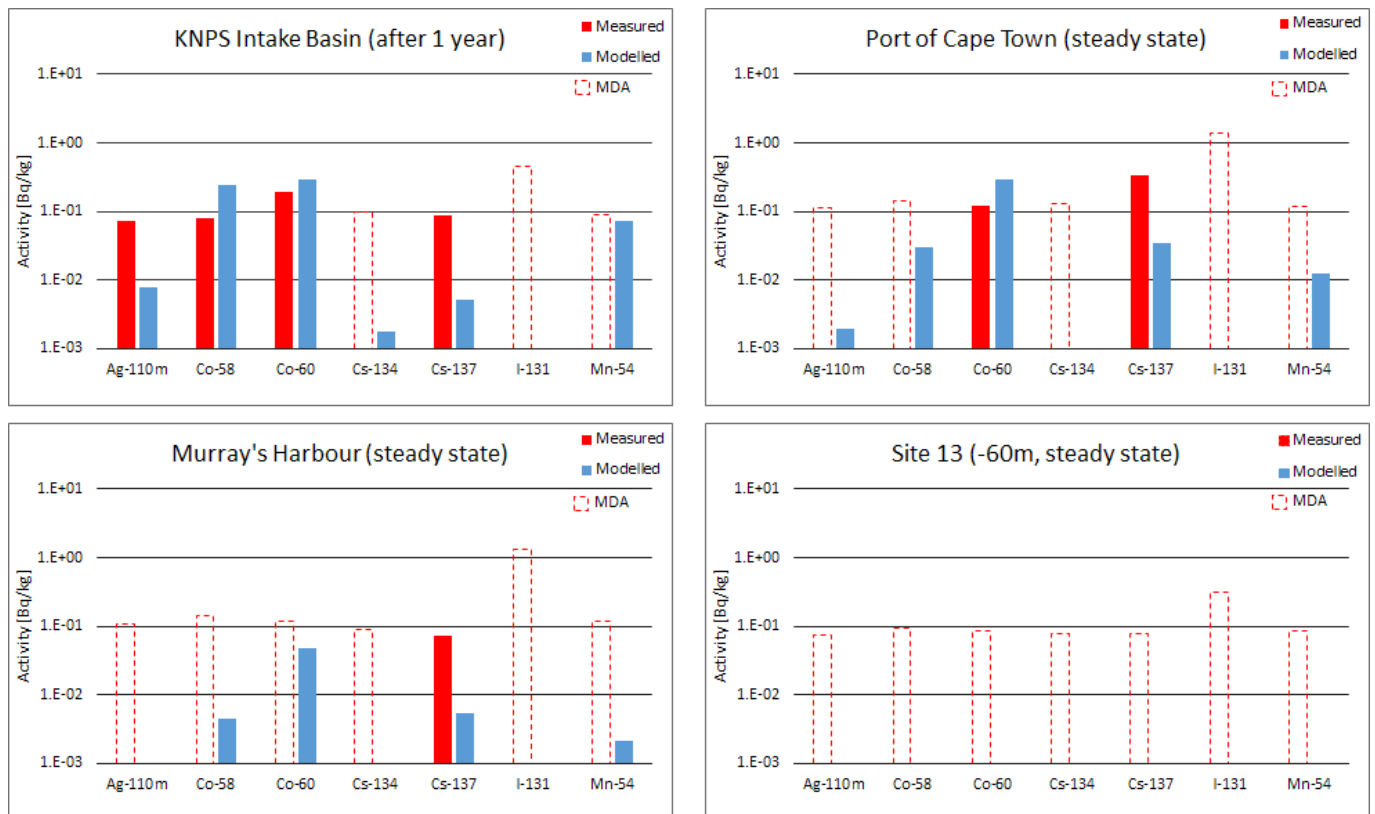


Figure 6-6: Comparison of measured and modelled radionuclide activity in bed sediment. The dotted red bars represent the Minimum Detectable Activity (MDA) of the radionuclide and are shown where measured activity was not sufficient to positively identify a radionuclide. The modelled bars (blue) indicate the predicted steady state concentration at all sites except in the KNPS intake basin which is continually dredged and thus only one year of accumulation is assumed.

In the KNPS intake basin, good agreement between modelled and measured activity is observed for the cobalt isotopes, while the model is found to under predict the accumulation of Ag-110m and Cs-137. For Cs-134 and Mn-54, no activity is measured while activity is predicted. Since the modelled activity is lower than the relevant MDA, this is a positive model calibration. For I-131, activity is neither measured nor predicted, owing to the 8 day half-life of I-131.

In the port of Cape Town, the trends are similar to those observed in the KNPS intake basin, with good agreement for Co-60 and an under prediction for Cs-137. For all other radionuclides, the predicted activity is below the MDA and is therefore considered to be positively calibrated.

In Murray's Harbour, only Cs-137 was measured, which has a long half-life of 30.2 years and a high affinity for adsorption. Similar to the other depo-centres, the model is shown to under predict the accumulation of



Cs-137. For all other radionuclides, the predicted accumulation is below the MDA and is therefore considered to be a positive calibration.

At Site 13, the deepest of the exposed sample locations, activity is not measured nor predicted. This serves to indicate that the location is not a permanent depo-centre and therefore further confirms the accuracy of the modelled suspended sediment dynamics.

The overall under prediction of the accumulation of Cs-137 may be caused by a higher affinity for adsorption (K_d) than was used in the model. These distribution coefficients are not known quantities and vary based on the nature of the particulate matter and environmental conditions. Furthermore, the repetition of one modelled year excludes any inter-annual trends in environmental conditions and the use of constant discharge concentrations precludes the short-term variability such as the co-occurrence of acute discharges with resuspension events. Considering the uncertainties in the input data and the limitations of the model, the overall calibration of the model to the measured activity is considered to be good.

A preliminary comparison indicated that the measured radionuclide activity in each of the depo-centres is significantly lower than the applicable Environmental Media Concentration Limits, although this will be investigated further by Eskom using the ERICA and PC-CREAM models.



6.5 Model Results

6.5.1 Results for Co-60

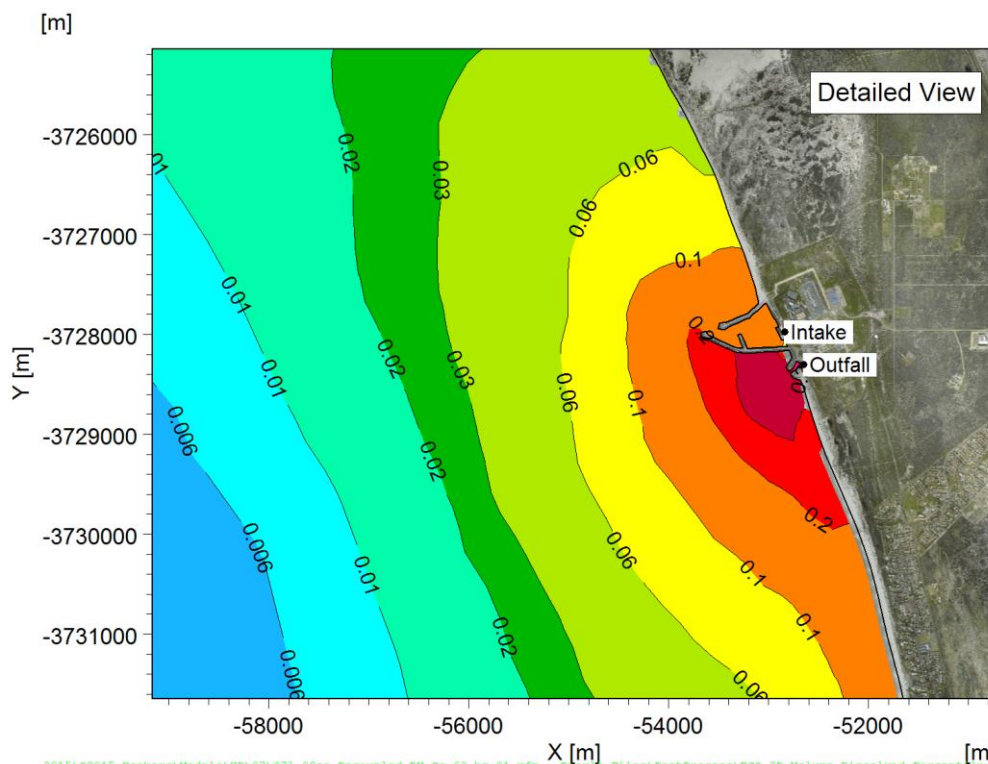
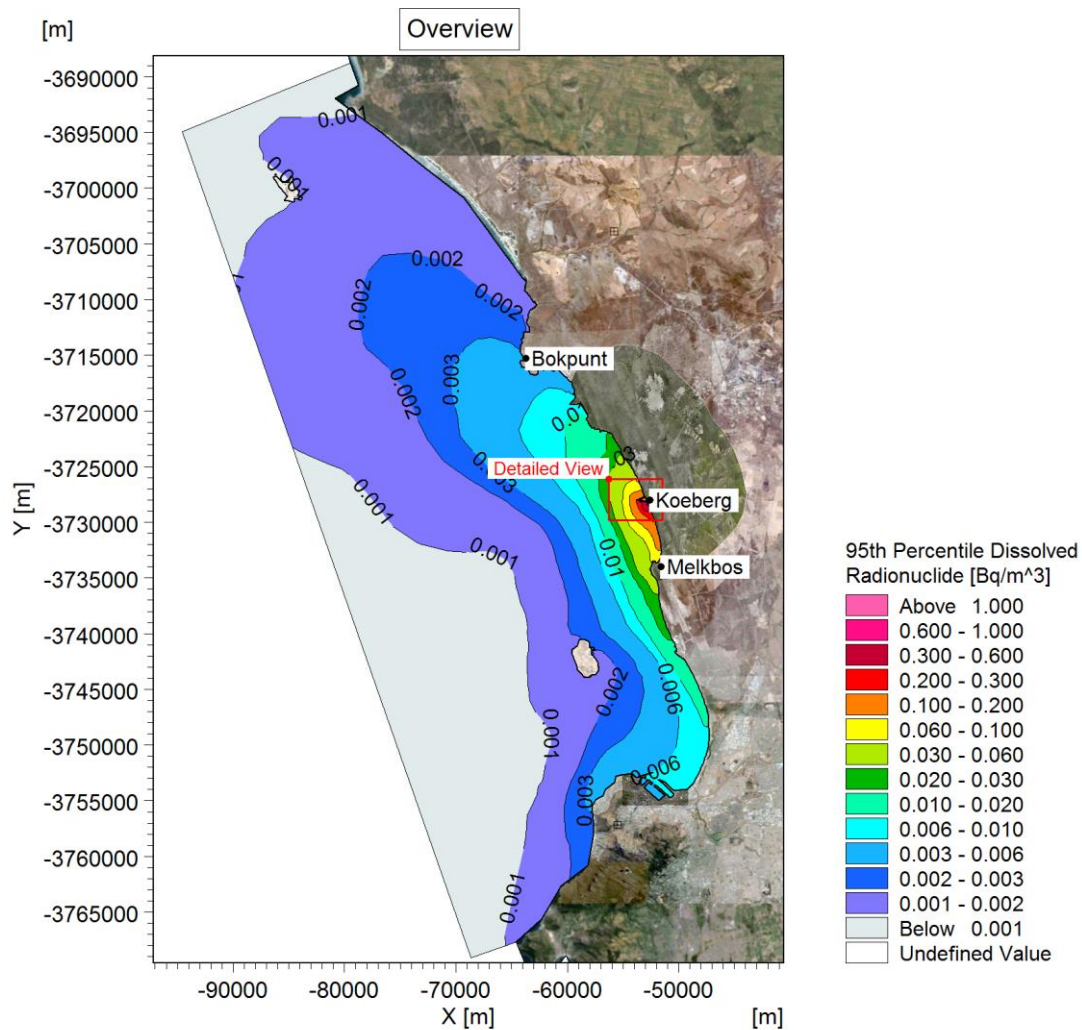
Recall that cobalt has a high affinity for adsorption ($K_d = 3 \times 10^5 \text{ L/kg}$) and is therefore an appropriate choice of radionuclide to indicate the dispersion of activity in both dissolved and adsorbed phases. Therefore, the model results for Co-60 are presented in this section, while the results for the remainder of the modelled radionuclides are presented in Annexure C. It is important to note that the colour scales of the figures differ between radionuclides. These scales were chosen to reflect modelled concentrations and were not based on environmental concentration limits. Areas shown on the plots therefore do not imply exceedance of environmental limits.

Figure 6-7 and Figure 6-8 present the near-surface and near-seabed 95th percentile concentration of activity dissolved in the water column. During summer conditions when south-easterly winds dominate, the plume is often advected northward. Due to Coriolis force, when currents flow northward along the coast, the surface currents are deflected offshore and the seabed currents are deflected onshore. This effect is enhanced by water column stratification which is characteristic of summer conditions. Therefore, to the north there is a big difference between the dispersion near the surface and seabed.

In winter months, north-westerly winds drive the plume southward. However, during winter the water column is generally well-mixed. Therefore, to the south the concentrations near the surface and near the seabed are similar.

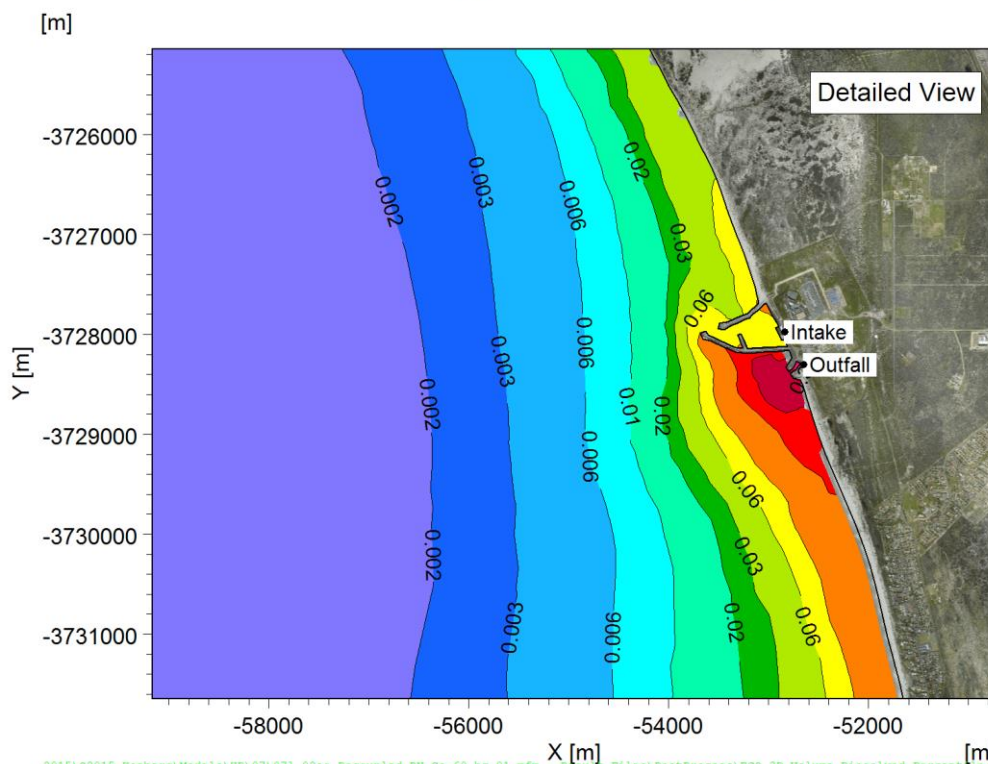
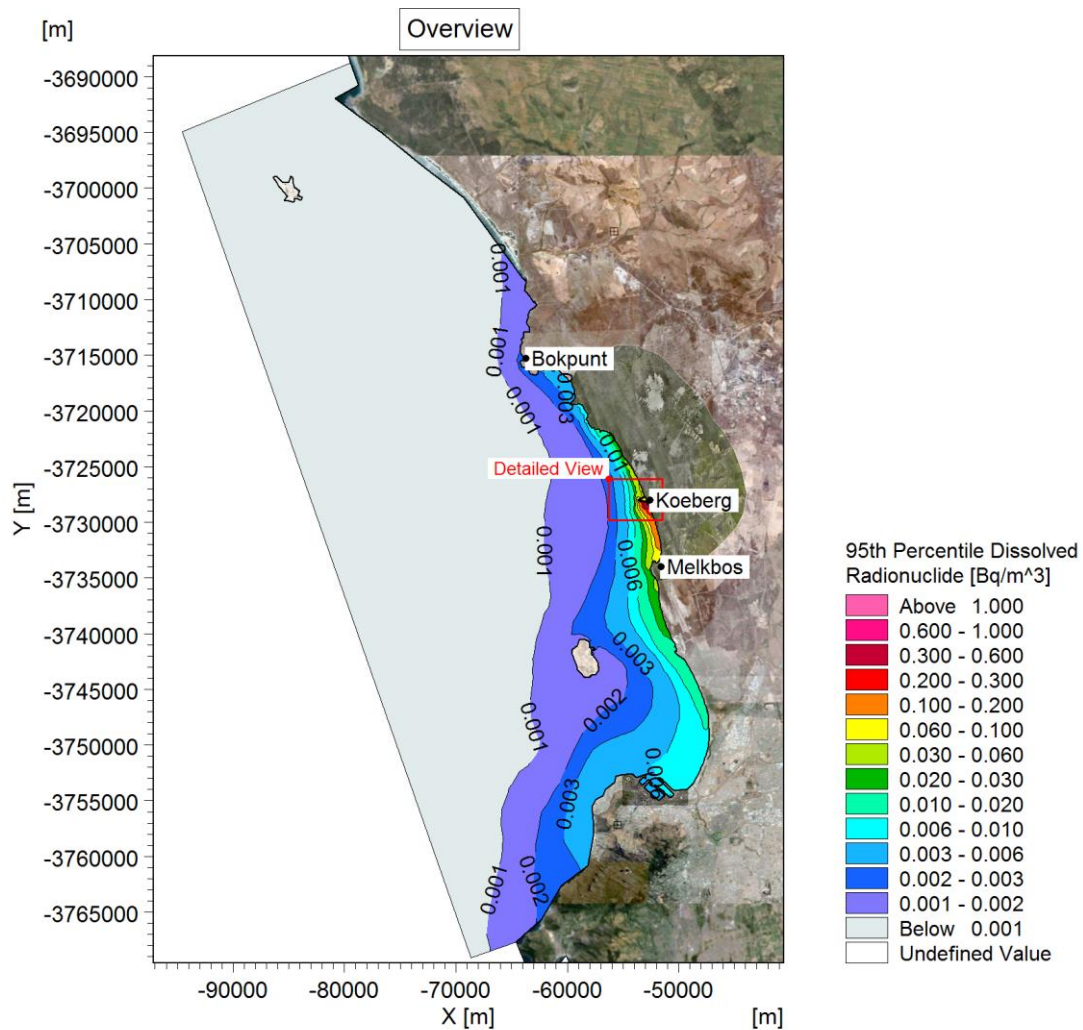
Figure 6-9 and Figure 6-10 present the near-surface and near-seabed 95th percentile concentration of activity adsorbed onto suspended sediment. In close proximity to the KNPS outfall, the dispersion of adsorbed radionuclides is similar to that of the dissolved radionuclides. However, as the plume moves further away from the source, the suspended matter settles deeper into the water column. This can be observed in the near-seabed layer which has a higher activity concentration than the surface layer due to settling of the particles from the surface and resuspension of particles from the seabed.

Figure 6-11 and Figure 6-12 present the maximum activity concentration in the seabed sediment over the first modelled year. As for the model calibration, the activity concentration was converted from Bq/m^2 to Bq/kg by assuming a mixing depth of 10 cm and a bulk density of 400 kg/m^3 . The highest concentrations are observed in the sheltered depo-centres, i.e. the KNPS intake basin, the Port of Cape Town and Murray's Harbour. Accumulation also occurs in exposed areas where the water depth is greater than approximately 70 m. The maximum concentration gradually reduces toward the shore, as the bed shear stress due to waves increases with decreasing water depth and therefore prevents long-term accumulation of fine sediment.



2015\S2015_Koeberg\Models\HD\07\071_02aa_Decoupled_RN_Co-60_bc_01.mfm - Result Files\PostProcess\ECO_3D_Volume_Dissolved_Percentile_95th_Lay6.png

Figure 6-7: 95th percentile concentration of dissolved Co-60 activity in the water column: near-surface.



2015\S2015_Koeberg\Models\HD\07\071_02aa_Decoupled_RN_Co-60_bc_01.mfm - Result Files\PostProcess\ECO_3D_Volume_Dissolved_Percentile_95th_Lay1.png

Figure 6-8: 95th percentile concentration of dissolved Co-60 activity in the water column: near-seabed.

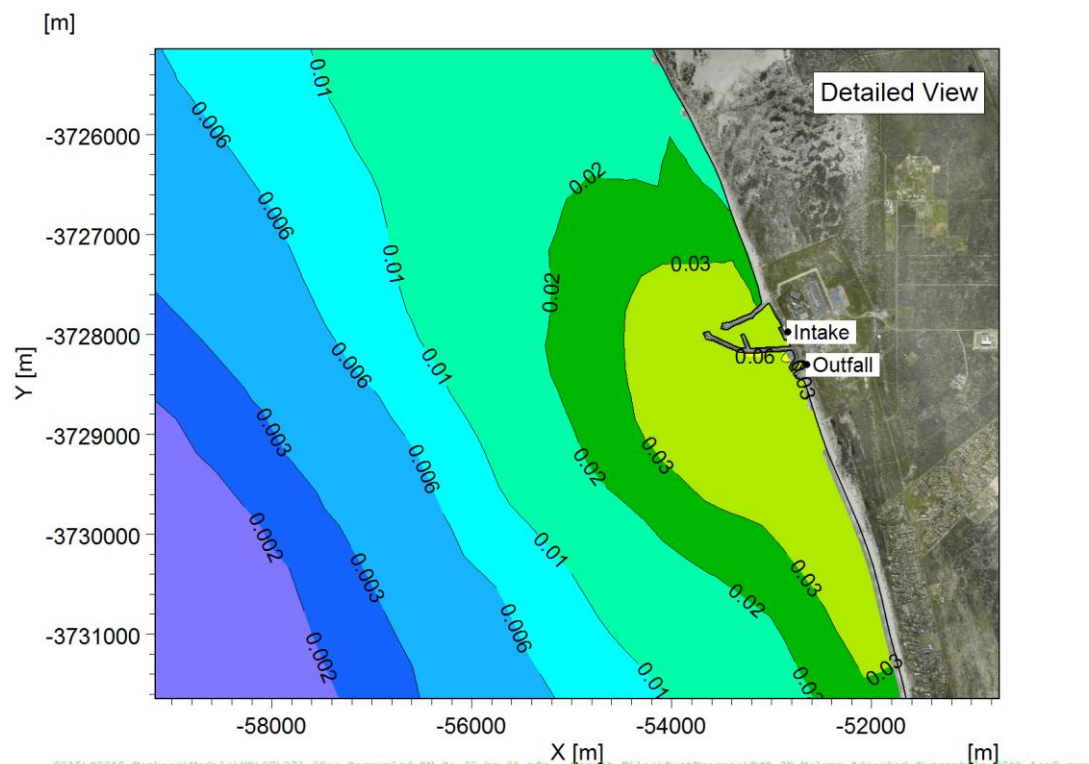
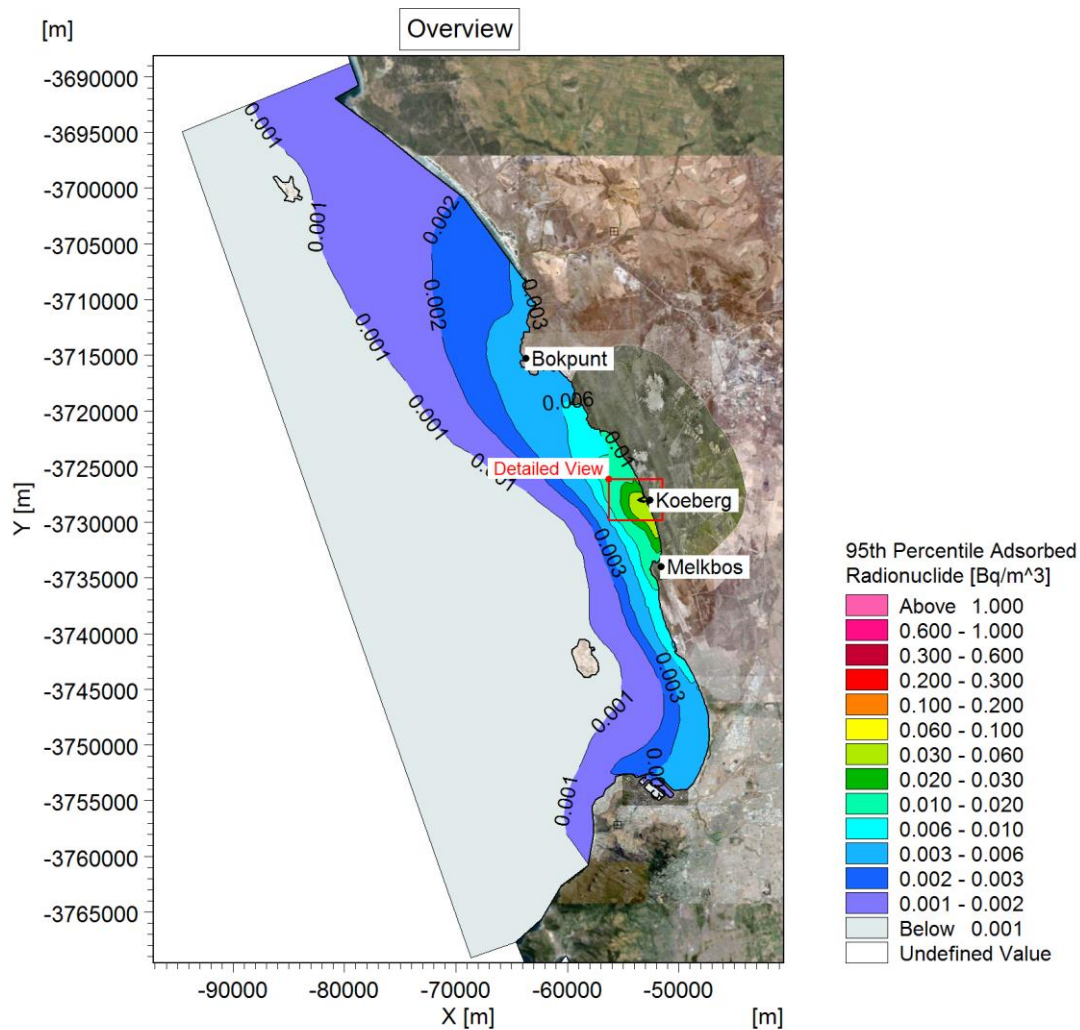
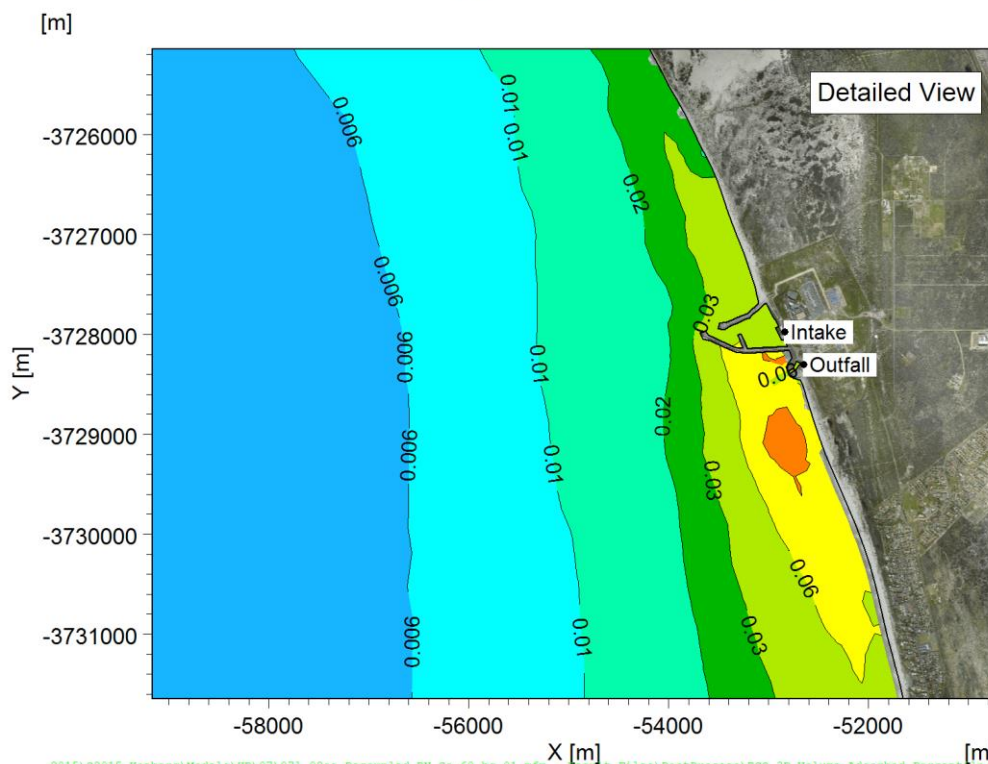
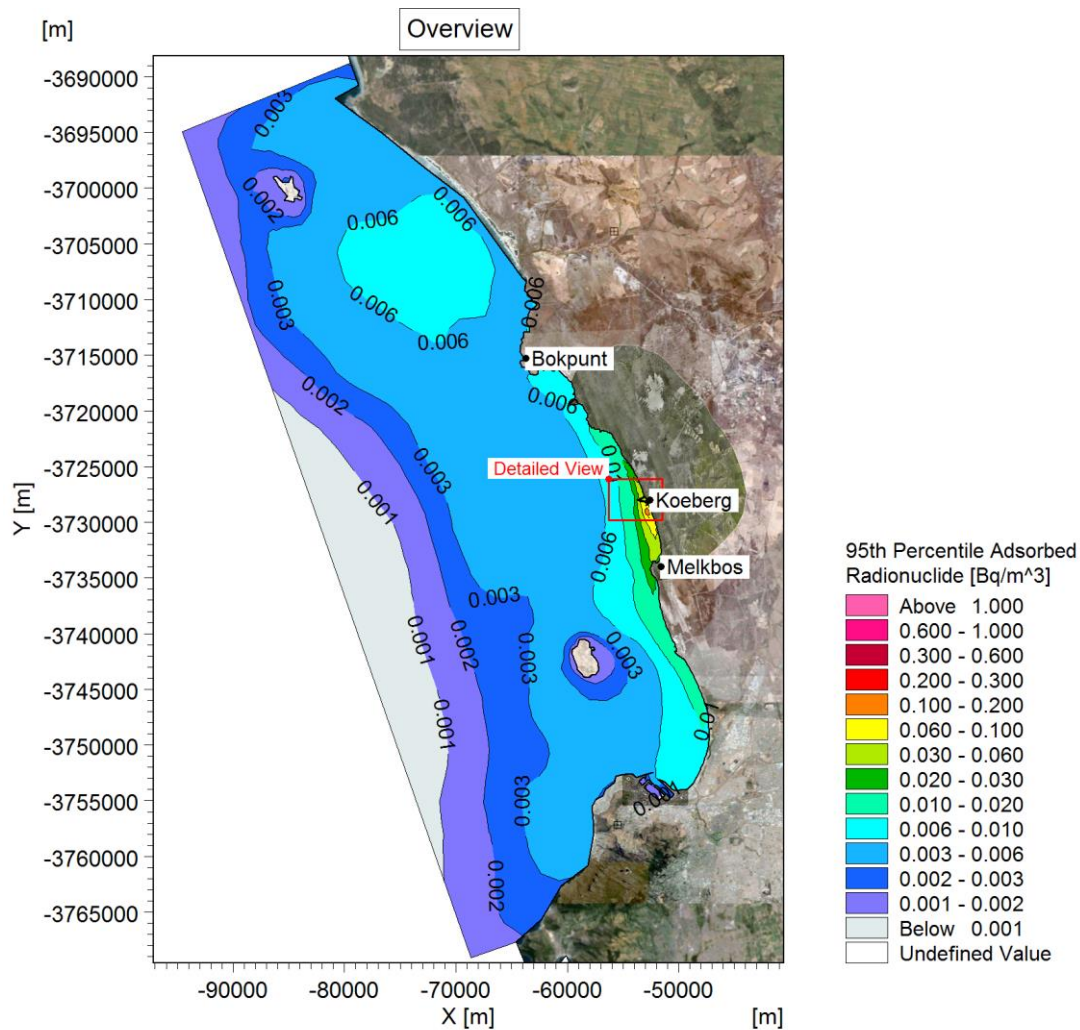


Figure 6-9: 95th percentile concentration of adsorbed Co-60 activity in the water column: near-surface.



2015\S2015_Koeberg\Models\HD\07\071_02aa_Decoupled_RM_Co-60_bc_01.nfm - Result Files\PostProcess\ECO_3D_Volume_Adsorbed_Percentile_95th_Lay1.png

Figure 6-10: 95th percentile concentration of adsorbed Co-60 activity in the water column: near-seabed.

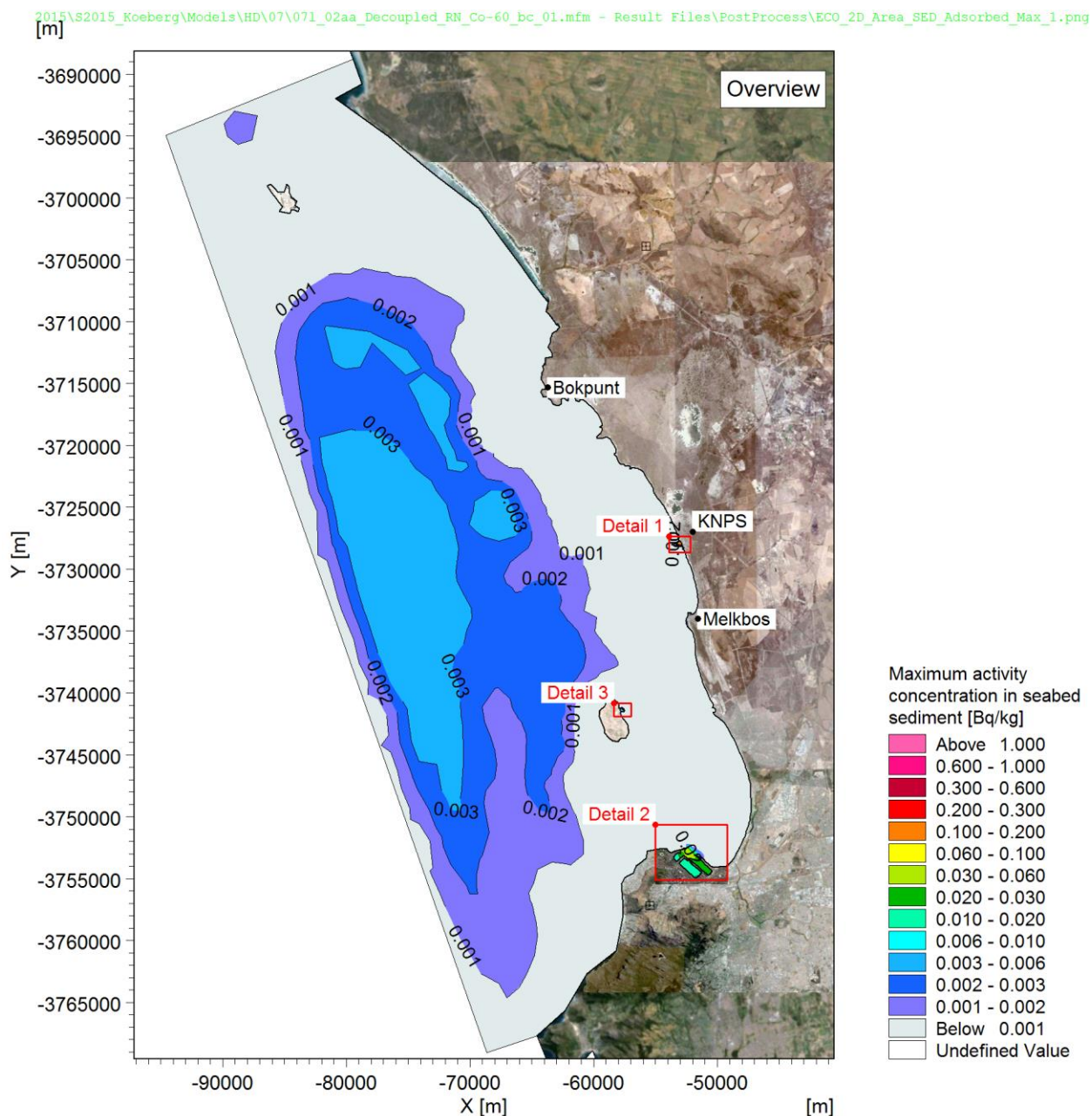


Figure 6-11: Maximum concentration of Co-60 activity in seabed sediment in one modelled year: overview.

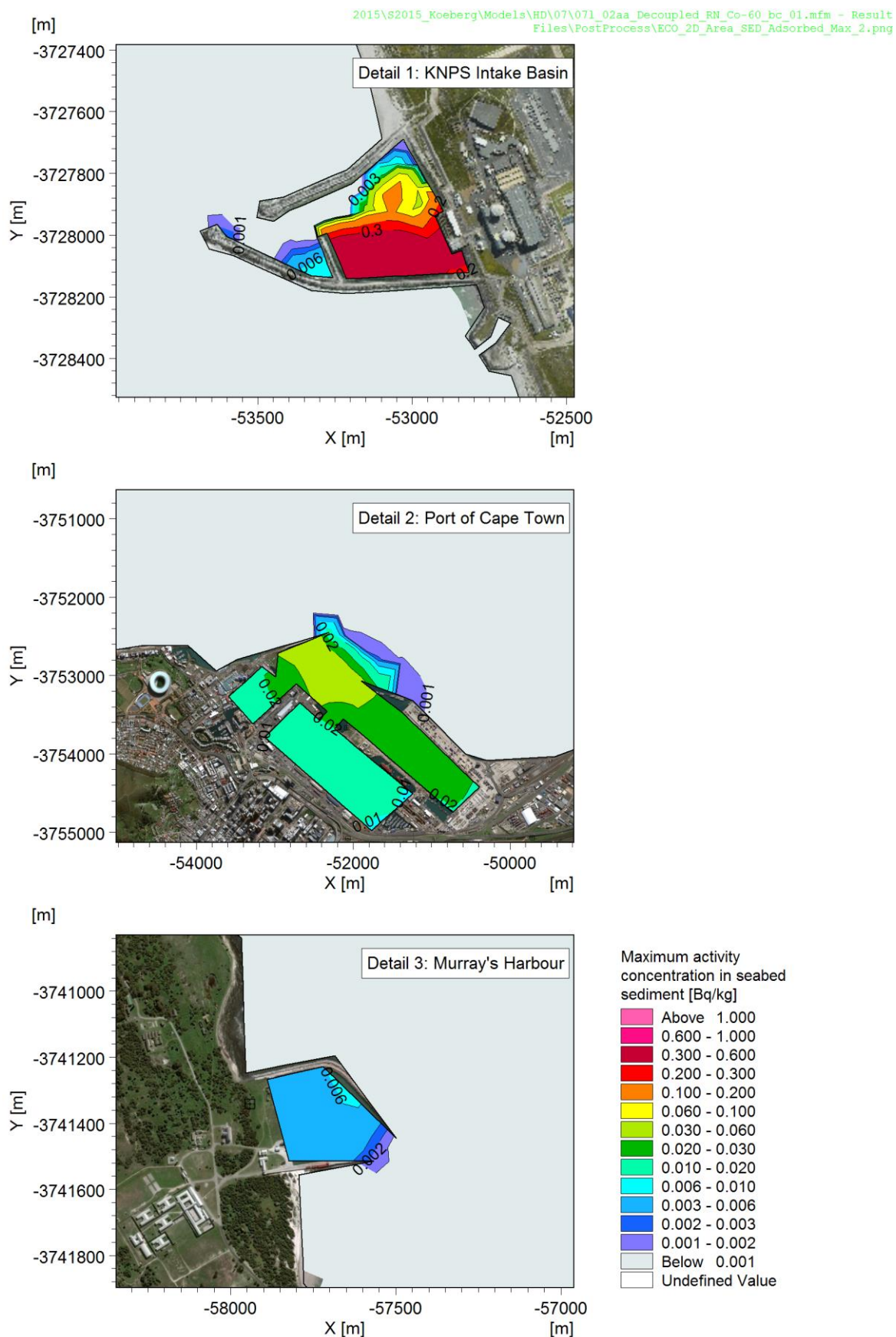


Figure 6-12: Maximum concentration of Co-60 activity in seabed sediment in one modelled year: detail of depo-centres.



Time series of the activity concentration in the seabed sediment at a single point in each of the three depo-centres are shown in Figure 6-13 for the four repetitions of the modelled year. The delay in the accumulation at the Port of Cape Town and Murray's Harbour are due to the travel time of the plume from its discharge point at KNPS.

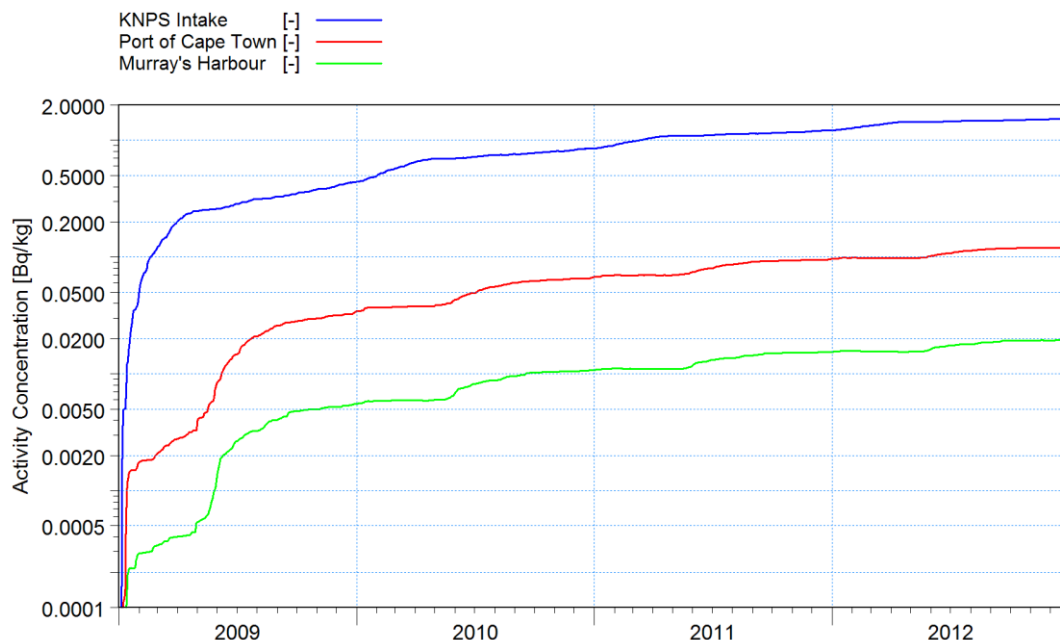


Figure 6-13: Time series of concentration of Co-60 activity in the seabed sediment at the three depo-centres. For comparative purposes, the concentration is plotted on a logarithmic scale.

A steady state will be reached when the activity decayed is balanced by the activity deposited. As can be observed from the time series, the activity concentrations have not reached steady state after the four modelled years. Therefore, steady state concentrations were forecast based on the trends observed in the four modelled years by determining the rate of change of activity concentration, as shown in Figure 6-14. These apply to the average over all the sample locations within a depo-centre.

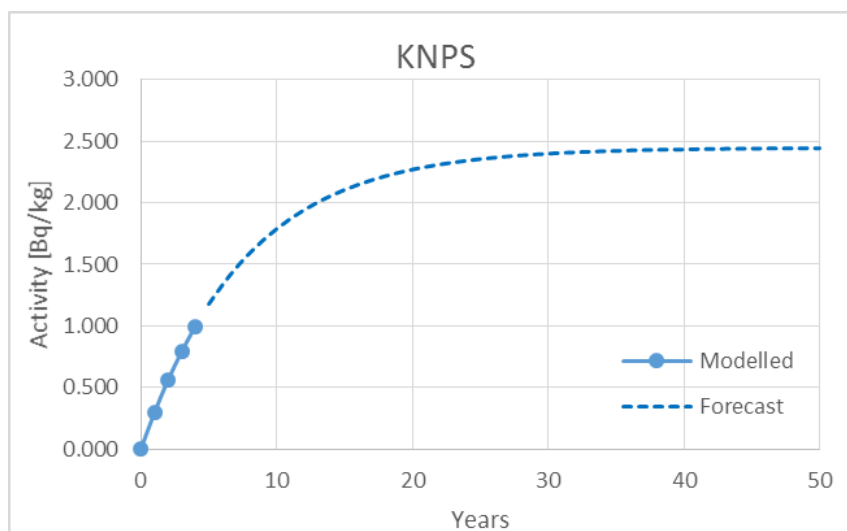


Figure 6-14: Predicted steady state concentration of Co-60 in the KNPS intake basin.

6.5.2 Results for Remaining Radionuclides

Results for the remainder of the modelled radionuclides are presented in Annexure C.

The steady state concentrations in the three depo-centres are listed in Table 6-4 for all modelled radionuclides. Generally, the activity concentration in the KNPS intake basin is approximately one order of magnitude greater than that in the port of Cape Town, which is approximately one order of magnitude greater than that in Murray's Harbour.

Table 6-4: Predicted steady state concentrations of radionuclides released from KNPS.

Radionuclide	Annual Load [Bq/y]	Kd (L/kg); Ocean Margin (IAEA, 2004)	Half-life (T _{1/2})	Steady State Activity Concentration in Bed Sediment [Bq/kg]		
				KNPS Intake Basin ⁽¹⁾	Port of Cape Town	Murray's Harbour
Ag-110m	1.28E+09	1.00E+04	249.76 days	0.013	0.002	0.000
C-14	2.05E+10	1.00E+03	5.70E3 years	1.132	0.167	0.026
Co-58	5.10E+09	3.00E+05	70.86 days	0.258	0.030	0.005
Co-60	1.62E+09		5.27 years	2.439	0.291	0.048
Cs-134	5.18E+08	4.00E+03	2.06 years	0.006	0.001	0.000
Cs-137	1.26E+09		30.17 years	0.232	0.034	0.005
H-3	4.14E+13	1.00E+00	12.32 years	Low ⁽²⁾	Low ⁽²⁾	Low ⁽²⁾
I-131	1.06E+08	7.00E+01	8.02 days	0.000	0.000	0.000
Mn-54	2.29E+08	2.00E+06	312.12 days	0.128	0.012	0.002

Notes:

- (1) Due to continuous dredging operations in the KNPS intake basin, the activity is not expected to reach steady state concentrations.
- (2) Tritium (H-3) has a very low affinity for adsorption to sediment ($K_d = 1$ L/kg).

6.6 PC CREAM Model Input Parameters

In addition to the modelling of the radionuclide dispersion, the model was also used to provide available hydrodynamic characteristics of local ocean compartments for use by Eskom in a box model called PC CREAM. The layouts of three compartments (or 'boxes') as agreed with Eskom are shown in Figure 6-15.

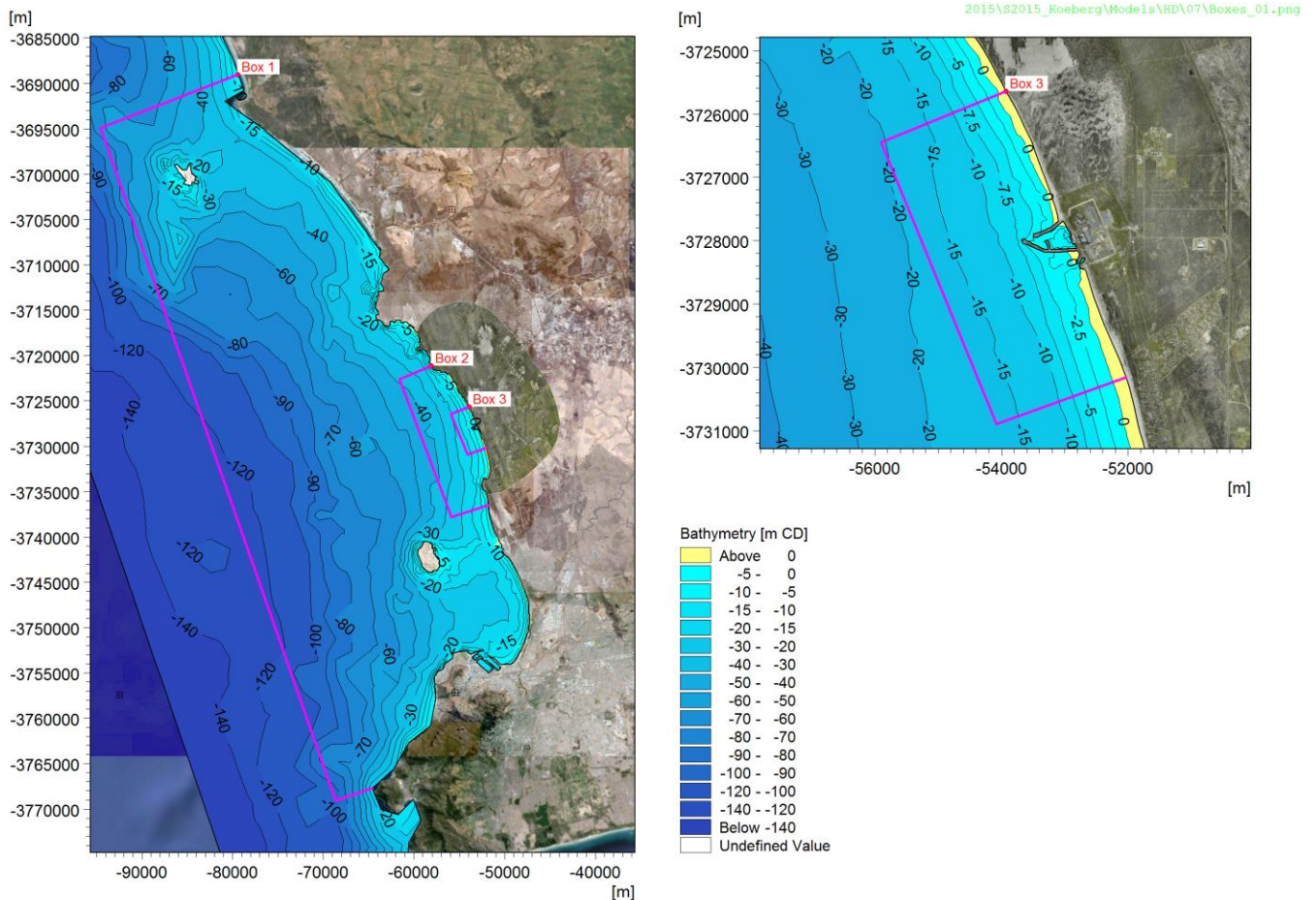


Figure 6-15: Layout of Boxes 1, 2 and 3 of which the PC CREAM input data are summarised in Table 6-5.

The characteristics of each of the boxes were calculated from the hydrodynamic and suspended sediment models used in this study and are presented in Table 6-5.



Table 6-5: PC CREAM required input parameters for local compartments.

Parameter	Unit	Value		
		Box 1	Box 2	Box 3
Volume	m ³	1.05E+11	2.15E+09	1.14E+08
Average water depth	m	66	23	11
Coastline length	m	135 000	22 000	5 900
Mean suspended sediment load	t/m ³	4.62E-06	4.76E-06	5.36E-06
95 th percentile suspended sediment load	t/m ³	7.70E-06	8.65E-06	1.24E-05
Net sedimentation rate	t/m ² /year	7.3E-04	6.6E-06	5.8E-05
Sediment density ⁽¹⁾	t/m ³	0.4	0.4	0.4
Diffusion rate	m ² /year	N/A ⁽²⁾	N/A ⁽²⁾	N/A ⁽²⁾
Volumetric exchange rate ⁽³⁾	m ³ /year	8.7E+12	8.8E+11	2.1E+11

Notes:

- (1) Assumed bulk density on seabed.
- (2) Diffusion within the seabed layer is not included in the model used here.
- (3) The volumetric exchange rate is the total volume of water passing through a compartment per year. Therefore, the residence time of a compartment can be found by dividing its volumetric exchange rate by its volume.

6.7 Summary

This section presented the development, setup and calibration of a radionuclide model used to predict the dispersion and fate of radionuclides released from KNPS, including accumulation in seabed sediment.

The model results were post-processed to present the 95th percentile concentrations of activity dissolved in the water column, the 95th percentile concentrations of activity adsorbed to sediment suspended in the water column and the maximum activity concentrations in the seabed sediment.



7. SUMMARY

Eskom is in the process of applying for a Coastal Waters Discharge Permit (CWDP) for the Koeberg Nuclear Power Station (KNPS) in terms of Section 69 of the Integrated Coastal Management Act (ICMA). PRDW were appointed by Eskom to undertake a specialist study to provide coastal processes information in support of this application.

To this end, this document provides a description of the hydrodynamic and geophysical characteristics of the study area, as required for the CWDP application. A description of the outfall structure and location are given. The various effluent streams released at KNPS were characterised in terms of the flow rate and frequency of each discharge as well as the concentrations of all constituents in the effluent streams.

Due to the complexity of the discharge characterisation, a screening process was undertaken to identify constituents which meet the ecological guidelines before the end of the discharge channel and therefore do not pose a significant threat to the environment. The constituents in the KNPS effluent which did not meet the screening assessment were temperature, chlorine, hydrazine and phosphate.

A 3D hydrodynamic model was set up to model the dispersion of the constituents which did not meet the screening criteria. The model was calibrated to available measurements of waves, currents and water temperature. The dispersion of the constituents was modelled for one full year (2009). As requested by the marine ecology specialist, the model results were post-processed to present plots of the duration that the water quality guidelines are exceeded, the 95th percentile concentrations (for continuous releases) and the maximum concentrations (for batch releases). Time series plots of near-surface and near-seabed concentration at the locations of sensitive receptors are also presented for the continuous release scenarios. The interpretation of these results in terms of ecological impacts was not done in this report, but is presented in the report of the Marine Ecology Specialist Study (Lwandle, 2017).

In addition to chemical constituents released from KNPS, some streams also contain radiological substances. To investigate the dispersion and fate of these substances, a model was developed to include the chemical and physical processes specific to radionuclides. This included adsorption-desorption kinetics, first order decay and the modelling of fine particulate matter. The model was calibrated to measured total suspended sediment concentrations in the water column, the location of fine sediment depo-centres and to radioactivity measured in grab samples of seabed sediment.

The model results were post-processed to show the 95th percentile concentrations of radionuclide activity dissolved in the water column and activity adsorbed to sediment suspended in the water column. The maximum concentration of activity in the seabed sediment from one modelled year was also presented as well as the predicted steady state concentrations in the sediment. From these results, the permanent depo-centres were identified as the KNPS intake basin, the Port of Cape Town, Murray's Harbour and offshore at depths greater than 70 m CD.

The interpretation of the radionuclide model results was not done in this report, but will be undertaken by Eskom. This will include a comparison between these results and those from the PC CREAM box model, and modelling the accumulation of radionuclides in marine biota using the ERICA model.



8. REFERENCES

- 7 Sea Geosciences, 2012. *Marine Sampling Investigation, Robben Island, Cape Town: Factual Report. Report No 7S_P12002_REV_1*, Cape Town: 7 Sea Geosciences.
- Abarnou, A. & Miossec, L., 1992. Chlorinated waters discharged to the marine environment: chemistry and environmental impact. An overview. *The Scenace of the Total Environment*, Issue 126, pp. 173-197.
- BEEMS, 2010a. *Hinkley Point: Model of Total Residual Oxidant (TRO) behaviour in seawater: theory, calibration & validation. Technical Report Series 2010 no. 0.92*, s.l.: British Energy Estuarine & Marine Studies (BEEMS). Copyright (c) 2011 EDF Energy..
- BEEMS, 2010b. *Hinkley Point: The decay of Total Residual Oxidant (TRO) measured in sea water samples. Technical Report Series 2010 no. 091*, s.l.: British Energy Estuarine & Marine Studies. Copyright (c) 2011 EDF Energy.
- BEEMS, 2010c. *Laboratory studies of the decay of Hydrazine measured in sea water samples. Technical Report Series 2010 No 146.*, s.l.: British Energy Estuarine & Marine Studies. Copyright (c) 2011 EDF Energy.
- BEEMS, 2011. *Chlorination by-products in power station cooling water. SAR 009 XS EP CBP*, s.l.: BEEMS Expert Panel. Copyright (c) 2011 EDF Energy.
- CGS, 2006. *Marine Operational Survey Report: Eskom Site Surveys, Koeberg, South Africa. Volume 2*, Bellville: Council for Geoscience.
- CSIR, 2003. *EIA for the Expansion of the Container Terminal Stacking Area at the Port fo Cape Town: Specialist Study on Physical Impacts of Dredging. CSIR Report ENV-S-C-2003-083*, Stellenbosch: CSIR.
- CSIR, 2016. *Draft Environmental Impact Assessment Report for the Proposed Construction, Operation and Decommissioning of a Seawater Reverse Osmosis Plant and Associated Infrastructure in Tongaat, Kwazulu-Natal. Chapter 6: Marine Ecology*, Pretoria: CSIR.
- DEA, 2014. *Generic Assessment Criteria for Coastal Waters Discharge Permits*, Cape Town: Department of Environmental Affairs: Oceans and Coasts.
- DHI, 2014a. *MIKE C-MAP, Extraction of World Wide Bathymetry Data and Tidal Information, User Guide*, Copenhagen, Denmark: Danish Hydraulics Institute.
- DHI, 2014b. *MIKE by DHI Flow Flexible Mesh Model, User Guide*, Copenhagen, Denmark: Danish Hydraulics Institute.
- DHI, 2014c. *MIKE by DHI Flow Flexible Mesh, Scientific Documentation*, Copenhagen, Denmark: Danish Hydraulics Institute.
- DHI, 2014d. *MIKE 21, Spectral Waves FM Module, User Guide*, Copenhagen, Denmark: Danish Hydraulics Institute.
- DHI, 2014e. *MIKE 21, Spectral Waves FM Module, Scientific Documentation*, Copenhagen, Denmark: Danish Hydraulics Institute.
- DHI, 2014f. *MIKE by DHI ECOLAB, User Guide*, Copenhagen: Danish Hydraulics Institute.
- DHI, 2014g. *MIKE by DHI ECOLAB, Scientific Documentation*, Copenhagen: Danish Hydraulics Institute.
- DHI, 2014h. *MIKE 21 & MIKE 3 Flow Model FM, Mud Transport Module, Scientific Documentation*, Copenhagen, Denmark: Danish Hydraulics Institute.



DWAF, 1995. *South African Water Quality Guidelines For Coastal Marine Waters, Volume 2, Recreational Use*, Pretoria: Department of Water Affairs and Forestry.

ECMWF, 2015. *European Centre for Medium-Range Weather Forecasts. ERA-Interim Project. Research Data Archive at the National Center for Atmospheric Research, Computational and Information Systems Laboratory*. [Online]

Available at: <http://apps.ecmwf.int/datasets/data/interim-full-daily/>

[Accessed 08 12 2015].

El-Dessouky, H. T. & Ettouney, H. M., 2002. *Fundamentals of Salt Water Desalination: Appendix A Thermodynamic Properties*. 1 ed. s.l.:Elsevier.

Environmental Health Canada, 2011. *Screening Assessment for the Challenge: Hydrazine. Chemical Abstracts Service Registry Number 302-01-2*, s.l.: Environmental Health Canada.

Fugro, 2007. *Survey Report for the Koeberg Site Extension, Eskom Site Surveys, South Africa*, Cape Town: Fugro Survey Africa (Pty) Ltd..

IAEA, 2004. *Sediment Distribution Coefficients and Concentration Factors for Biota in the Marine Environment. Technical Reports Series no. 422*, Vienna: International Atomic Energy Agency.

Jiangning, Z. et al., 2009. The decay kinetics of residual chlorine in cooling seawater simulation experiments. *Acta Oceanologica Sinica*, 28(2), pp. 54-59.

Lwandle, 2017. *KNPS Marine Discharge Assessment in support of the CWDP Application: Marine Ecology Specialist Study. Doc Ref: LT-267 Rev-06*, Cape Town: Lwandle Technologies (Pty) Ltd..

NCEP, 2012. *National Weather Service Environmental Modeling Centre*. [Online]

Available at: <http://polar.ncep.noaa.gov>

[Accessed 14 November 2012].

Nyffeler, U. P., Li, Y.-H. & Santschi, P. H., 1984. A kinetic approach to describe trace-element distribution between particles and solution in natural aquatic systems. *Geochimica et Cosmochimica Acta*, Volume 48, pp. 1513-1522.

Periáñez, R., 2000. Modelling the tidal dispersion of ¹³⁷Cs and ^{239,240}Pu in the English Channel. *Journal of Environmental Radioactivity*, Issue 49, pp. 259-277.

Periáñez, R., 2005. Modelling the dispersion of radionuclides by a river plume: Application to the Rhone river. *Continental Shelf Research*, Issue 25, pp. 1583-1603.

Periáñez, R., 2012. Modelling the environmental behaviour of pollutants in Algeciras Bay (south Spain). *Marine Pollution Bulletin*, Issue 64, pp. 221-232.

PRDW, 2012. *Eskom Nuclear Sites, Site Safety Reports, Numerical Modelling of Coastal Processes, Duynfontein, Report No. 1010/4/101*, Cape Town: PRDW (Pty) Ltd.

PRDW, 2013. *Koeberg Nuclear Power Station, Oceanographic Engineering Services, Outlet Near and Far-Field Dispersion Modelling. Doc No 1105/01*, Cape Town: PRDW (Pty) Ltd..

Pulfrich, A. & Steffani, N., 2014. *Marine Environmental Impact Assessment for the Seawater Intake Structure and Brine Disposal System of the Proposed Desalination Plant at Volwaterbaai*, Tokai: PISCES Environmental Services (Pty) Ltd..

SANHO, 2016. *South African Tide Tables*. 2016 ed. Tokai: South African Navy Hydrographic Office.



Sohn, J. et al., 2004. Disinfectant decay and disinfection by-products formation model development: chlorination and ozonation by-products. *Water Research*, Issue 38, pp. 2461-2478.

Tritan Survey cc, 2008. *Eskom - Koeberg, Beach Profile Survey Ref.7145*, Wynberg: Tritan Survey cc.

UNEP, 1984. *GESAMP: Thermal discharges in the marine environment. UNEP Regional Seas Reports and Studies No. 45*, s.l.: United Nations Environment Programme.

Van Ballegooyen, R. C. et al., 2006. *Ben Schoeman Dock Berth Deepening Project: Dredging and Disposal of Dredge Spoil Modelling Specialist Study. CSIR Report No CSIR/NRE/ECO/ER/2006/0228/C*, Stellenbosch: CSIR.

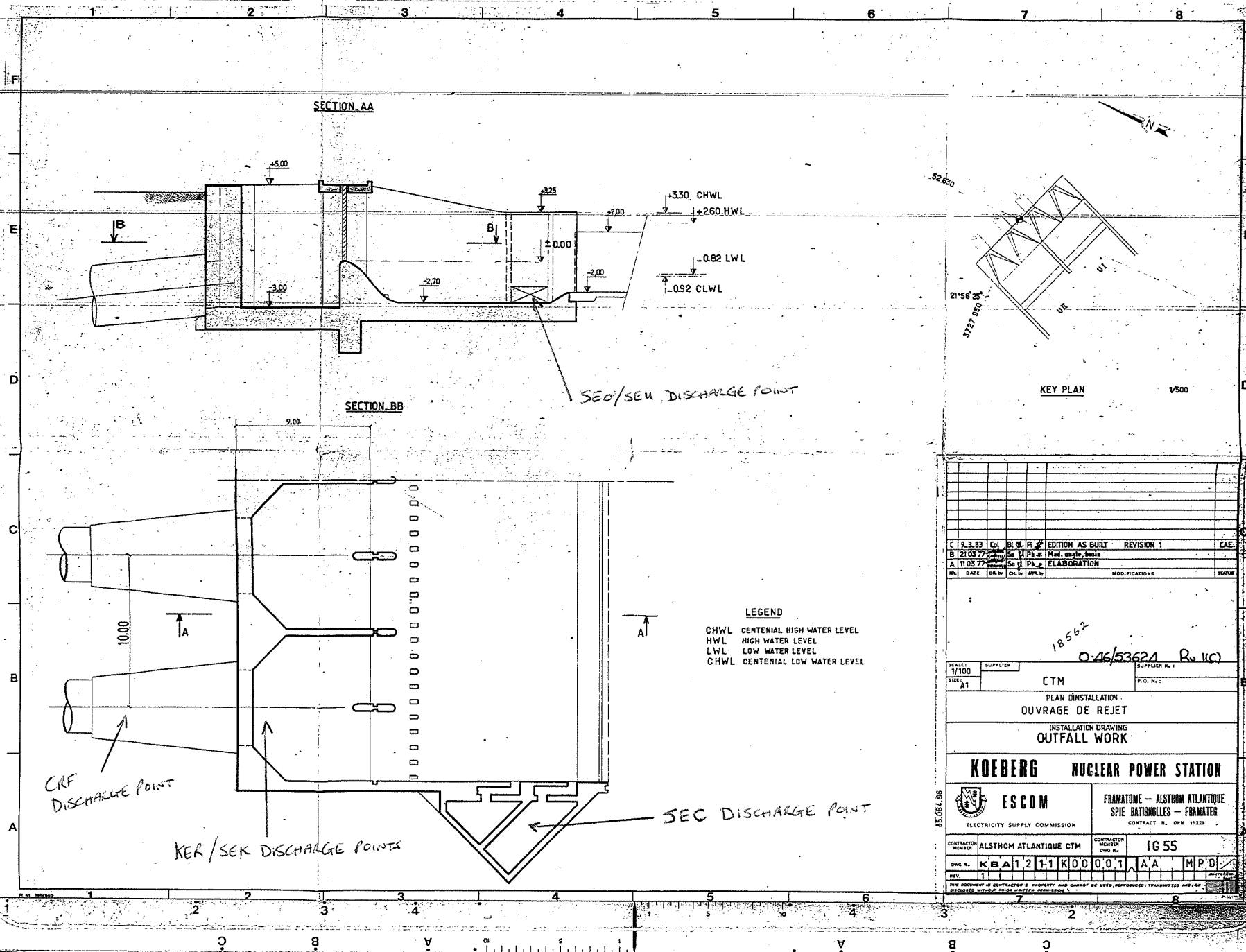
Van Ballegooyen, R., Steffani, N. & Pulfrich, A., 2007. *Environmental Impact Assessment: Proposed Reverse Osmosis Plant, Iron-ore Handling Facility, Port of Saldanha - Marine Impact Assessment Specialist Study, Joint CSIR/Piscus Report, CSIR/NRE/ECO/ER/2007/0419/C, 190pp+189pp App.*, Pretoria: CSIR.

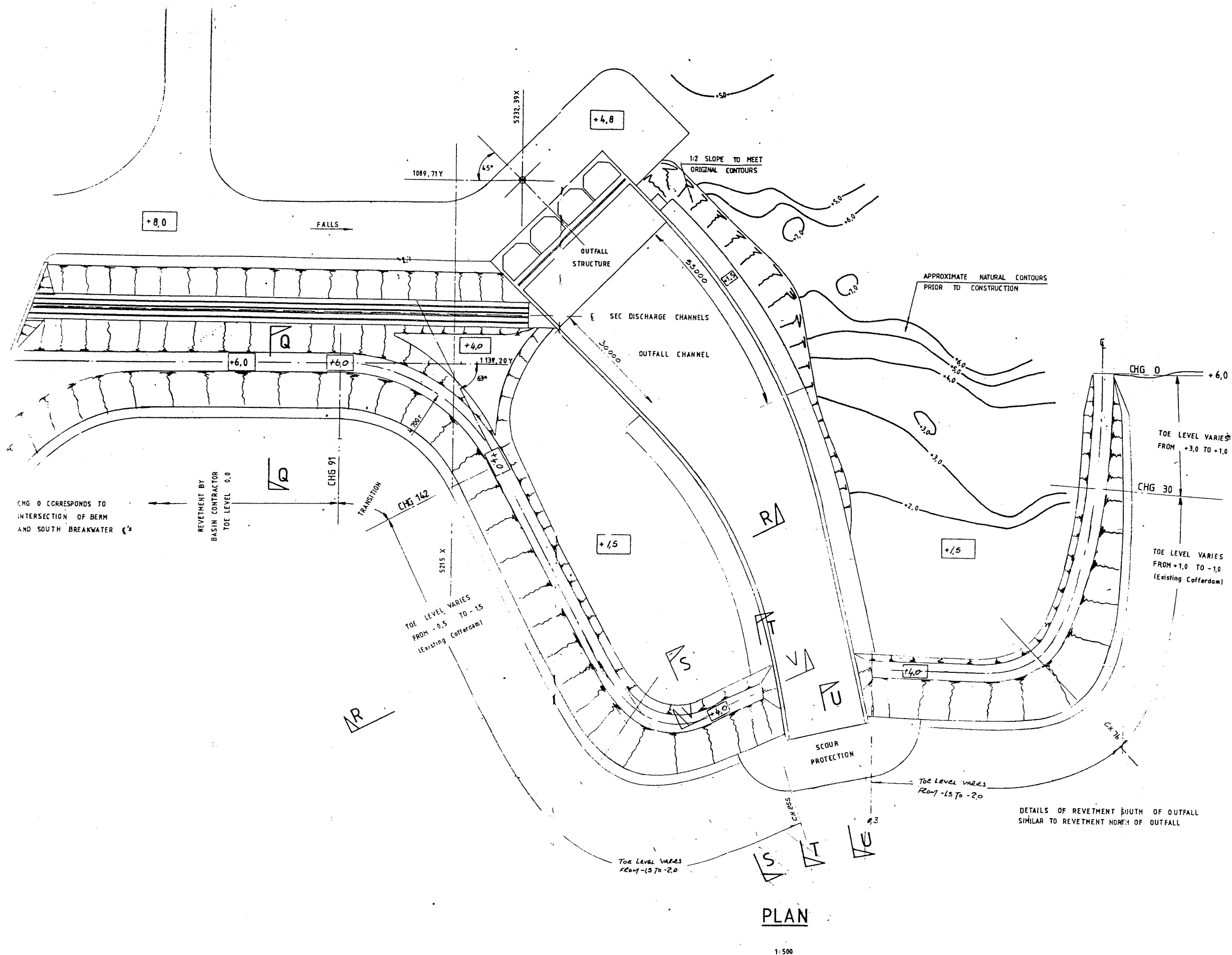
Watermeyer, Sir William Halcrow and Partners, Elliot, J. & Legge, Piesold & Uhlmann, 1972. *Report on comparative studies of alternative cooling water intake and outfall systems. Koeberg Nuclear Power Station. Report submitted to the Electricity Supply Commission, February 1972*, Cape Town: s.n.

WLPU, Sir William Halcrow and Partners, 1972. *Koeberg Nuclear Power Station: Report on comparative studies of alternative cooling water intake and outfall systems*, Cape Town: Watermeyer, Legge, Piesold & Uhlmann, Sir William Halcrow and Partners..



ANNEXURE A | DRAWINGS OF KOEBERG NUCLEAR POWER STATION OUTFALL CHANNEL





PLAN

NOTES

REVISIONS

CLIENT

PROJECT

DRAWING TITLE

WATERMEYER PRESTEDGE RETIEF

UNION CASTLE HOUSE,
PIERHEAD,
VICTORIA & ALFRED WATERFRONT,
CAPE TOWN, 8001.
PO BOX 50023, WATERFRONT, 8002.
TEL. (021) 418-3830 FAX (021) 418-3834

ENGINEER GK Prestledge

CHECKED	APPROVED
---------	----------

SCALE	NIS	DATE
-------	-----	------

DNG No:

201/11/ 11

REV. 00

DWG No: 201/11/11

REV. 00



ANNEXURE B | RESULTS OF CHEMICAL DISPERSION MODELLING



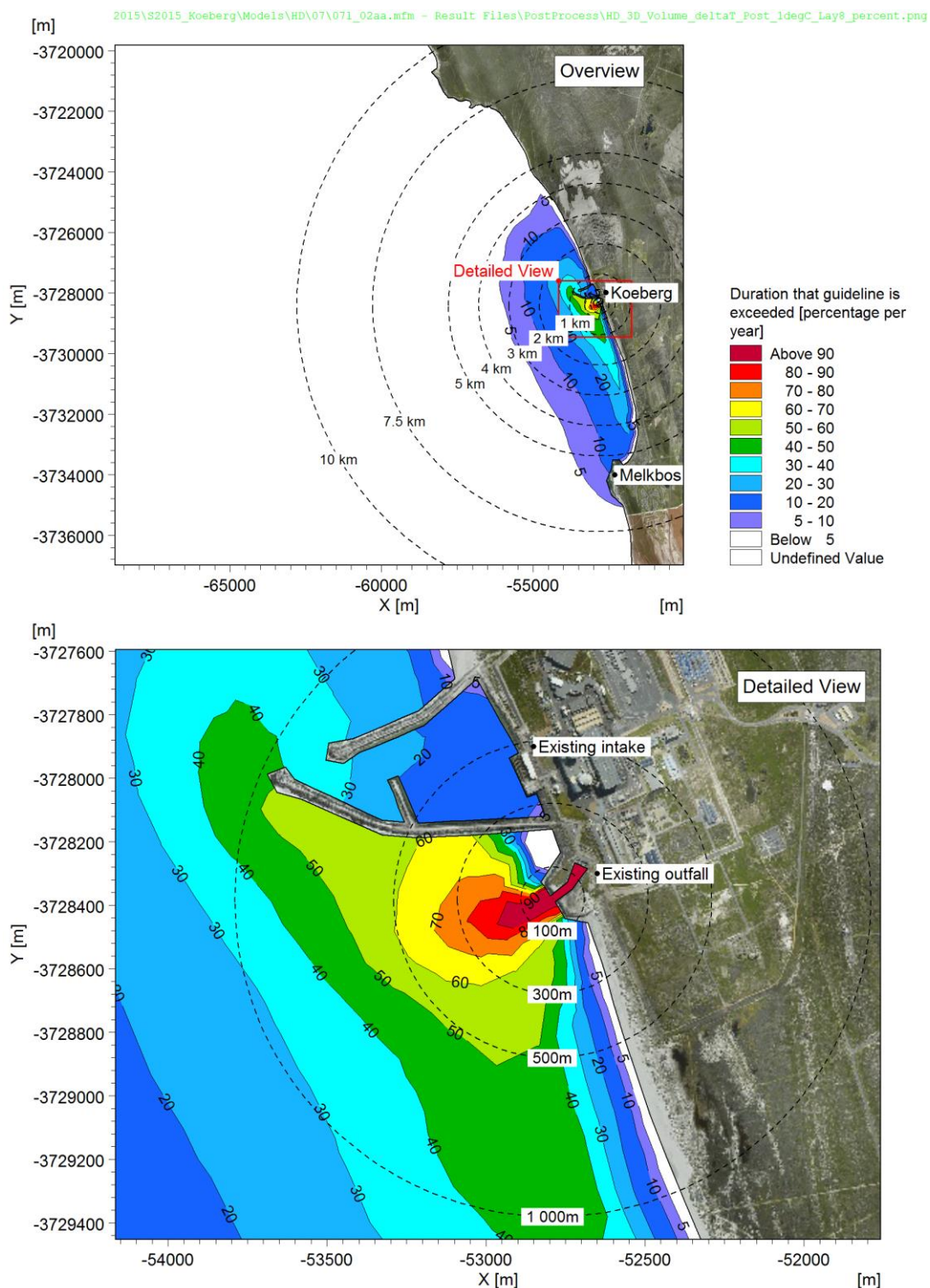
Figure B-1: Percentage of time during which the guideline increase in temperature ($\Delta T = 1^\circ\text{C}$) is exceeded near the surface: plant operation at full capacity.....	5
Figure B-2: Percentage of time during which the guideline increase in temperature ($\Delta T = 1^\circ\text{C}$) is exceeded near the seabed: plant operation at full capacity.....	6
Figure B-3: Percentage of time during which the guideline increase in temperature ($\Delta T = 2^\circ\text{C}$) is exceeded near the surface: plant operation at full capacity.....	7
Figure B-4: Percentage of time during which the guideline increase in temperature ($\Delta T = 2^\circ\text{C}$) is exceeded near the seabed: plant operation at full capacity.....	8
Figure B-5: Percentage of time during which the guideline increase in temperature ($\Delta T = 3^\circ\text{C}$) is exceeded near the surface: plant operation at full capacity.....	9
Figure B-6: Percentage of time during which the guideline increase in temperature ($\Delta T = 3^\circ\text{C}$) is exceeded near the seabed: plant operation at full capacity.....	10
Figure B-7: 95 th Percentile near-surface increase in temperature: plant operation at full capacity.	11
Figure B-8: 95 th Percentile near-seabed increase in temperature: plant operation at full capacity.....	12
Figure B-9: 95 th Percentile near-surface absolute temperature: plant operation at full capacity.....	13
Figure B-10: 95 th Percentile near-seabed absolute temperature: plant operation at full capacity.	14
Figure B-11: Time series of near-surface and near-seabed increase in temperature at the rocks to the south (see Figure 5-15): plant operation at full capacity.....	15
Figure B-12: Time series of near-surface and near-seabed increase in temperature 1 km offshore of the discharge point (see Figure 5-15): plant operation at full capacity.	16
Figure B-13: Time series of near-surface and near-seabed increase in temperature 100 m offshore of the discharge point (see Figure 5-15): plant operation at full capacity.	17
Figure B-14: Time series of near-surface and near-seabed increase in temperature at the breakwater head (see Figure 5-15): plant operation at full capacity.	18
Figure B-15: Time series of near-surface and near-seabed increase in temperature at Northern Blinders 2 (see Figure 5-15): plant operation at full capacity.	19
Figure B-16: Time series of near-surface and near-seabed increase in temperature at Northern Blinders 1 (see Figure 5-15): plant operation at full capacity.	20
Figure B-17: Time series of near-surface absolute temperature at the rocks to the south (see Figure 5-15): plant operation at full capacity.	21
Figure B-18: Time series of near-seabed absolute temperature at the rocks to the south (see Figure 5-15): plant operation at full capacity.	22
Figure B-19: Time series of near-surface absolute temperature 1 km offshore of the discharge point (see Figure 5-15): plant operation at full capacity.....	23
Figure B-20: Time series of near-seabed absolute temperature 1 km offshore of the discharge point (see Figure 5-15): plant operation at full capacity.	24
Figure B-21: Time series of near-surface absolute temperature 100 m offshore of the discharge point (see Figure 5-15): plant operation at full capacity.....	25
Figure B-22: Time series of near-seabed absolute temperature 100 m offshore of the discharge point (see Figure 5-15): plant operation at full capacity.....	26
Figure B-23: Time series of near-surface absolute temperature at the breakwater head (see Figure 5-15): plant operation at full capacity.	27
Figure B-24: Time series of near-seabed absolute temperature at the breakwater head (see Figure 5-15): plant operation at full capacity.	28



Figure B-25: Time series of near-surface absolute temperature at Northern Blinders 2 (see Figure 5-15): plant operation at full capacity.	29
Figure B-26: Time series of near-seabed absolute temperature at Northern Blinders 2 (see Figure 5-15): plant operation at full capacity.	30
Figure B-27: Time series of near-surface absolute temperature at Northern Blinders 1 (see Figure 5-15): plant operation at full capacity.	31
Figure B-28: Time series of near-seabed absolute temperature at Northern Blinders 1 (see Figure 5-15): plant operation at full capacity.	32
Figure B-29: Maximum absolute temperature near the surface: pump trip scenario.	33
Figure B-30: Maximum absolute temperature near the seabed: pump trip scenario.	34
Figure B-31: Percentage of time during which the guideline concentration for free chlorine (0.003 mg/l) is exceeded near the surface: plant operation at full capacity.	35
Figure B-32: Percentage of time during which the guideline concentration for free chlorine (0.003 mg/l) is exceeded near the seabed: plant operation at full capacity.	36
Figure B-33: Percentage of time during which the guideline concentration for free chlorine (0.01 mg/l) is exceeded near the surface: plant operation at full capacity.	37
Figure B-34: Percentage of time during which the guideline concentration for free chlorine (0.01 mg/l) is exceeded near the seabed: plant operation at full capacity.	38
Figure B-35: 95 th Percentile near-surface concentration of free chlorine: plant operation at full capacity.	39
Figure B-36: 95 th Percentile near-seabed concentration of free chlorine: plant operation at full capacity.	40
Figure B-37: Time series of near-surface and near-seabed TRO concentration at the rocks to the south (see Figure 5-15): plant operation at full capacity.	41
Figure B-38: Time series of near-surface and near-seabed TRO concentration 1 km offshore of the discharge point (see Figure 5-15): plant operation at full capacity.	42
Figure B-39: Time series of near-surface and near-seabed TRO concentration 100 m offshore of the discharge point (see Figure 5-15): plant operation at full capacity.	43
Figure B-40: Time series of near-surface and near-seabed TRO concentration at the breakwater head (see Figure 5-15): plant operation at full capacity.	44
Figure B-41: Time series of near-surface and near-seabed TRO concentration at Northern Blinders 2 (see Figure 5-15): plant operation at full capacity.	45
Figure B-42: Time series of near-surface and near-seabed TRO concentration at Northern Blinders 1 (see Figure 5-15): plant operation at full capacity.	46
Figure B-43: Maximum annual duration that the guideline concentration for hydrazine (0.0002 mg/l) is exceeded near the surface: plant operation at full capacity (two units operational).	47
Figure B-44: Maximum annual duration that the guideline concentration for hydrazine (0.0002 mg/l) is exceeded near the seabed: plant operation at full capacity (two units operational).	48
Figure B-45: Maximum annual duration that the guideline concentration for hydrazine (0.0025 mg/l) is exceeded near the surface: plant operation at full capacity (two units operational).	49
Figure B-46: Maximum annual duration that the guideline concentration for hydrazine (0.0025 mg/l) is exceeded near the seabed: plant operation at full capacity (two units operational).	50
Figure B-47: Maximum near-surface hydrazine concentration: plant operation at full capacity (two units operational).	51
Figure B-48: Maximum near-seabed hydrazine concentration: plant operation at full capacity (two units operational).	52
Figure B-49: Maximum annual duration that the guideline concentration for hydrazine (0.0002 mg/l) is exceeded near the surface: exceptional discharges associated with refuelling outages (one unit operational). ...	53

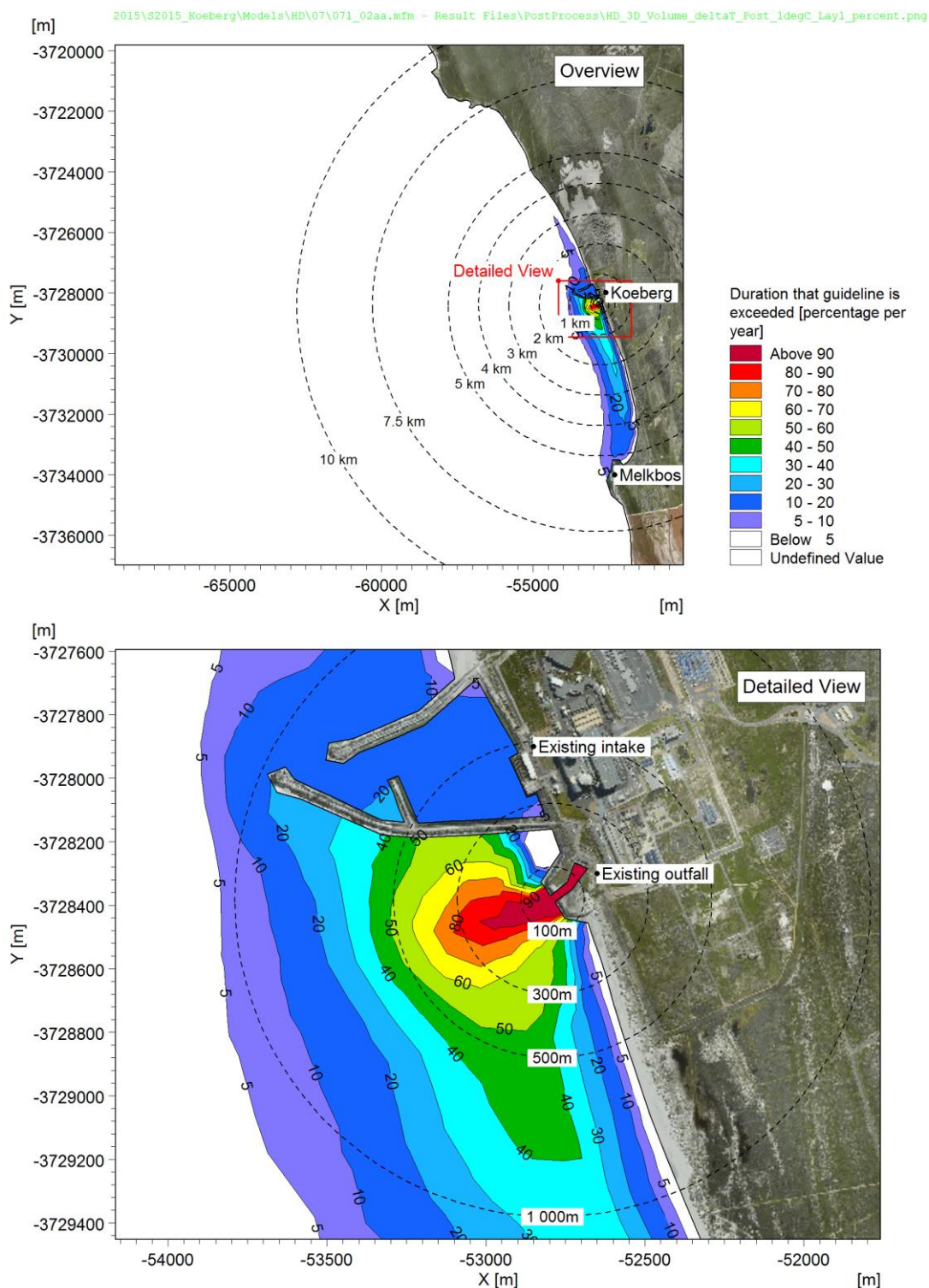


Figure B-50: Maximum annual duration that the guideline concentration for hydrazine (0.0002 mg/l) is exceeded near the seabed: exceptional discharges associated with refuelling outages (one unit operational). ...	54
Figure B-51: Maximum annual duration that the guideline concentration for hydrazine (0.0025 mg/l) is exceeded near the surface: exceptional discharges associated with refuelling outages (one unit operational). ...	55
Figure B-52: Maximum annual duration that the guideline concentration for hydrazine (0.0025 mg/l) is exceeded near the seabed: exceptional discharges associated with refuelling outages (one unit operational). ...	56
Figure B-53: Maximum near-surface hydrazine concentration: exceptional discharges associated with refuelling outages (one unit operational).....	57
Figure B-54: Maximum near-seabed hydrazine concentration: exceptional discharges associated with refuelling outages (one unit operational).....	58
Figure B-55: Maximum annual duration that the guideline concentration for phosphate (0.053 mg/l) is exceeded near the surface: exceptional discharges during refuelling outages (one unit operational).	59
Figure B-56: Maximum annual duration that the guideline concentration for phosphate (0.053 mg/l) is exceeded near the seabed: exceptional discharges during refuelling outages (one unit CRF operational).	60
Figure B-57: Maximum near-surface phosphate concentration: exceptional discharges during refuelling outages (one unit operational).	61
Figure B-58: Maximum near-seabed phosphate concentration: exceptional discharges during refuelling outages (one unit CRF operational).	62



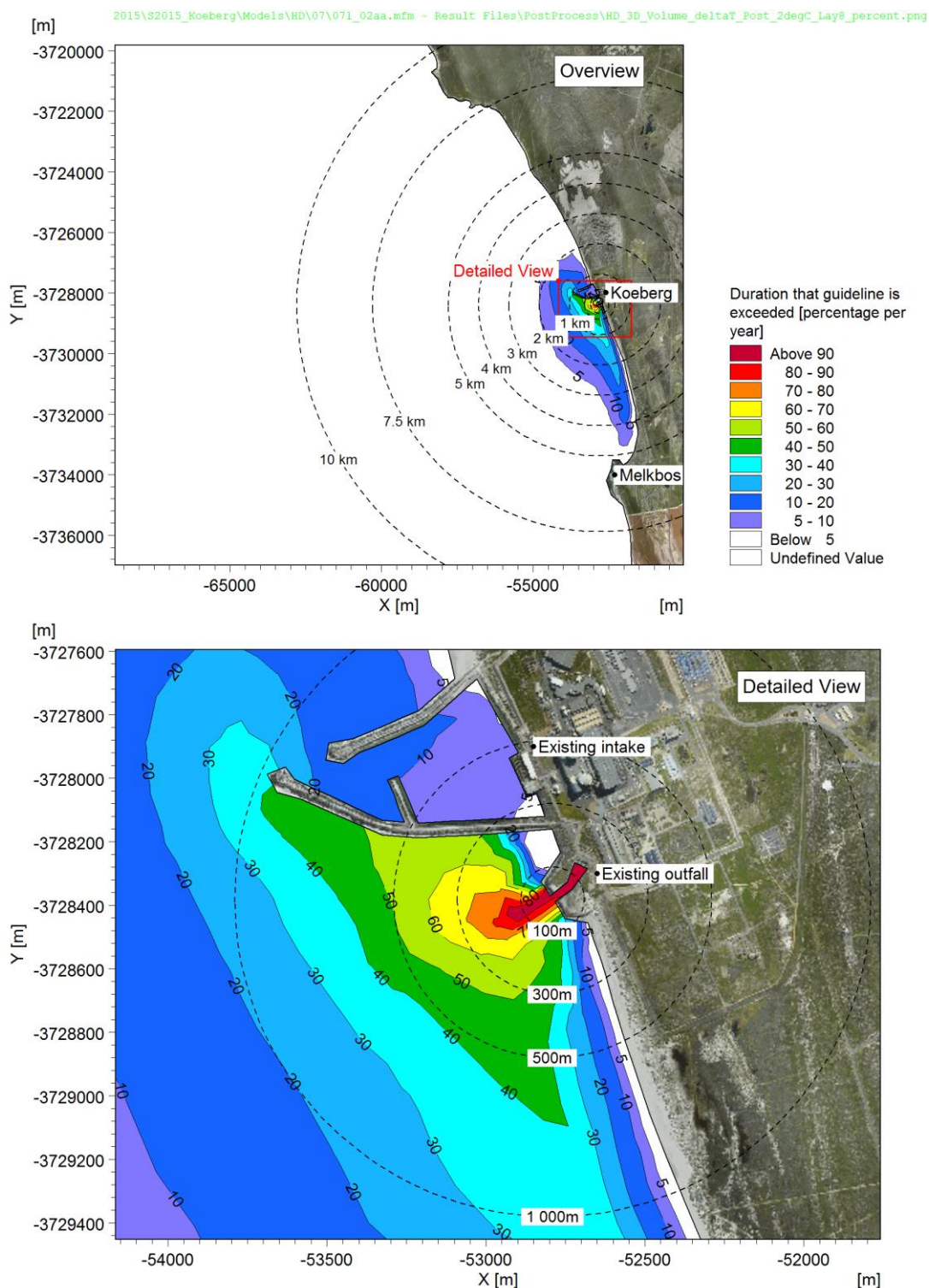
Stream	Discharge [m ³ /h]	ΔT [°C]	Duration [h]	Release interval [days]	Total duration per year [hrs]
CRF	327 888	11.7	continuous		
SEC	12 700	12	continuous		

Figure B-1: Percentage of time during which the guideline increase in temperature ($\Delta T = 1^\circ\text{C}$) is exceeded near the surface: plant operation at full capacity.



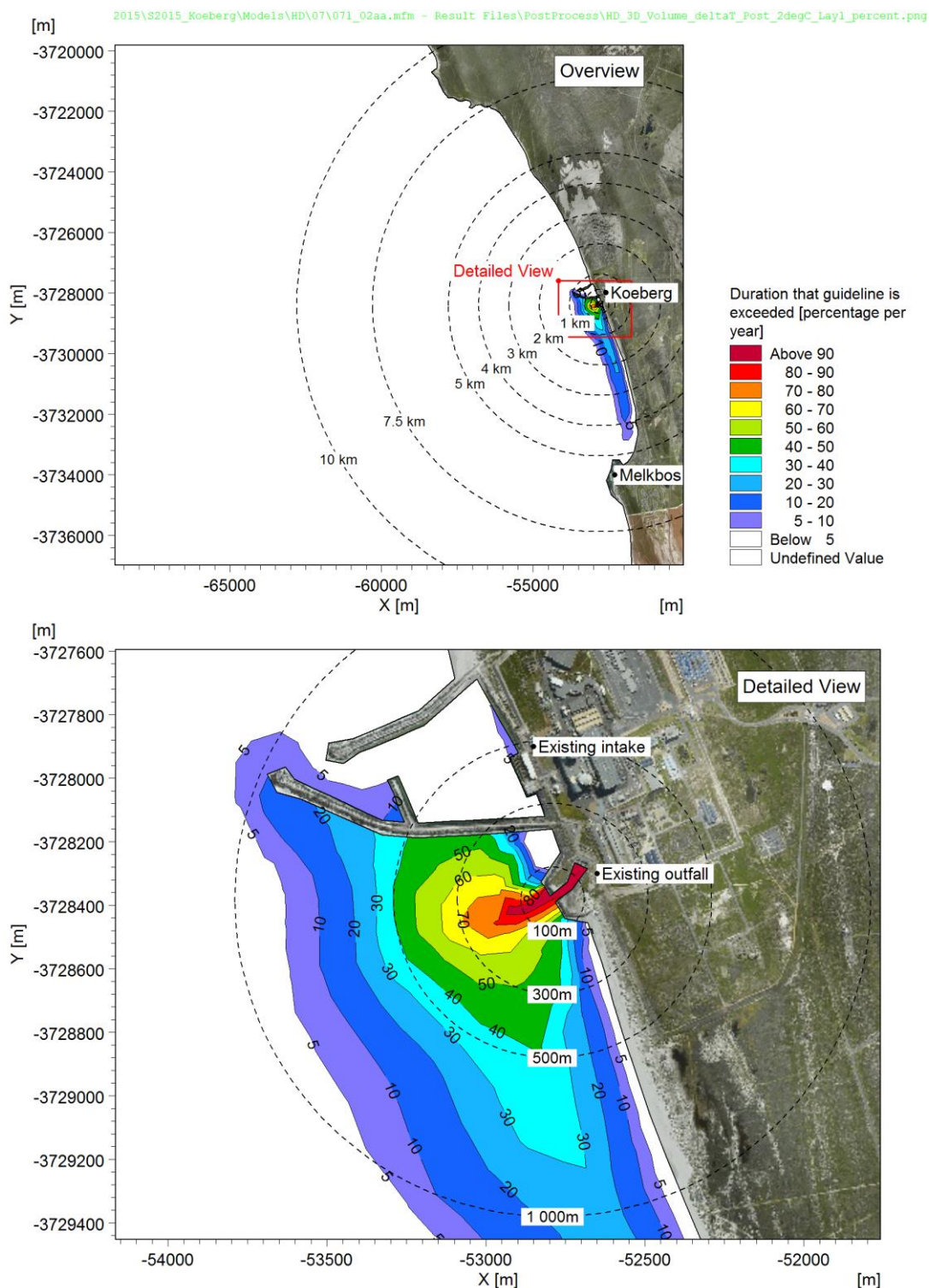
Stream	Discharge [m ³ /h]	ΔT [°C]	Duration [h]	Release interval [days]	Total duration per year [hrs]
CRF	327 888	11.7	continuous		
SEC	12 700	12	continuous		

Figure B-2: Percentage of time during which the guideline increase in temperature ($\Delta T = 1^\circ\text{C}$) is exceeded near the seabed: plant operation at full capacity.



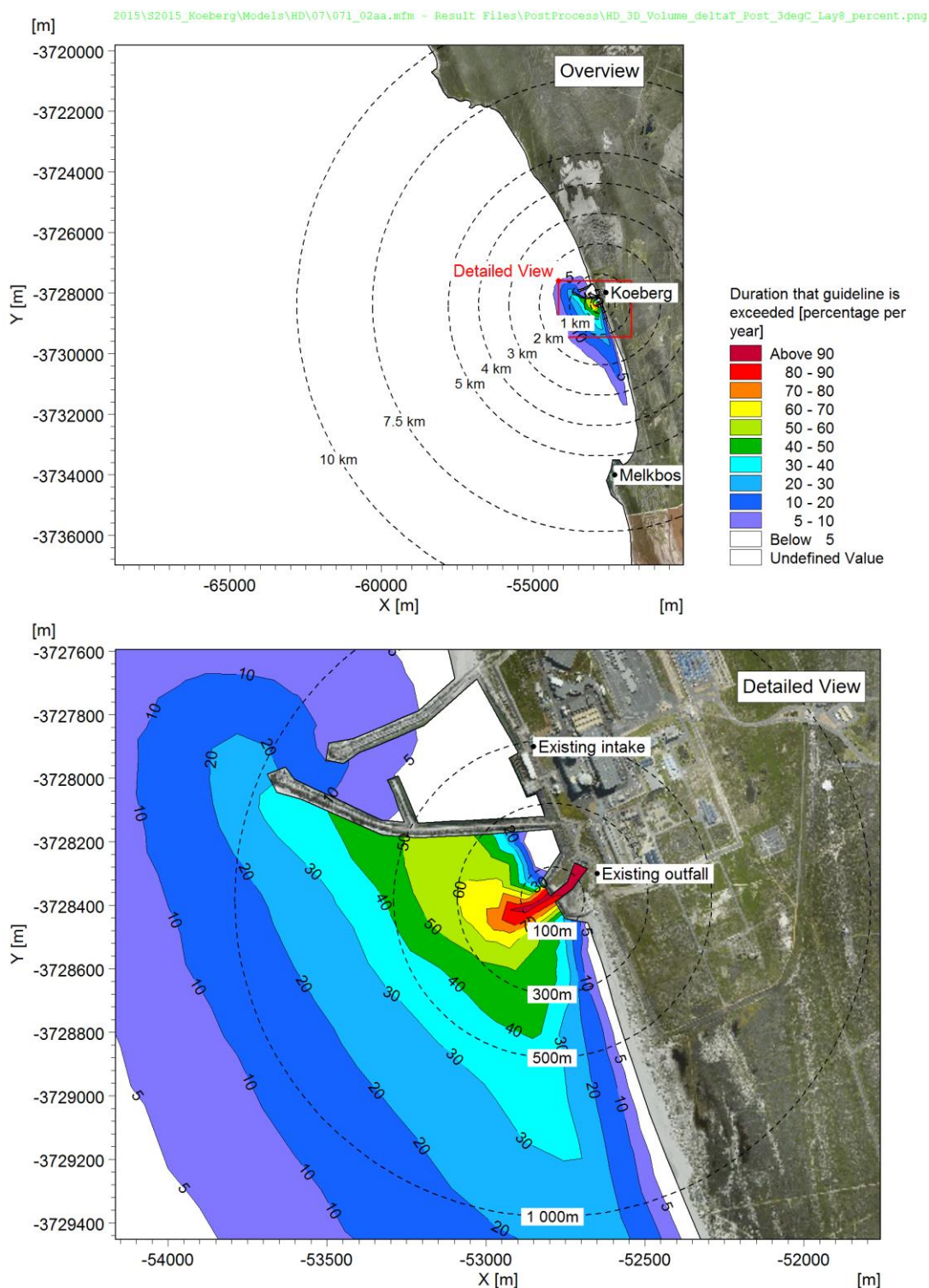
Stream	Discharge [m ³ /h]	ΔT [°C]	Duration [h]	Release interval [days]	Total duration per year [hrs]
CRF	327 888	11.7	continuous		
SEC	12 700	12	continuous		

Figure B-3: Percentage of time during which the guideline increase in temperature ($\Delta T = 2^\circ\text{C}$) is exceeded near the surface: plant operation at full capacity.



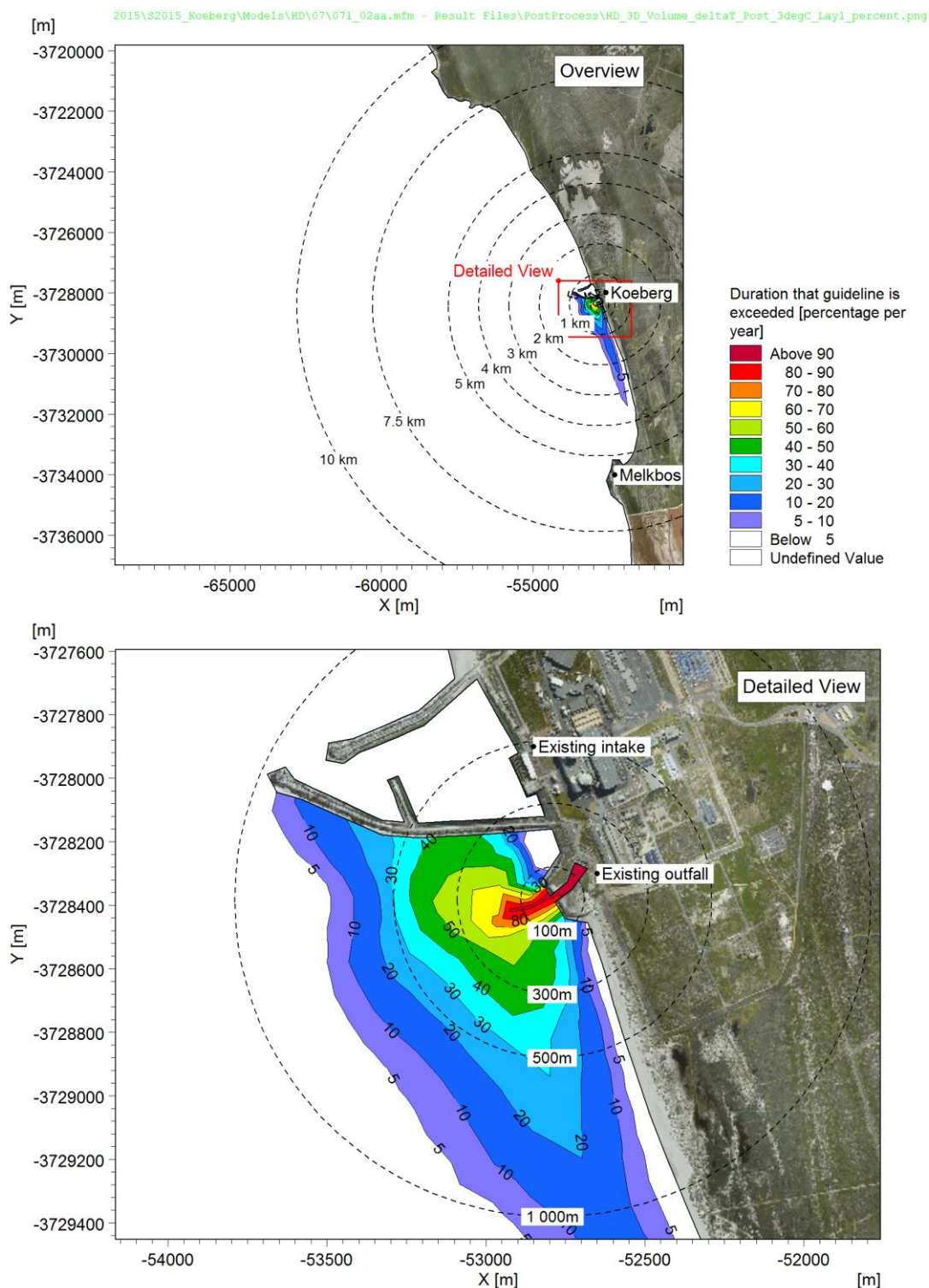
Stream	Discharge [m ³ /h]	ΔT [°C]	Duration [h]	Release interval [days]	Total duration per year [hrs]
CRF	327 888	11.7	continuous		
SEC	12 700	12	continuous		

Figure B-4: Percentage of time during which the guideline increase in temperature ($\Delta T = 2^\circ\text{C}$) is exceeded near the seabed: plant operation at full capacity.



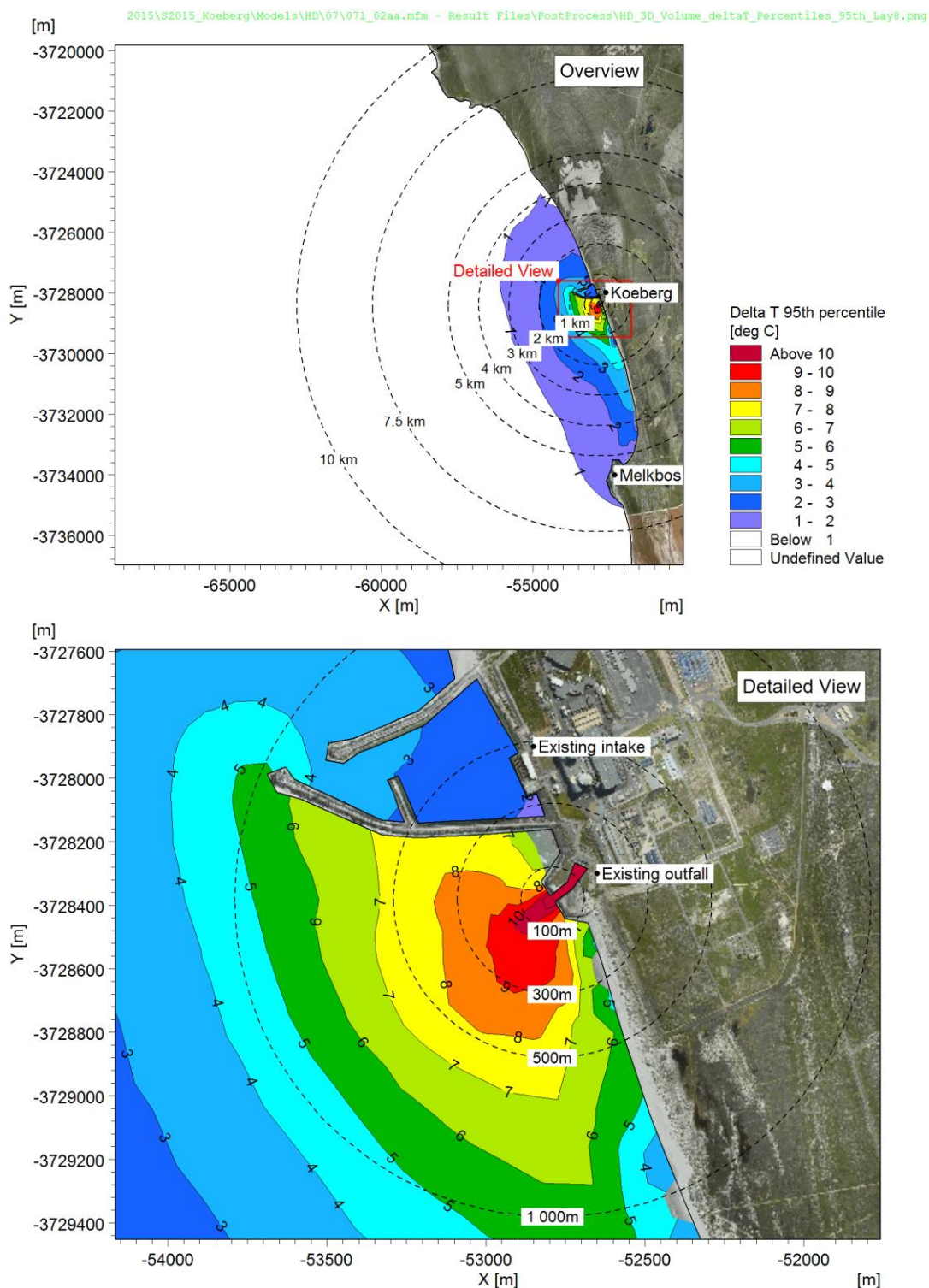
Stream	Discharge [m ³ /h]	ΔT [°C]	Duration [h]	Release interval [days]	Total duration per year [hrs]
CRF	327 888	11.7	continuous		
SEC	12 700	12	continuous		

Figure B-5: Percentage of time during which the guideline increase in temperature ($\Delta T = 3^{\circ}\text{C}$) is exceeded near the surface: plant operation at full capacity.



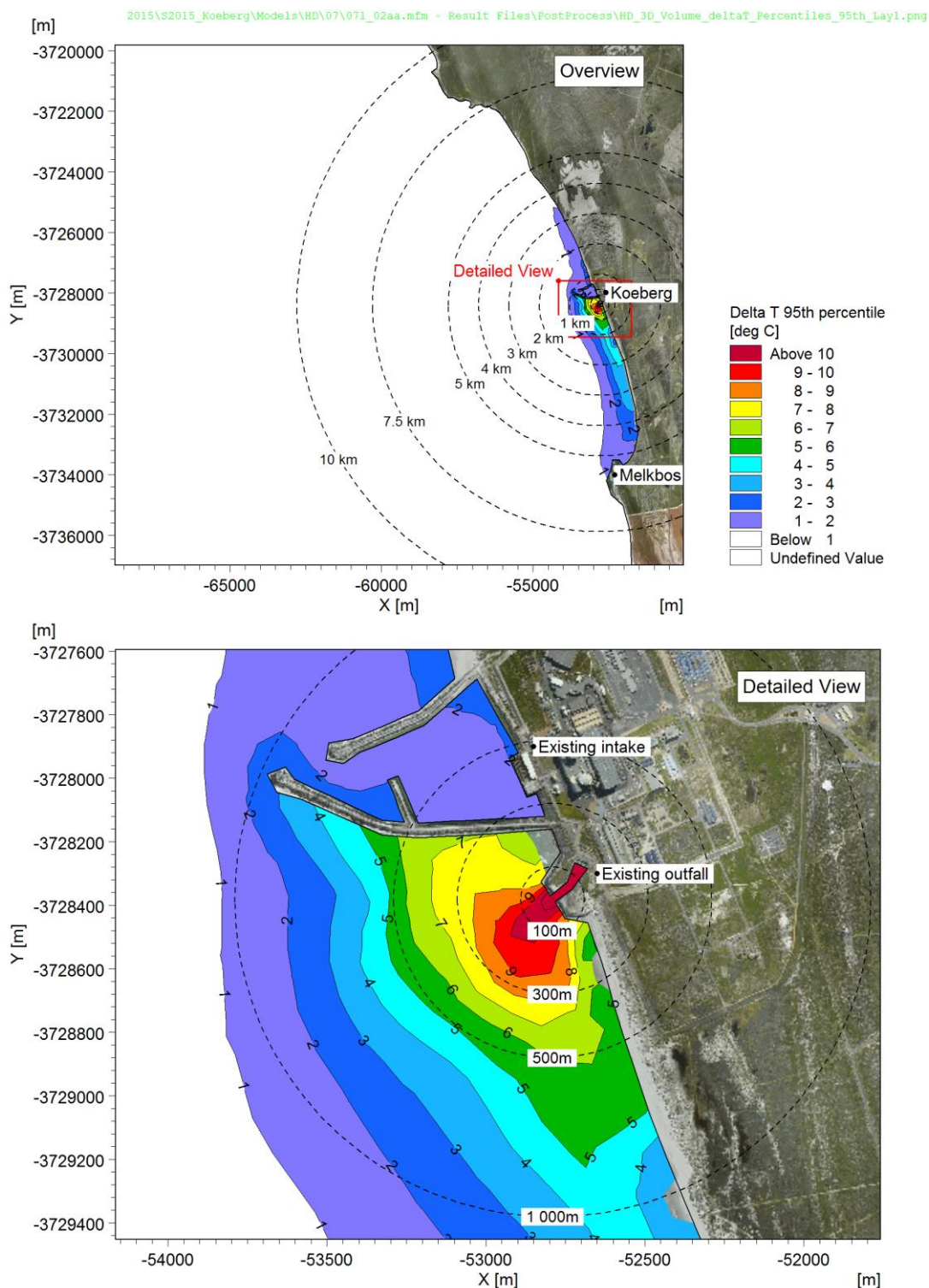
Stream	Discharge [m ³ /h]	ΔT [°C]	Duration [h]	Release interval [days]	Total duration per year [hrs]
CRF	327 888	11.7	continuous		
SEC	12 700	12	continuous		

Figure B-6: Percentage of time during which the guideline increase in temperature ($\Delta T = 3^{\circ}\text{C}$) is exceeded near the seabed: plant operation at full capacity.



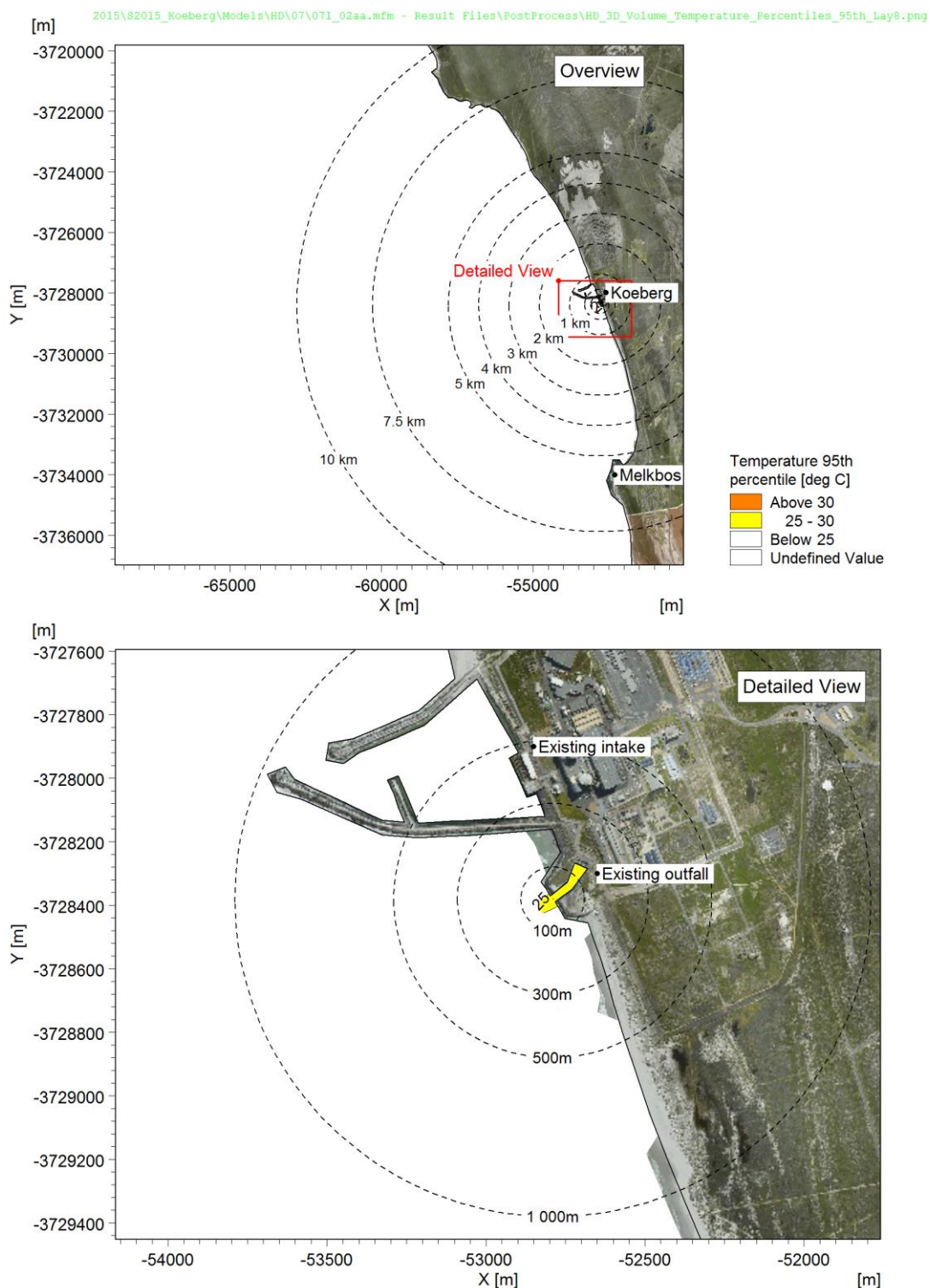
Stream	Discharge [m ³ /h]	ΔT [°C]	Duration [h]	Release interval [days]	Total duration per year [hrs]
CRF	327 888	11.7	continuous		
SEC	12 700	12	continuous		

Figure B-7: 95th Percentile near-surface increase in temperature: plant operation at full capacity.



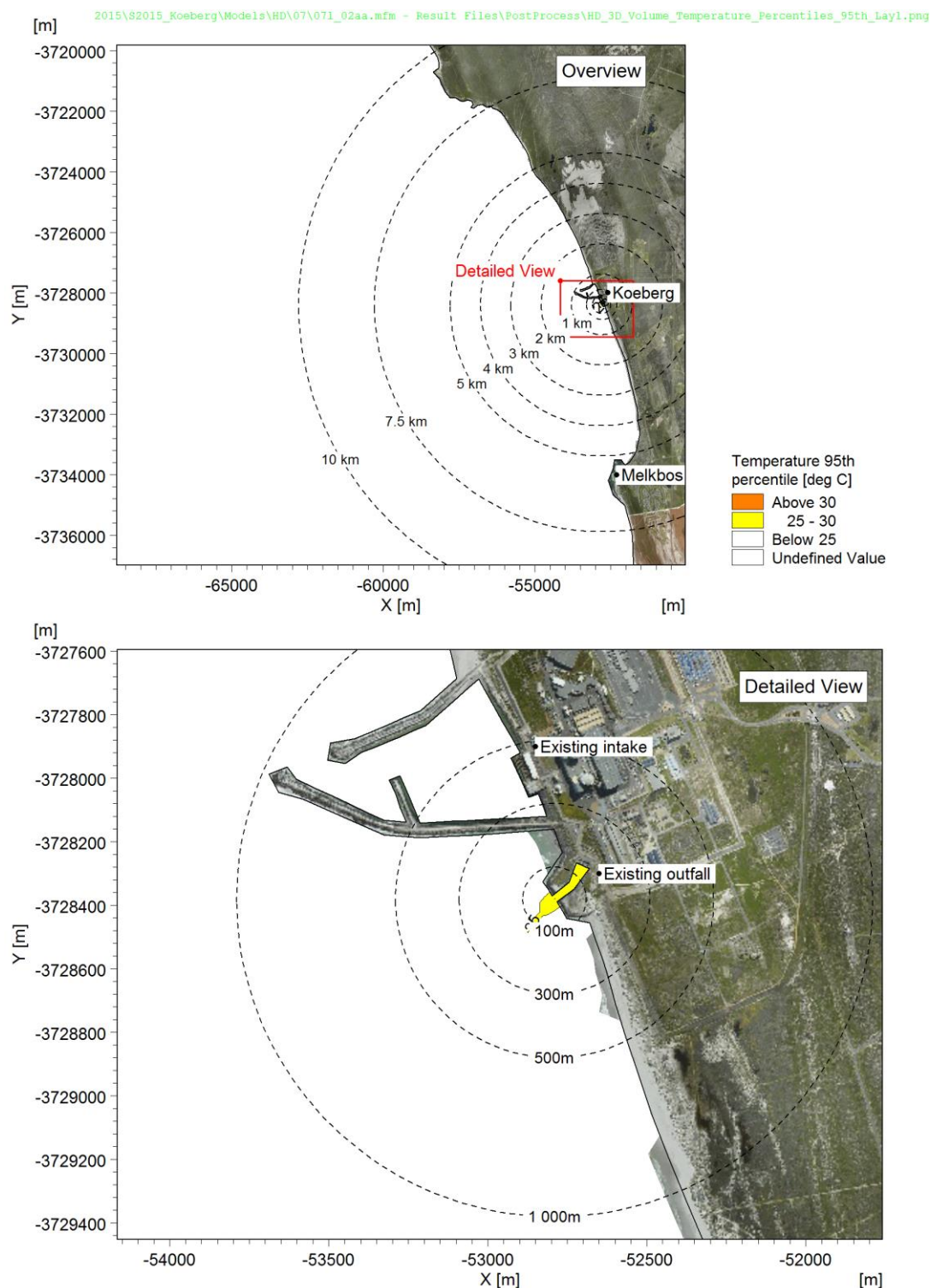
Stream	Discharge [m ³ /h]	ΔT [°C]	Duration [h]	Release interval [days]	Total duration per year [hrs]
CRF	327 888	11.7	continuous		
SEC	12 700	12	continuous		

Figure B-8: 95th Percentile near-seabed increase in temperature: plant operation at full capacity.



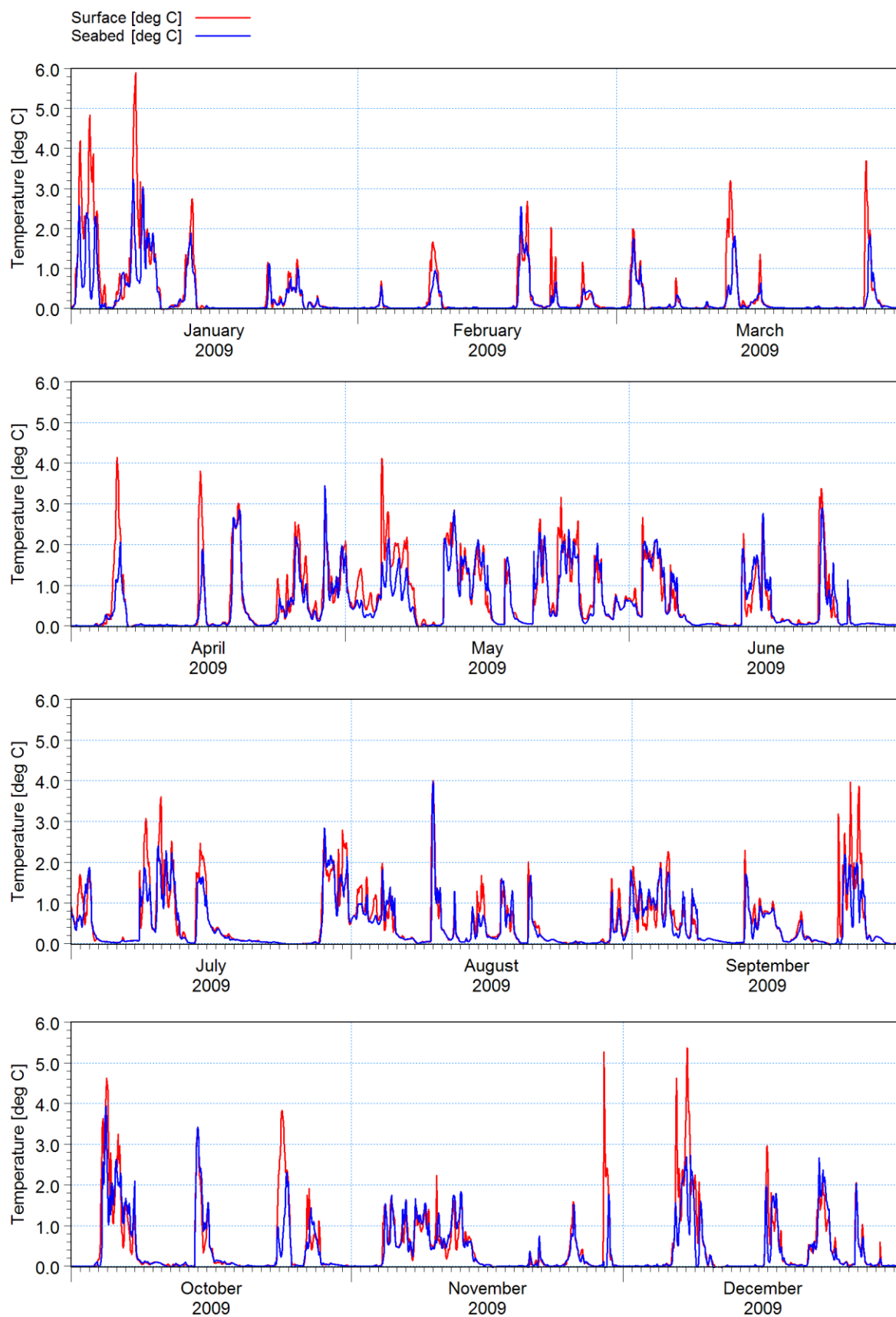
Stream	Discharge [m ³ /h]	ΔT [°C]	Duration [h]	Release interval [days]	Total duration per year [hrs]
CRF	327 888	11.7	continuous		
SEC	12 700	12	continuous		

Figure B-9: 95th Percentile near-surface absolute temperature: plant operation at full capacity.



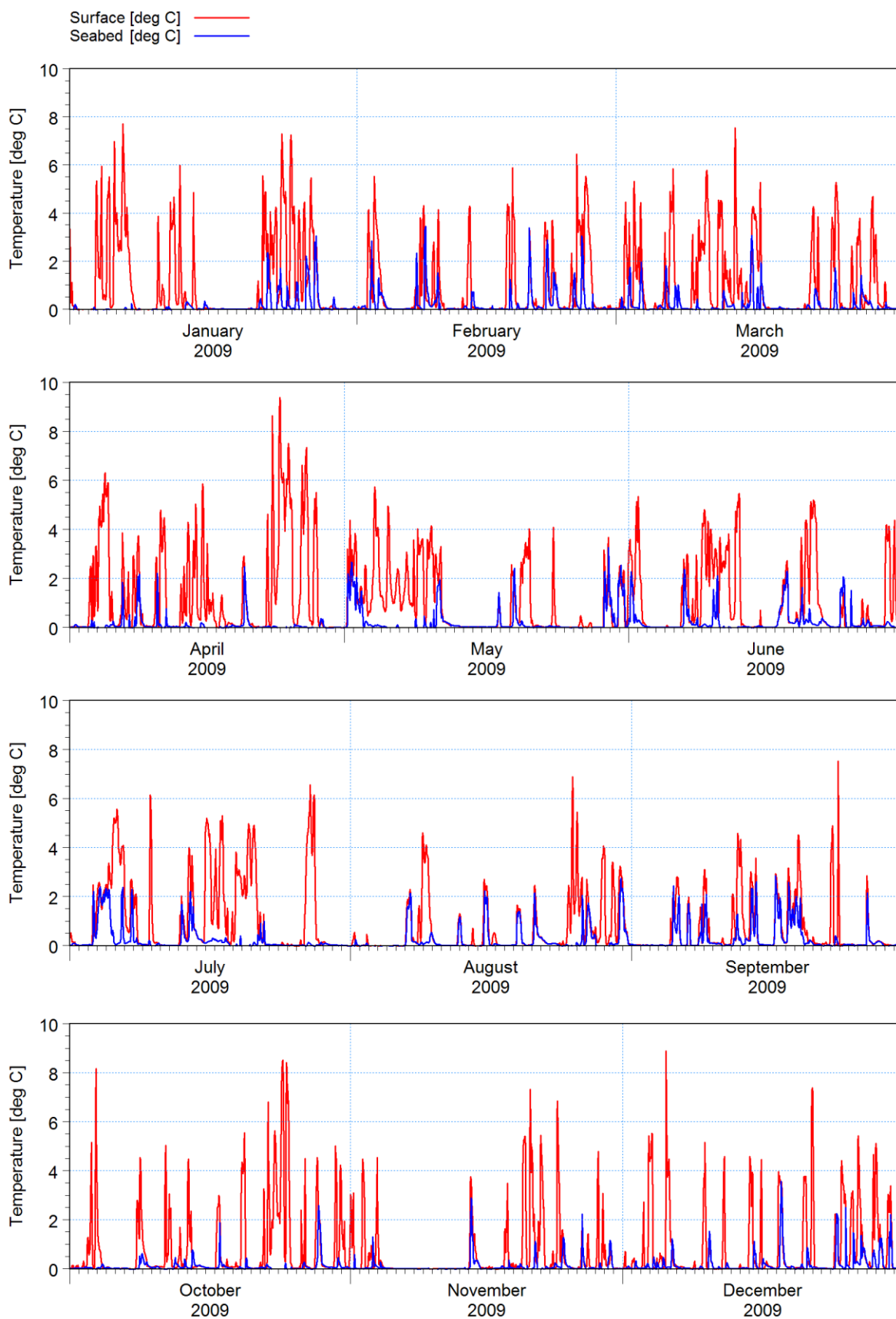
Stream	Discharge [m ³ /h]	ΔT [°C]	Duration [h]	Release interval [days]	Total duration per year [hrs]
CRF	327 888	11.7	continuous		
SEC	12 700	12	continuous		

Figure B-10: 95th Percentile near-seabed absolute temperature: plant operation at full capacity.



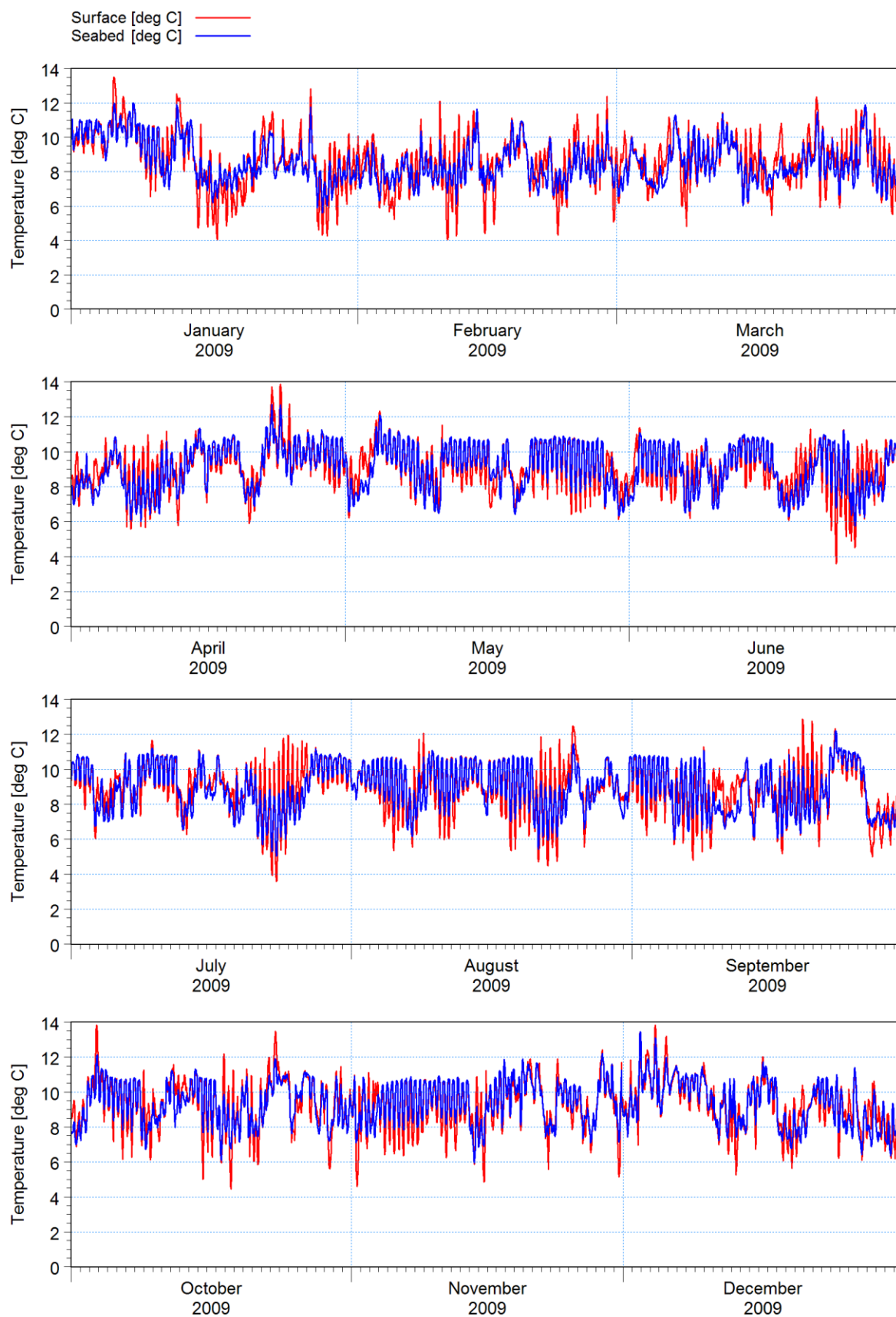
2015\S2015_Koeberg\Models\HD\07\071_02aa.mfm - Result Files\PostProcess\Timeseries\deltaT_SR.png

Figure B-11: Time series of near-surface and near-seabed increase in temperature at the rocks to the south (see Figure 5-15): plant operation at full capacity.



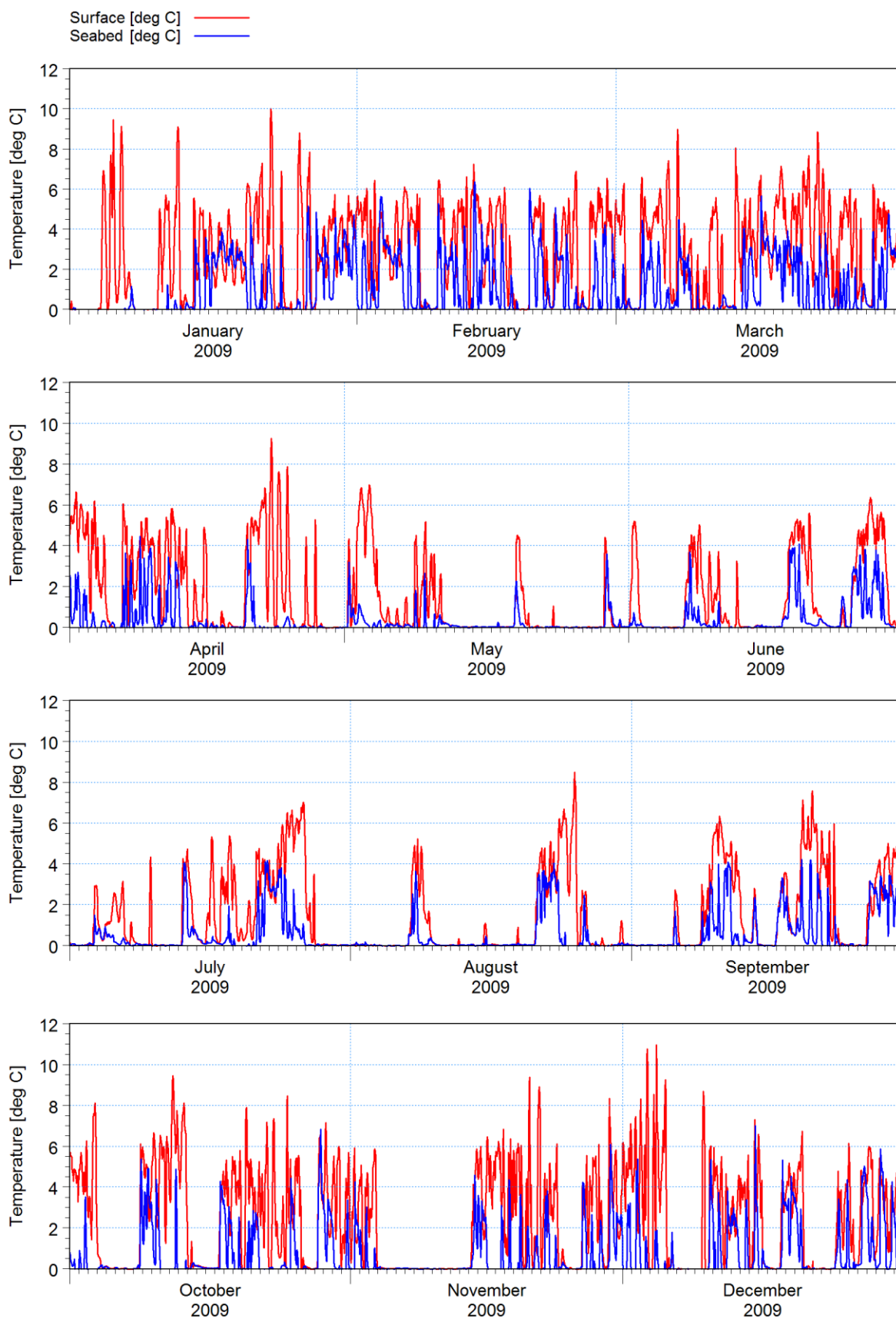
2015\S2015_Koeberg\Models\HD\07\071_02aa.mfm - Result Files\PostProcess\Timeseries\deltaT_1000m.png

Figure B-12: Time series of near-surface and near-seabed increase in temperature 1 km offshore of the discharge point (see Figure 5-15): plant operation at full capacity.



2015\S2015_Koeberg\Models\HD\07\071_02aa.mfm - Result Files\PostProcess\Timeseries\deltaT_100m.png

Figure B-13: Time series of near-surface and near-seabed increase in temperature 100 m offshore of the discharge point (see Figure 5-15): plant operation at full capacity.



2015\S2015_Koeberg\Models\HD\07\071_02aa.mfm - Result Files\PostProcess\Timeseries\deltaT_BW.png

Figure B-14: Time series of near-surface and near-seabed increase in temperature at the breakwater head (see Figure 5-15): plant operation at full capacity.

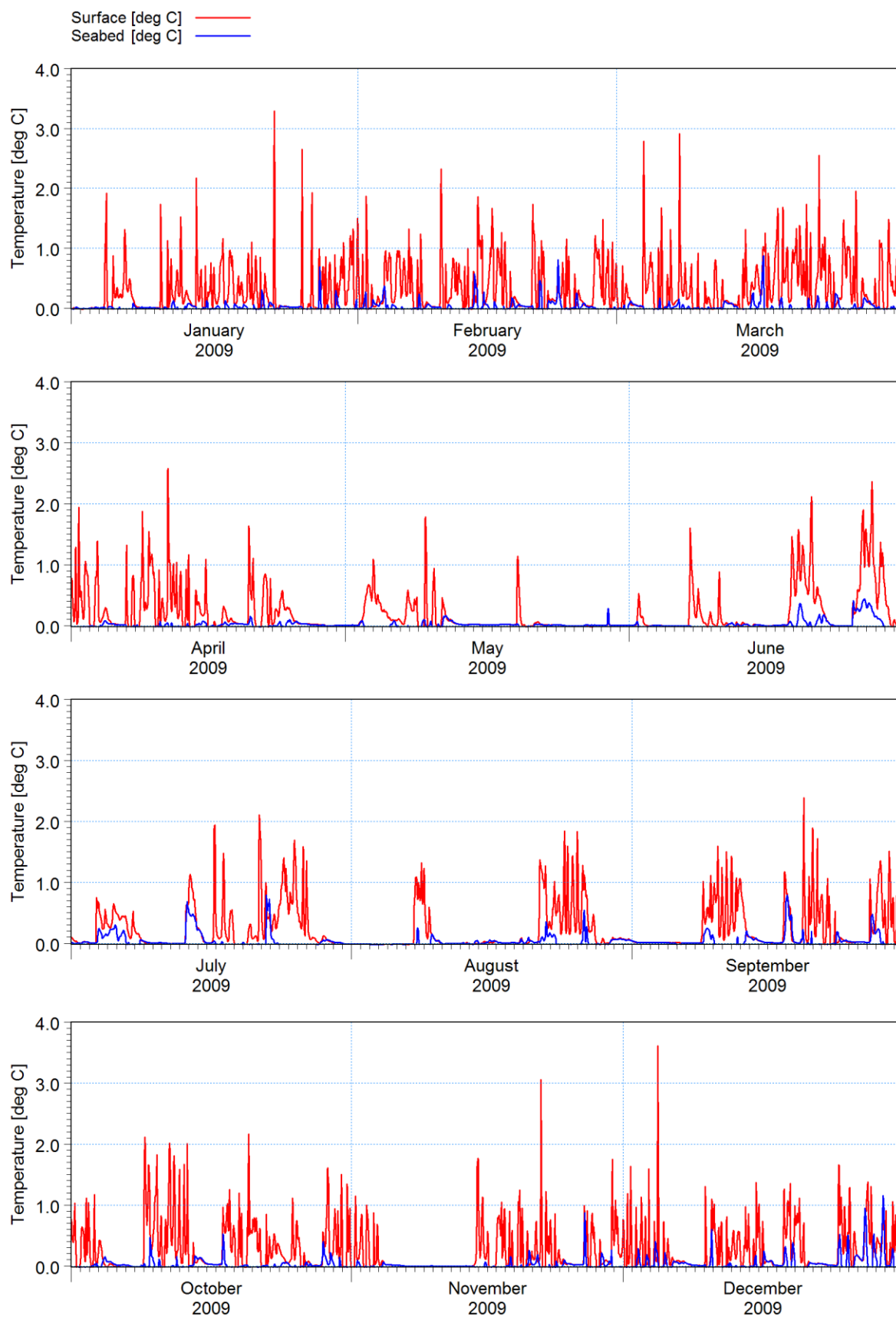
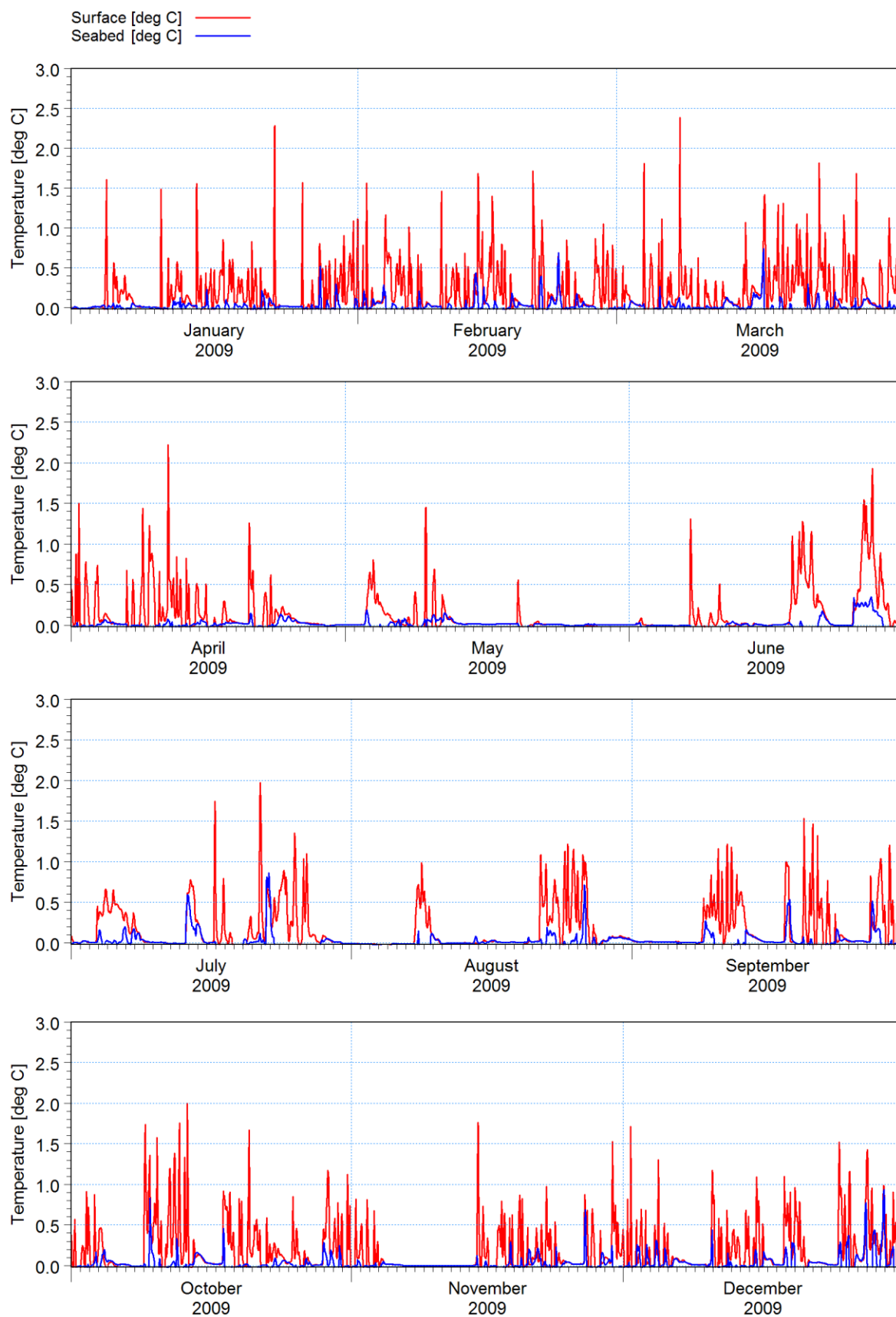
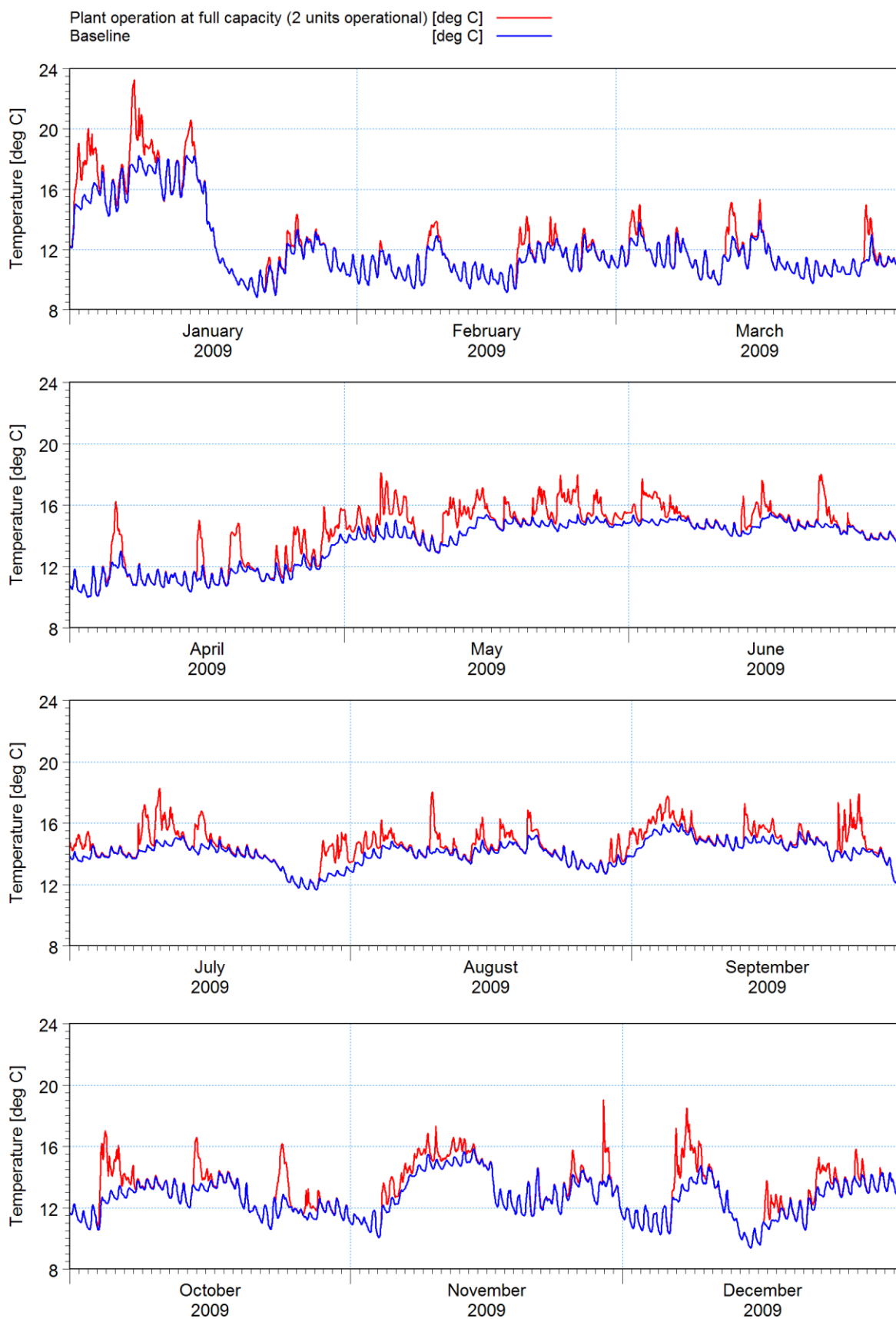


Figure B-15: Time series of near-surface and near-seabed increase in temperature at Northern Blinders 2 (see Figure 5-15): plant operation at full capacity.



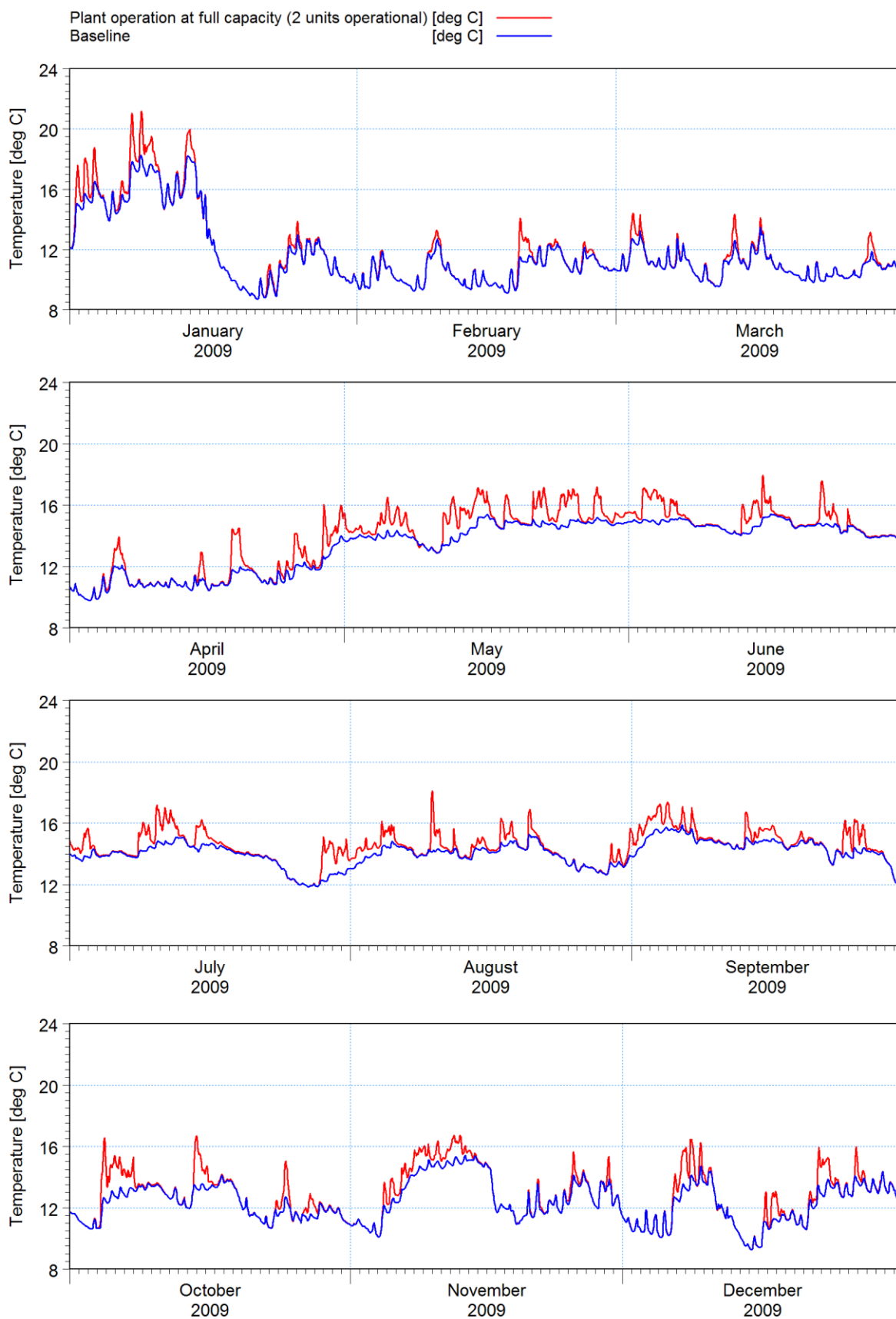
2015\S2015_Koeberg\Models\HD\07\071_02aa.mfm - Result Files\PostProcess\Timeseries\deltaT_NB1.png

Figure B-16: Time series of near-surface and near-seabed increase in temperature at Northern Blinders 1 (see Figure 5-15): plant operation at full capacity.



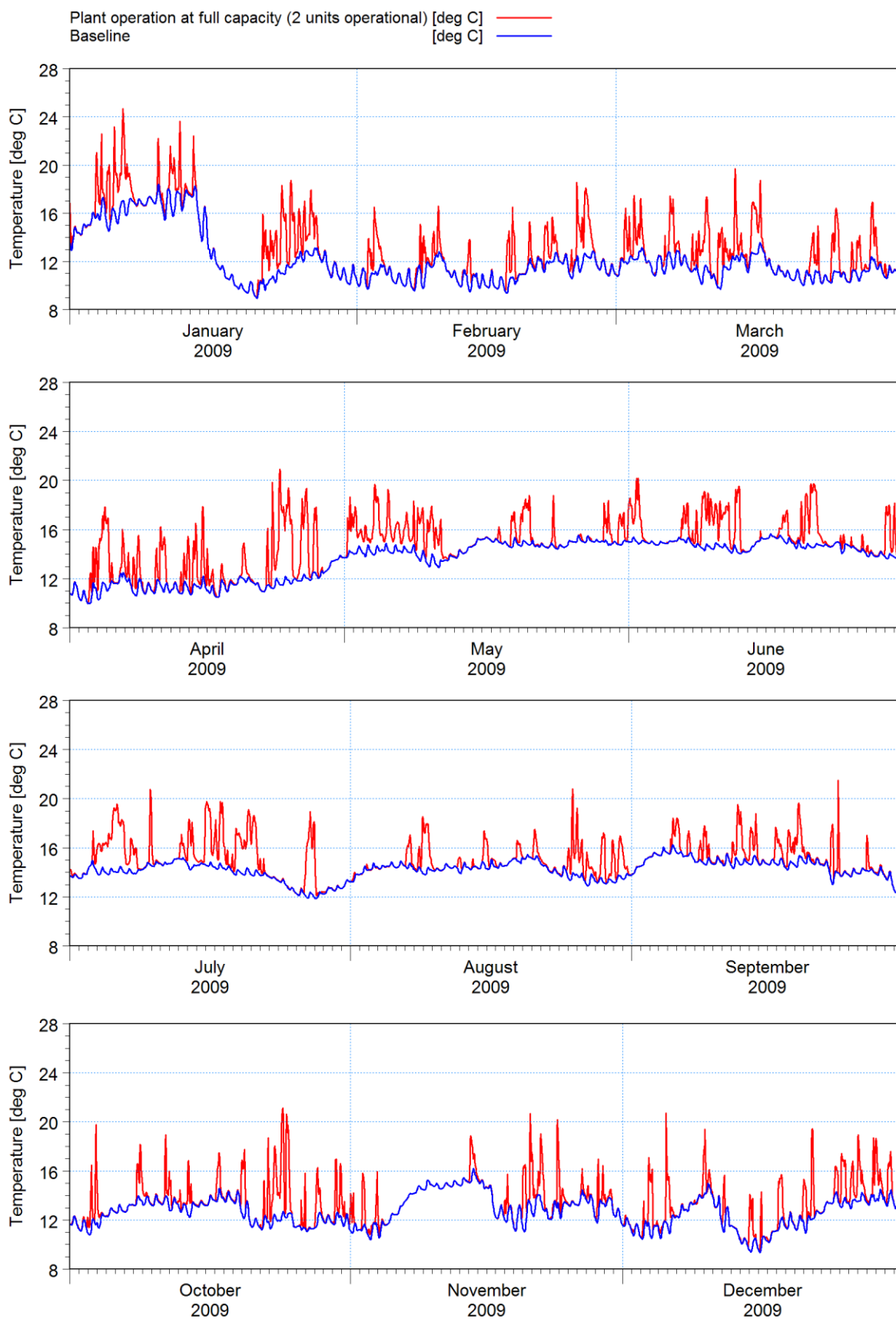
2015\S2015_Koeberg\Models\HD\07\071_02aa.mfm - Result Files\PostProcess\Timeseries\AbsTemp_SR_Lay8.png

Figure B-17: Time series of near-surface absolute temperature at the rocks to the south (see Figure 5-15): plant operation at full capacity.



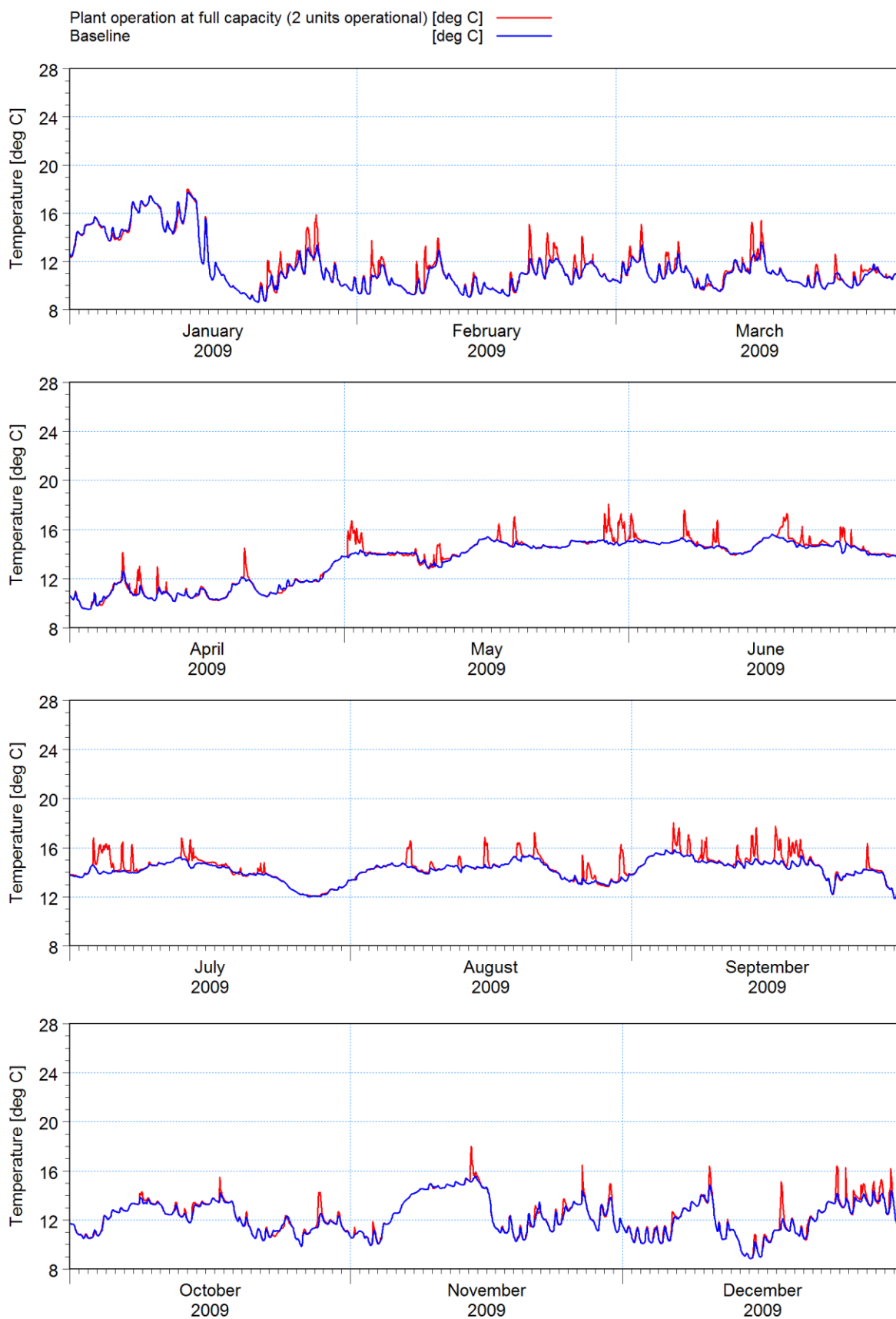
2015\S2015_Koeberg\Models\HD\07\071_02aa.mfm - Result Files\PostProcess\Timeseries\AbsTemp_SR_Lay1.png

Figure B-18: Time series of near-seabed absolute temperature at the rocks to the south (see Figure 5-15): plant operation at full capacity.



2015\S2015_Koeberg\Models\HD\07\071_02aa.mfm - Result Files\PostProcess\Timeseries\AbsTemp_1000m_Lay8.png

Figure B-19: Time series of near-surface absolute temperature 1 km offshore of the discharge point (see Figure 5-15): plant operation at full capacity.



2015\S2015_Koeberg\Models\HD\07\071_02aa.mfm - Result Files\PostProcess\Timeseries\AbsTemp_1000m_Lay1.png

Figure B-20: Time series of near-seabed absolute temperature 1 km offshore of the discharge point (see Figure 5-15): plant operation at full capacity.

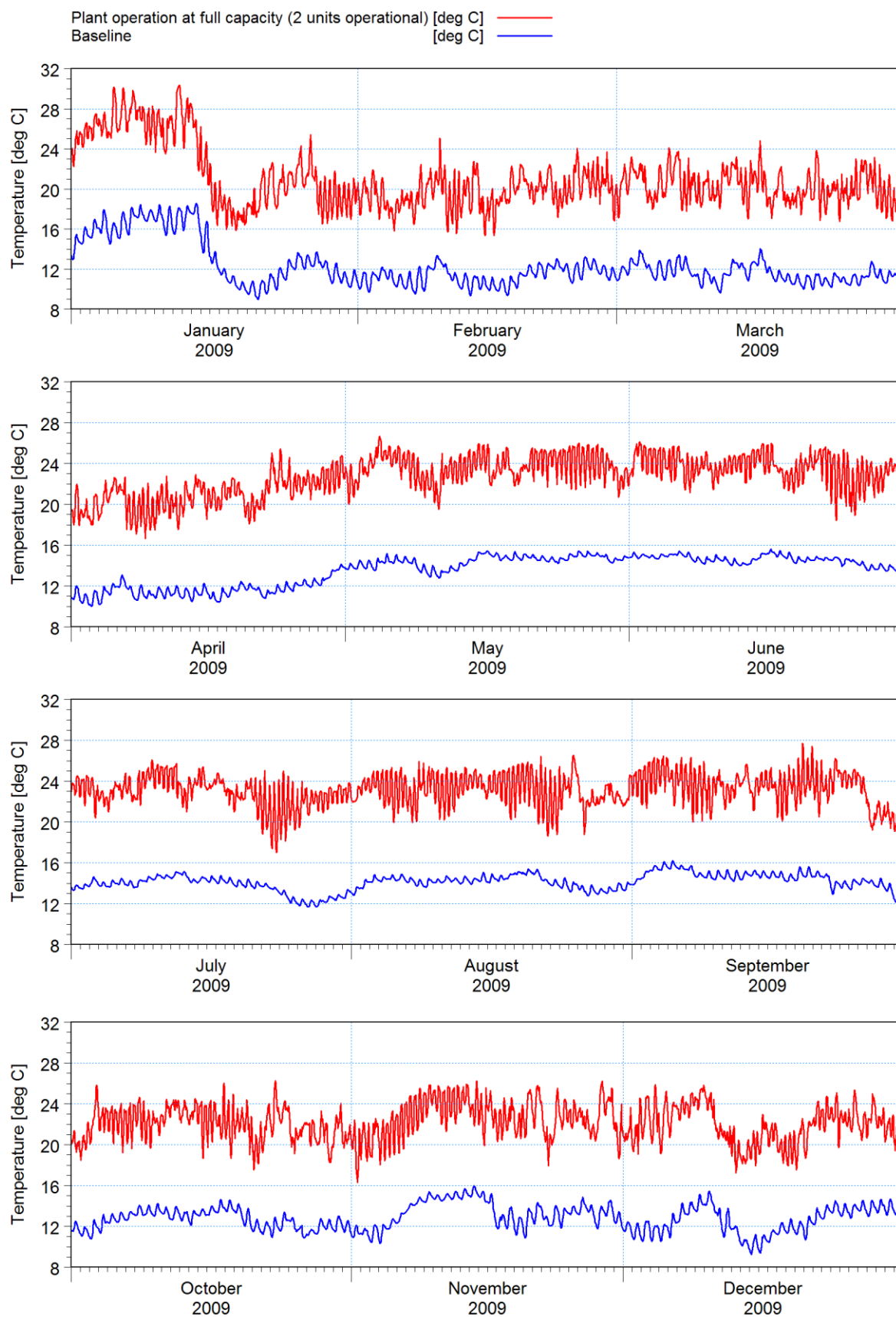


Figure B-21: Time series of near-surface absolute temperature 100 m offshore of the discharge point (see Figure 5-15): plant operation at full capacity.

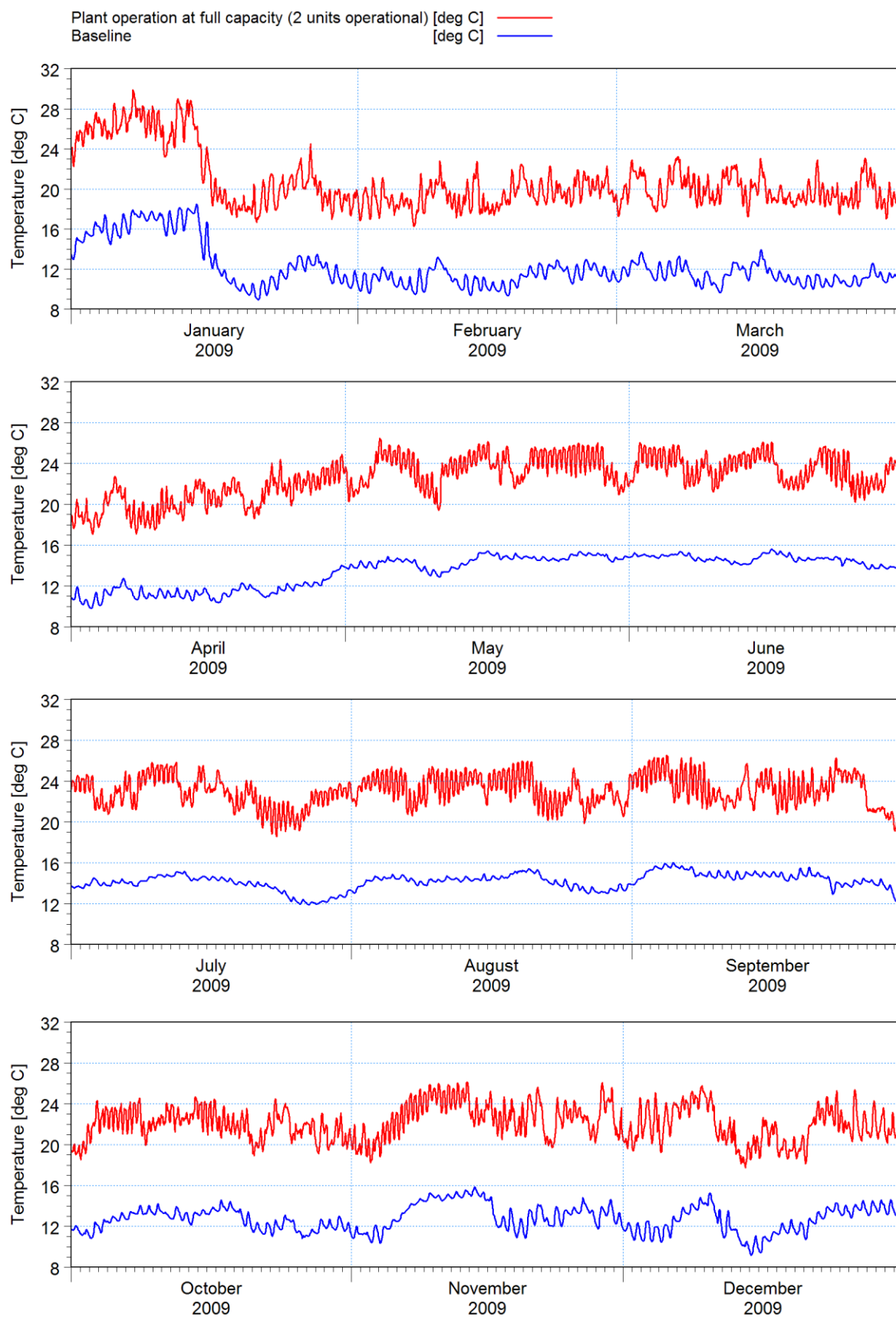
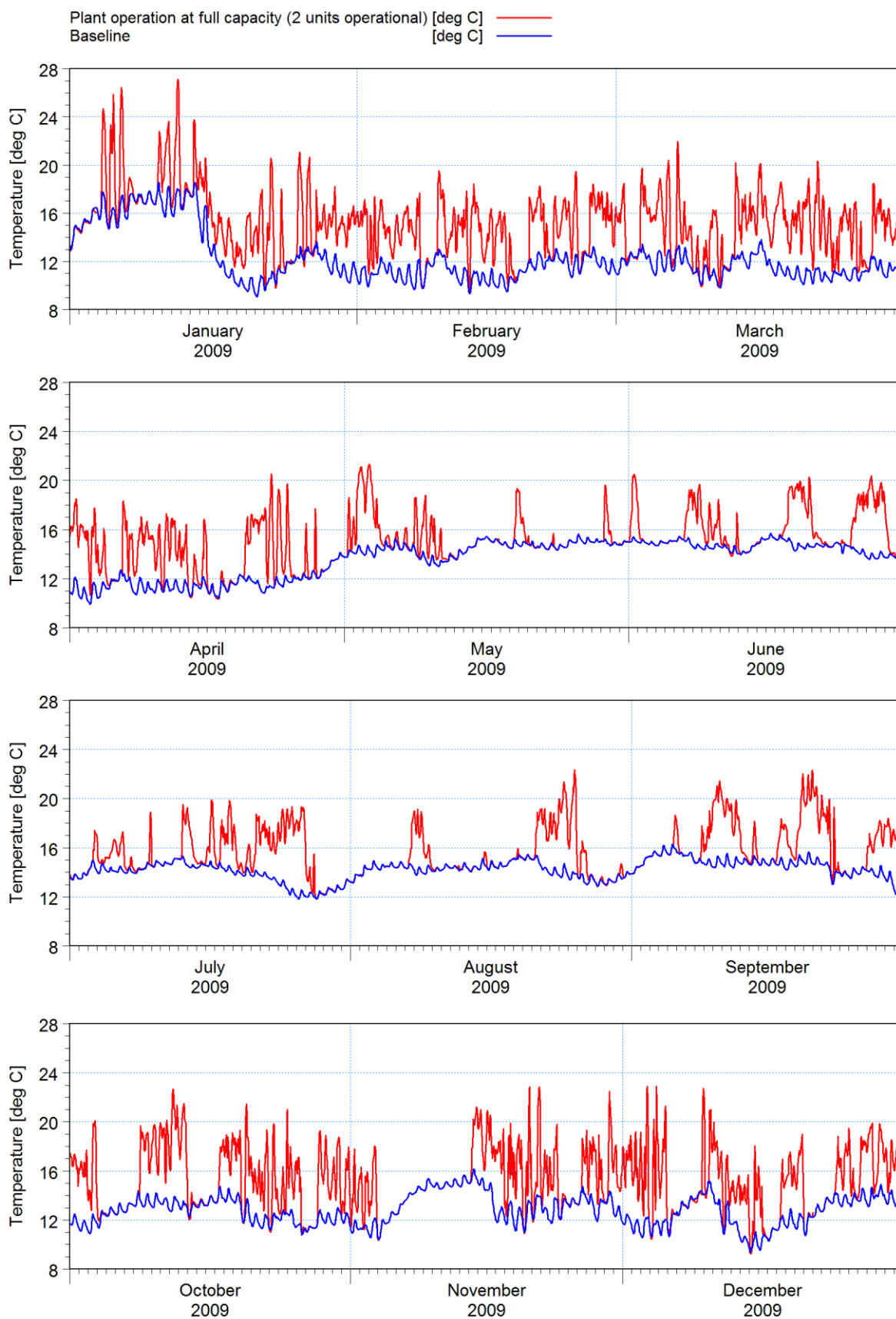
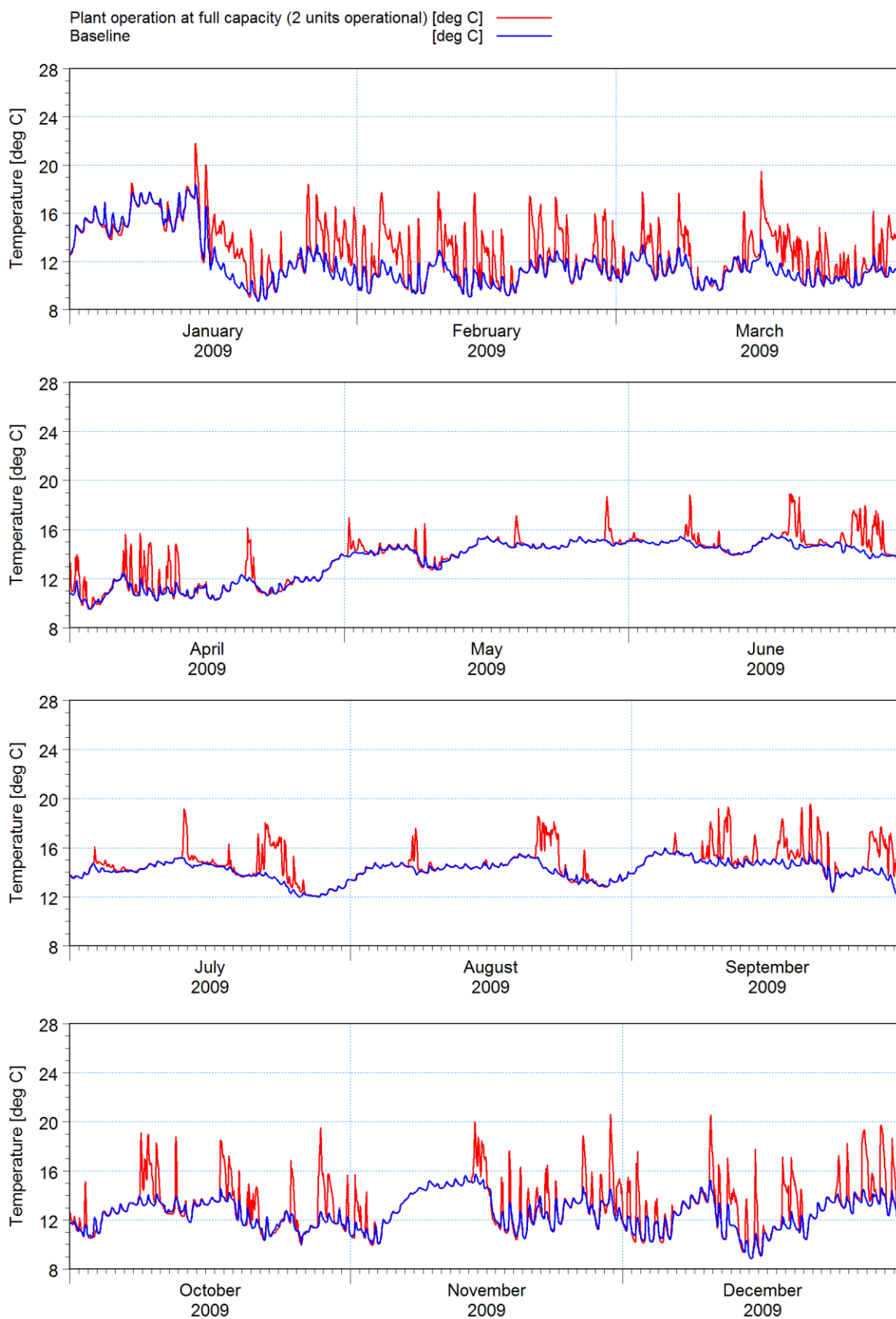


Figure B-22: Time series of near-seabed absolute temperature 100 m offshore of the discharge point (see Figure 5-15): plant operation at full capacity.



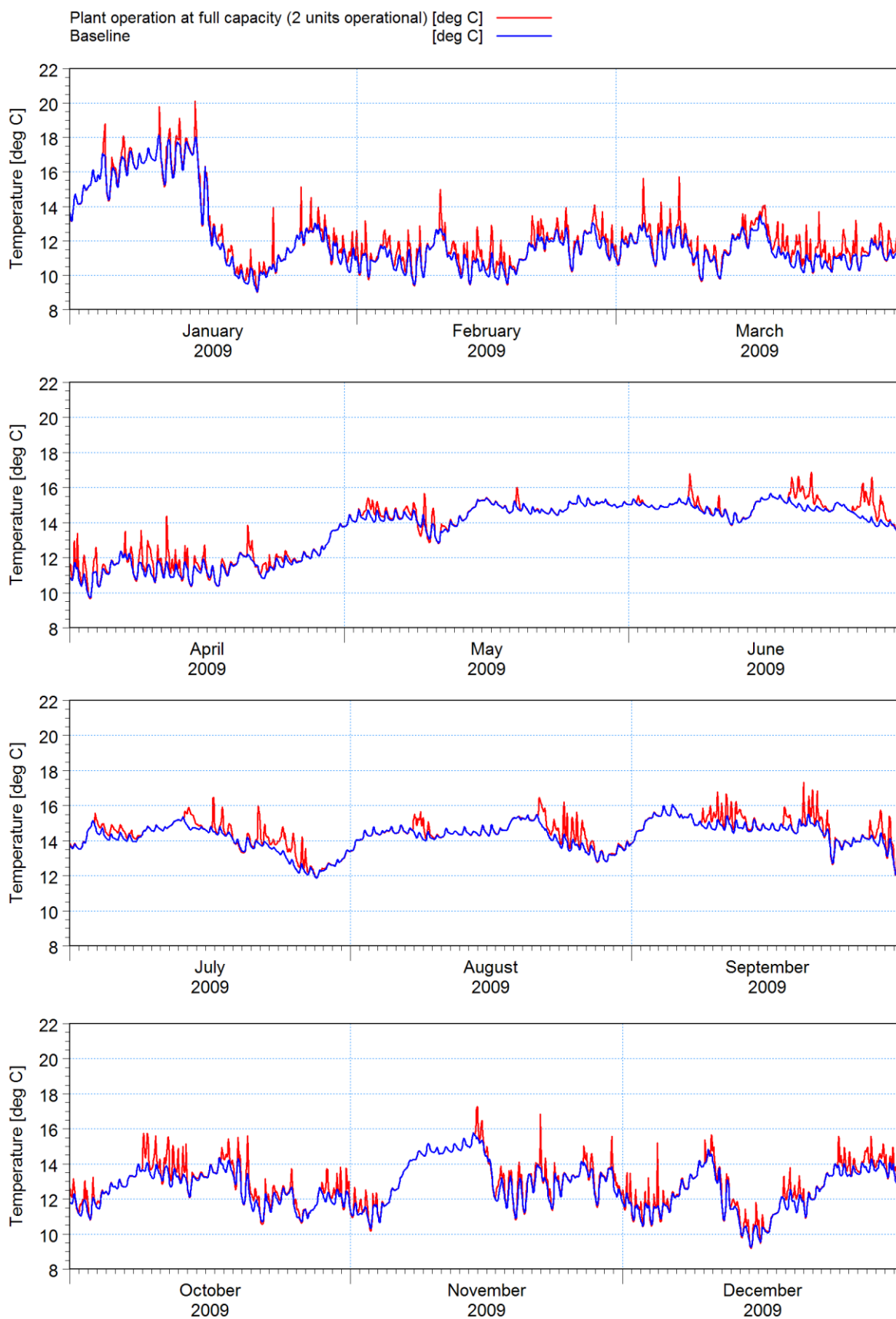
2015\S2015_Koeberg\Models\HD\07\071_02aa.mfm - Result Files\PostProcess\Timeseries\AbsTemp_BW_Lay8.png

Figure B-23: Time series of near-surface absolute temperature at the breakwater head (see Figure 5-15): plant operation at full capacity.



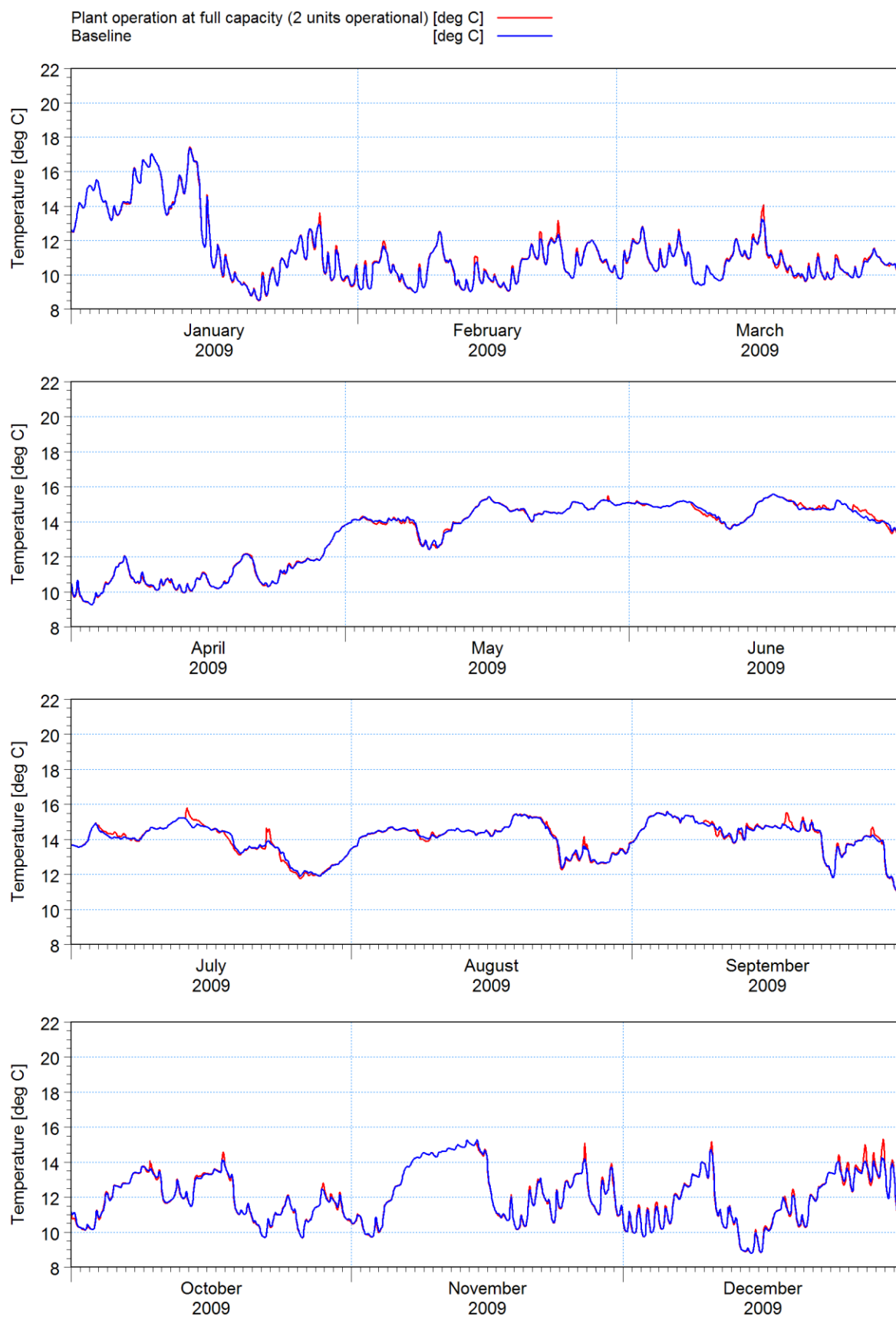
2015\S2015_Koeberg\Models\HD\07\071_02aa.mfm - Result Files\PostProcess\Timeseries\AbsTemp_BW_Lay1.png

Figure B-24: Time series of near-seabed absolute temperature at the breakwater head (see Figure 5-15): plant operation at full capacity.



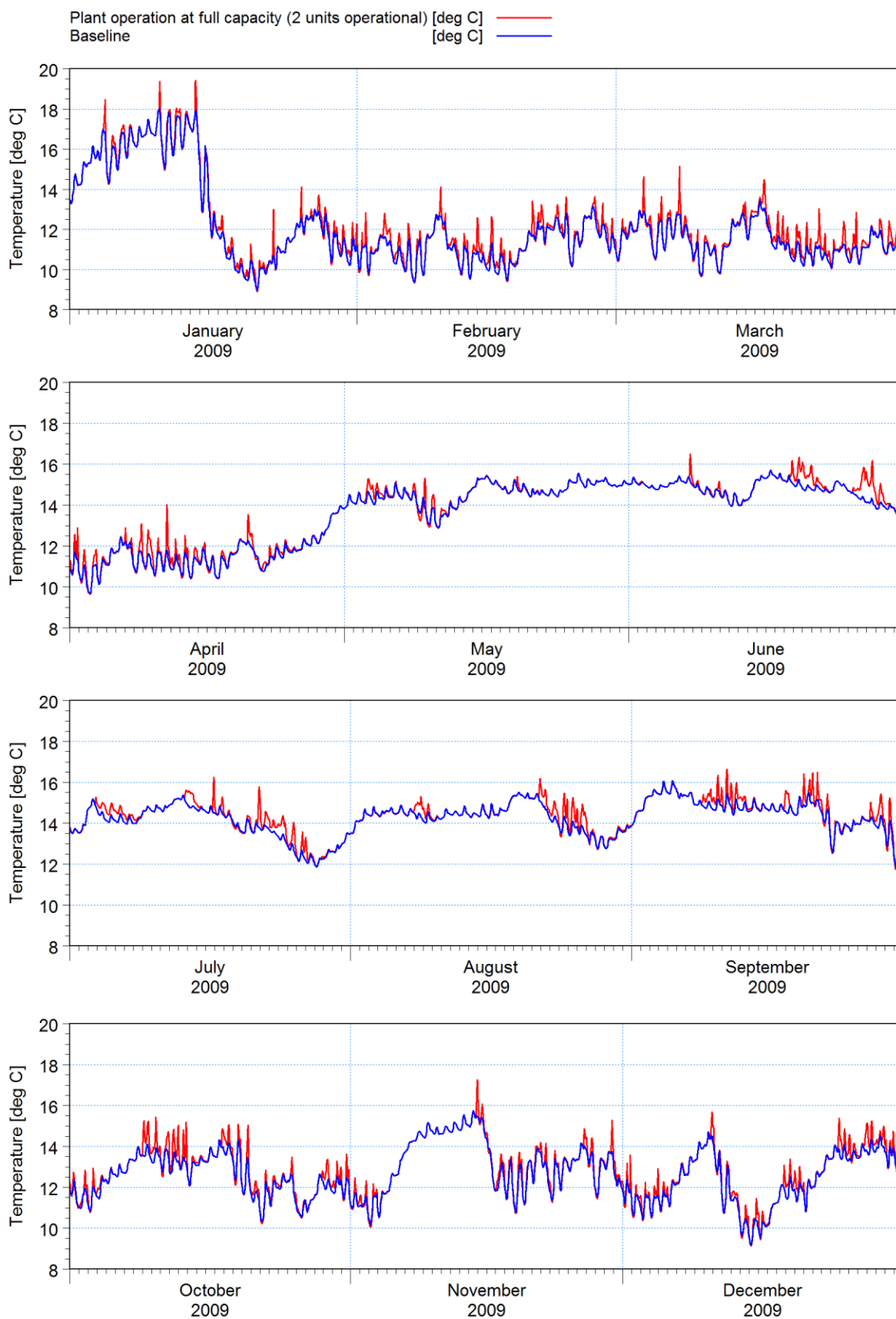
2015\S2015_Koeberg\Models\HD\07\071_02aa.mfm - Result Files\PostProcess\Timeseries\AbsTemp_NB2_Lay8.png

**Figure B-25: Time series of near-surface absolute temperature at Northern Blinders 2 (see Figure 5-15):
plant operation at full capacity.**



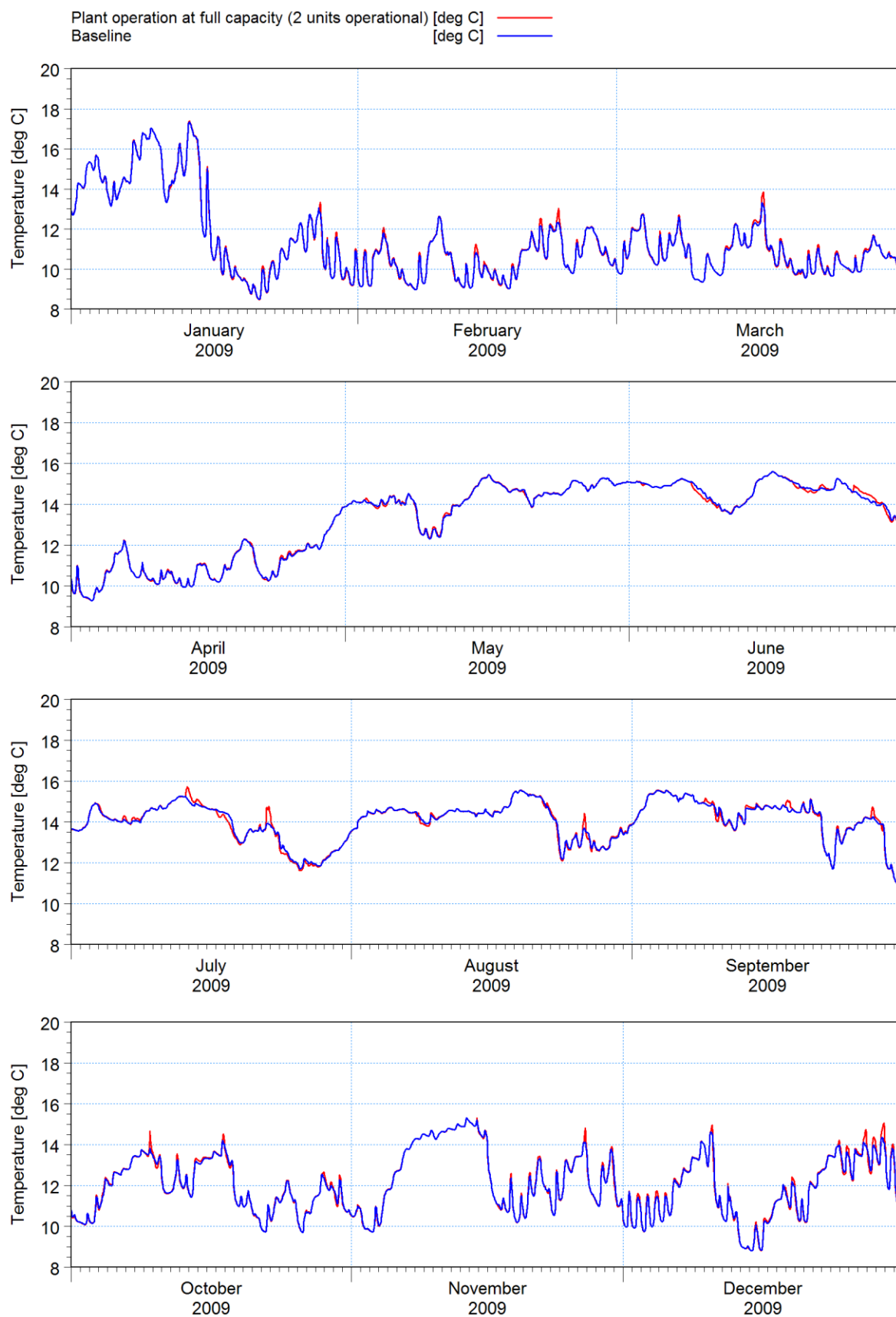
2015\S2015_Koeberg\Models\HD\07\071_02aa.mfm - Result Files\PostProcess\Timeseries\AbsTemp_NB2_Lay1.png

Figure B-26: Time series of near-seabed absolute temperature at Northern Blinders 2 (see Figure 5-15): plant operation at full capacity.



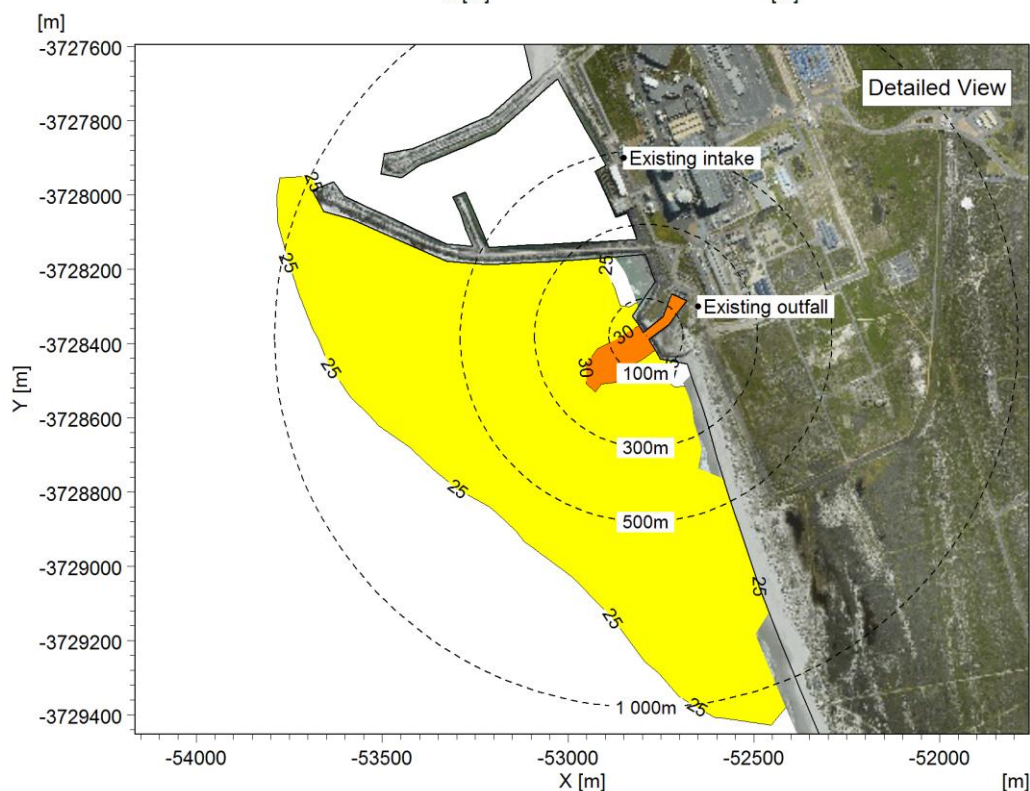
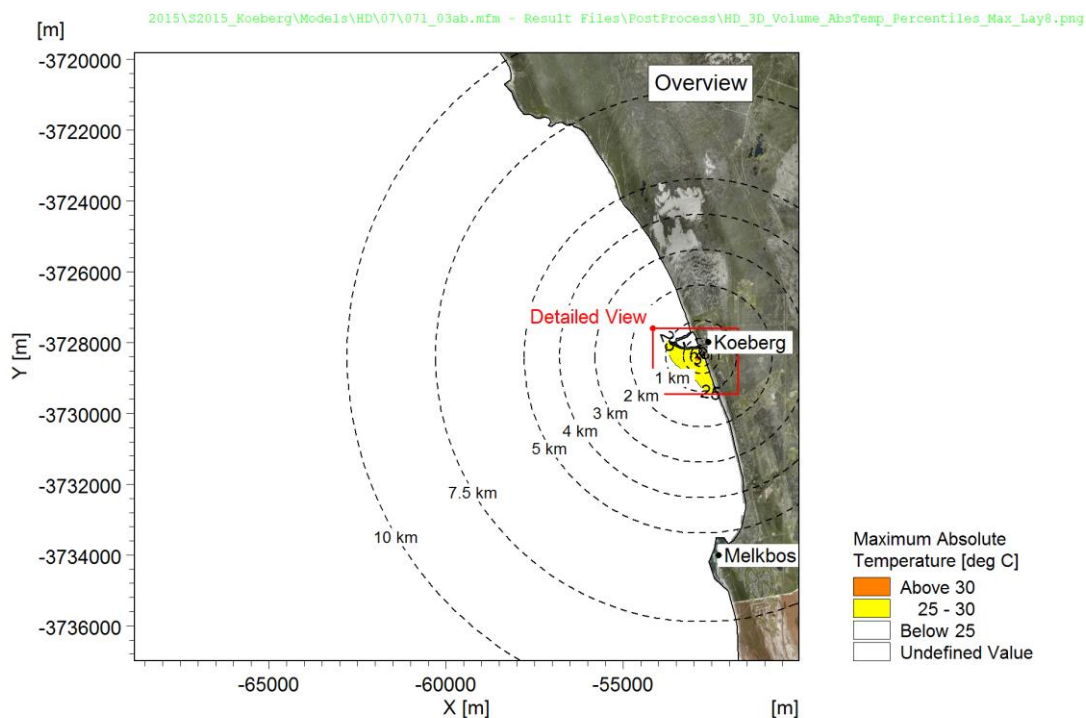
2015\S2015_Koeberg\Models\HD\07\071_02aa.mfm - Result Files\PostProcess\Timeseries\AbsTemp_NB1_Lay8.png

Figure B-27: Time series of near-surface absolute temperature at Northern Blinders 1 (see Figure 5-15): plant operation at full capacity.



2015\S2015_Koeberg\Models\HD\07\071_02aa.mfm - Result Files\PostProcess\Timeseries\AbsTemp_NB1_Lay1.png

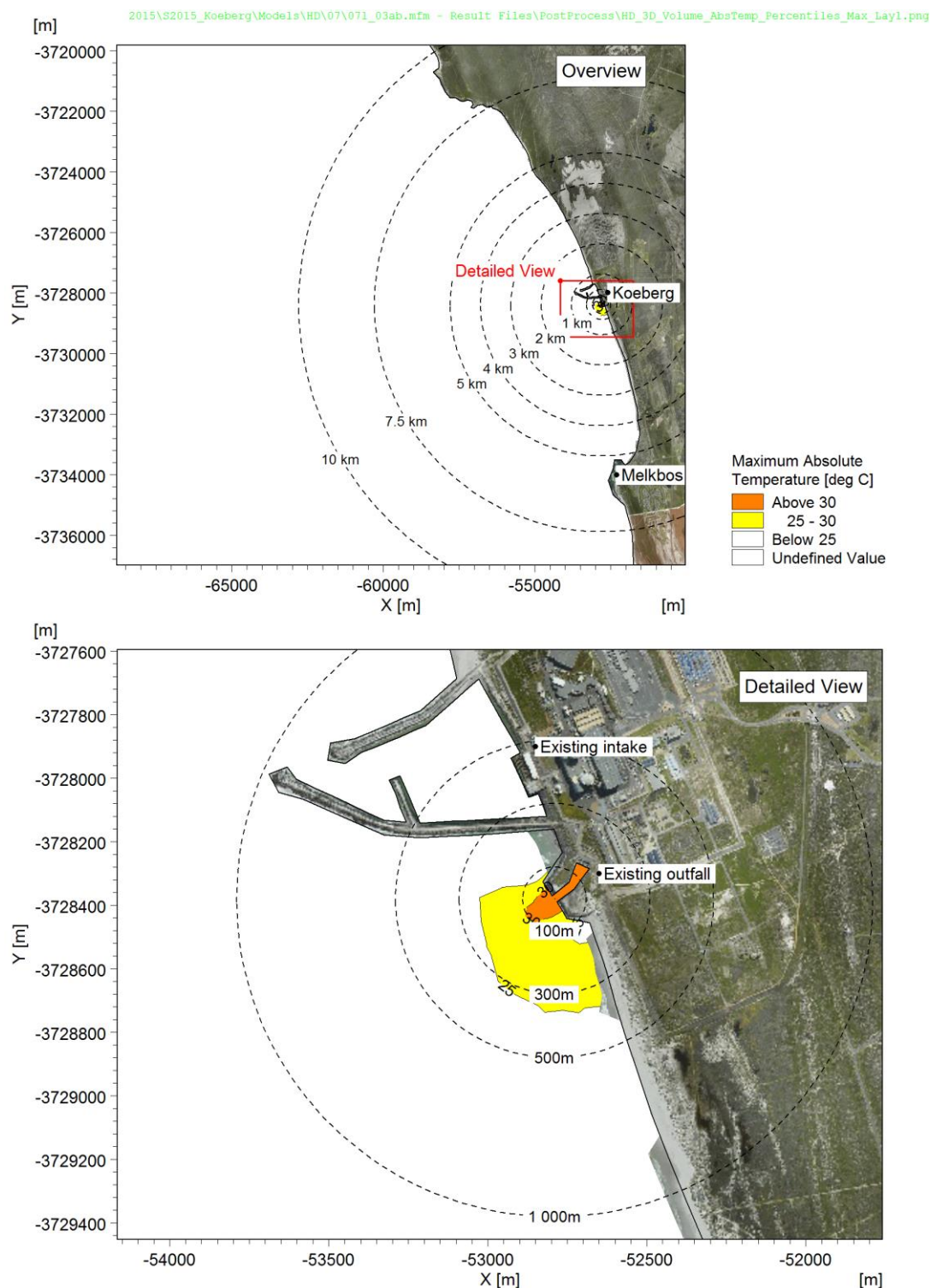
Figure B-28: Time series of near-seabed absolute temperature at Northern Blinders 1 (see Figure 5-15): plant operation at full capacity.



Stream	Discharge [m ³ /h]	ΔT [°C]	Duration [h]	Release interval [days]	Total duration per year [hrs]
CRF	163 944	11.7	continuous		
	81 972	22.7	12	Abnormal	.. ⁽¹⁾
SEC	12 700	12	continuous		

(1) Since this batch release only occurs under abnormal operation, the real number of releases expected to occur per year is unknown.

Figure B-29: Maximum absolute temperature near the surface: pump trip scenario.

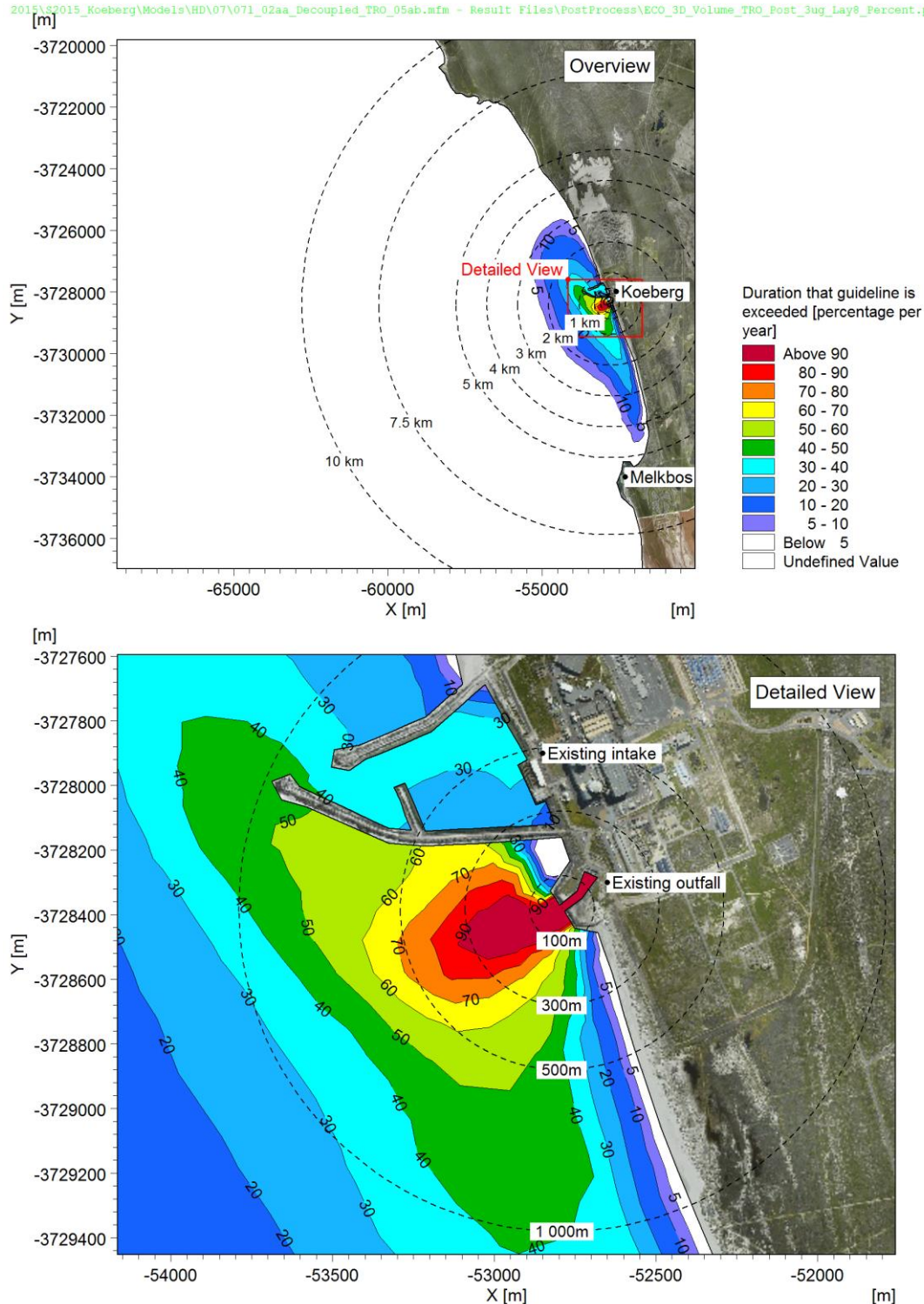


Stream	Discharge [m ³ /h]	ΔT [°C]	Duration [h]	Release interval [days]	Total duration per year [hrs]
CRF	163 944	11.7	continuous		
	81 972	22.7	12	Abnormal	.. ⁽¹⁾
SEC	12 700	12	continuous		

(1) Since this batch release only occurs under abnormal operation, the real number of releases expected to occur per year is unknown.

Figure B-30: Maximum absolute temperature near the seabed: pump trip scenario.

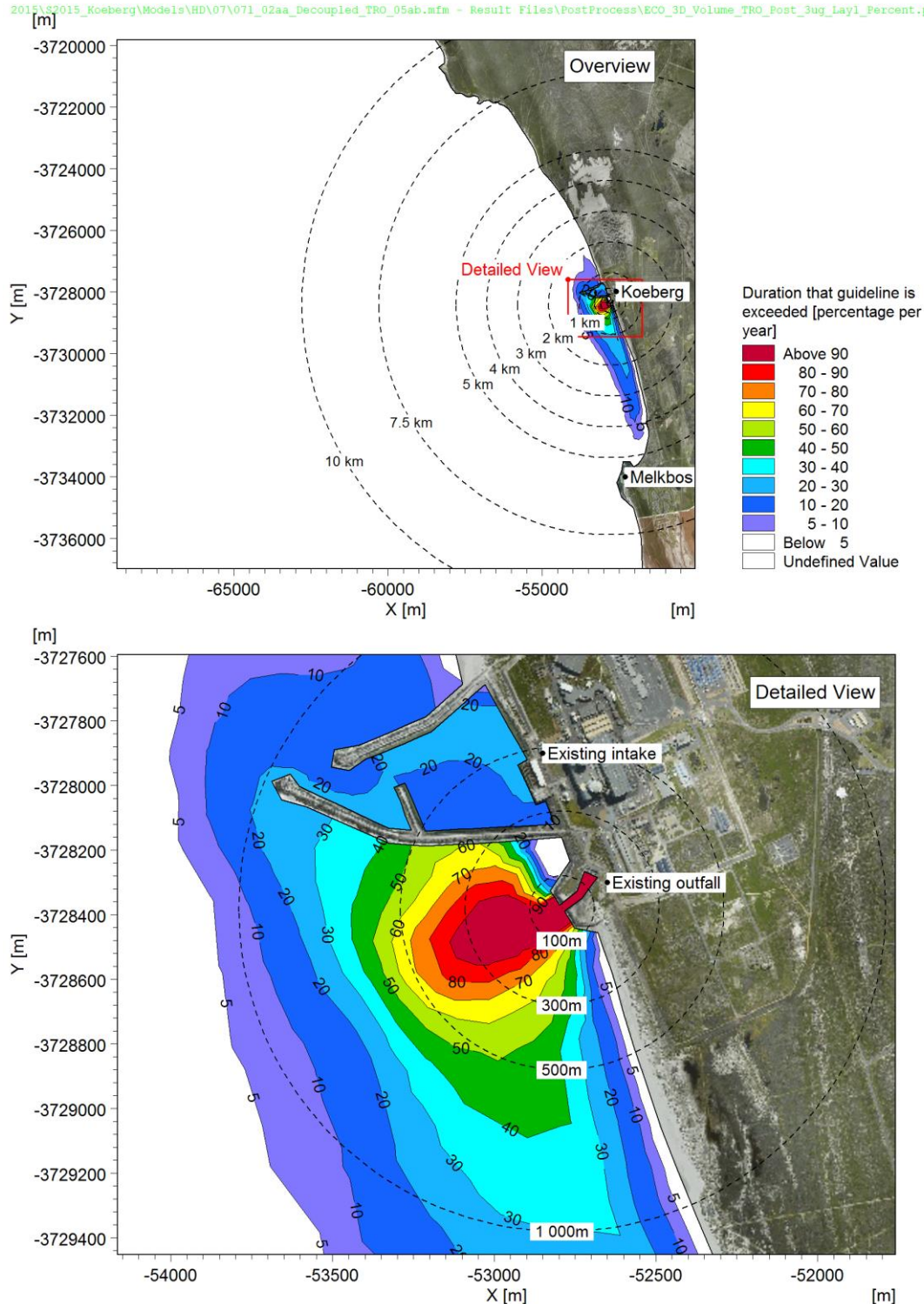
2015\82015_Koeberg\Models\HD\07\071_02aa_Decoupled_TRO_05ab.mfm - Result Files\PostProcess\ECO_3D_Volume_TRO_Post_3ug_Lay8_Percent.png



Stream	Discharge [m³/h]	Concentration [mg/l]	Load [kg/h]	Duration [h]	Release interval [days]	Total duration per year [hrs]	Total Annual Load [kg]
CRF	327 888	0.5	164	continuous		8766	1 437 133
SEC	12 700	1	13	continuous		8336	105 861
		2	25	8	7	417	10 603
		25	318	0.5	14	13	4 142
SEU	28	5	0.14	continuous		8766	1 227

Figure B-31: Percentage of time during which the guideline concentration for free chlorine (0.003 mg/l) is exceeded near the surface: plant operation at full capacity.

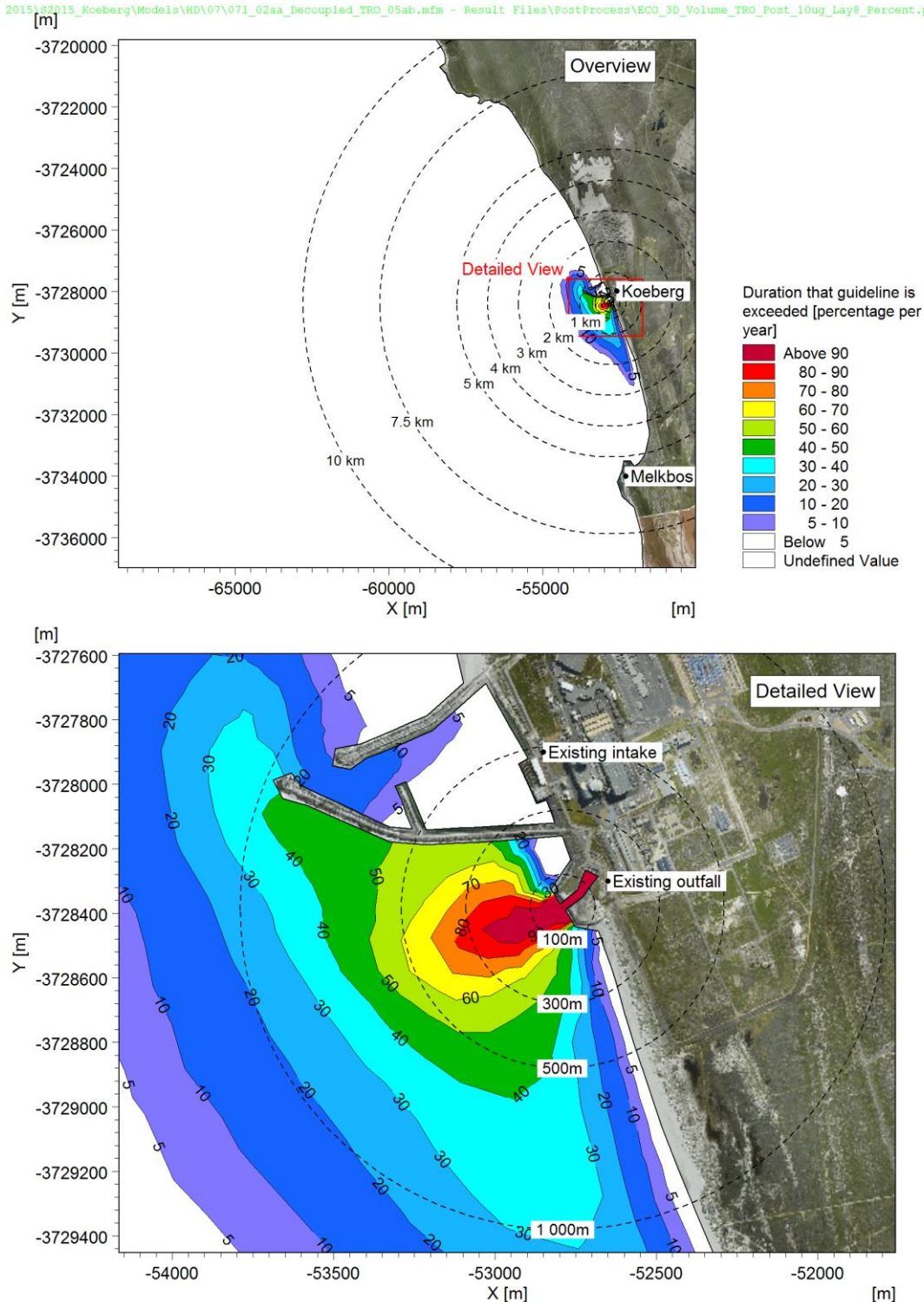
2015\82015_Koeberg\Models\HD\07\071_02aa_Decoupled_TRO_05ab.mfm - Result Files\PostProcess\ECO_3D_Volume_TRO_Post_3ug_Lay1_Percent.png



Stream	Discharge [m³/h]	Concentration [mg/l]	Load [kg/h]	Duration [h]	Release interval [days]	Total duration per year [hrs]	Total Annual Load [kg]
CRF	327 888	0.5	164	continuous		8766	1 437 133
SEC	12 700	1	13	continuous		8336	105 861
		2	25	8	7	417	10 603
		25	318	0.5	14	13	4 142
SEU	28	5	0.14	continuous		8766	1 227

Figure B-32: Percentage of time during which the guideline concentration for free chlorine (0.003 mg/l) is exceeded near the seabed: plant operation at full capacity.

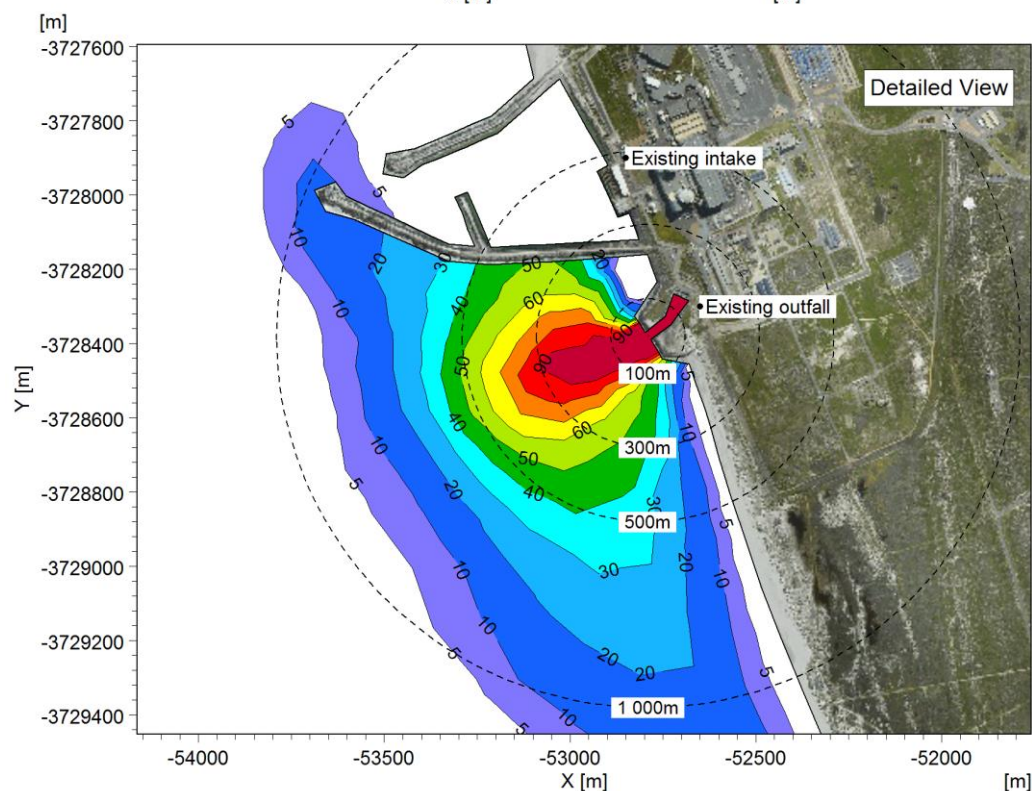
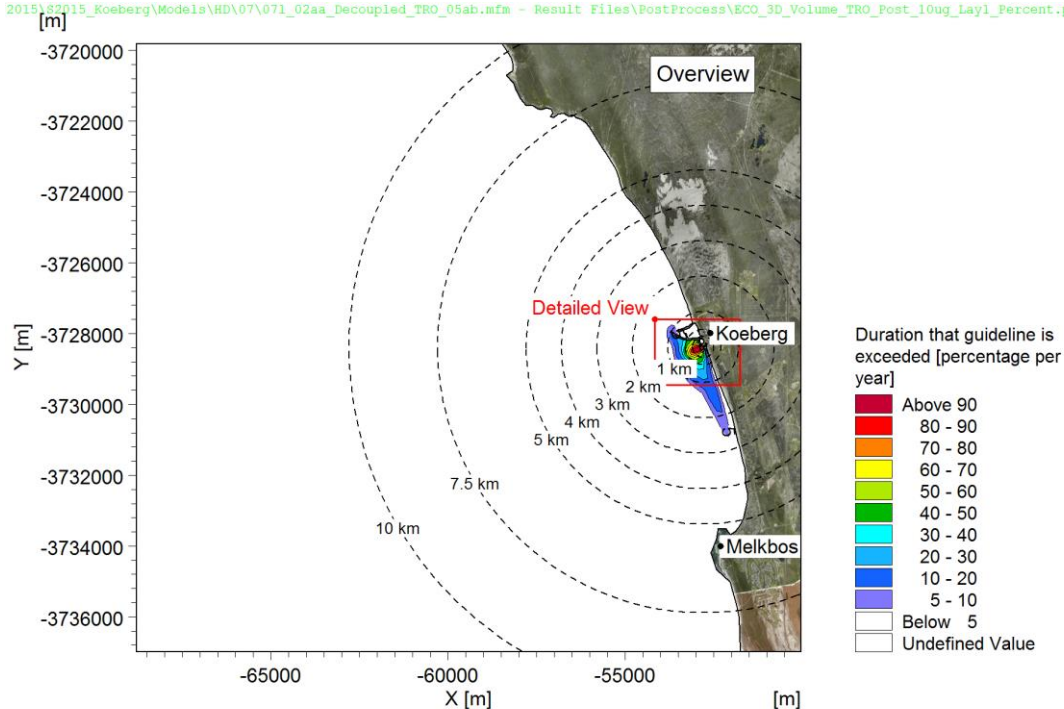
2015\82215_Koeberg\Models\HD\07\071_02aa_Decoupled_TRO_05ab.mfm - Result Files\PostProcess\ECO_3D_Volume_TRO_Post_10ug_Lay8_Percent.png



Stream	Discharge [m ³ /h]	Concentration [mg/l]	Load [kg/h]	Duration [h]	Release interval [days]	Total duration per year [hrs]	Total Annual Load [kg]
CRF	327 888	0.5	164	continuous		8766	1 437 133
SEC	12 700	1	13	continuous		8336	105 861
		2	25	8	7	417	10 603
		25	318	0.5	14	13	4 142
SEU	28	5	0.14	continuous		8766	1 227

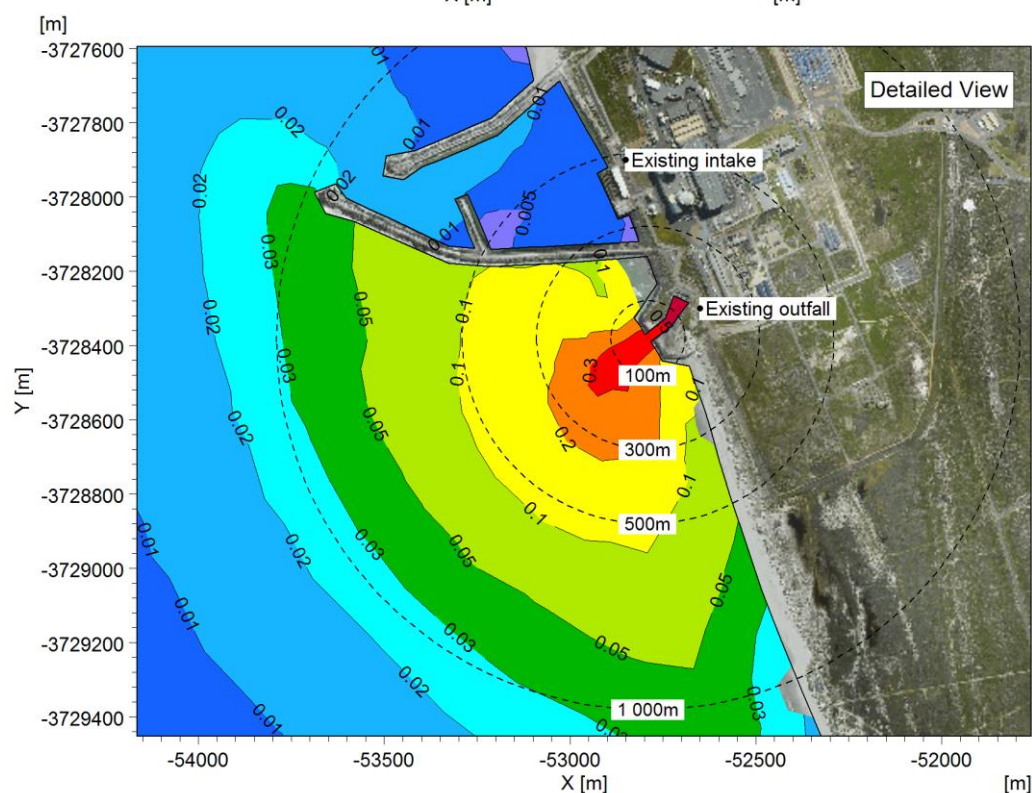
Figure B-33: Percentage of time during which the guideline concentration for free chlorine (0.01 mg/l) is exceeded near the surface: plant operation at full capacity.

2015\82215_Koeberg\Models\HD\07\071_02aa_Decoupled_TRO_05ab.mfm - Result Files\PostProcess\ECO_3D_Volume_TRO_Post_10ug_Lay1_Percent.png



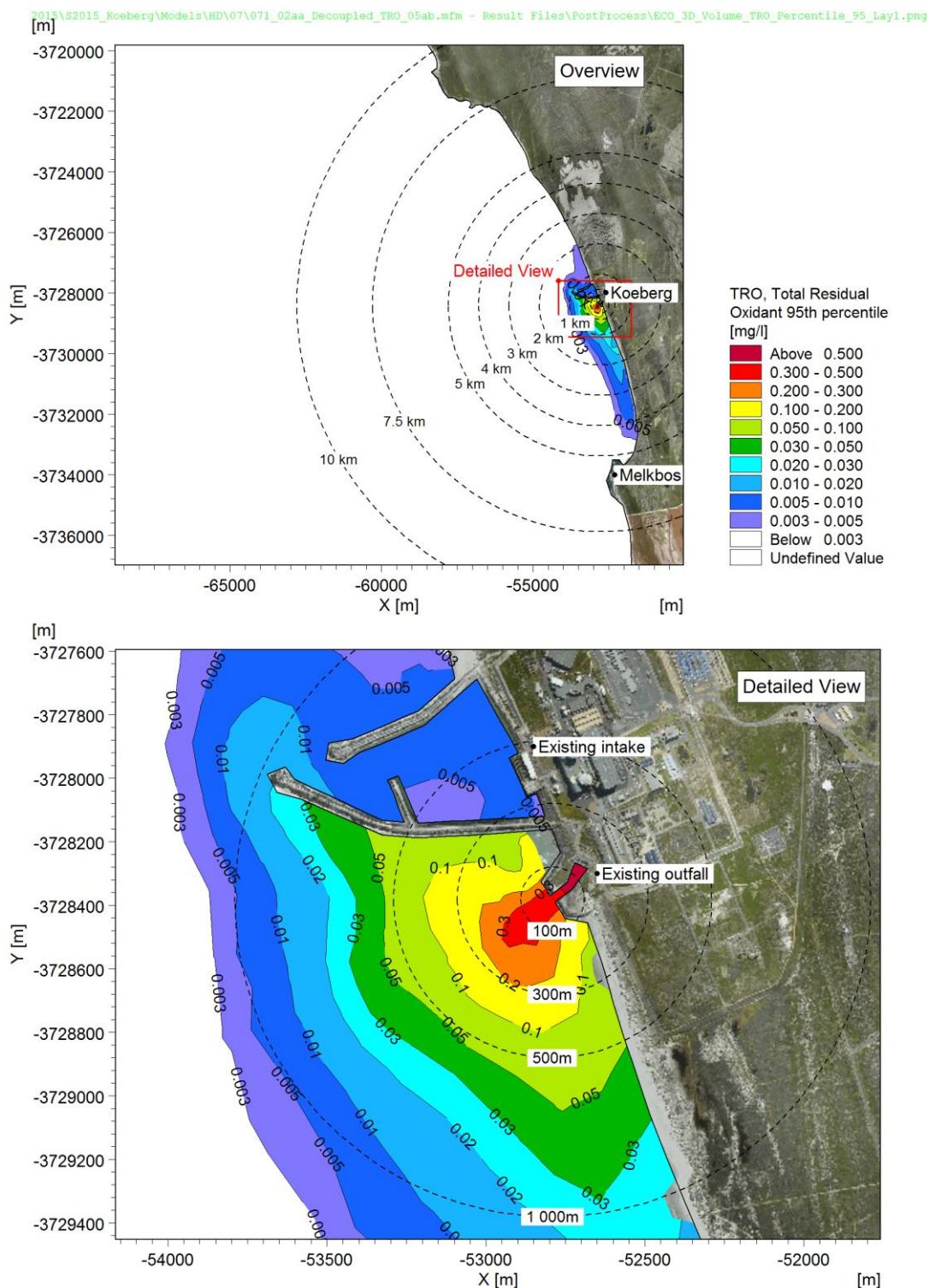
Stream	Discharge [m³/h]	Concentration [mg/l]	Load [kg/h]	Duration [h]	Release interval [days]	Total duration per year [hrs]	Total Annual Load [kg]
CRF	327 888	0.5	164	continuous		8766	1 437 133
SEC	12 700	1	13	continuous		8336	105 861
		2	25	8	7	417	10 603
		25	318	0.5	14	13	4 142
SEU	28	5	0.14	continuous		8766	1 227

Figure B-34: Percentage of time during which the guideline concentration for free chlorine (0.01 mg/l) is exceeded near the seabed: plant operation at full capacity.



Stream	Discharge [m³/h]	Concentration [mg/l]	Load [kg/h]	Duration [h]	Release interval [days]	Total duration per year [hrs]	Total Annual Load [kg]
CRF	327 888	0.5	164	continuous		8766	1 437 133
SEC	12 700	1	13	continuous		8336	105 861
		2	25	8	7	417	10 603
		25	318	0.5	14	13	4 142
SEU	28	5	0.14	continuous		8766	1 227

Eskom



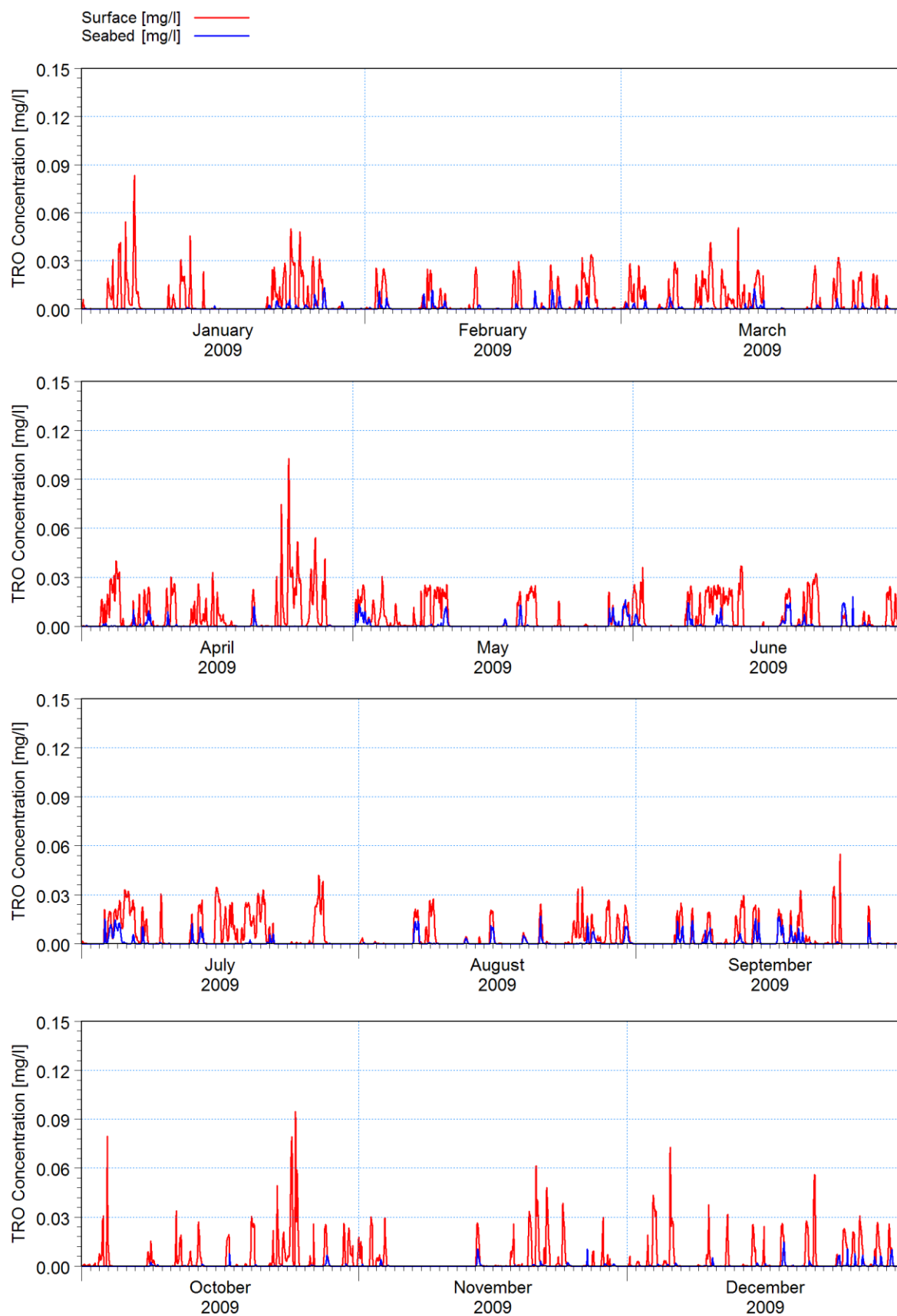
Stream	Discharge [m ³ /h]	Concentration [mg/l]	Load [kg/h]	Duration [h]	Release interval [days]	Total duration per year [hrs]	Total Annual Load [kg]
CRF	327 888	0.5	164	continuous		8766	1 437 133
SEC	12 700	1	13	continuous		8336	105 861
		2	25	8	7	417	10 603
		25	318	0.5	14	13	4 142
SEU	28	5	0.14	continuous		8766	1 227

Figure B-36: 95th Percentile near-seabed concentration of free chlorine: plant operation at full capacity.



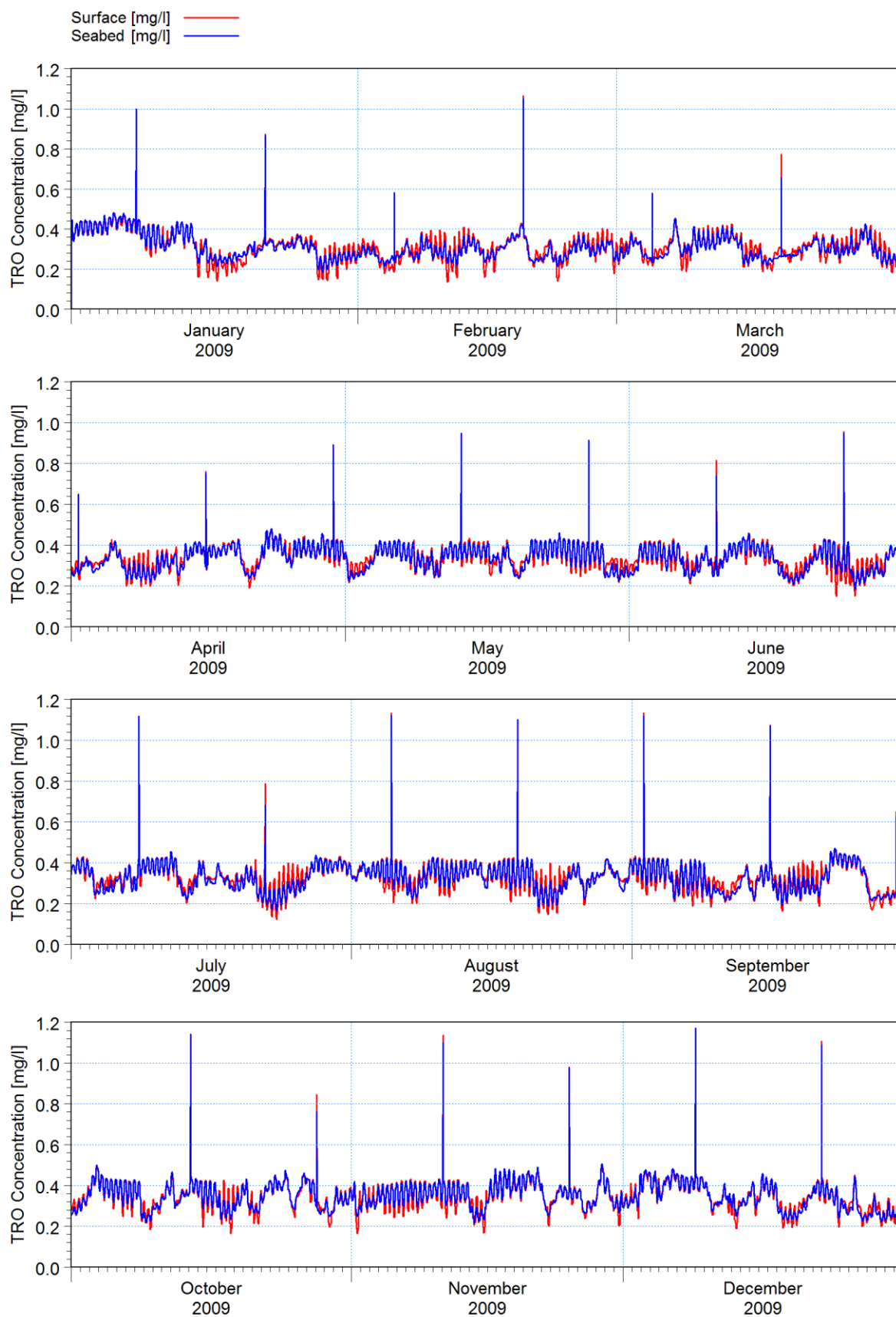
2015\S2015_Koeberg\Models\HD\07\071_02aa_Decoupled_TRO_05ab.mfm - Result Files\PostProcess\Timeseries\TRO_SR.png

Figure B-37: Time series of near-surface and near-seabed TRO concentration at the rocks to the south (see Figure 5-15): plant operation at full capacity.



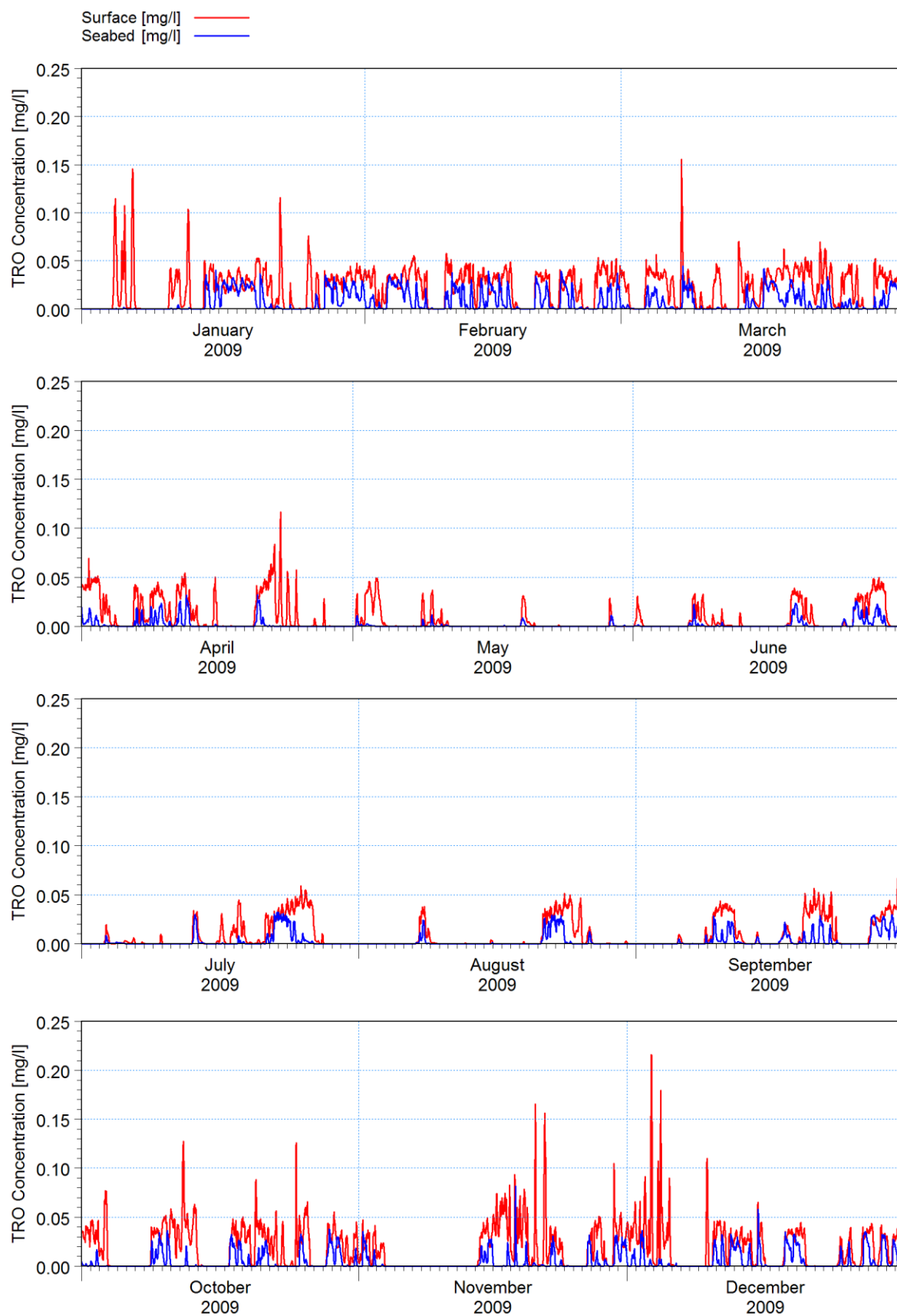
2015\S2015_Koeberg\Models\HD\07\071_02aa_Decoupled_TRO_05ab.mfm - Result Files\PostProcess\Timeseries\TRO_1000m.png

Figure B-38: Time series of near-surface and near-seabed TRO concentration 1 km offshore of the discharge point (see Figure 5-15): plant operation at full capacity.



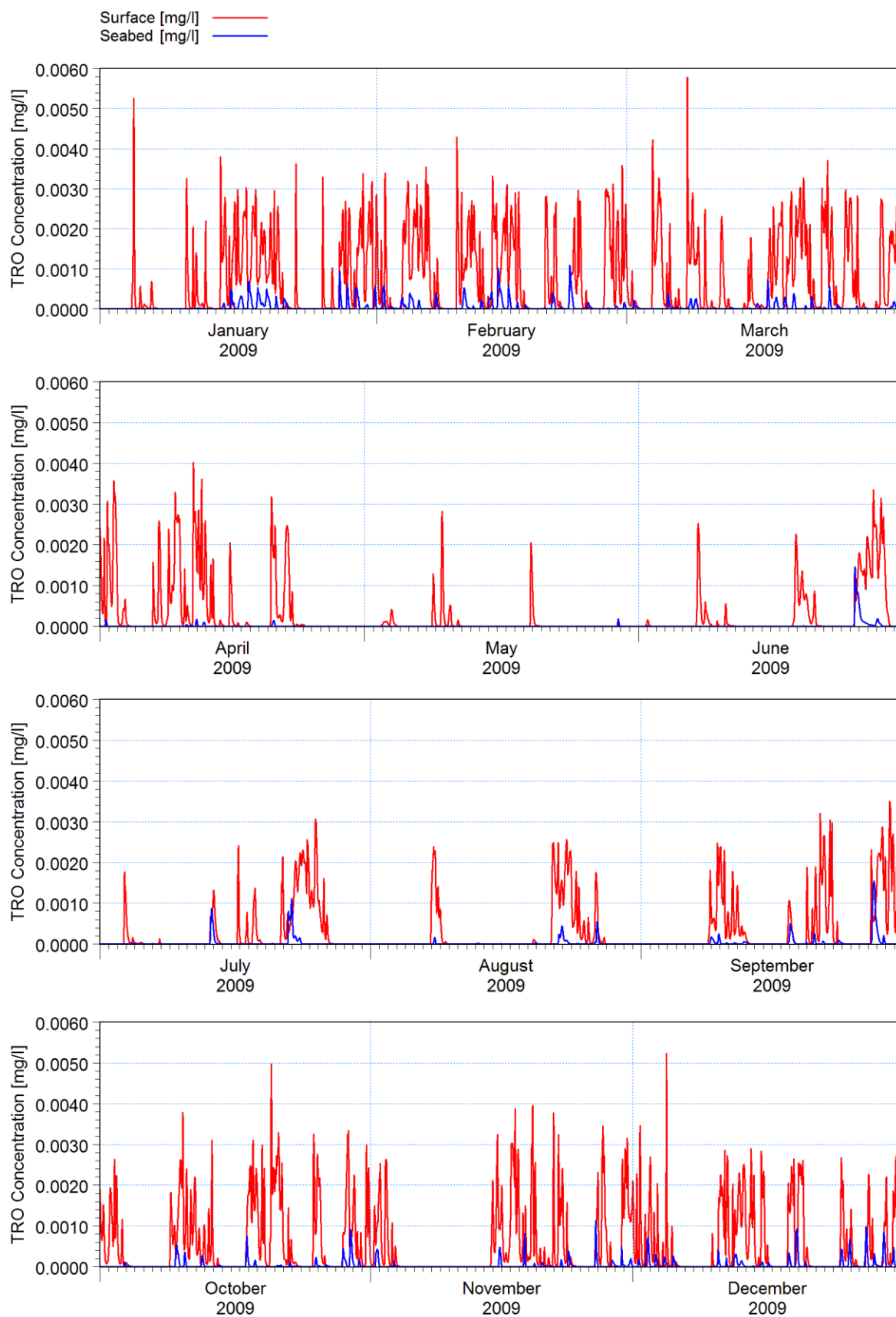
2015\S2015_Koeberg\Models\HD\07\071_02aa_Decoupled_TRO_05ab.mfm - Result Files\PostProcess\Timeseries\TRO_100m.png

Figure B-39: Time series of near-surface and near-seabed TRO concentration 100 m offshore of the discharge point (see Figure 5-15): plant operation at full capacity.



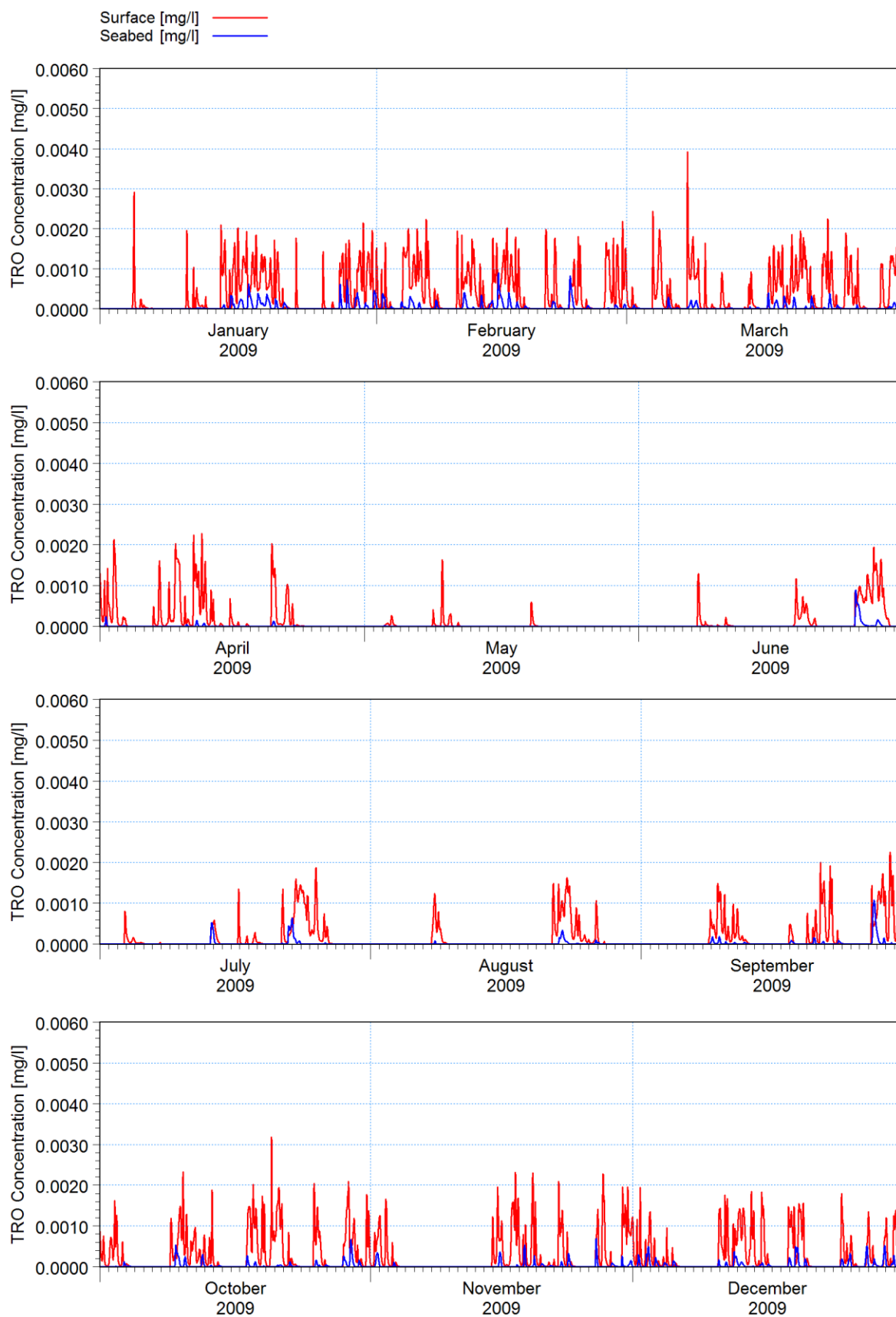
2015\S2015_Koeberg\Models\HD\07\071_02aa_Decoupled_TRO_05ab.mfm - Result Files\PostProcess\Timeseries\TRO_BW.png

Figure B-40: Time series of near-surface and near-seabed TRO concentration at the breakwater head (see Figure 5-15): plant operation at full capacity.



2015\S2015_Koeberg\Models\HD\07\071_02aa_Decoupled_TRO_05ab.mfm - Result Files\PostProcess\Timeseries\TRO_NB2.png

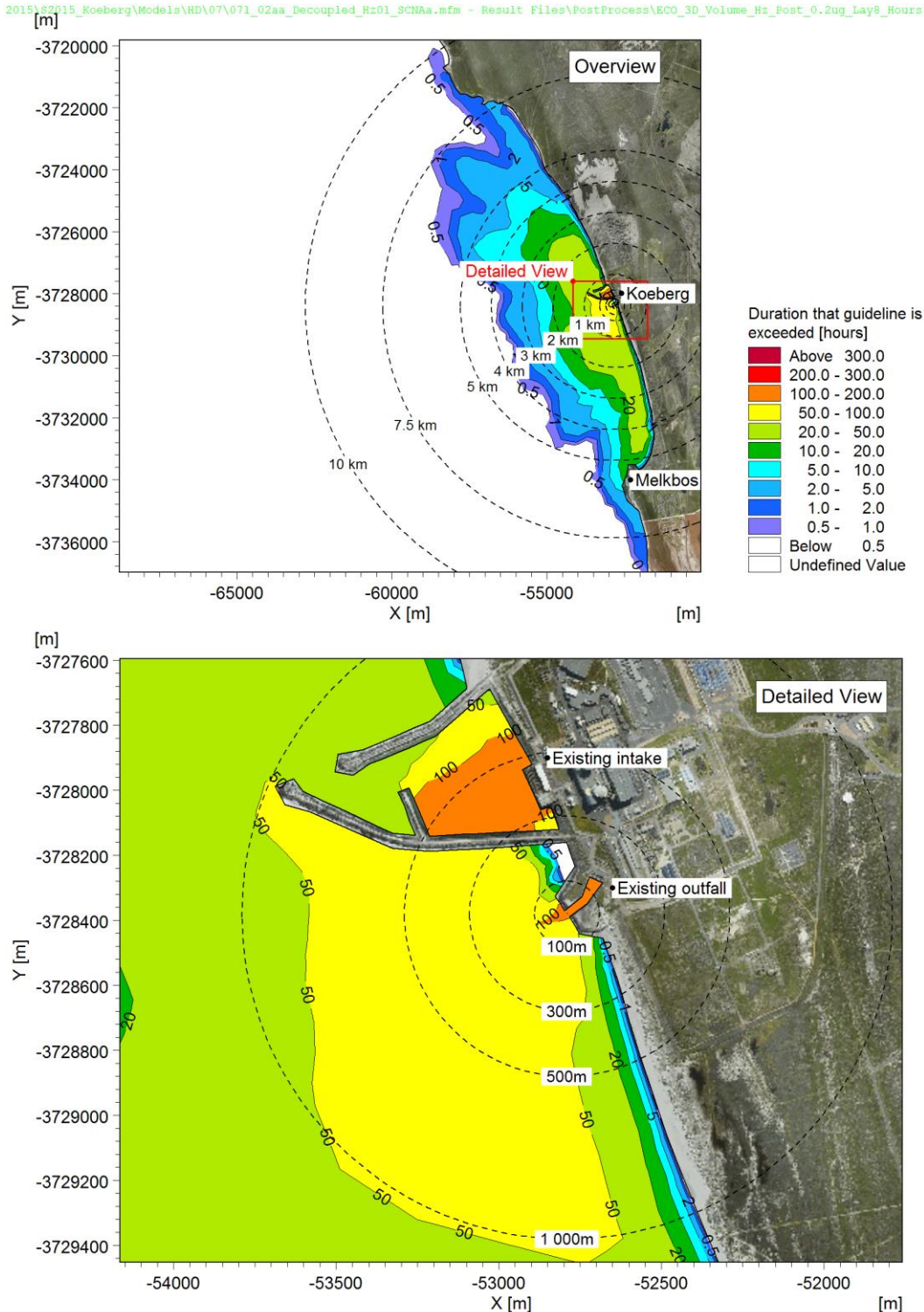
Figure B-41: Time series of near-surface and near-seabed TRO concentration at Northern Blinders 2 (see Figure 5-15): plant operation at full capacity.



2015\S2015_Koeberg\Models\HD\07\071_02aa_Decoupled_TRO_05ab.mfm - Result Files\PostProcess\Timeseries\TRO_NB1.png

Figure B-42: Time series of near-surface and near-seabed TRO concentration at Northern Blinders 1 (see Figure 5-15): plant operation at full capacity.

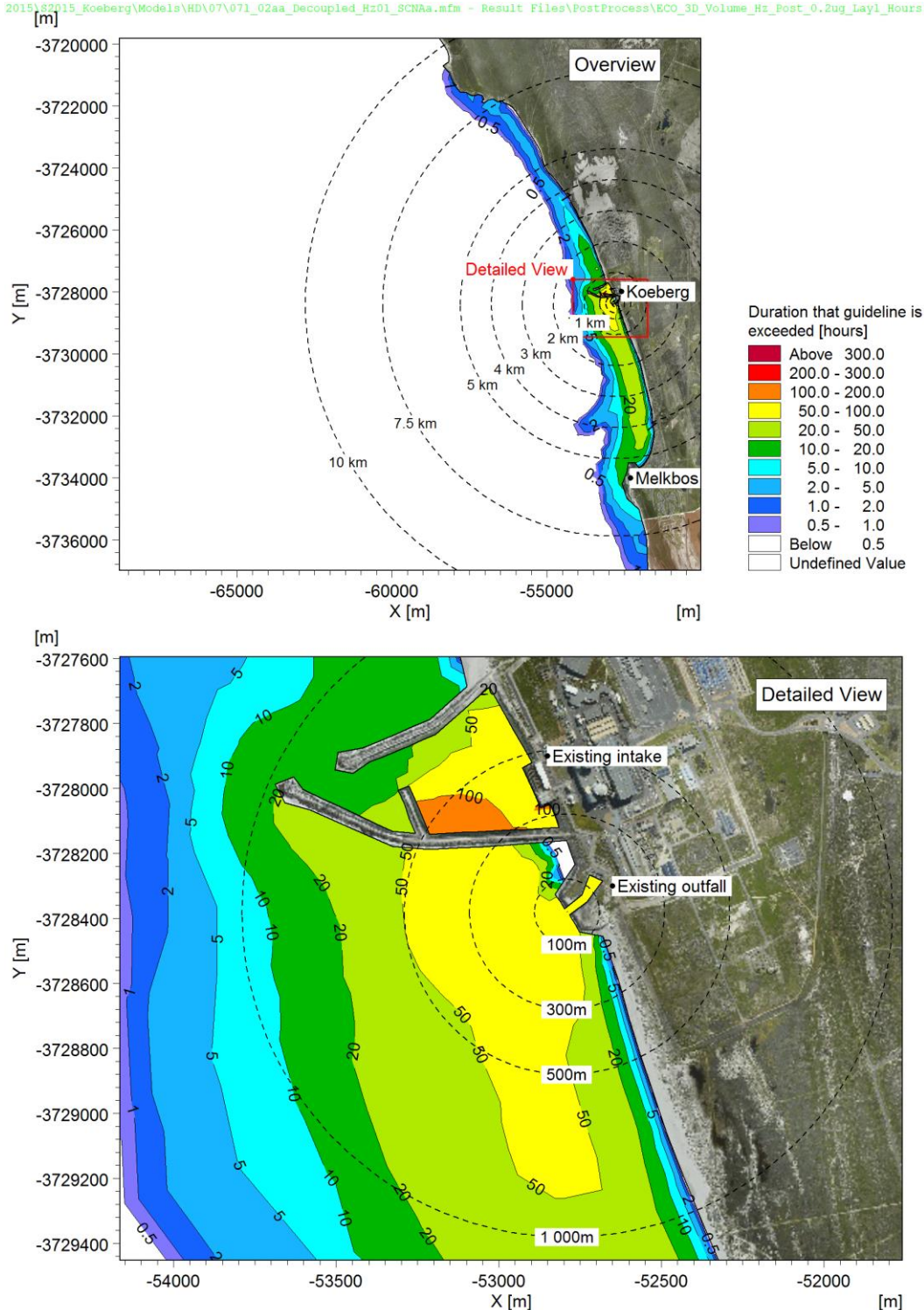
2015\62215_Koeberg\Models\HD\07\071_02aa_Decoupled_Hz01_SCNAa.mfm - Result Files\PostProcess\ECO_3D_Volume_Hz_Post_0.2ug_Lay8_Hours.png



Stream	Discharge [m³/h]	Concentration [mg/l]	Load [kg/h]	Duration [h]	Release interval [days]	Total duration per year [hrs]	Total Annual Load [kg]
SEK_A	300	0.2	0.06	6	1	2 192	131
XCA_A	60	300	18	0.42	Monthly	5.00	90
XCA_B	60	300	18	1.17	Twice per year	2.33	42

Figure B-43: Maximum annual duration that the guideline concentration for hydrazine (0.0002 mg/l) is exceeded near the surface: plant operation at full capacity (two units operational).

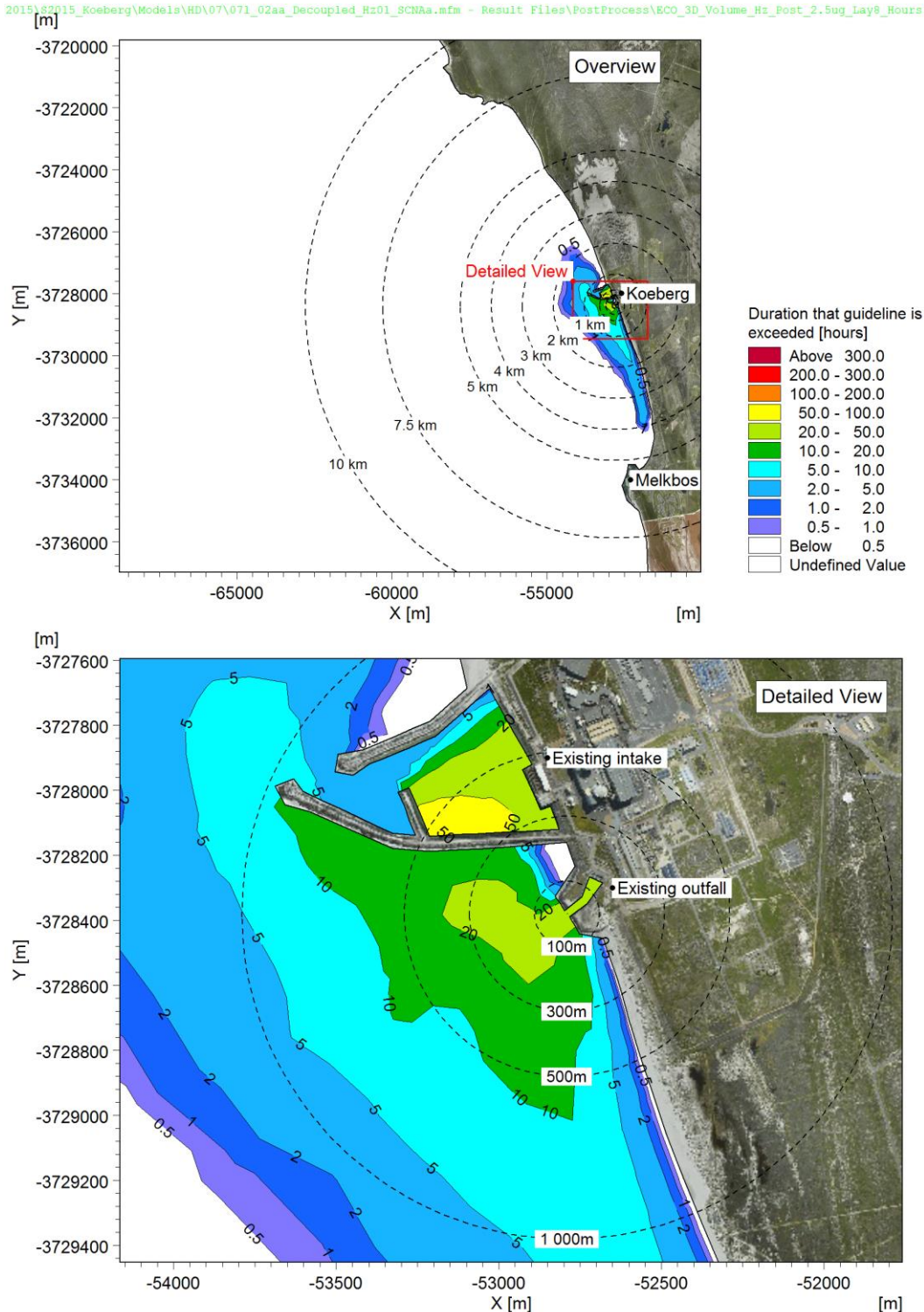
2015\62215_Koeberg\Models\HD\07\071_02aa_Decoupled_Hz01_SCNAa.mfm - Result Files\PostProcess\ECO_3D_Volume_Hz_Post_0.2ug_Lay1_Hours.png



Stream	Discharge [m³/h]	Concentration [mg/l]	Load [kg/h]	Duration [h]	Release interval [days]	Total duration per year [hrs]	Total Annual Load [kg]
SEK_A	300	0.2	0.06	6	1	2 192	131
XCA_A	60	300	18	0.42	Monthly	5.00	90
XCA_B	60	300	18	1.17	Twice per year	2.33	42

Figure B-44: Maximum annual duration that the guideline concentration for hydrazine (0.0002 mg/l) is exceeded near the seabed: plant operation at full capacity (two units operational).

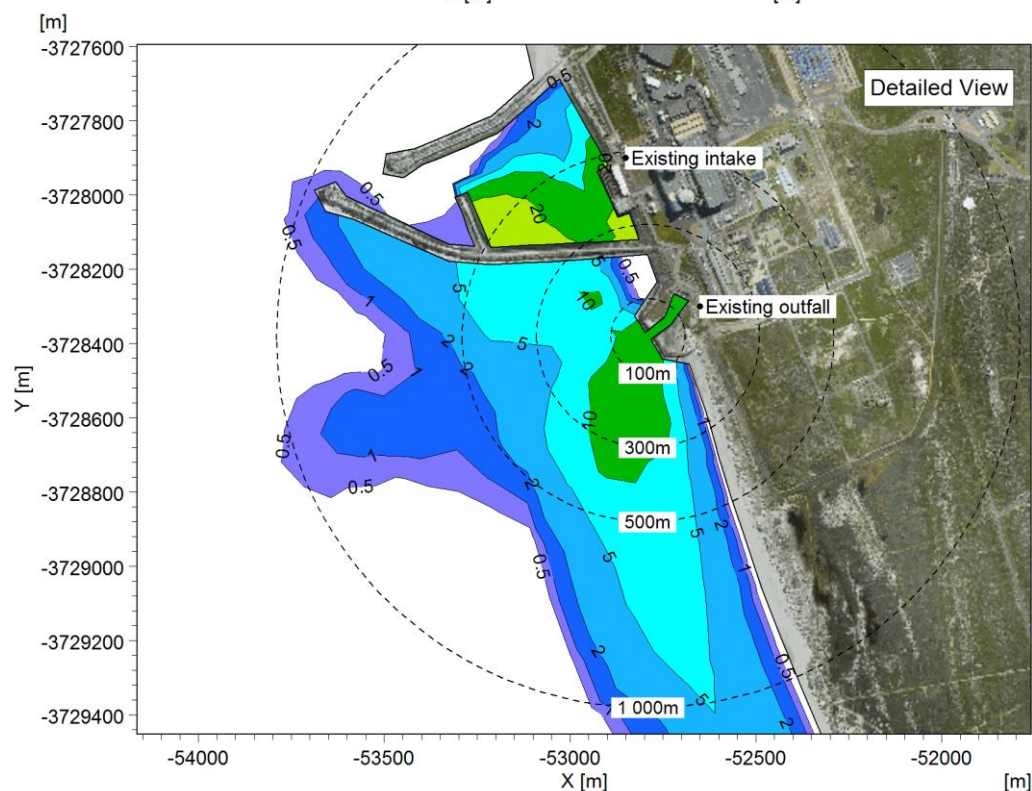
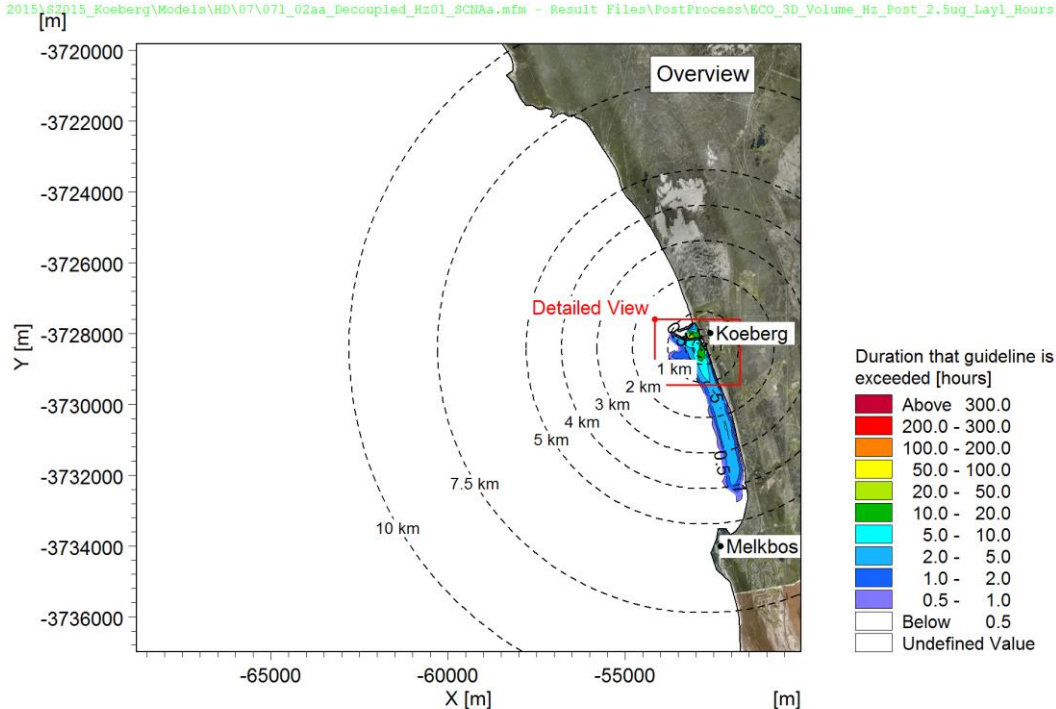
2015\62215_Koeberg\Models\HD\07\071_02aa_Decoupled_Hz01_SCNAa.mfm - Result Files\PostProcess\ECO_3D_Volume_Hz_Post_2.5ug_Lay8_Hours.png



Stream	Discharge [m³/h]	Concentration [mg/l]	Load [kg/h]	Duration [h]	Release interval [days]	Total duration per year [hrs]	Total Annual Load [kg]
SEK_A	300	0.2	0.06	6	1	2 192	131
XCA_A	60	300	18	0.42	Monthly	5.00	90
XCA_B	60	300	18	1.17	Twice per year	2.33	42

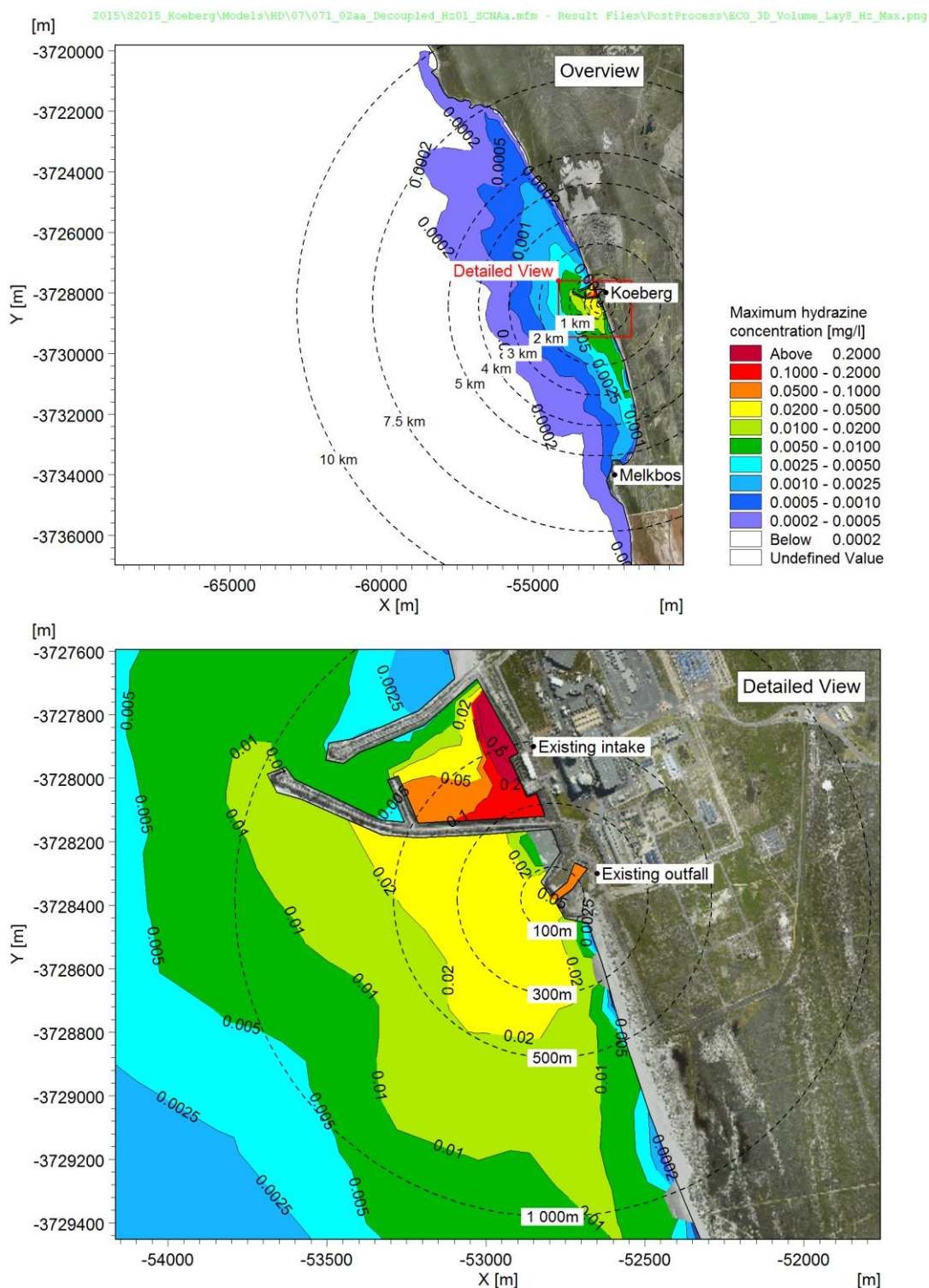
Figure B-45: Maximum annual duration that the guideline concentration for hydrazine (0.0025 mg/l) is exceeded near the surface: plant operation at full capacity (two units operational).

2015\82215_Koeberg\Models\HD\07\071_02aa_Decoupled_Hz01_SCNAa.mfm - Result Files\PostProcess\ECO_3D_Volume_Hz_Post_2.5ug_Lay1_Hours.png



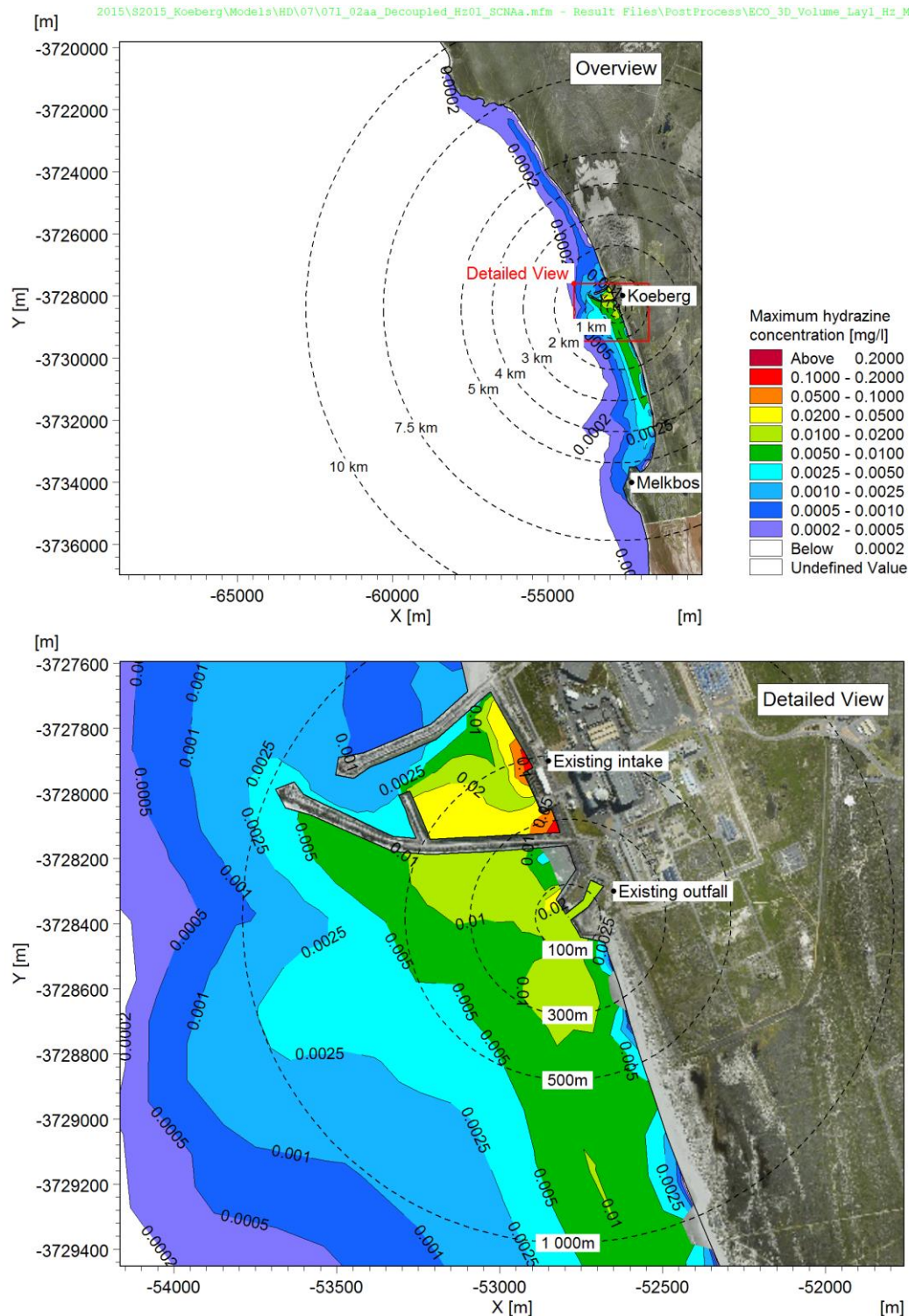
Stream	Discharge [m³/h]	Concentration [mg/l]	Load [kg/h]	Duration [h]	Release interval [days]	Total duration per year [hrs]	Total Annual Load [kg]
SEK_A	300	0.2	0.06	6	1	2 192	131
XCA_A	60	300	18	0.42	Monthly	5.00	90
XCA_B	60	300	18	1.17	Twice per year	2.33	42

Figure B-46: Maximum annual duration that the guideline concentration for hydrazine (0.0025 mg/l) is exceeded near the seabed: plant operation at full capacity (two units operational).



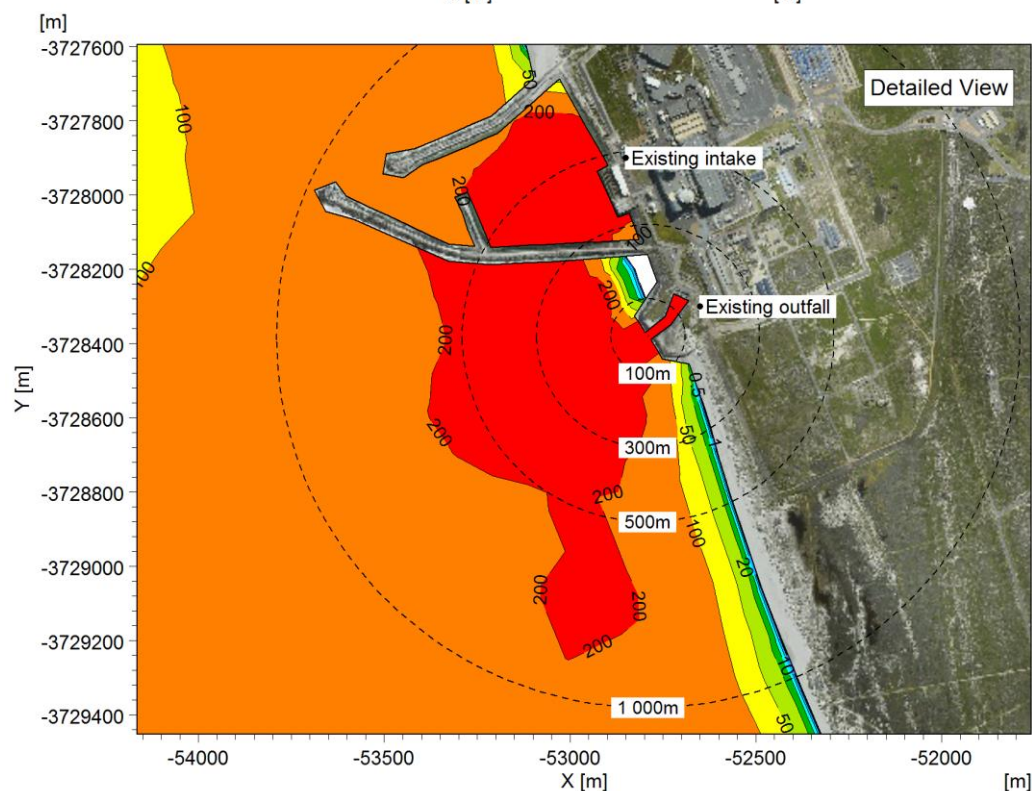
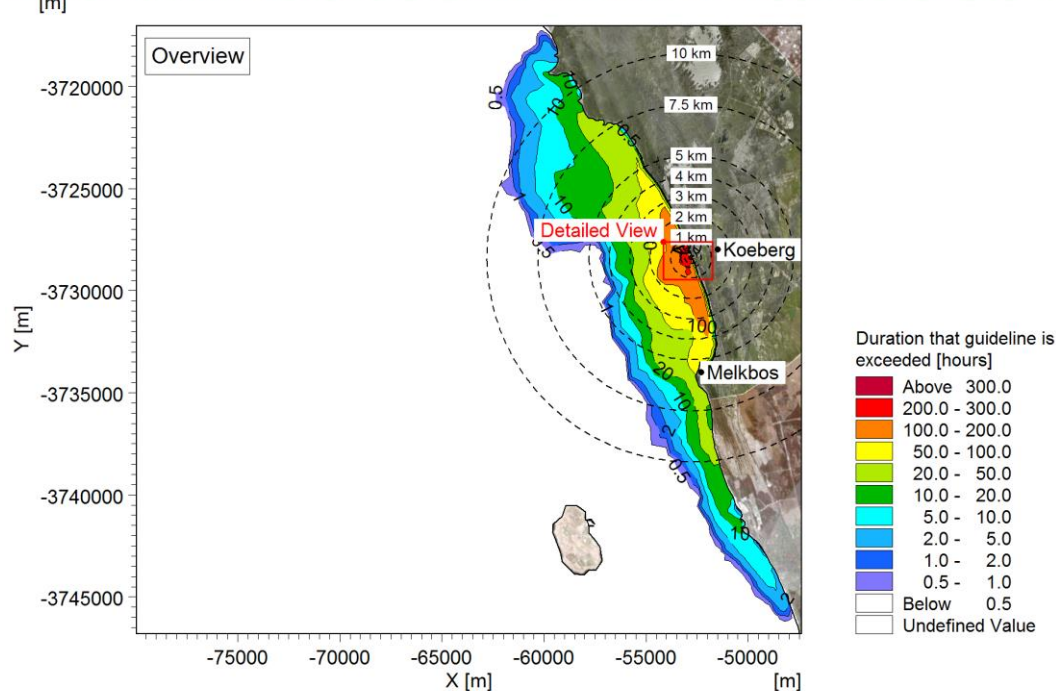
Stream	Discharge [m³/h]	Concentration [mg/l]	Load [kg/h]	Duration [h]	Release interval [days]	Total duration per year [hrs]	Total Annual Load [kg]
SEK_A	300	0.2	0.06	6	1	2 192	131
XCA_A	60	300	18	0.42	Monthly	5.00	90
XCA_B	60	300	18	1.17	Twice per year	2.33	42

Figure B-47: Maximum near-surface hydrazine concentration: plant operation at full capacity (two units operational).



Stream	Discharge [m³/h]	Concentration [mg/l]	Load [kg/h]	Duration [h]	Release interval [days]	Total duration per year [hrs]	Total Annual Load [kg]
SEK_A	300	0.2	0.06	6	1	2 192	131
XCA_A	60	300	18	0.42	Monthly	5.00	90
XCA_B	60	300	18	1.17	Twice per year	2.33	42

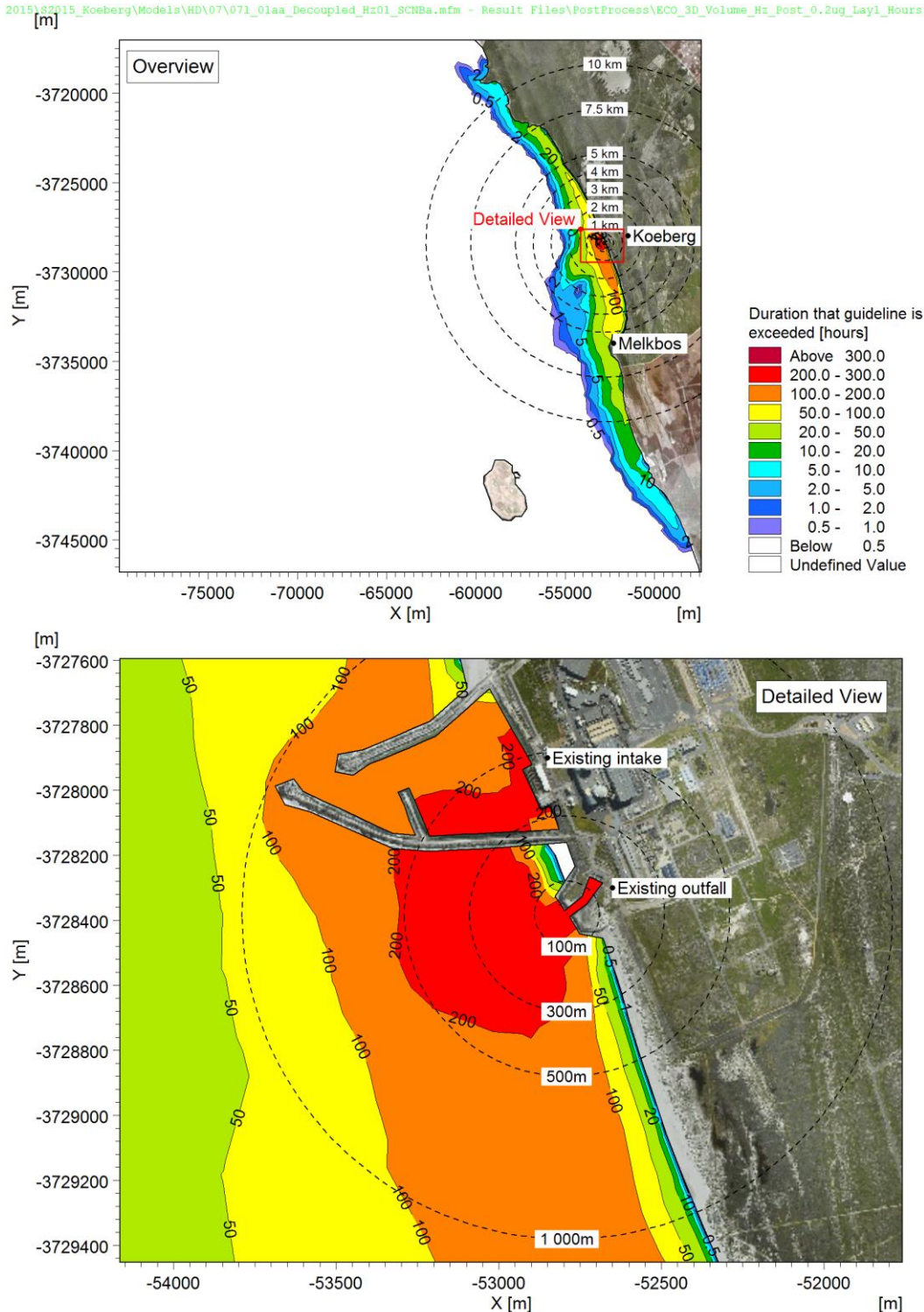
Figure B-48: Maximum near-seabed hydrazine concentration: plant operation at full capacity (two units operational).



Stream	Discharge [m³/h]	Concentration [mg/l]	Load [kg/h]	Duration [h]	Release interval during outage [days]	Total duration per year ⁽¹⁾ [hrs]	Total Annual Load [kg]
SEK_B	60	250	15	0.50	1	21	315
SEK_C	60	250	15	1.67	7	10	150
XCA_A	60	300	18	0.42	once per outage	0.83	15

(1) Total annual duration calculated assuming hydrazine discharges to occur for three weeks per outage, two outages per year.

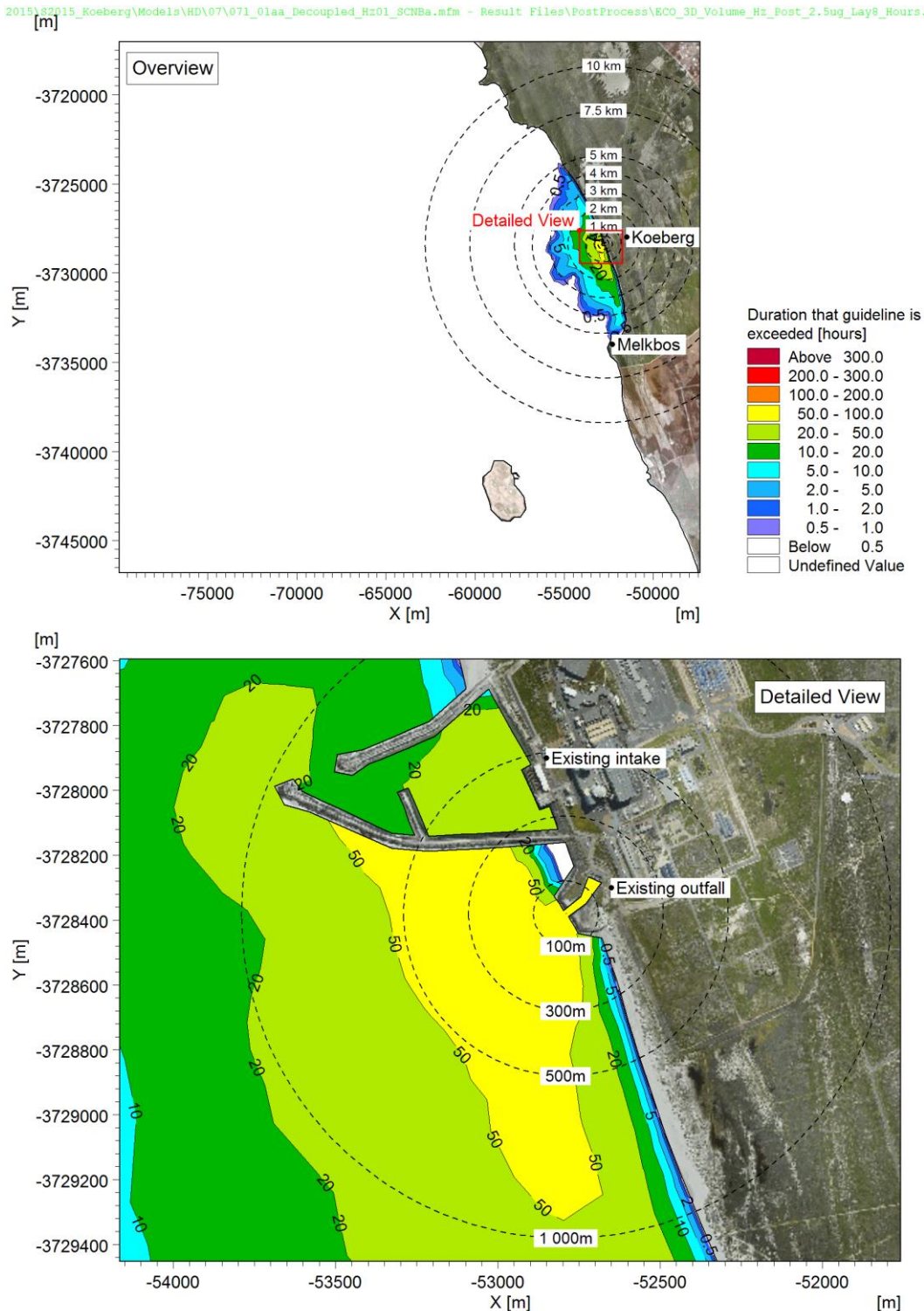
Figure B-49: Maximum annual duration that the guideline concentration for hydrazine (0.0002 mg/l) is exceeded near the surface: exceptional discharges associated with refuelling outages (one unit operational).



Stream	Discharge [m ³ /h]	Concentration [mg/l]	Load [kg/h]	Duration [h]	Release interval during outage [days]	Total duration per year ⁽¹⁾ [hrs]	Total Annual Load [kg]
SEK_B	60	250	15	0.50	1	21	315
SEK_C	60	250	15	1.67	7	10	150
XCA_A	60	300	18	0.42	once per outage	0.83	15

(1) Total annual duration calculated assuming hydrazine discharges to occur for three weeks per outage, two outages per year.

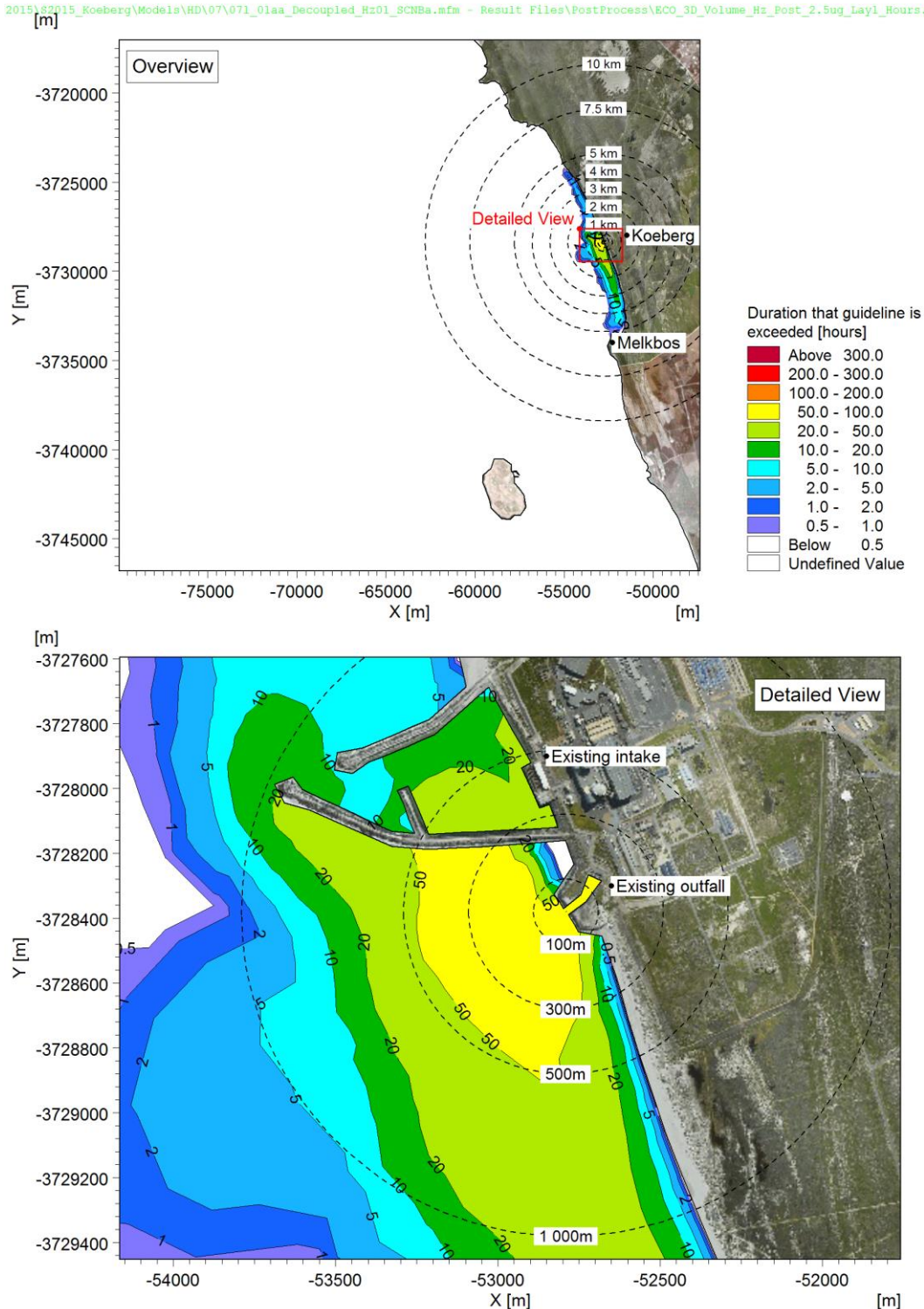
Figure B-50: Maximum annual duration that the guideline concentration for hydrazine (0.0002 mg/l) is exceeded near the seabed: exceptional discharges associated with refuelling outages (one unit operational).



Stream	Discharge [m³/h]	Concentration [mg/l]	Load [kg/h]	Duration [h]	Release interval during outage [days]	Total duration per year ⁽¹⁾ [hrs]	Total Annual Load [kg]
SEK_B	60	250	15	0.50	1	21	315
SEK_C	60	250	15	1.67	7	10	150
XCA_A	60	300	18	0.42	once per outage	0.83	15

(1) Total annual duration calculated assuming hydrazine discharges to occur for three weeks per outage, two outages per year.

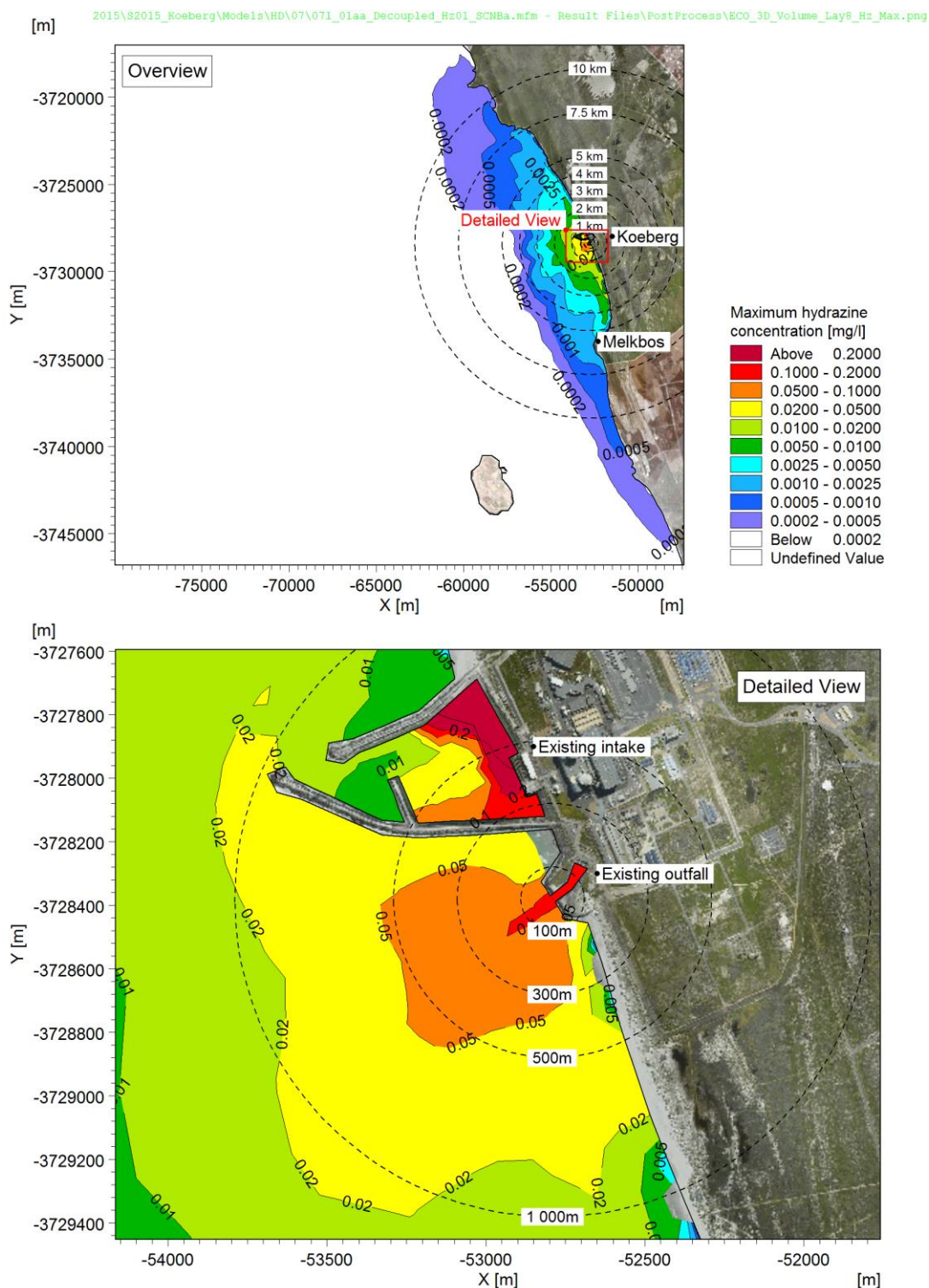
Figure B-51: Maximum annual duration that the guideline concentration for hydrazine (0.0025 mg/l) is exceeded near the surface: exceptional discharges associated with refuelling outages (one unit operational).



Stream	Discharge [m ³ /h]	Concentration [mg/l]	Load [kg/h]	Duration [h]	Release interval during outage [days]	Total duration per year ⁽¹⁾ [hrs]	Total Annual Load [kg]
SEK_B	60	250	15	0.50	1	21	315
SEK_C	60	250	15	1.67	7	10	150
XCA_A	60	300	18	0.42	once per outage	0.83	15

(1) Total annual duration calculated assuming hydrazine discharges to occur for three weeks per outage, two outages per year.

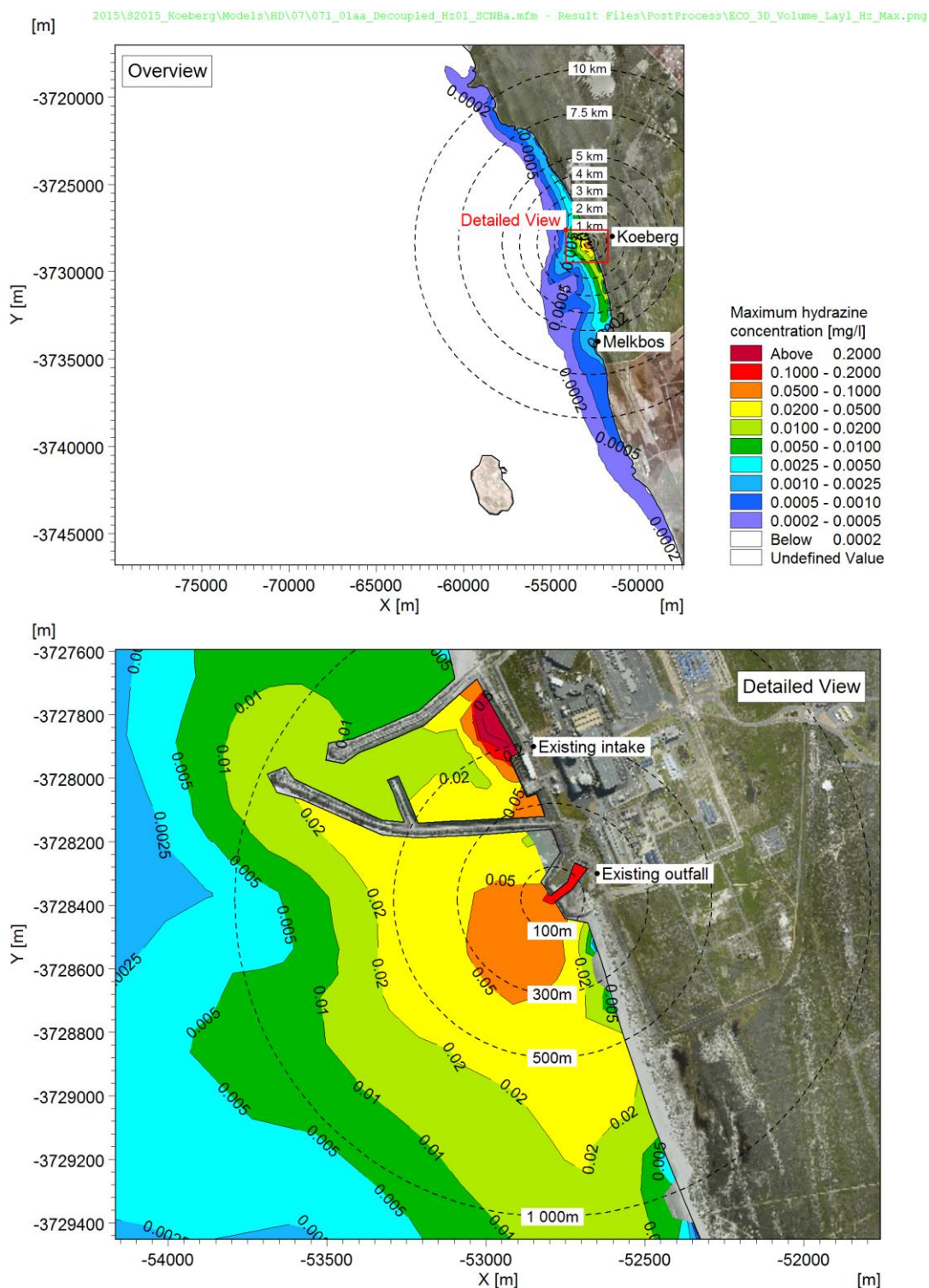
Figure B-52: Maximum annual duration that the guideline concentration for hydrazine (0.0025 mg/l) is exceeded near the seabed: exceptional discharges associated with refuelling outages (one unit operational).



Stream	Discharge [m ³ /h]	Concentration [mg/l]	Load [kg/h]	Duration [h]	Release interval during outage [days]	Total duration per year ⁽¹⁾ [hrs]	Total Annual Load [kg]
SEK_B	60	250	15	0.50	1	21	315
SEK_C	60	250	15	1.67	7	10	150
XCA_A	60	300	18	0.42	once per outage	0.83	15

(1) Total annual duration calculated assuming hydrazine discharges to occur for three weeks per outage, two outages per year.

Figure B-53: Maximum near-surface hydrazine concentration: exceptional discharges associated with refuelling outages (one unit operational).

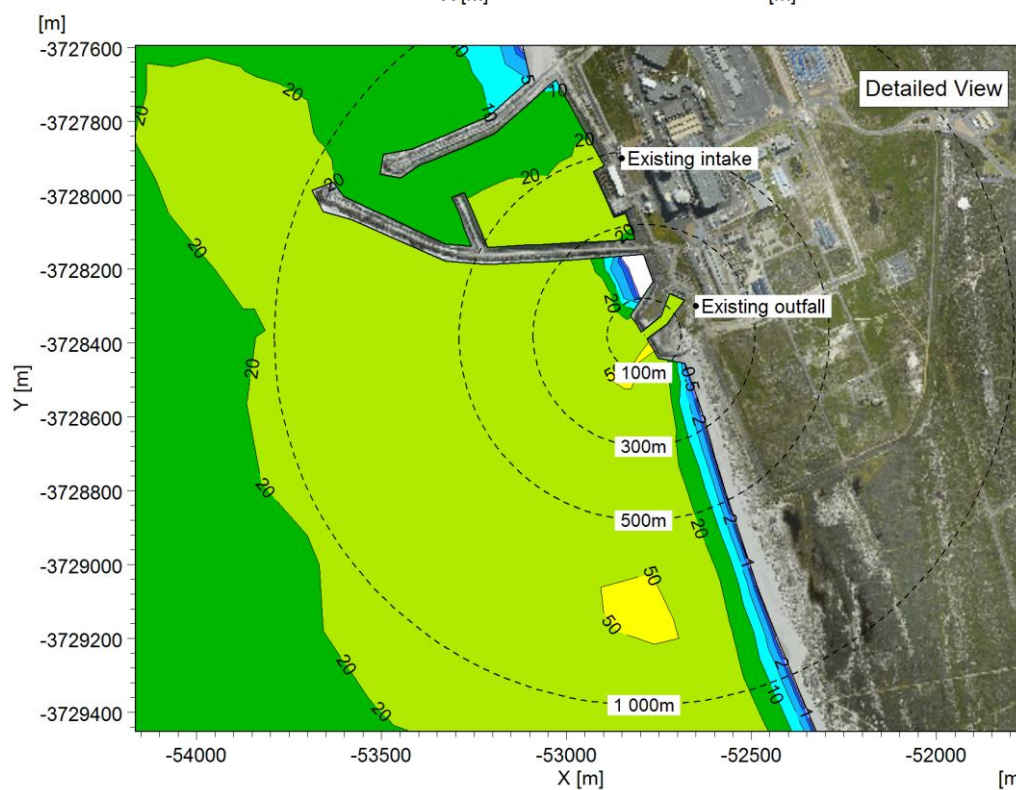
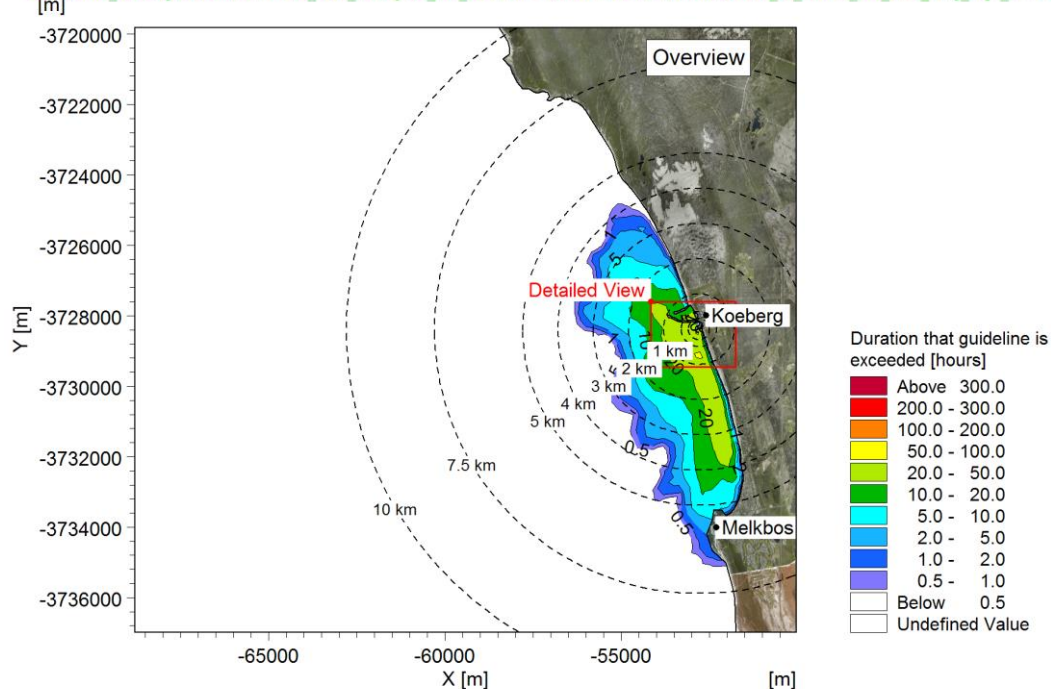


Stream	Discharge [m ³ /h]	Concentration [mg/l]	Load [kg/h]	Duration [h]	Release interval during outage [days]	Total duration per year ⁽¹⁾ [hrs]	Total Annual Load [kg]
SEK_B	60	250	15	0.50	1	21	315
SEK_C	60	250	15	1.67	7	10	150
XCA_A	60	300	18	0.42	once per outage	0.83	15

(1) Total annual duration calculated assuming hydrazine discharges to occur for three weeks per outage, two outages per year.

Figure B-54: Maximum near-seabed hydrazine concentration: exceptional discharges associated with refuelling outages (one unit operational).

2015\S2015_Koeberg\Models\HD\07\07i_01aa_Decoupled_PO4_01a.mfm - Result Files\PostProcess\ECO_3D_Volume_PO4_Post_53ug_Lay8_Hours.png

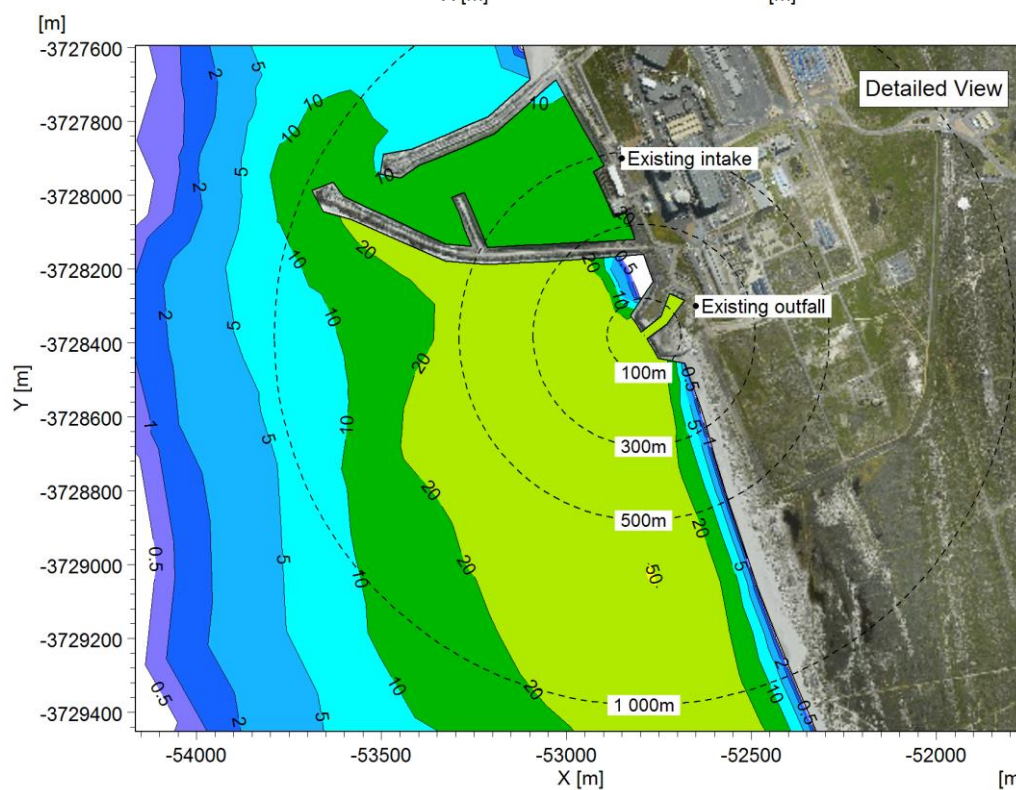
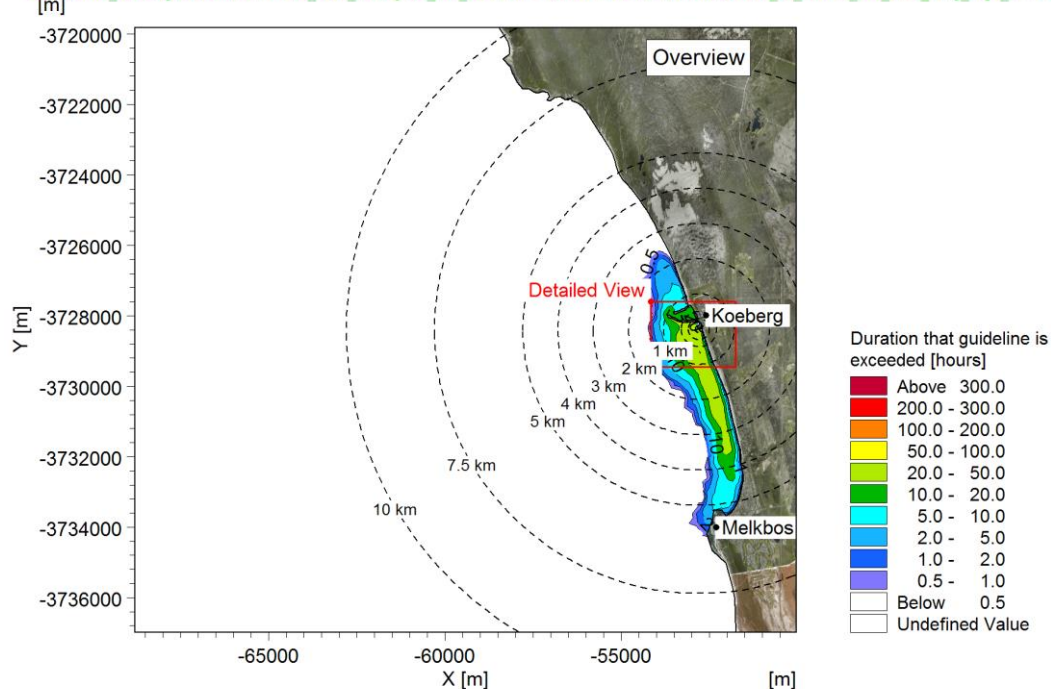


Stream	Discharge [m³/h]	Concentration [mg/l]	Load [kg/h]	Duration [h]	Release characterisation during outage	Total duration per year [hrs]	Total Annual Load [kg]
Leaks	0.804	613	0.493		continuous	8 766	4318
SEK	60	550	33	2	daily for three days	12 ⁽¹⁾	396
KER	25	1 250	31	5	two releases, two days apart	20 ⁽¹⁾	625
DEL via SEO-S	20	1 250	25	2	single release	2 ⁽¹⁾	50
DEL via SEO-N	20	1 250	25	2	single release	2 ⁽¹⁾	50

⁽¹⁾Total annual duration calculated assuming two outages per year. SEO-S and SEO-N releases do not occur during the same outage.

Figure B-55: Maximum annual duration that the guideline concentration for phosphate (0.053 mg/l) is exceeded near the surface: exceptional discharges during refuelling outages (one unit operational).

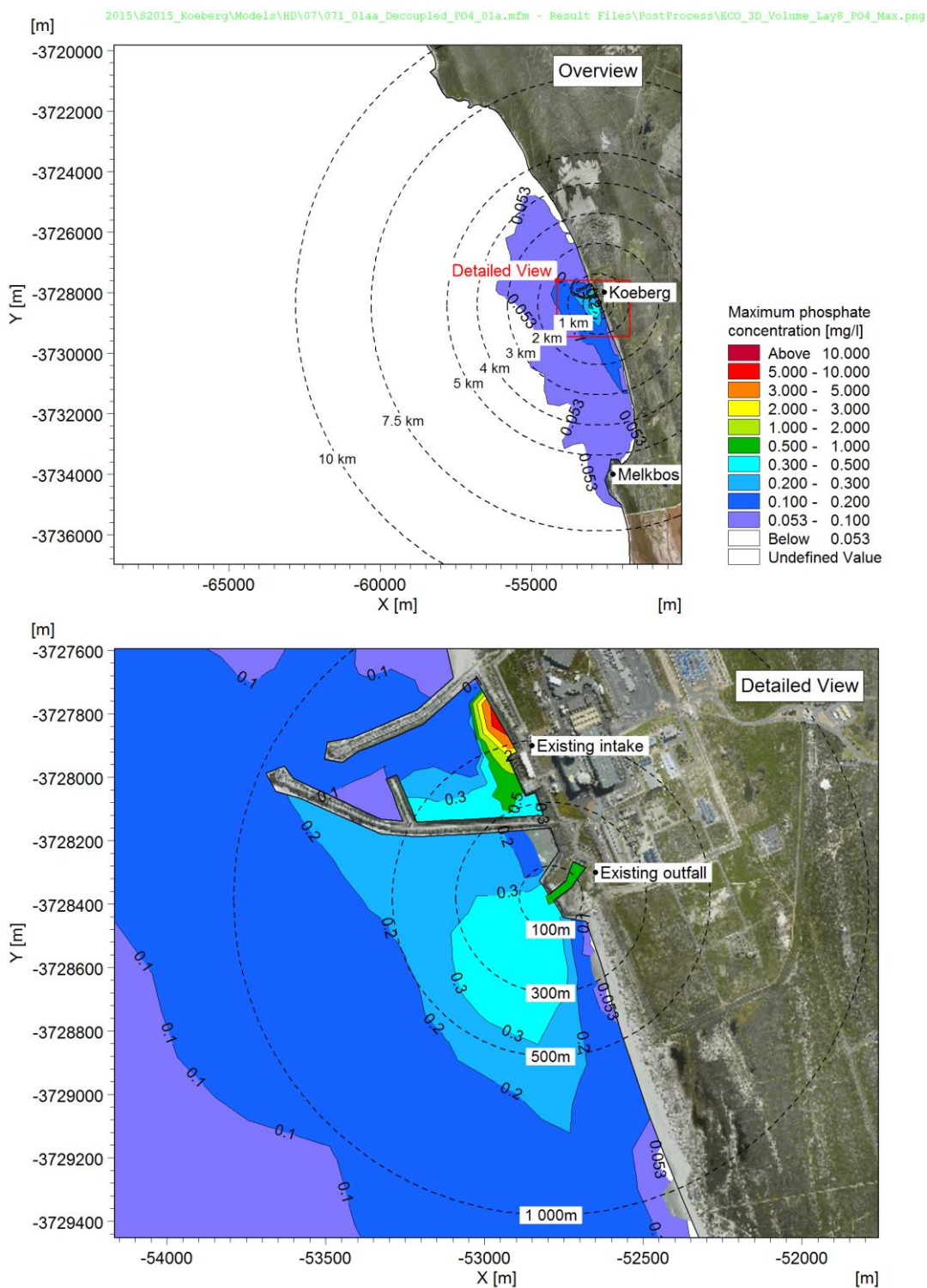
2015\S2015_Koeberg\Models\HD\07\07i_01aa_Decoupled_PO4_01a.mfm - Result Files\PostProcess\ECO_3D_Volume_PO4_Post_53ug_Lay1_Hours.png



Stream	Discharge [m³/h]	Concentration [mg/l]	Load [kg/h]	Duration [h]	Release characterisation during outage	Total duration per year [hrs]	Total Annual Load [kg]
Leaks	0.804	613	0.493		continuous	8 766	4318
SEK	60	550	33	2	daily for three days	12 ⁽¹⁾	396
KER	25	1 250	31	5	two releases, two days apart	20 ⁽¹⁾	625
DEL via SEO-S	20	1 250	25	2	single release	2 ⁽¹⁾	50
DEL via SEO-N	20	1 250	25	2	single release	2 ⁽¹⁾	50

⁽¹⁾Total annual duration calculated assuming two outages per year. SEO-S and SEO-N releases do not occur during the same outage.

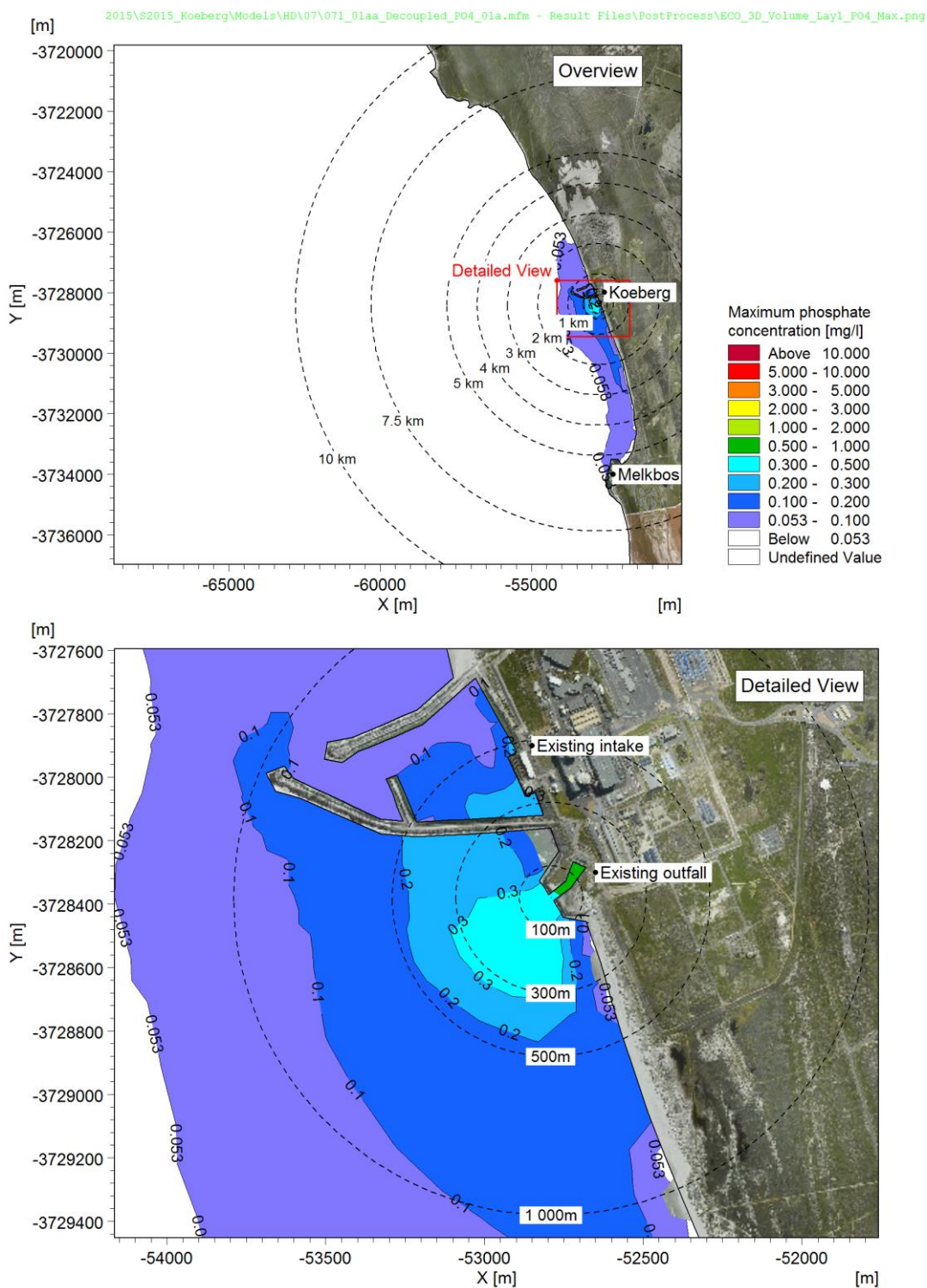
Figure B-56: Maximum annual duration that the guideline concentration for phosphate (0.053 mg/l) is exceeded near the seabed: exceptional discharges during refuelling outages (one unit CRF operational).



Stream	Discharge [m ³ /h]	Concentration [mg/l]	Load [kg/h]	Duration [h]	Release characterisation during outage	Total duration per year [hrs]	Total Annual Load [kg]
Leaks	0.804	613	0.493		continuous	8 766	4318
SEK	60	550	33	2	daily for three days	12 ⁽¹⁾	396
KER	25	1 250	31	5	two releases, two days apart	20 ⁽¹⁾	625
DEL via SEO-S	20	1 250	25	2	single release	2 ⁽¹⁾	50
DEL via SEO-N	20	1 250	25	2	single release	2 ⁽¹⁾	50

⁽¹⁾Total annual duration calculated assuming two outages per year. SEO-S and SEO-N releases do not occur during the same outage.

Figure B-57: Maximum near-surface phosphate concentration: exceptional discharges during refuelling outages (one unit operational).



Stream	Discharge [m³/h]	Concentration [mg/l]	Load [kg/h]	Duration [h]	Release characterisation during outage	Total duration per year [hrs]	Total Annual Load [kg]
Leaks	0.804	613	0.493		continuous	8 766	4318
SEK	60	550	33	2	daily for three days	12 ⁽¹⁾	396
KER	25	1 250	31	5	two releases, two days apart	20 ⁽¹⁾	625
DEL via SEO-S	20	1 250	25	2	single release	2 ⁽¹⁾	50
DEL via SEO-N	20	1 250	25	2	single release	2 ⁽¹⁾	50

⁽¹⁾Total annual duration calculated assuming two outages per year. SEO-S and SEO-N releases do not occur during the same outage.

Figure B-58: Maximum near-seabed phosphate concentration: exceptional discharges during refuelling outages (one unit CRF operational).



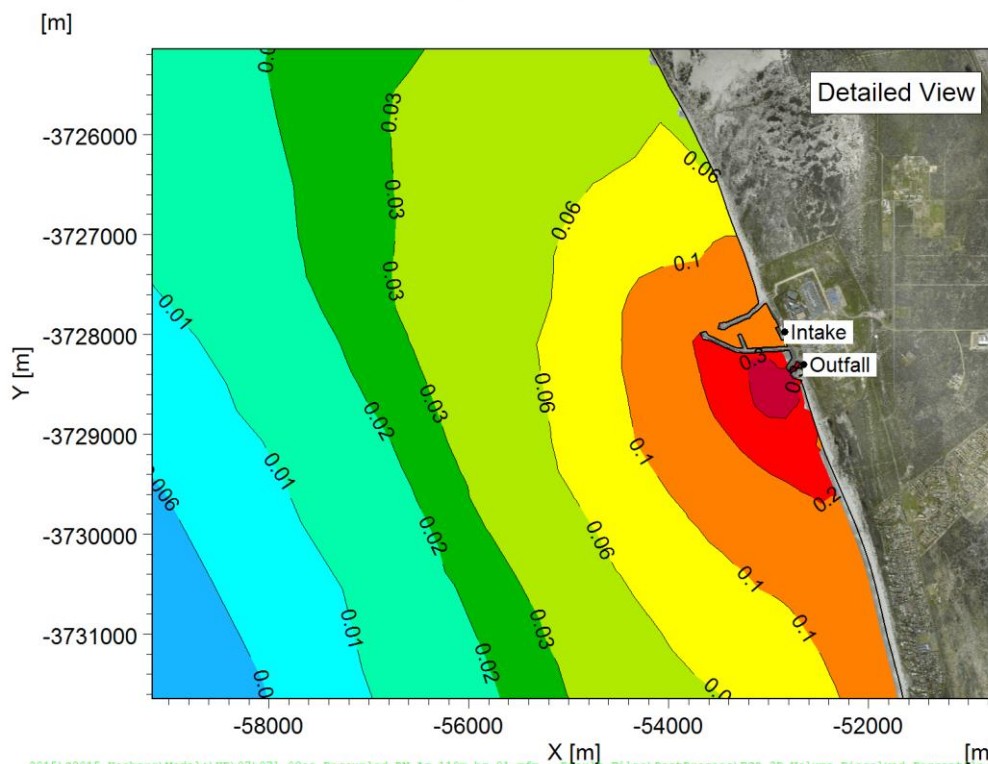
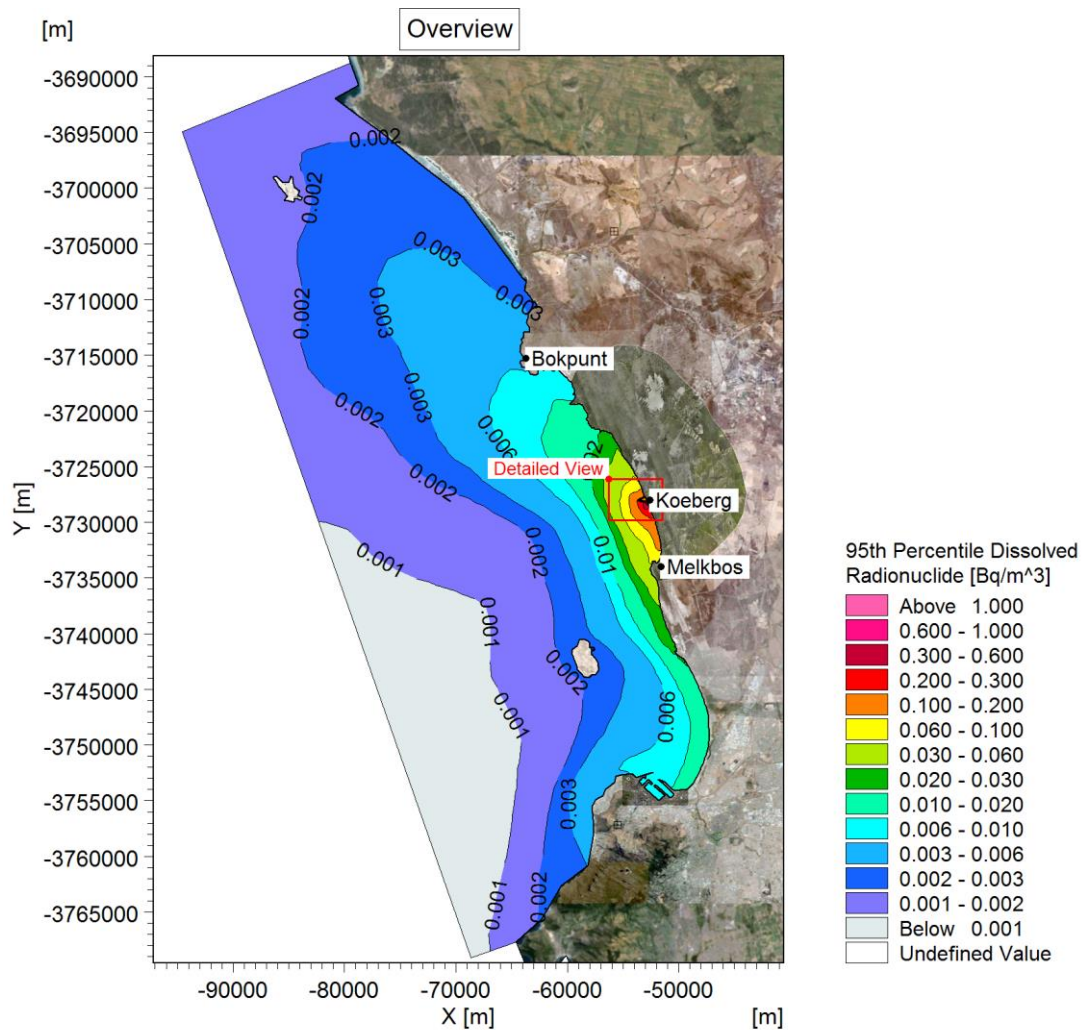
ANNEXURE C | ADDITIONAL RESULTS OF RADIONUCLIDE DISPERSION MODELLING



Figure C-1: 95 th percentile concentration of dissolved Ag-110m activity in the water column: near-surface.	4
Figure C-2: 95 th percentile concentration of dissolved Ag-110m activity in the water column: near-seabed.....	5
Figure C-3: 95 th percentile concentration of adsorbed Ag-110m activity in the water column: near-surface.	6
Figure C-4: 95 th percentile concentration of adsorbed Ag-110m activity in the water column: near-seabed.	7
Figure C-5: Maximum concentration of Ag-110m activity in seabed sediment in one modelled year: overview.	8
Figure C-6: Maximum concentration of Ag-110m activity in seabed sediment in one modelled year: detail of depo- centres.	9
Figure C-7: Time series of concentration of Ag-110m activity in the seabed sediment at the three depo-centres. For comparative purposes, the concentration is plotted on a logarithmic scale.....	10
Figure C-8: 95 th percentile concentration of dissolved C-14 activity in the water column: near-surface.....	11
Figure C-9: 95 th percentile concentration of dissolved C-14 activity in the water column: near-seabed.....	12
Figure C-10: 95 th percentile concentration of adsorbed C-14 activity in the water column: near-surface.	13
Figure C-11: 95 th percentile concentration of adsorbed C-14 activity in the water column: near-seabed.....	14
Figure C-12: Maximum concentration of C-14 activity in seabed sediment in one modelled year: overview.	15
Figure C-13: Maximum concentration of C-14 activity in seabed sediment in one modelled year: detail of depo- centres.	16
Figure C-14: Time series of concentration of C-14 activity in the seabed sediment at the three depo-centres. For comparative purposes, the concentration is plotted on a logarithmic scale.....	17
Figure C-15: 95 th percentile concentration of dissolved Co-58 activity in the water column: near-surface.	18
Figure C-16: 95 th percentile concentration of dissolved Co-58 activity in the water column: near-seabed.....	19
Figure C-17: 95 th percentile concentration of adsorbed Co-58 activity in the water column: near-surface.	20
Figure C-18: 95 th percentile concentration of adsorbed Co-58 activity in the water column: near-seabed.	21
Figure C-19: Maximum concentration of Co-58 activity in seabed sediment in one modelled year: overview.	22
Figure C-20: Maximum concentration of Co-58 activity in seabed sediment in one modelled year: detail of depo- centres.	23
Figure C-21: Time series of concentration of Co-58 activity in the seabed sediment at the three depo-centres. For comparative purposes, the concentration is plotted on a logarithmic scale.....	24
Figure C-22: 95 th percentile concentration of dissolved Cs-134 activity in the water column: near-surface.	25
Figure C-23: 95 th percentile concentration of dissolved Cs-134 activity in the water column: near-seabed.	26
Figure C-24: 95 th percentile concentration of adsorbed Cs-134 activity in the water column: near-surface.....	27
Figure C-25: 95 th percentile concentration of adsorbed Cs-134 activity in the water column: near-seabed.	28
Figure C-26: Maximum concentration of Cs-134 activity in seabed sediment in one modelled year: overview.....	29
Figure C-27: Maximum concentration of Cs-134 activity in seabed sediment in one modelled year: detail of depo- centres.	30
Figure C-28: Time series of concentration of Cs-134 activity in the seabed sediment at the three depo-centres. For comparative purposes, the concentration is plotted on a logarithmic scale.....	31
Figure C-29: 95 th percentile concentration of dissolved Cs-137 activity in the water column: near-surface.	32
Figure C-30: 95 th percentile concentration of dissolved Cs-137 activity in the water column: near-seabed.	33
Figure C-31: 95 th percentile concentration of adsorbed Cs-137 activity in the water column: near-surface.....	34
Figure C-32: 95 th percentile concentration of adsorbed Cs-137 activity in the water column: near-seabed.	35
Figure C-33: Maximum concentration of Cs-137 activity in seabed sediment in one modelled year: overview.....	36
Figure C-34: Maximum concentration of Cs-137 activity in seabed sediment in one modelled year: detail of depo- centres.	37

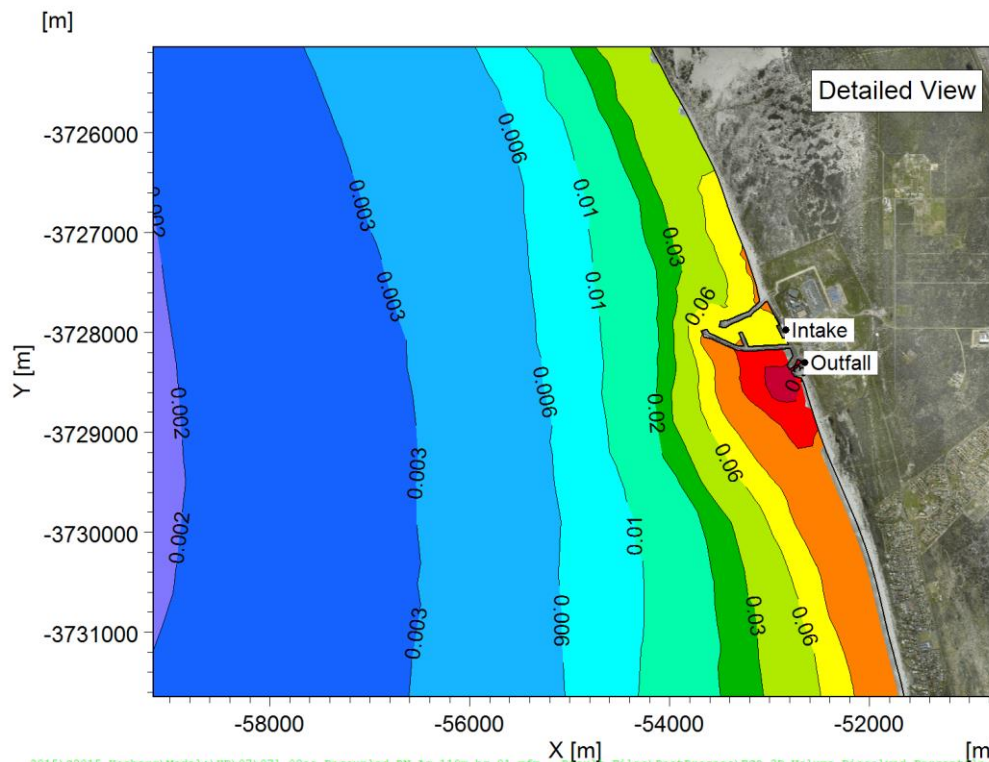
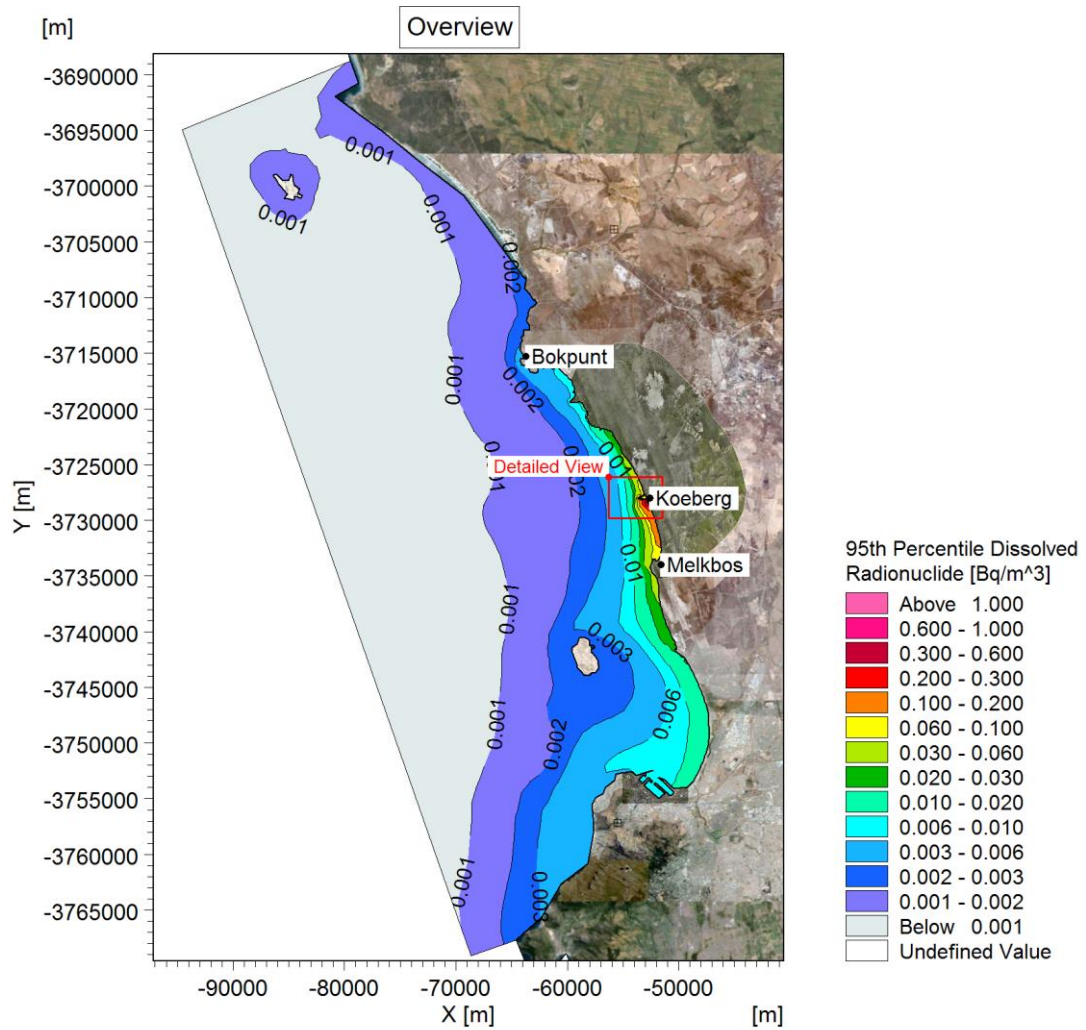


Figure C-35: Time series of concentration of Cs-137 activity in the seabed sediment at the three depo-centres. For comparative purposes, the concentration is plotted on a logarithmic scale.....	38
Figure C-36: 95 th percentile concentration of dissolved H-3 activity in the water column: near-surface.	39
Figure C-37: 95 th percentile concentration of dissolved H-3 activity in the water column: near-seabed.	40
Figure C-38: 95 th percentile concentration of adsorbed H-3 activity in the water column: near-surface.	41
Figure C-39: 95 th percentile concentration of adsorbed H-3 activity in the water column: near-seabed.	42
Figure C-40: Maximum concentration of H-3 activity in seabed sediment in one modelled year: overview.	43
Figure C-41: Maximum concentration of H-3 activity in seabed sediment in one modelled year: detail of depo-centres.	44
Figure C-42: Time series of concentration of H-3 activity in the seabed sediment at the three depo-centres. For comparative purposes, the concentration is plotted on a logarithmic scale.....	45
Figure C-43: 95 th percentile concentration of dissolved I-131 activity in the water column: near-surface.....	46
Figure C-44: 95 th percentile concentration of dissolved I-131 activity in the water column: near-seabed.	47
Figure C-45: 95 th percentile concentration of adsorbed I-131 activity in the water column: near-surface.....	48
Figure C-46: 95 th percentile concentration of adsorbed I-131 activity in the water column: near-seabed.....	49
Figure C-47: Maximum concentration of I-131 activity in seabed sediment in one modelled year: overview.	50
Figure C-48: Maximum concentration of I-131 activity in seabed sediment in one modelled year: detail of depo-centres.	51
Figure C-49: Time series of concentration of I-131 activity in the seabed sediment at the three depo-centres. For comparative purposes, the concentration is plotted on a logarithmic scale.....	52
Figure C-50: 95 th percentile concentration of dissolved Mn-54 activity in the water column: near-surface.	53
Figure C-51: 95 th percentile concentration of dissolved Mn-54 activity in the water column: near-seabed.	54
Figure C-52: 95 th percentile concentration of adsorbed Mn-54 activity in the water column: near-surface.	55
Figure C-53: 95 th percentile concentration of adsorbed Mn-54 activity in the water column: near-seabed.	56
Figure C-54: Maximum concentration of Mn-54 activity in seabed sediment in one modelled year: overview.	57
Figure C-55: Maximum concentration of Mn-54 activity in seabed sediment in one modelled year: detail of depo-centres.	58
Figure C-56: Time series of concentration of Mn-54 activity in the seabed sediment at the three depo-centres. For comparative purposes, the concentration is plotted on a logarithmic scale.....	59



2015\S2015_Koeberg\Models\RD\07\071_02aa_Decoupled_RN_Ag-110m_bc_01.mfm - Result Files\PostProcess\ECO_3D_Volume_Dissolved_Percentile_95th_Lay6.png

Figure C-1: 95th percentile concentration of dissolved Ag-110m activity in the water column: near-surface.



2015\S2015_Koeberg\Models\RD\07\071_02aa_Decoupled_RN_Ag-110m_bc_01.mfm - Result Files\PostProcess\ECO_3D_Volume_Dissolved_Percentile_95th_Lay1.png

Figure C-2: 95th percentile concentration of dissolved Ag-110m activity in the water column: near-seabed.

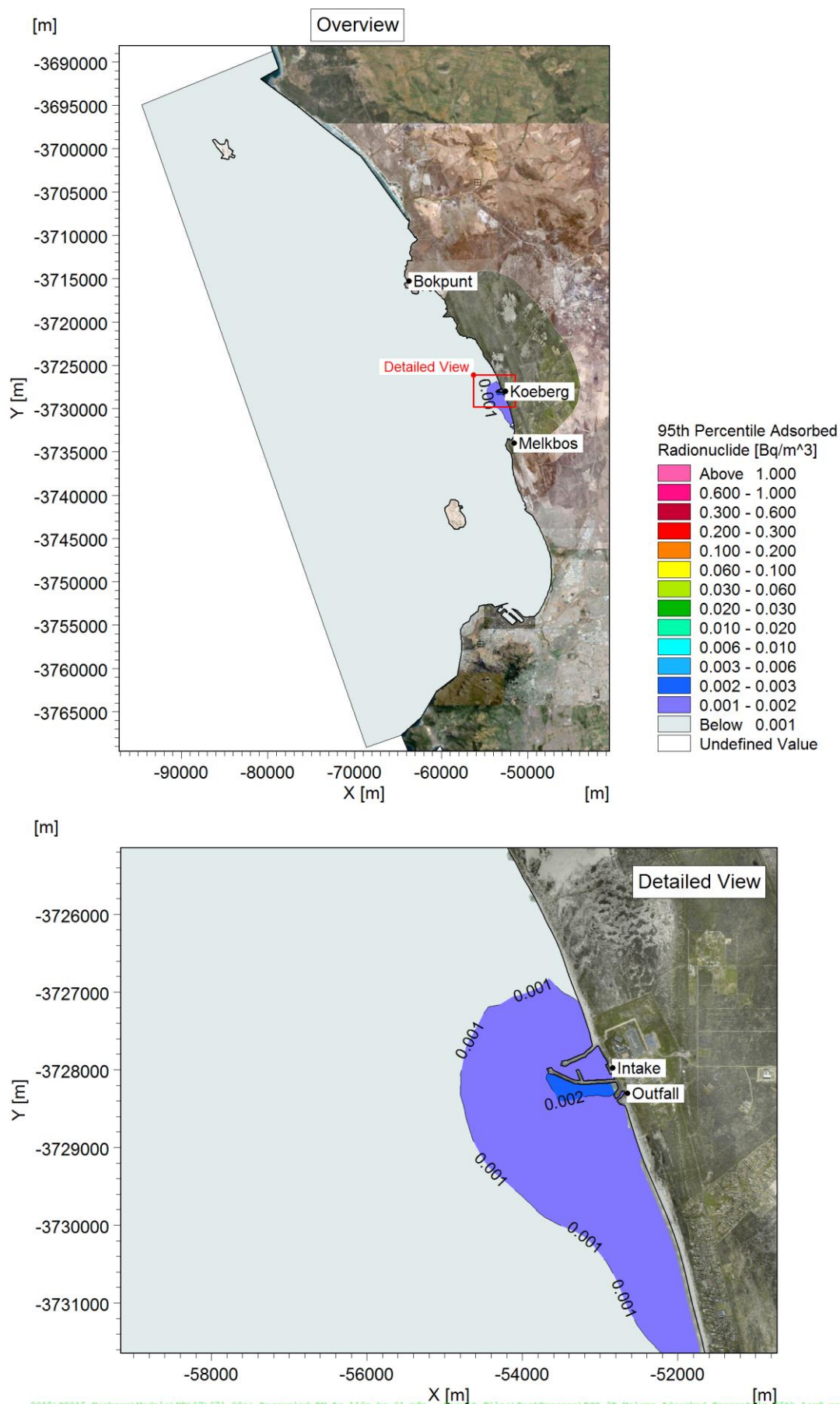


Figure C-3: 95th percentile concentration of adsorbed Ag-110m activity in the water column: near-surface.

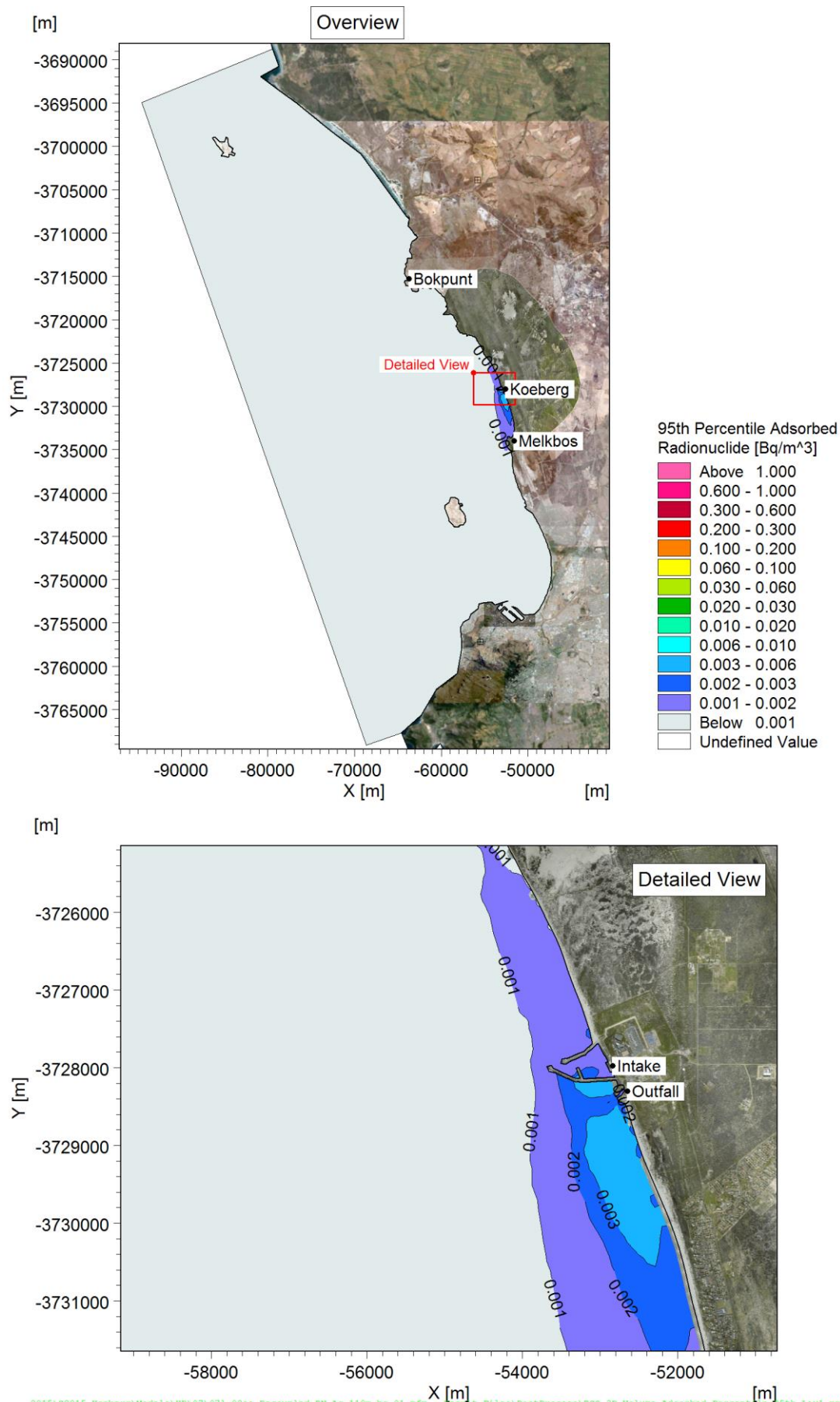


Figure C-4: 95th percentile concentration of adsorbed Ag-110m activity in the water column: near-seabed.

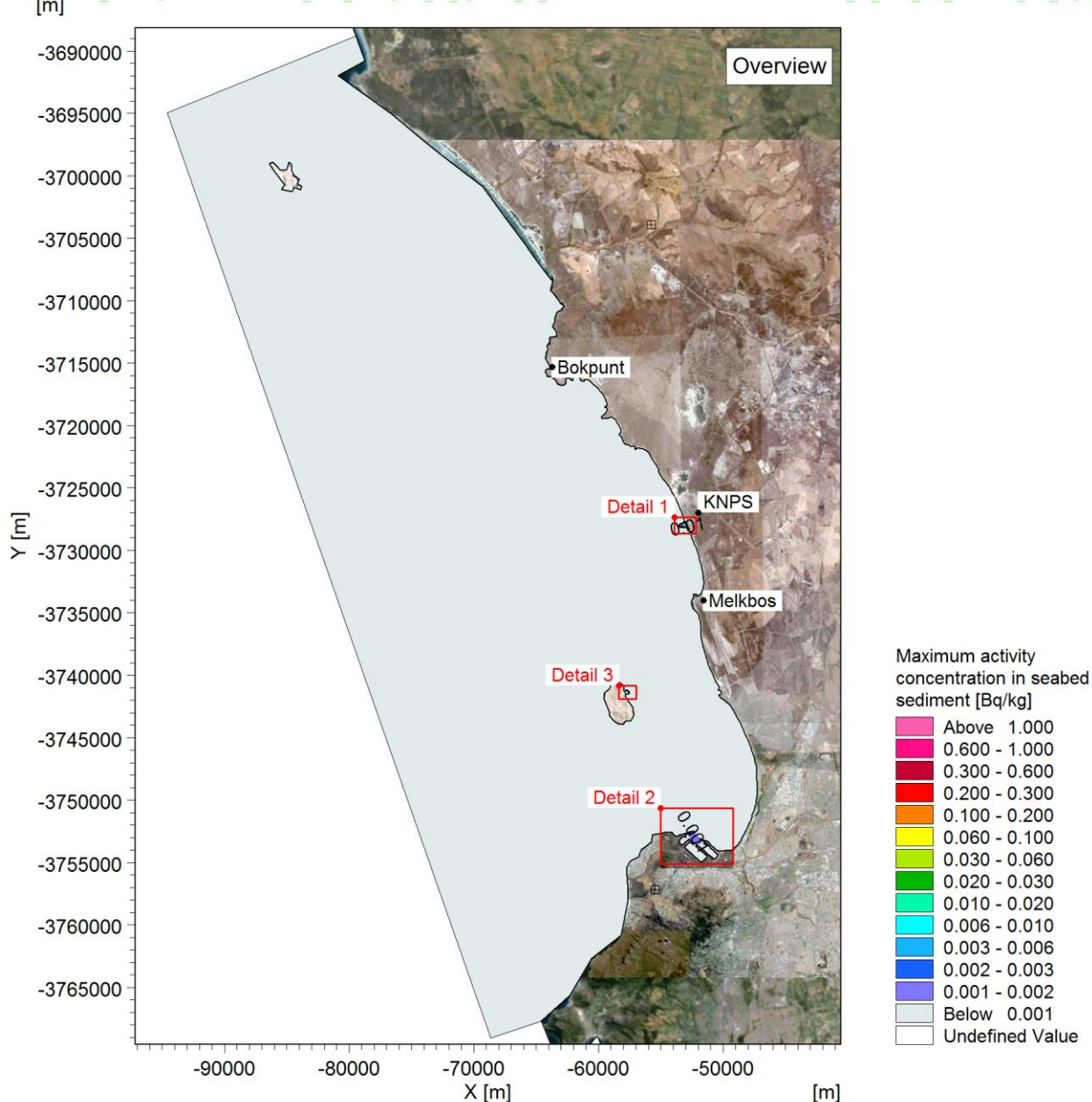


Figure C-5: Maximum concentration of Ag-110m activity in seabed sediment in one modelled year: overview.

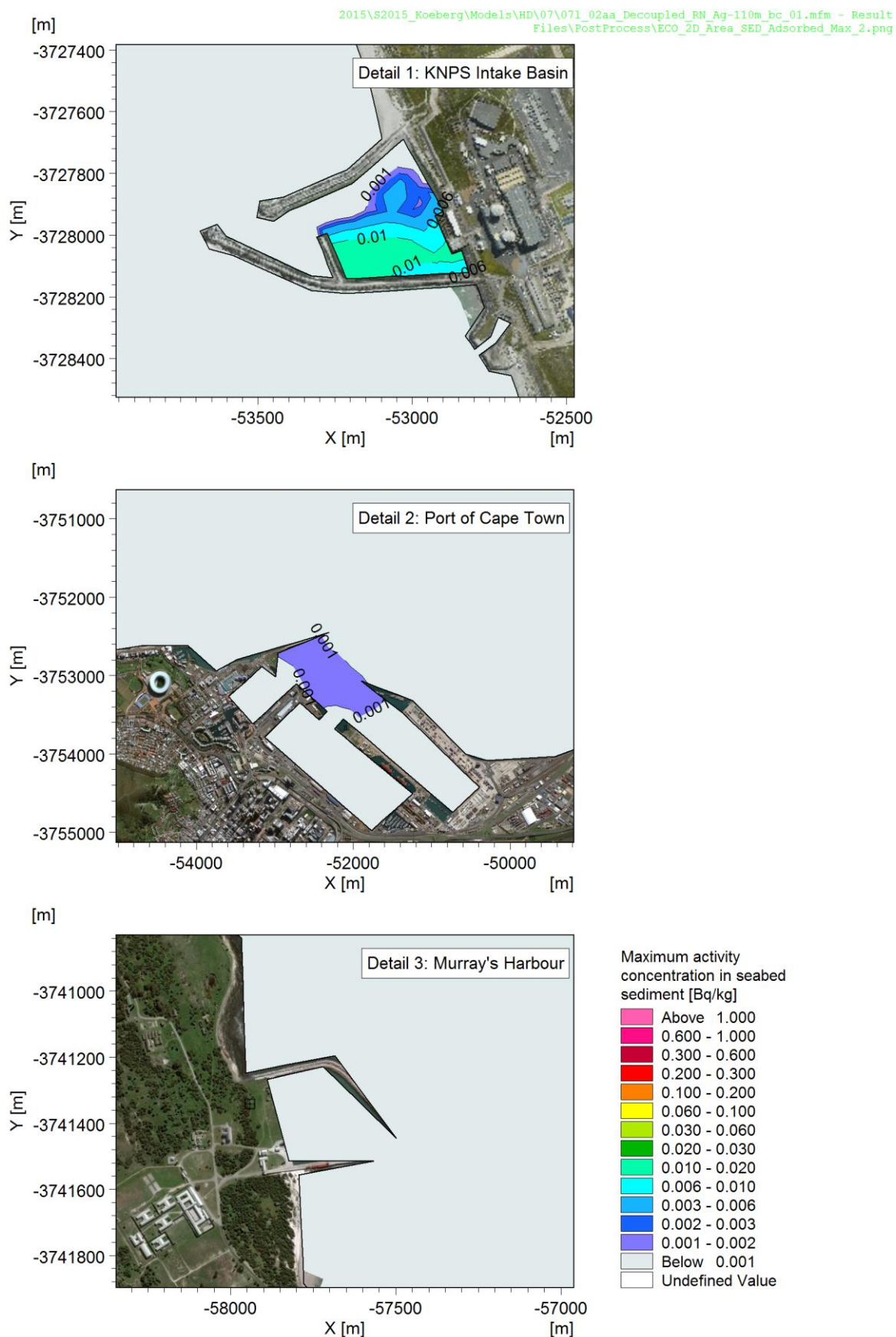
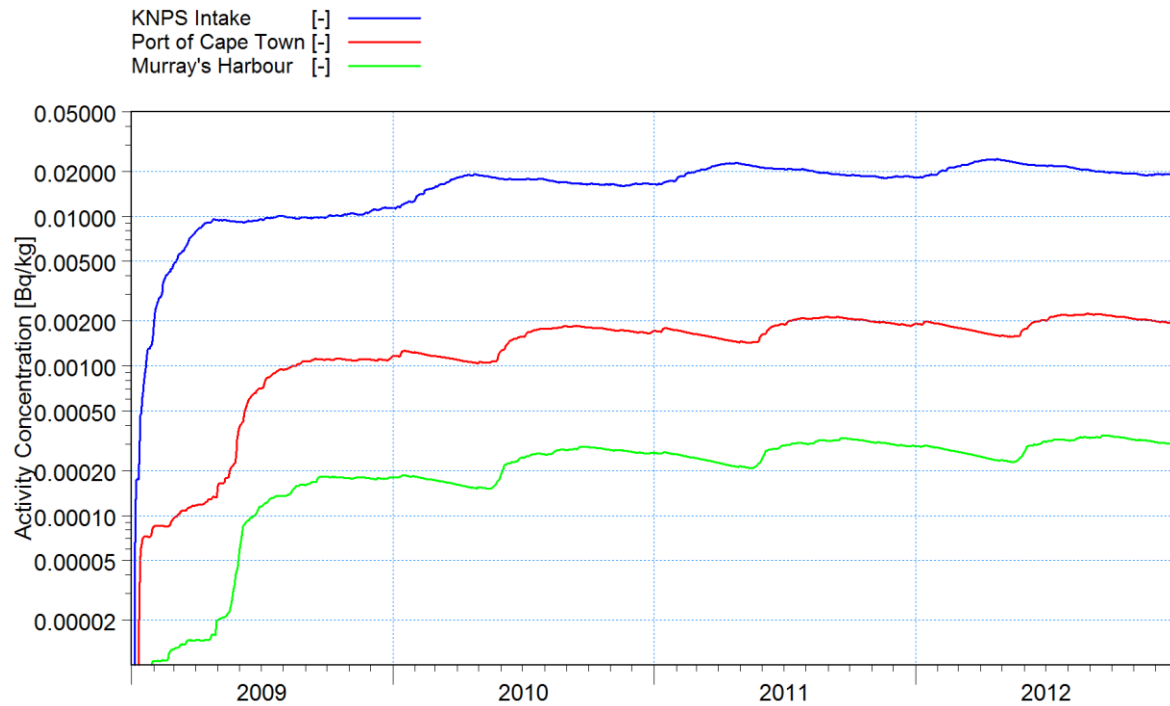


Figure C-6: Maximum concentration of Ag-110m activity in seabed sediment in one modelled year: detail of depo-centres.



2015\S2015_Koeberg\Models\HD\07\071_02aa_Decoupled_RN\TS_Ag-110m.png

Figure C-7: Time series of concentration of Ag-110m activity in the seabed sediment at the three depocentres. For comparative purposes, the concentration is plotted on a logarithmic scale.

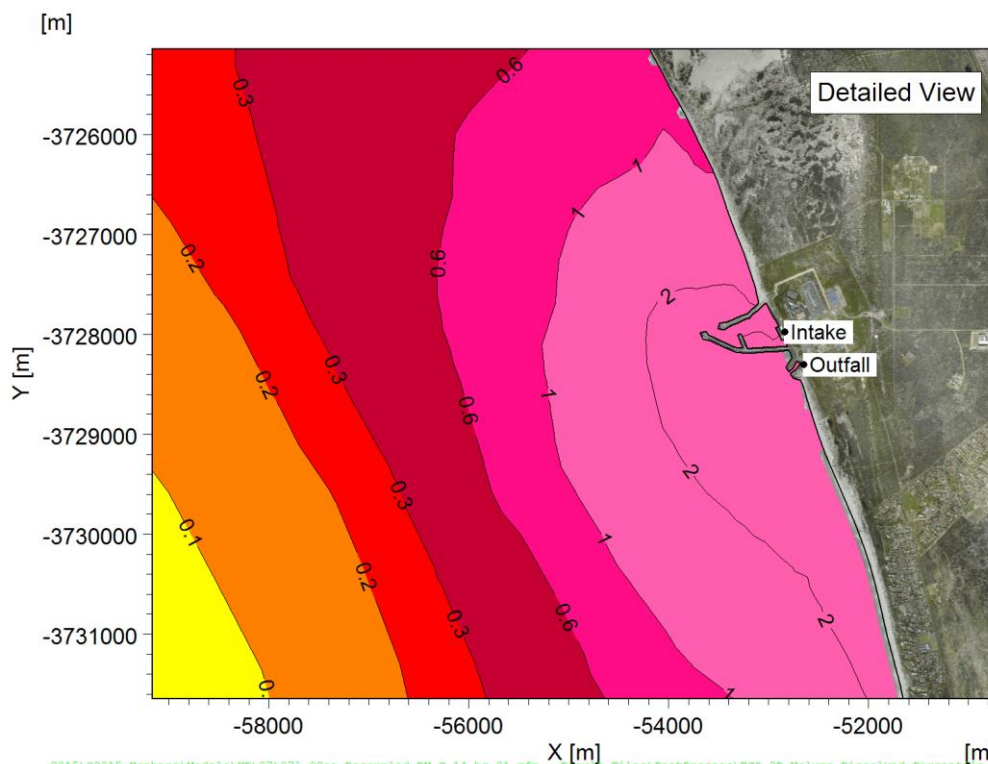
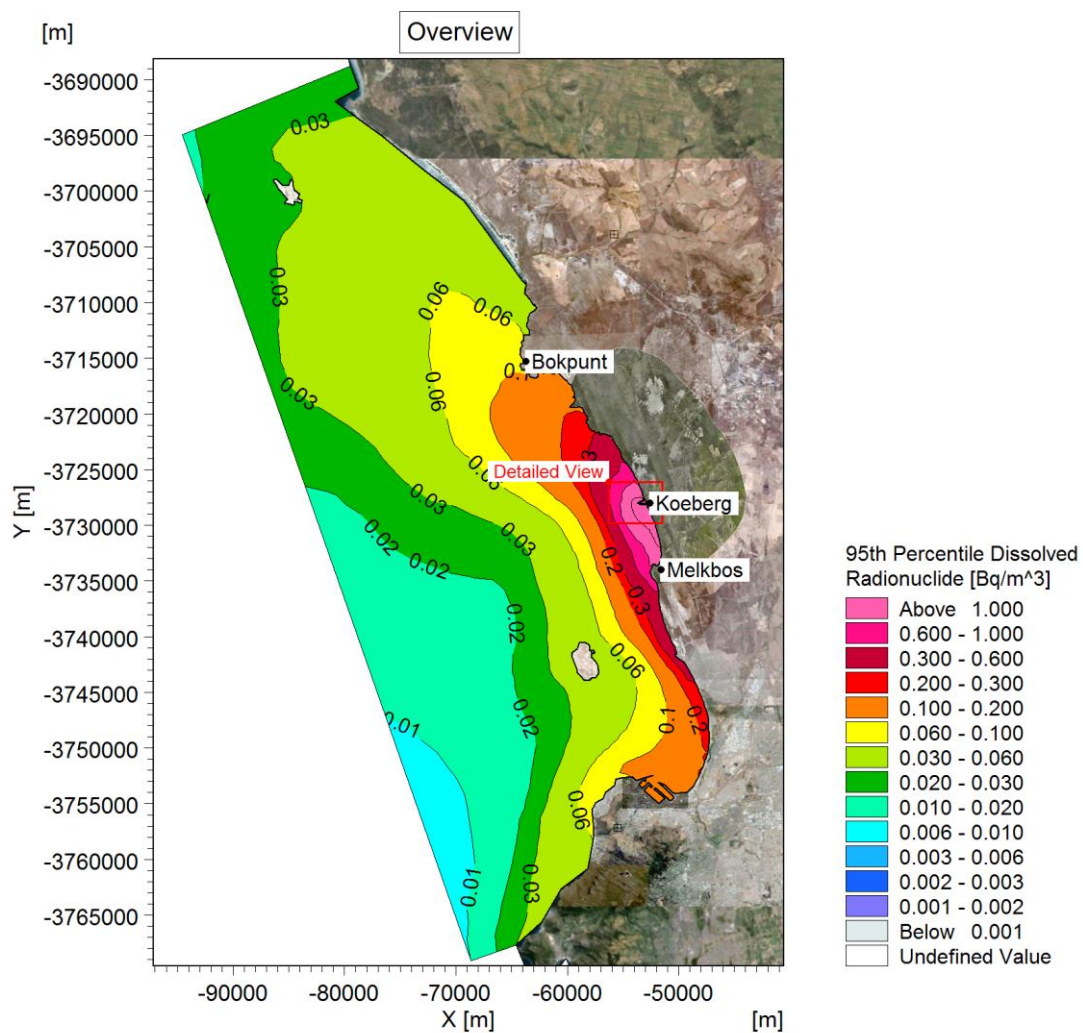


Figure C-8: 95th percentile concentration of dissolved C-14 activity in the water column: near-surface.

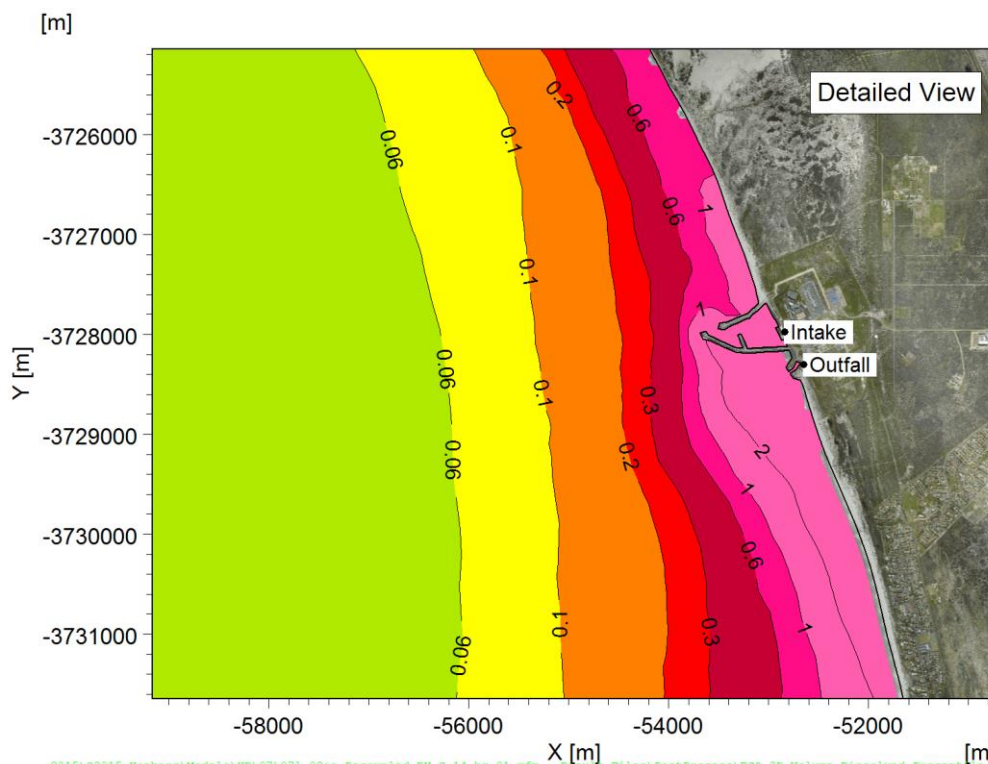
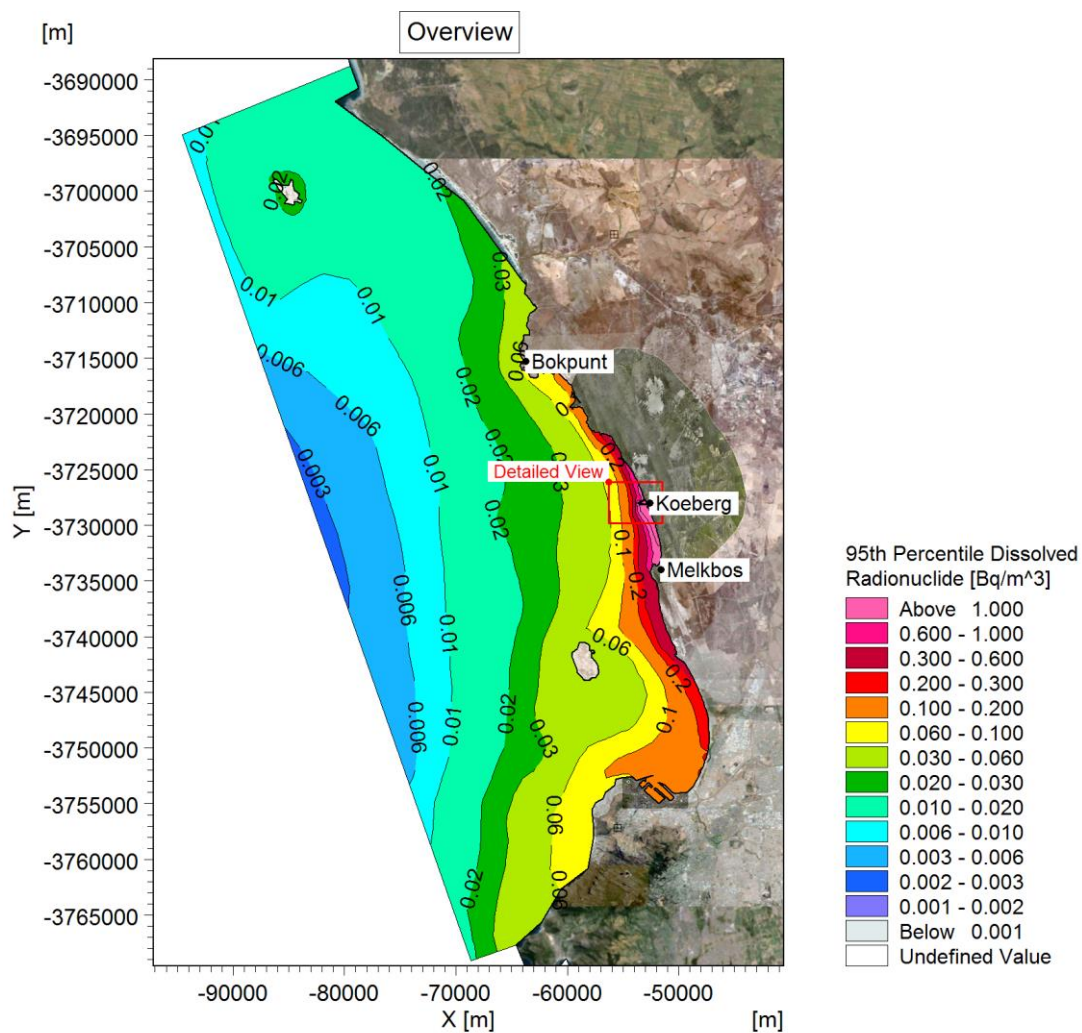


Figure C-9: 95th percentile concentration of dissolved C-14 activity in the water column: near-seabed.

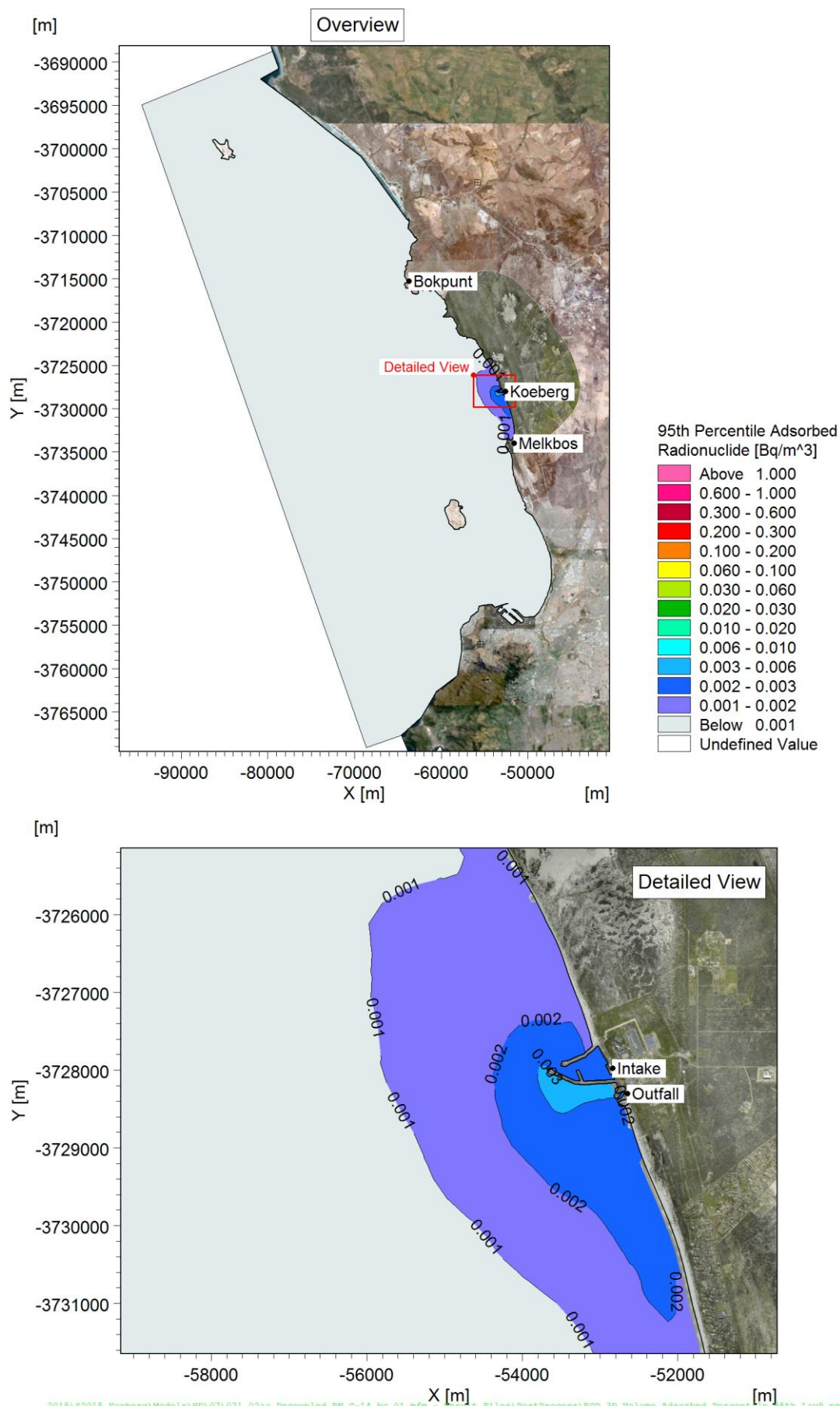


Figure C-10: 95th percentile concentration of adsorbed C-14 activity in the water column: near-surface.

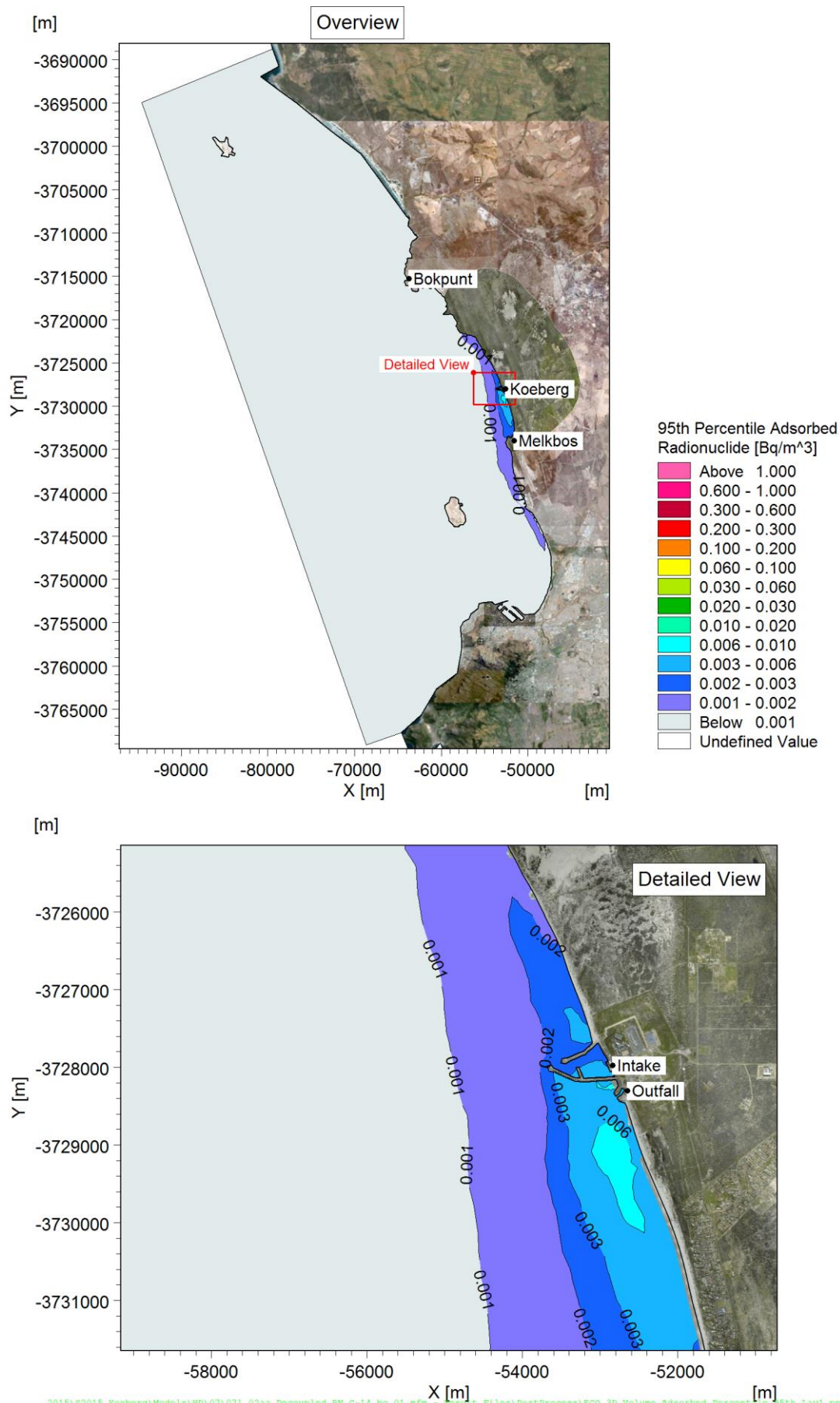


Figure C-11: 95th percentile concentration of adsorbed C-14 activity in the water column: near-seabed.

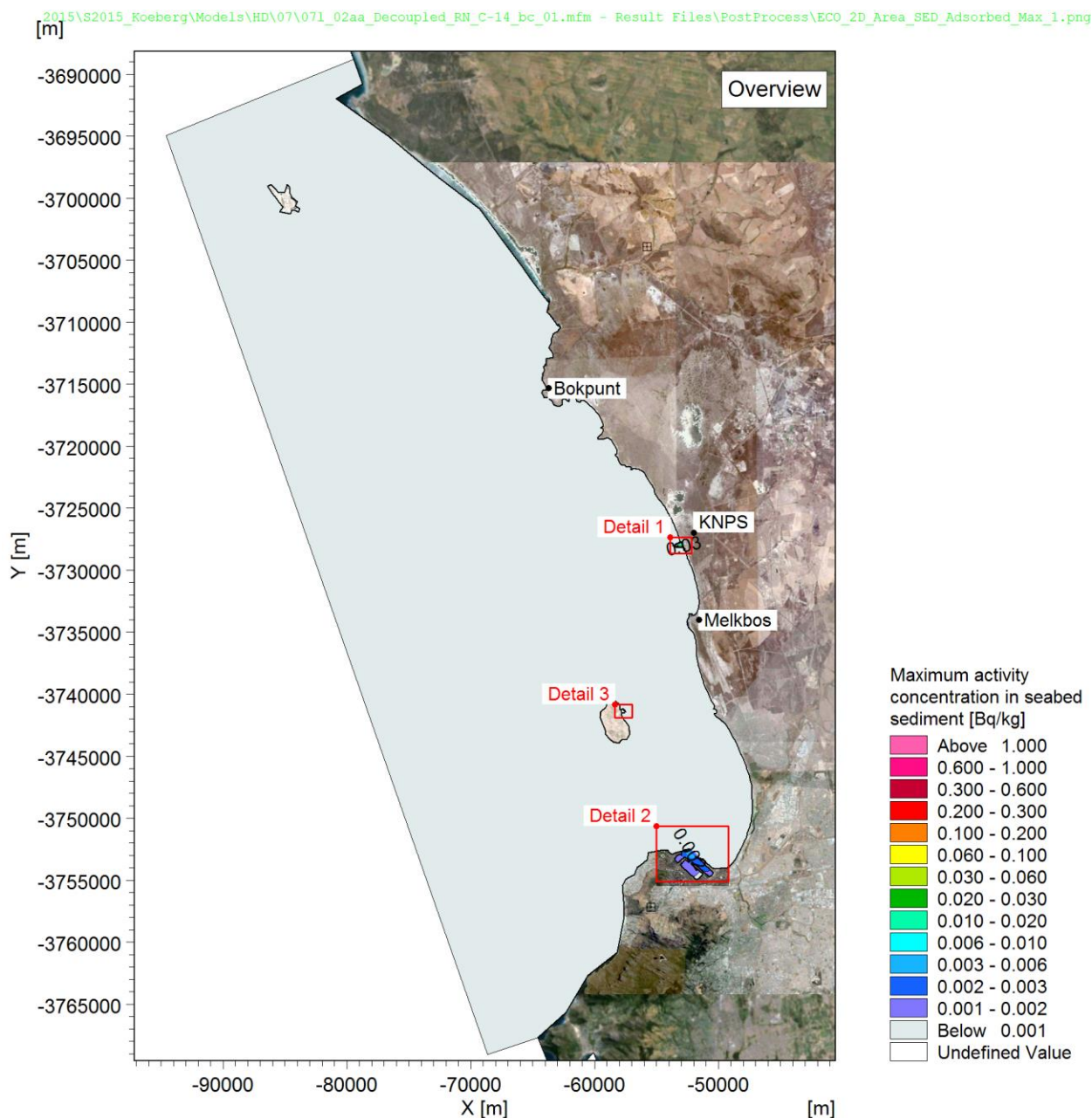


Figure C-12: Maximum concentration of C-14 activity in seabed sediment in one modelled year: overview.

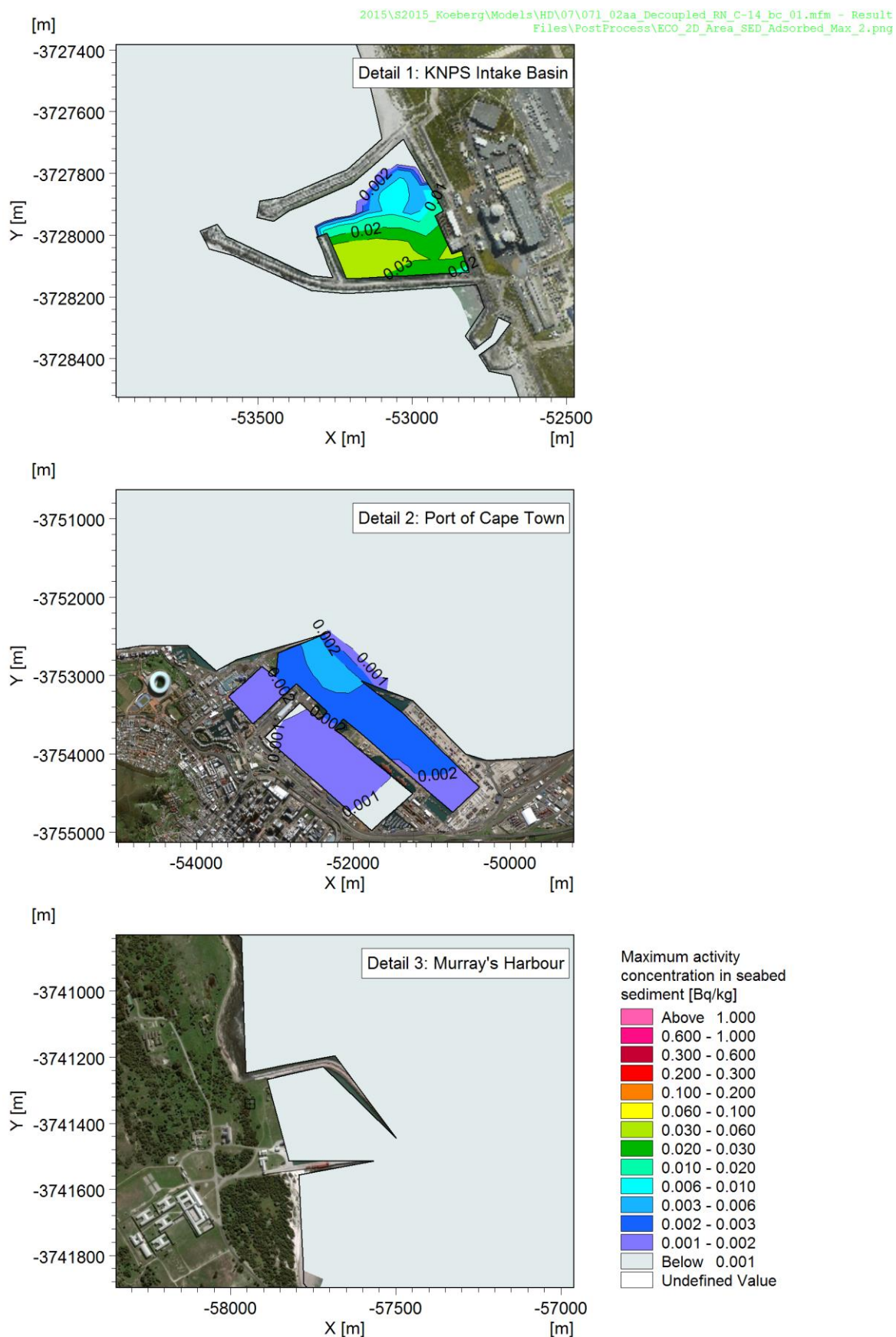
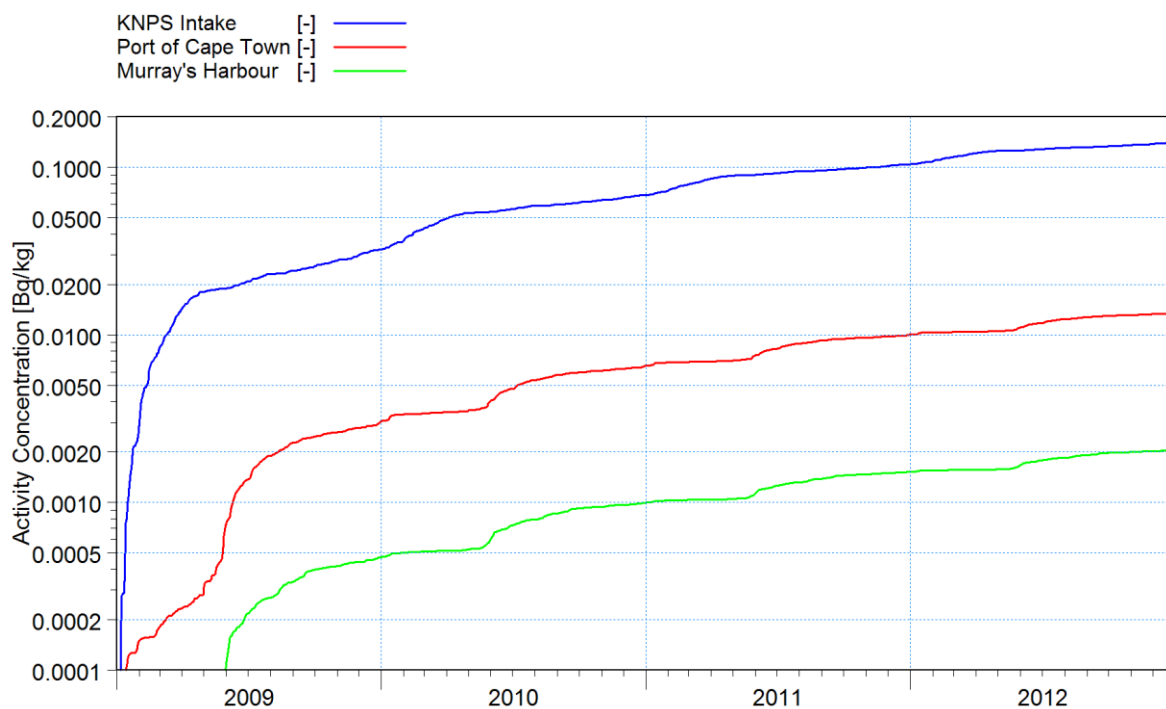


Figure C-13: Maximum concentration of C-14 activity in seabed sediment in one modelled year: detail of depo-centres.



2015\S2015_Koeberg\Models\HD\07\071_02aa_Decoupled_RN\TS_C-14.png

Figure C-14: Time series of concentration of C-14 activity in the seabed sediment at the three depositions. For comparative purposes, the concentration is plotted on a logarithmic scale.

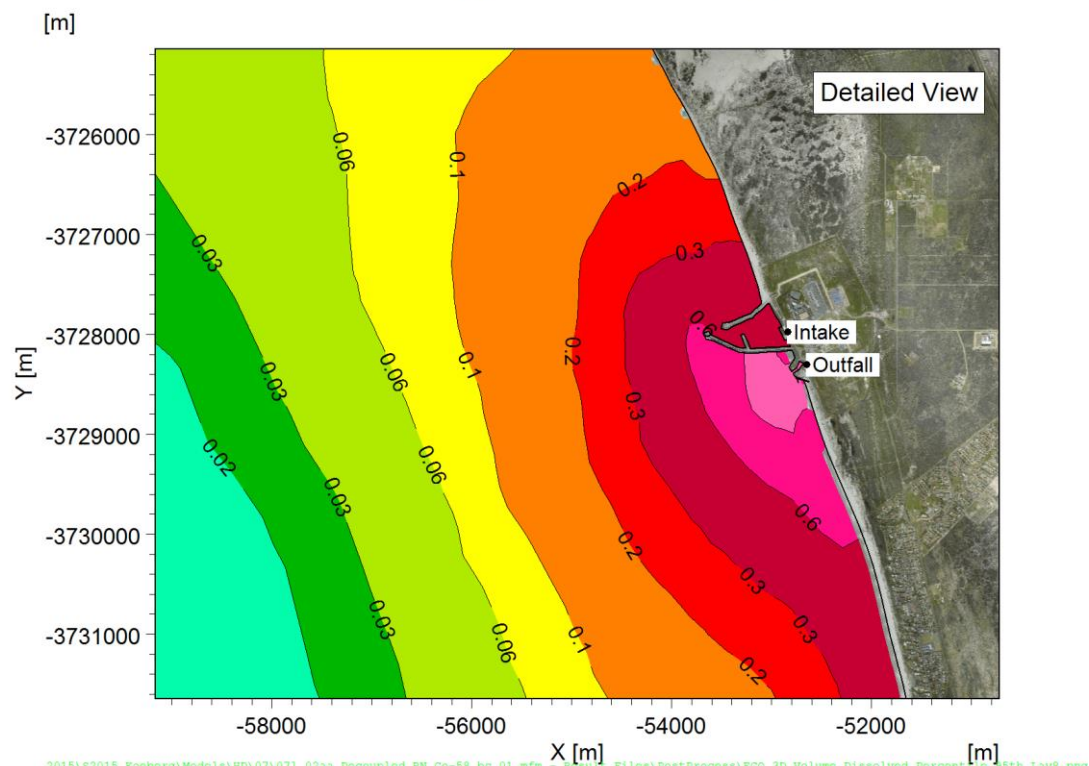
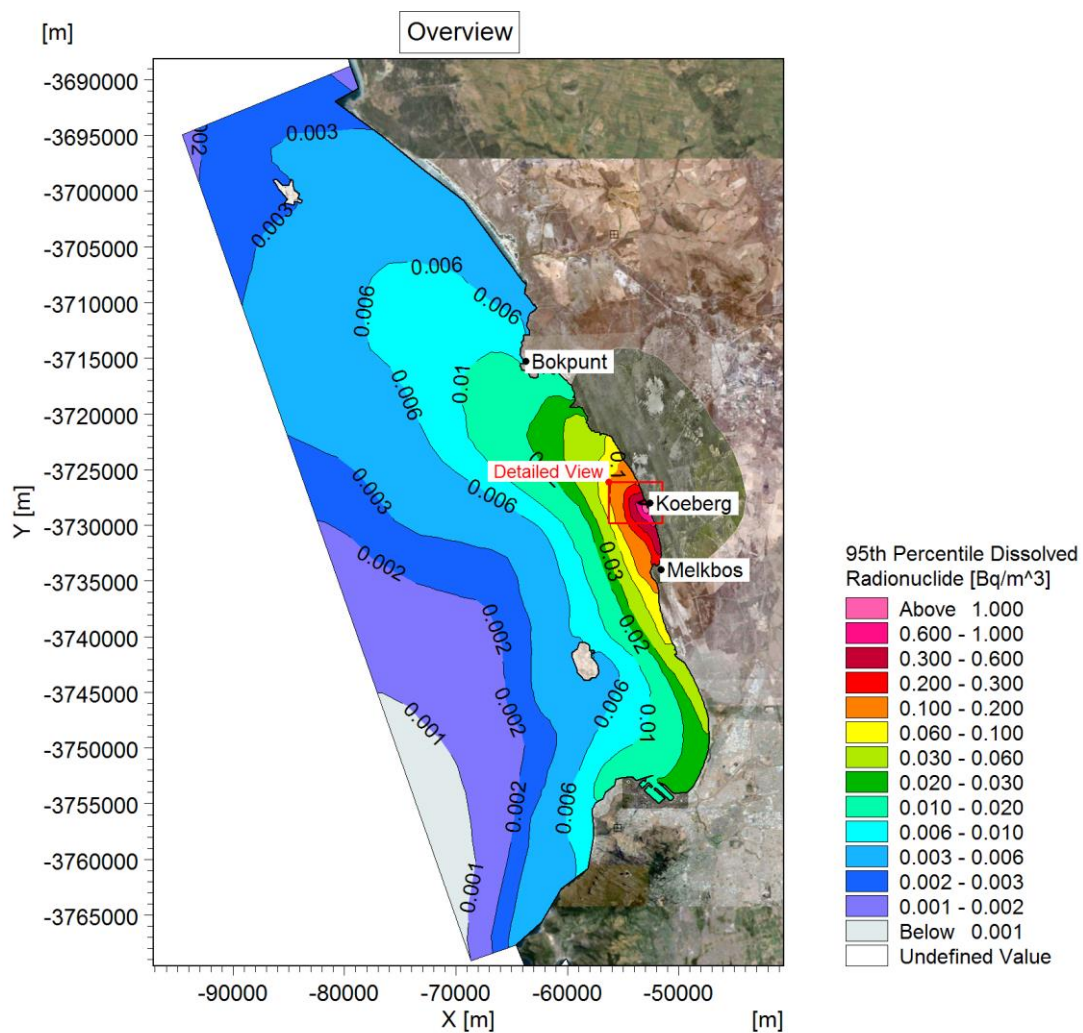
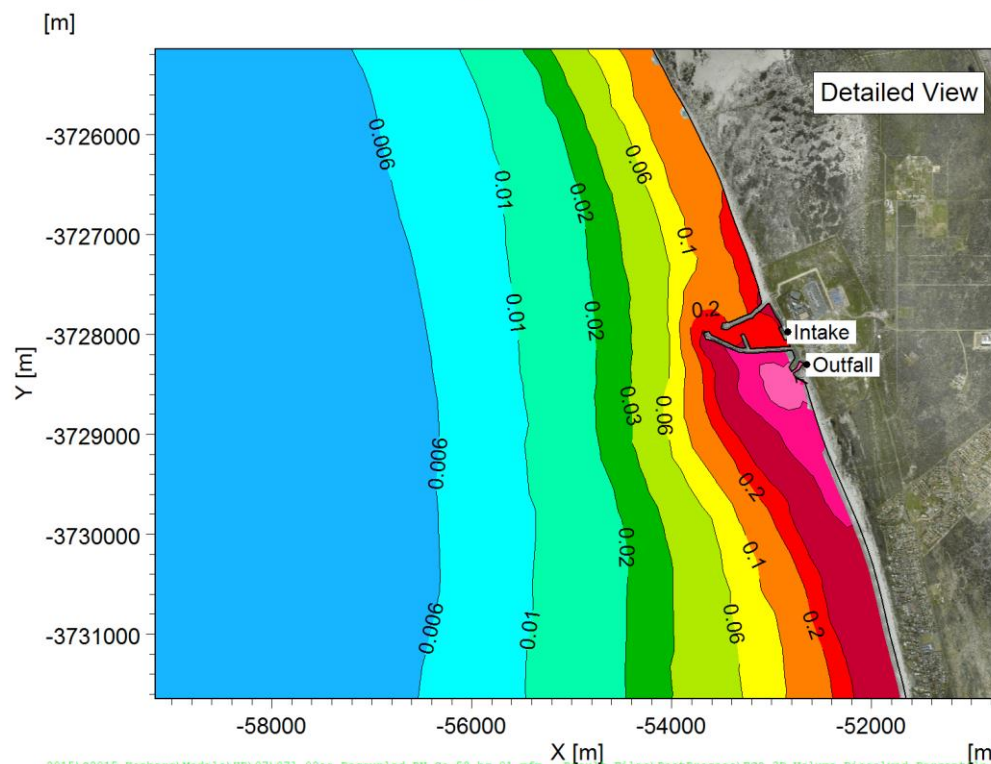
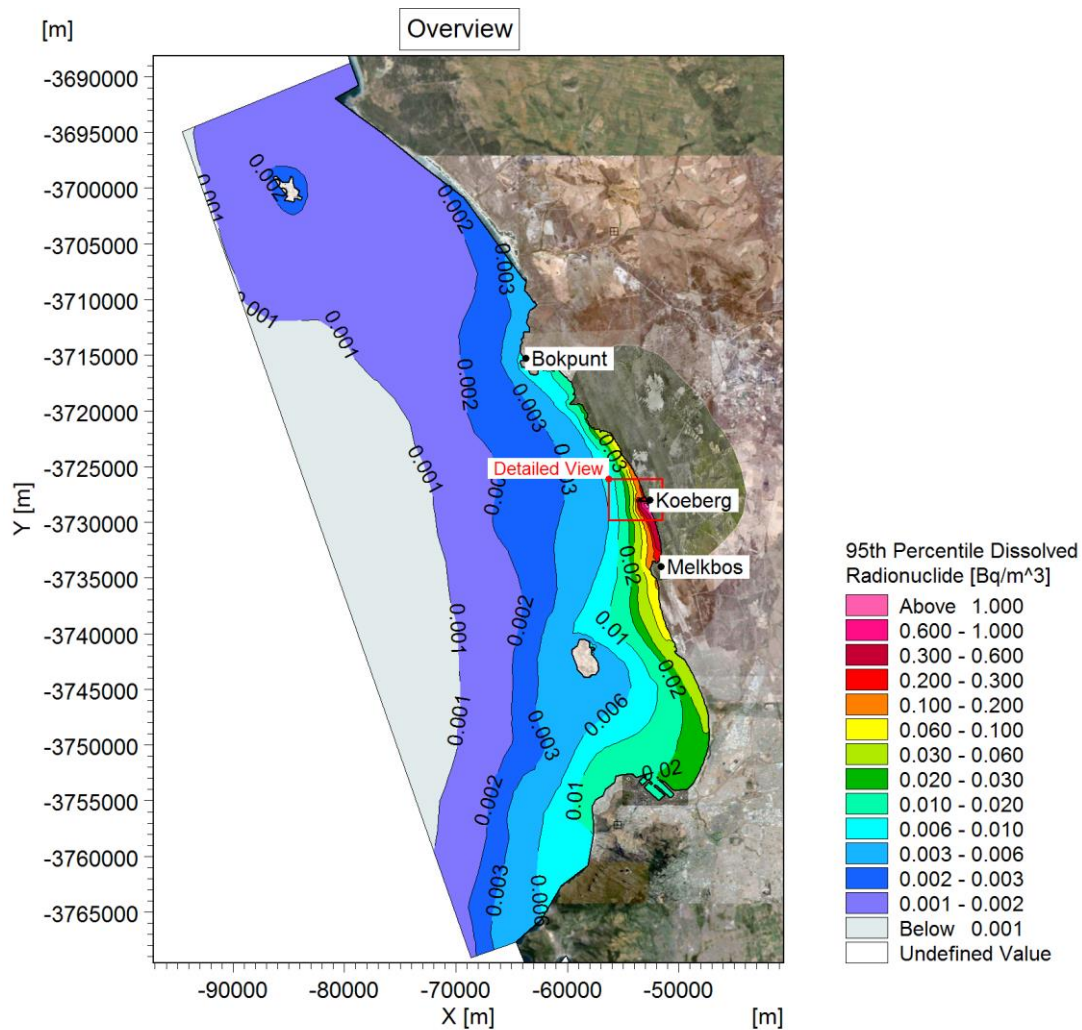


Figure C-15: 95th percentile concentration of dissolved Co-58 activity in the water column: near-surface.



2015\S2015_Koeberg\Models\HD\07\071_02aa_Decoupled_RN_Co-58_bc_01.mfm - Result Files\PostProcess\ECO_3D_Volume_Dissolved_Percentile_95th_Lay1.png

Figure C-16: 95th percentile concentration of dissolved Co-58 activity in the water column: near-seabed.

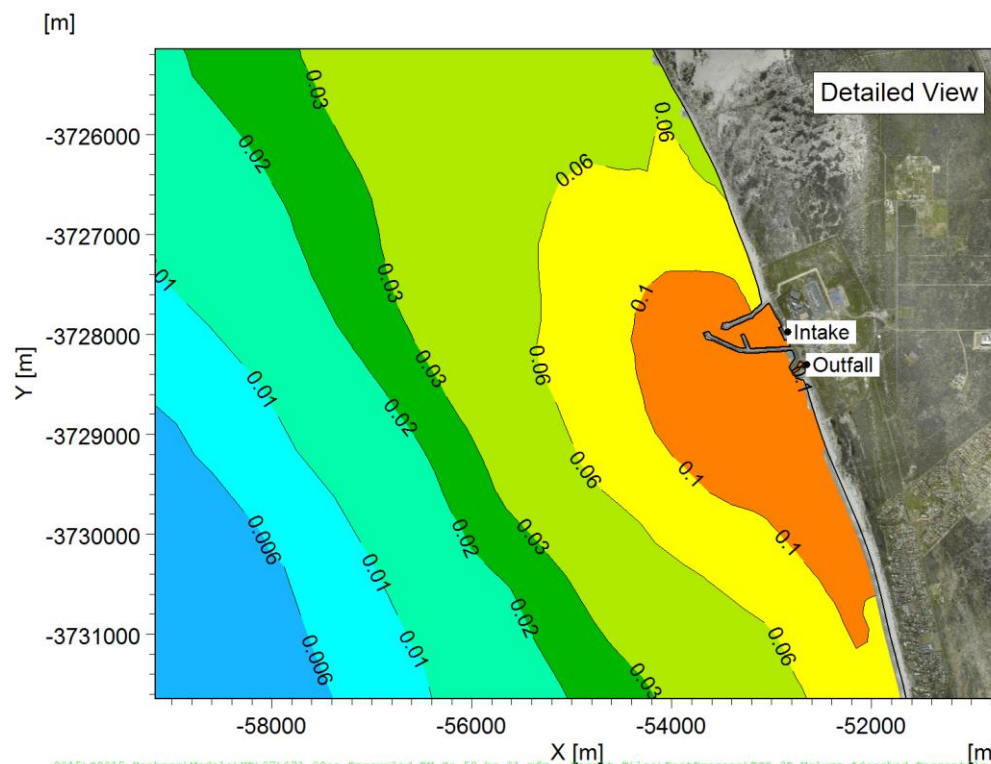
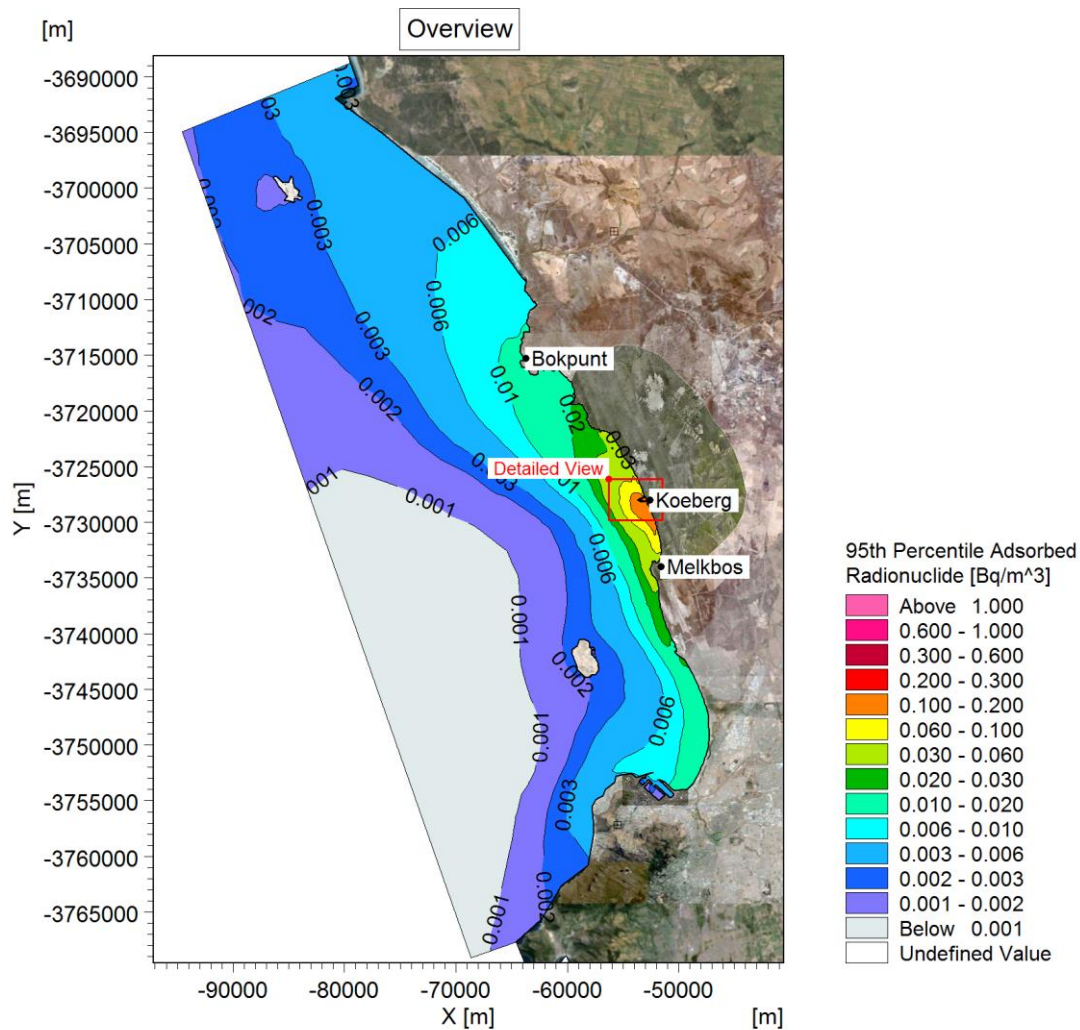


Figure C-17: 95th percentile concentration of adsorbed Co-58 activity in the water column: near-surface.

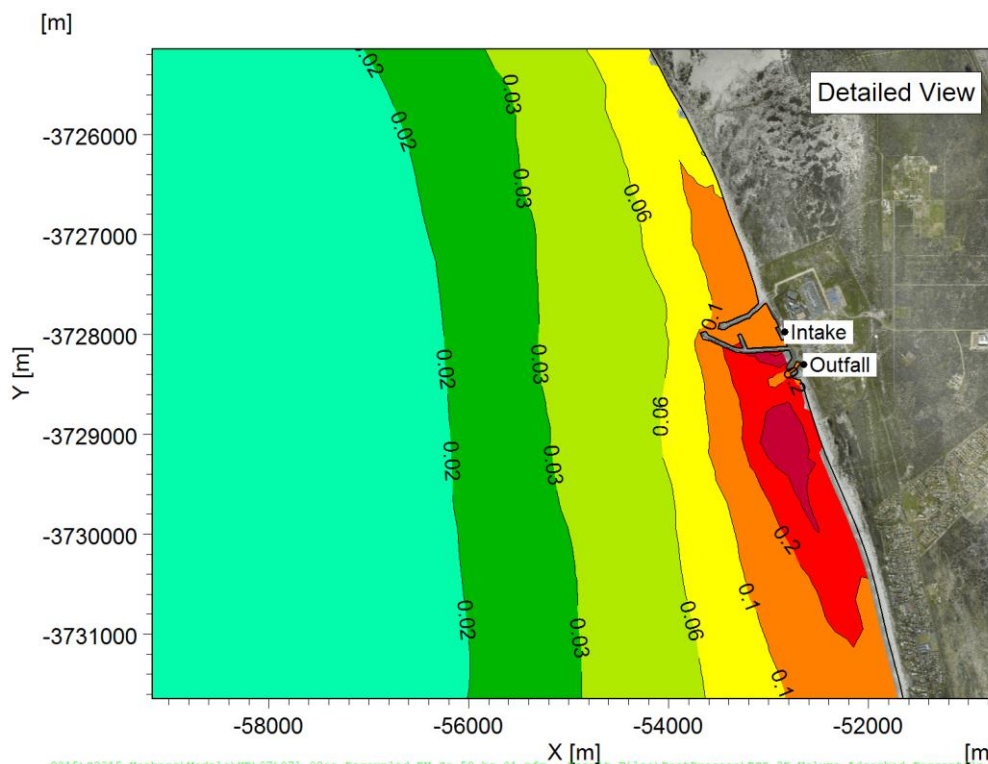
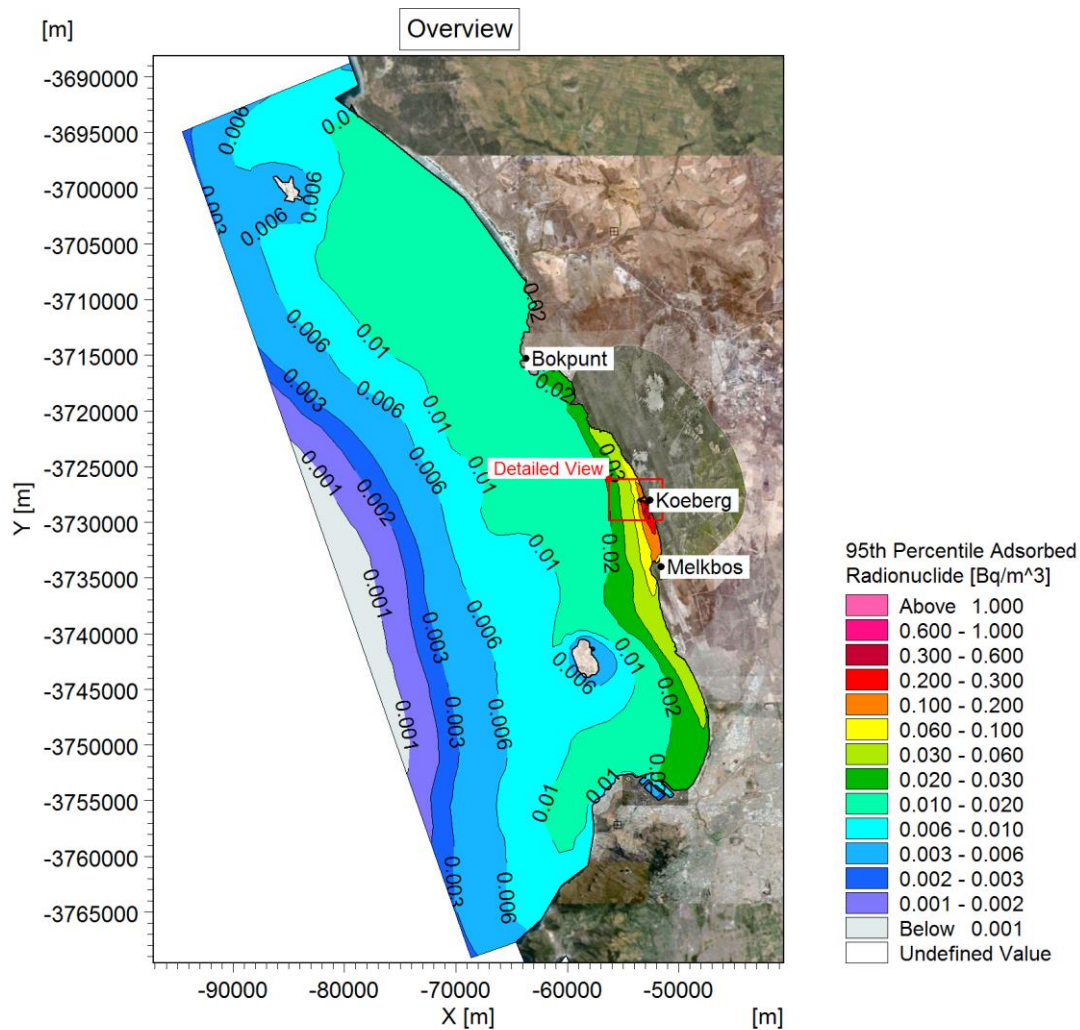


Figure C-18: 95th percentile concentration of adsorbed Co-58 activity in the water column: near-seabed.

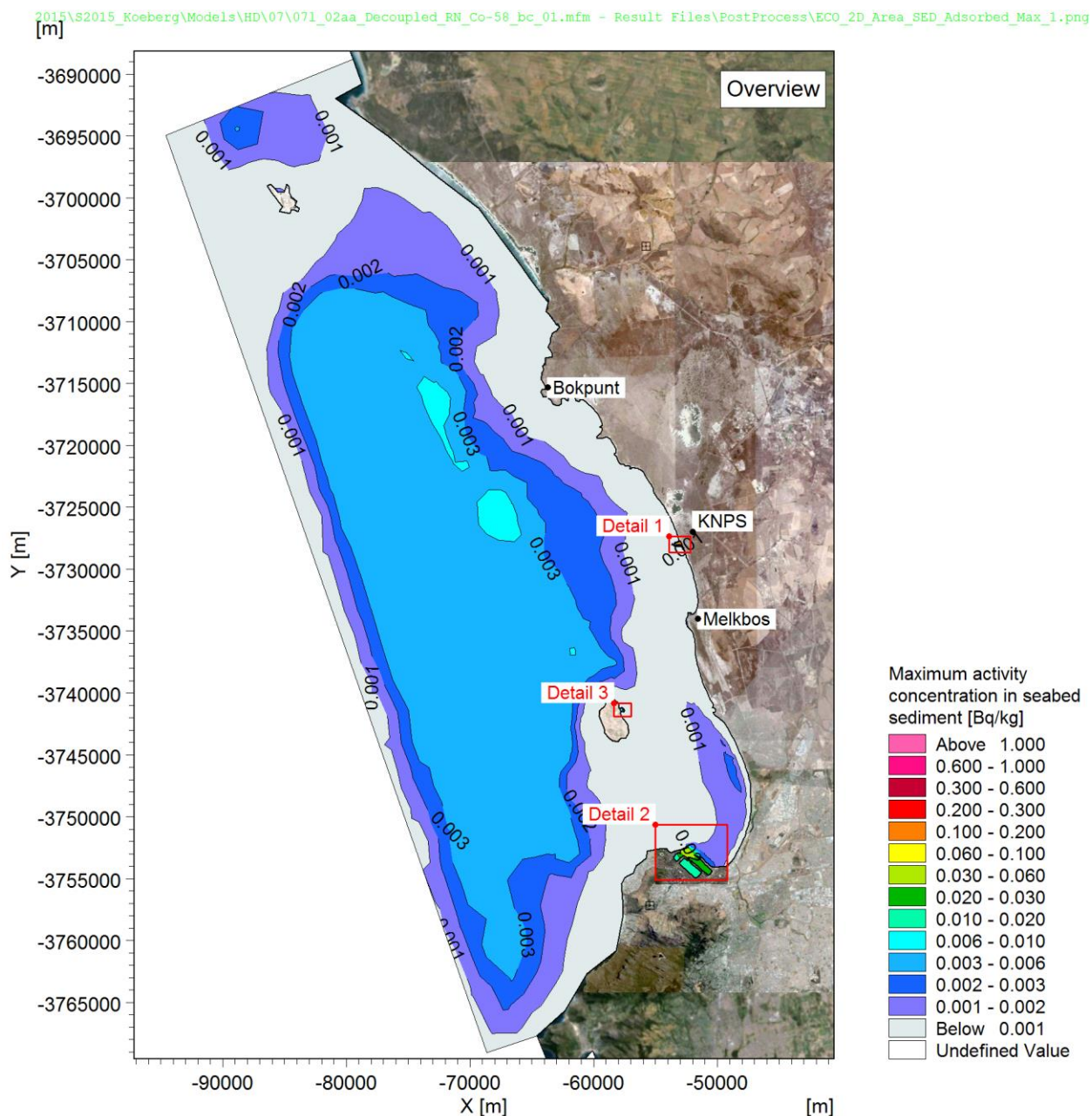


Figure C-19: Maximum concentration of Co-58 activity in seabed sediment in one modelled year: overview.

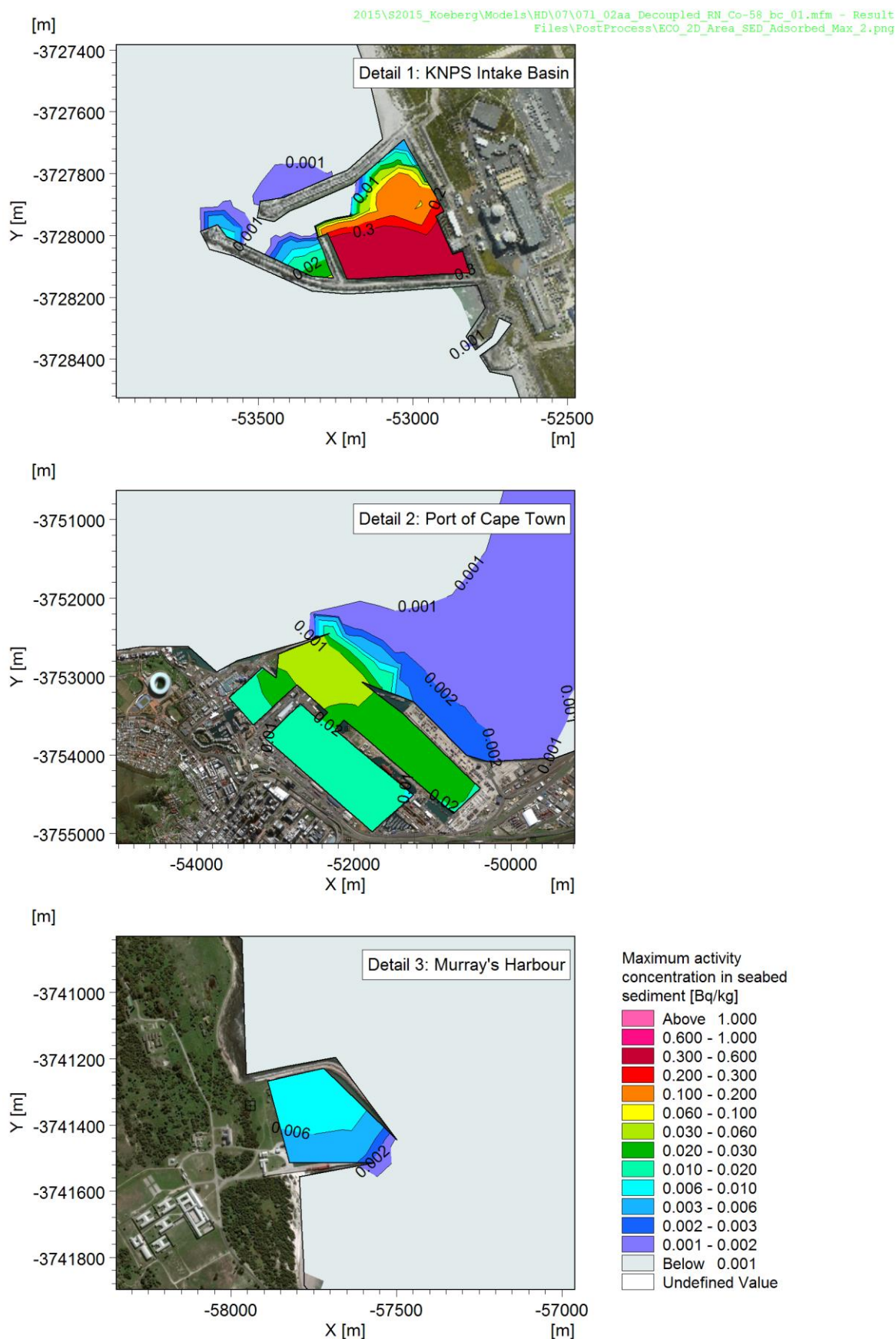
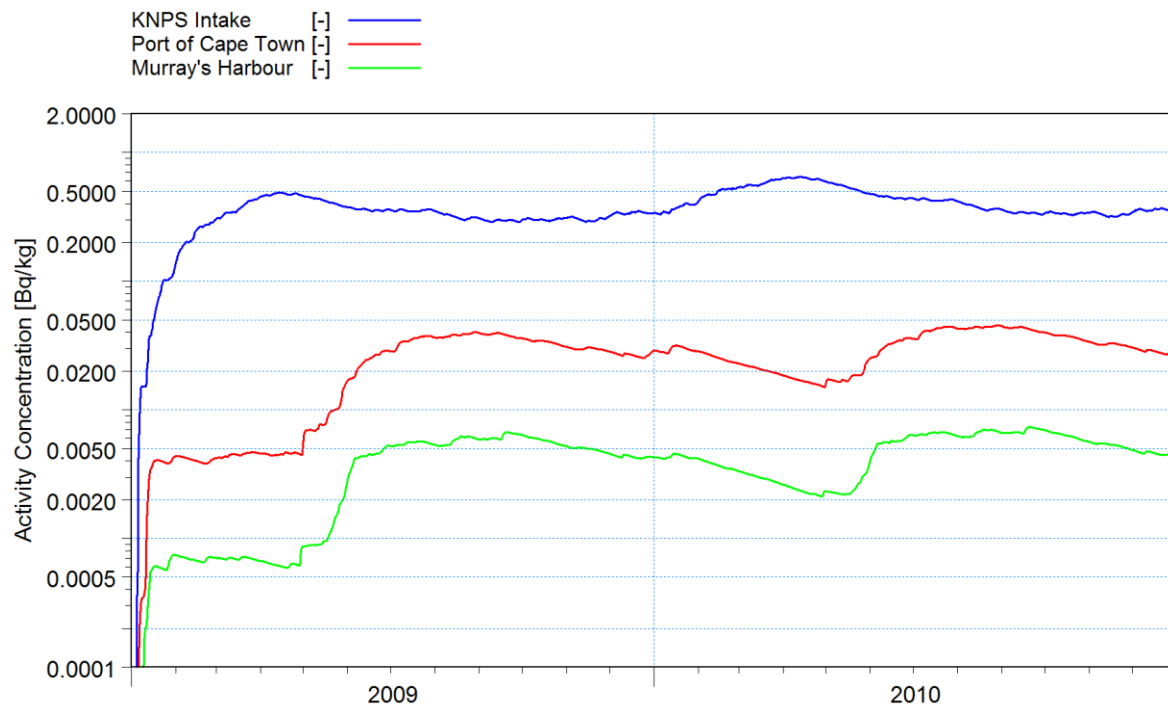
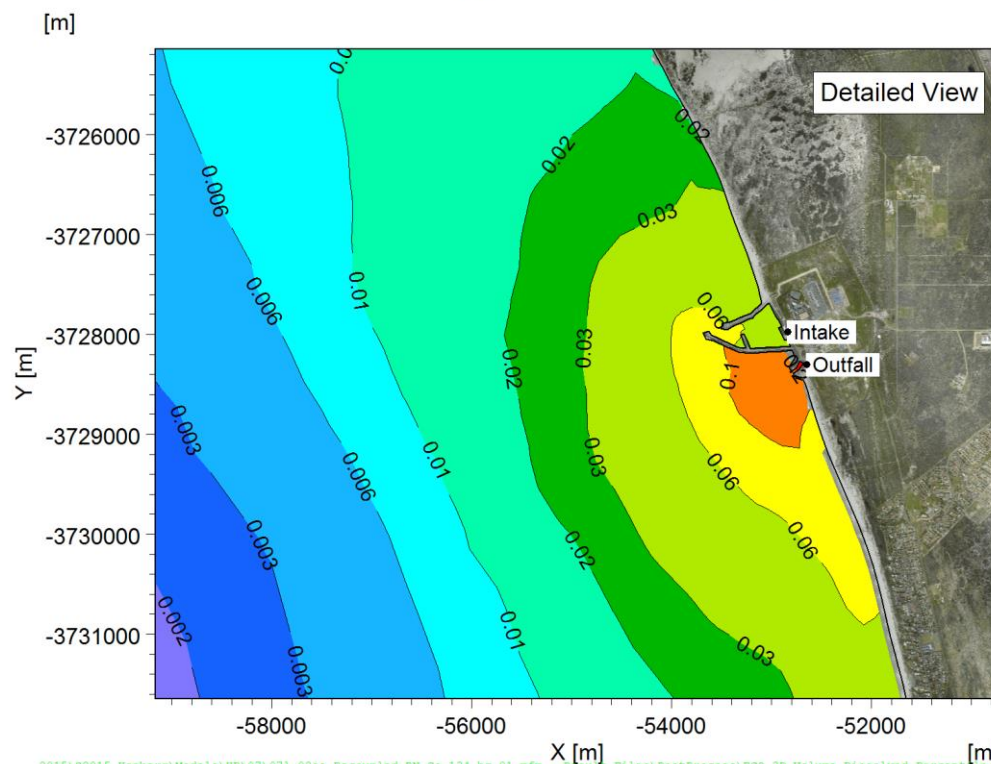
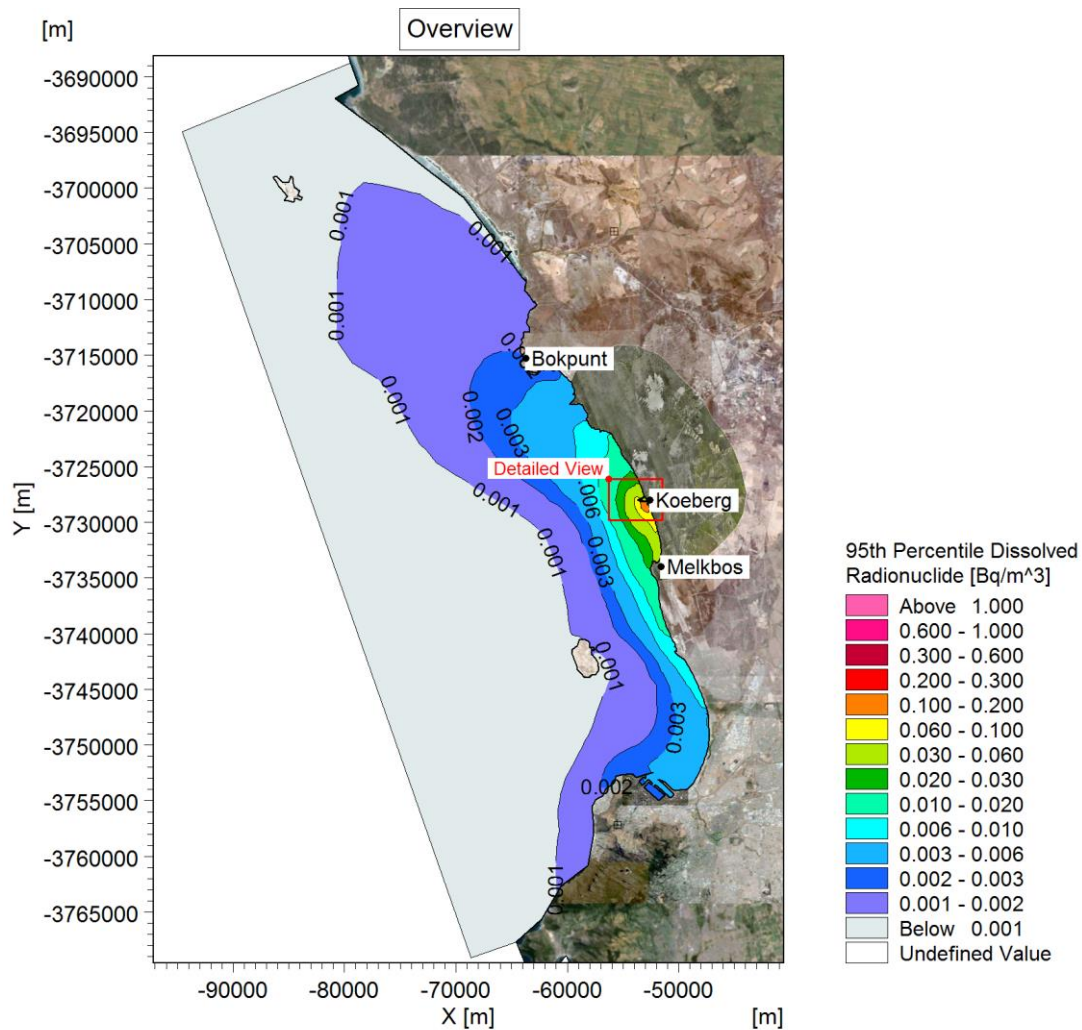


Figure C-20: Maximum concentration of Co-58 activity in seabed sediment in one modelled year: detail of depo-centres.



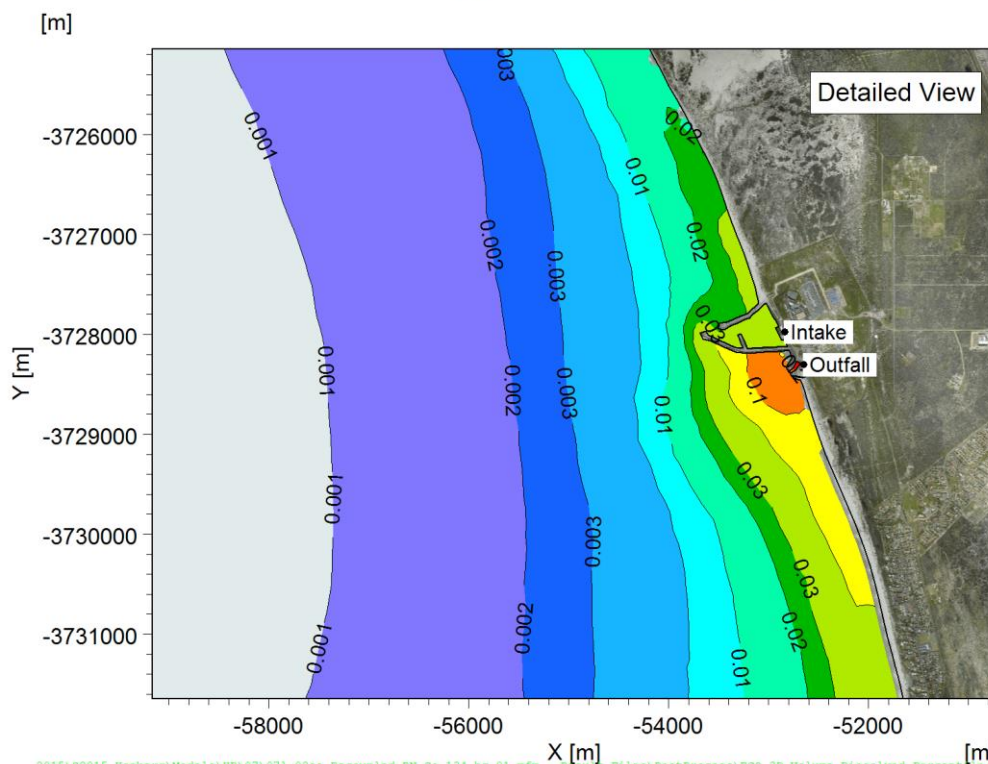
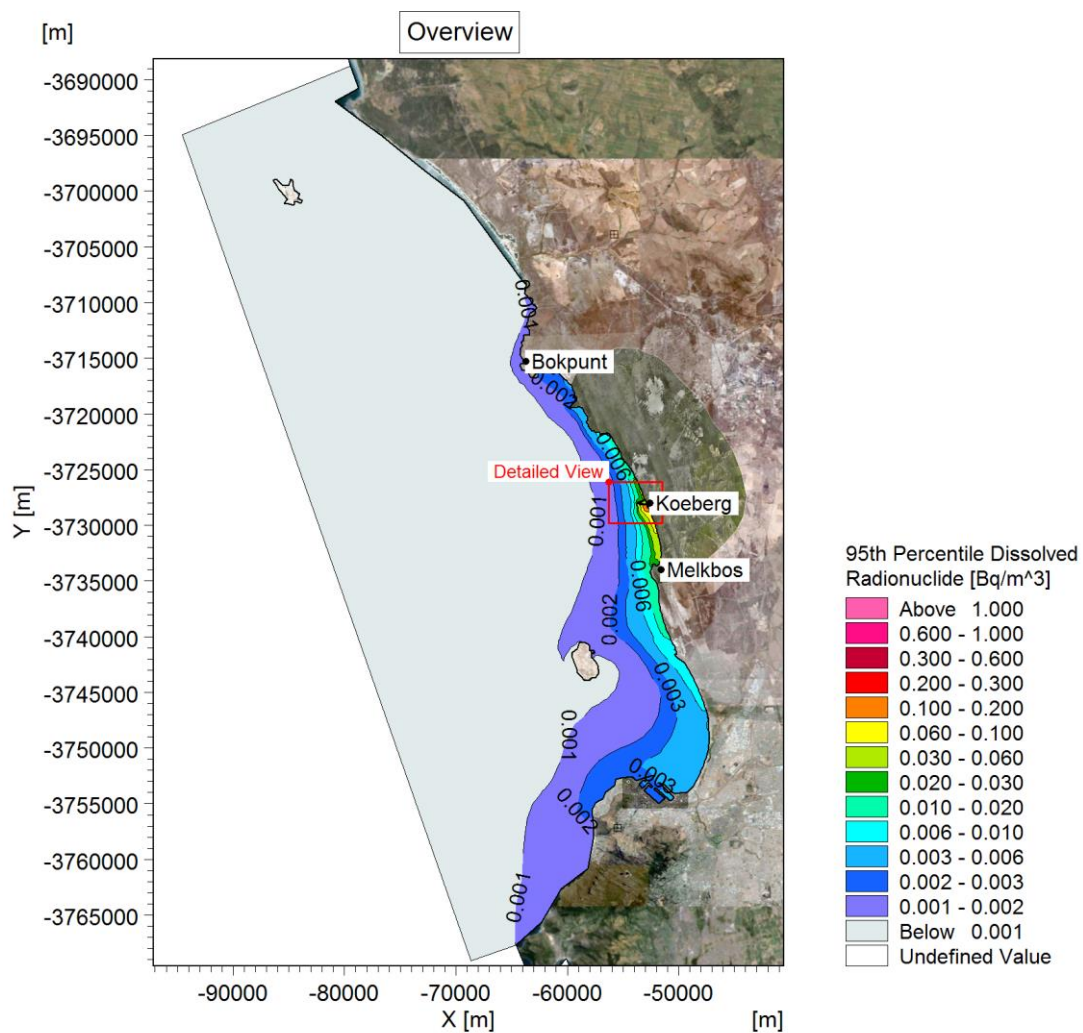
2015\S2015_Koeberg\Models\HD\07\071_02aa_Decoupled_RN\TS_Co-58.png

Figure C-21: Time series of concentration of Co-58 activity in the seabed sediment at the three depositions. For comparative purposes, the concentration is plotted on a logarithmic scale.



2015\B2015_Koeberg\Models\HD\07\071_02aa_Decoupled_RN-Cs-134_bc_01.mfm - Result Files\PostProcess\ECO_3D_Volume_Dissolved_Percentile_95th_Lay6.png

Figure C-22: 95th percentile concentration of dissolved Cs-134 activity in the water column: near-surface.



2015\B2015_Koeberg\Models\HD\07\071_02aa_Decoupled_RN-Cs-134_bc_01.mfm - Result Files\PostProcess\ECO_3D_Volume_Dissolved_Percentile_95th_Lay1.png

Figure C-23: 95th percentile concentration of dissolved Cs-134 activity in the water column: near-seabed.

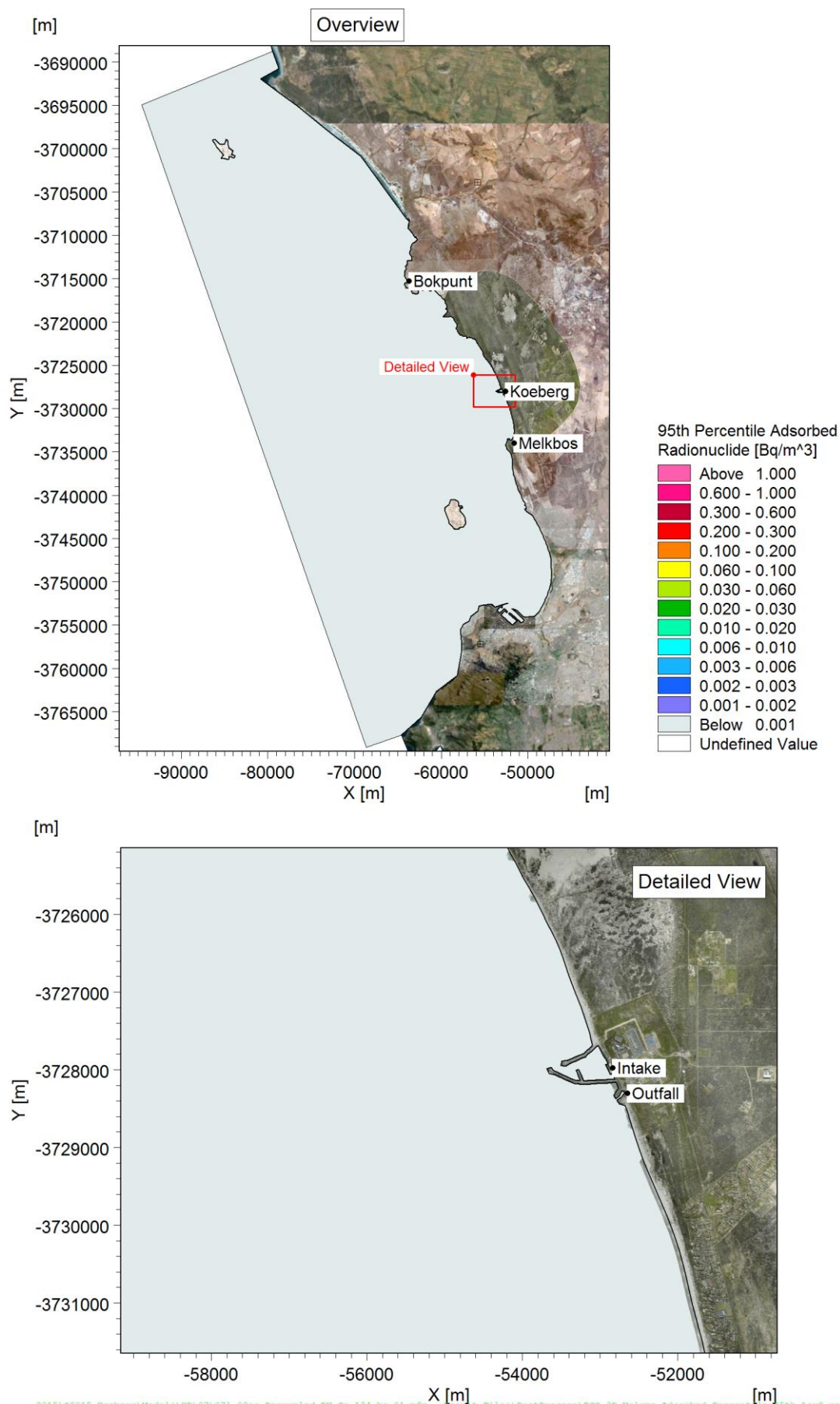


Figure C-24: 95th percentile concentration of adsorbed Cs-134 activity in the water column: near-surface.

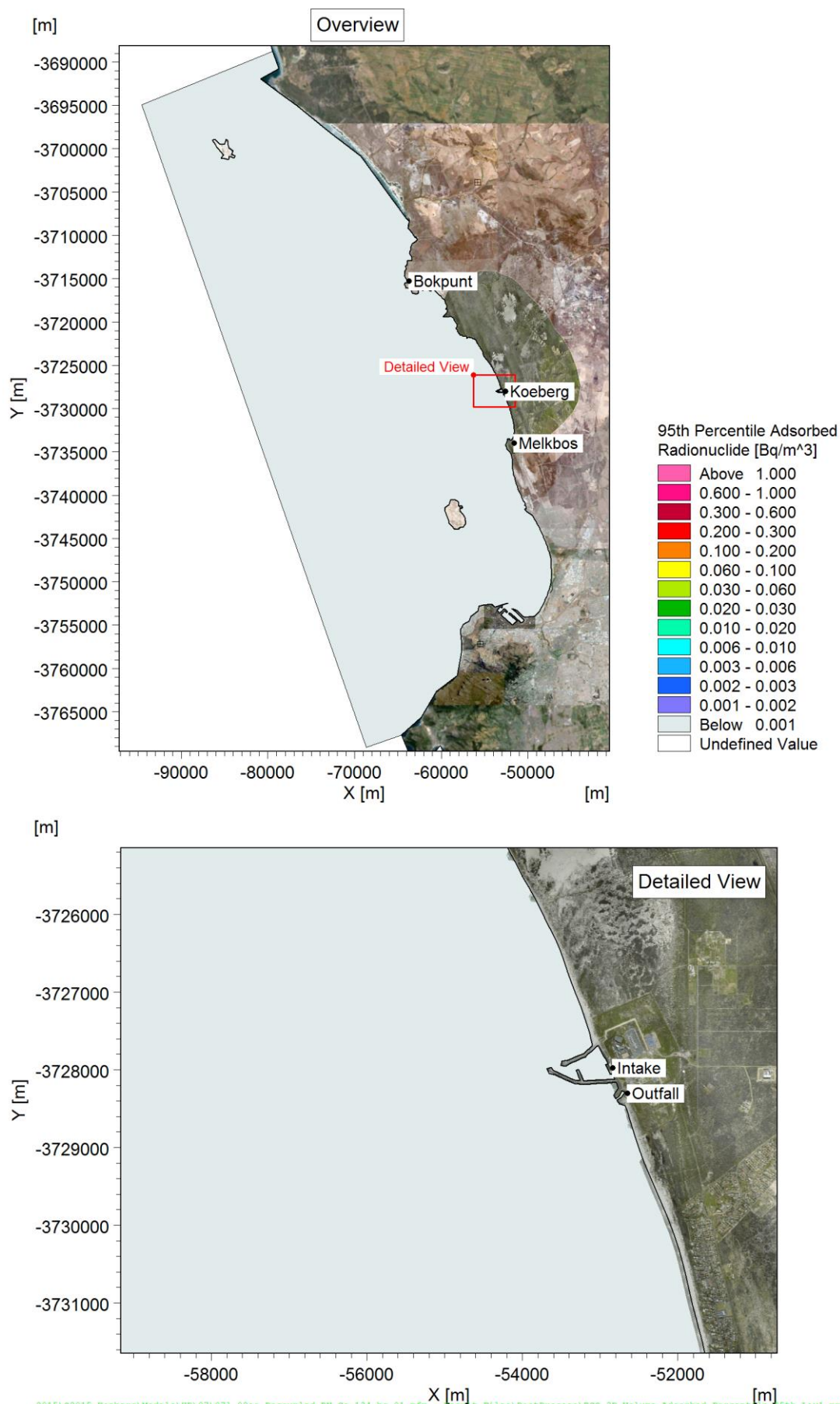


Figure C-25: 95th percentile concentration of adsorbed Cs-134 activity in the water column: near-seabed.

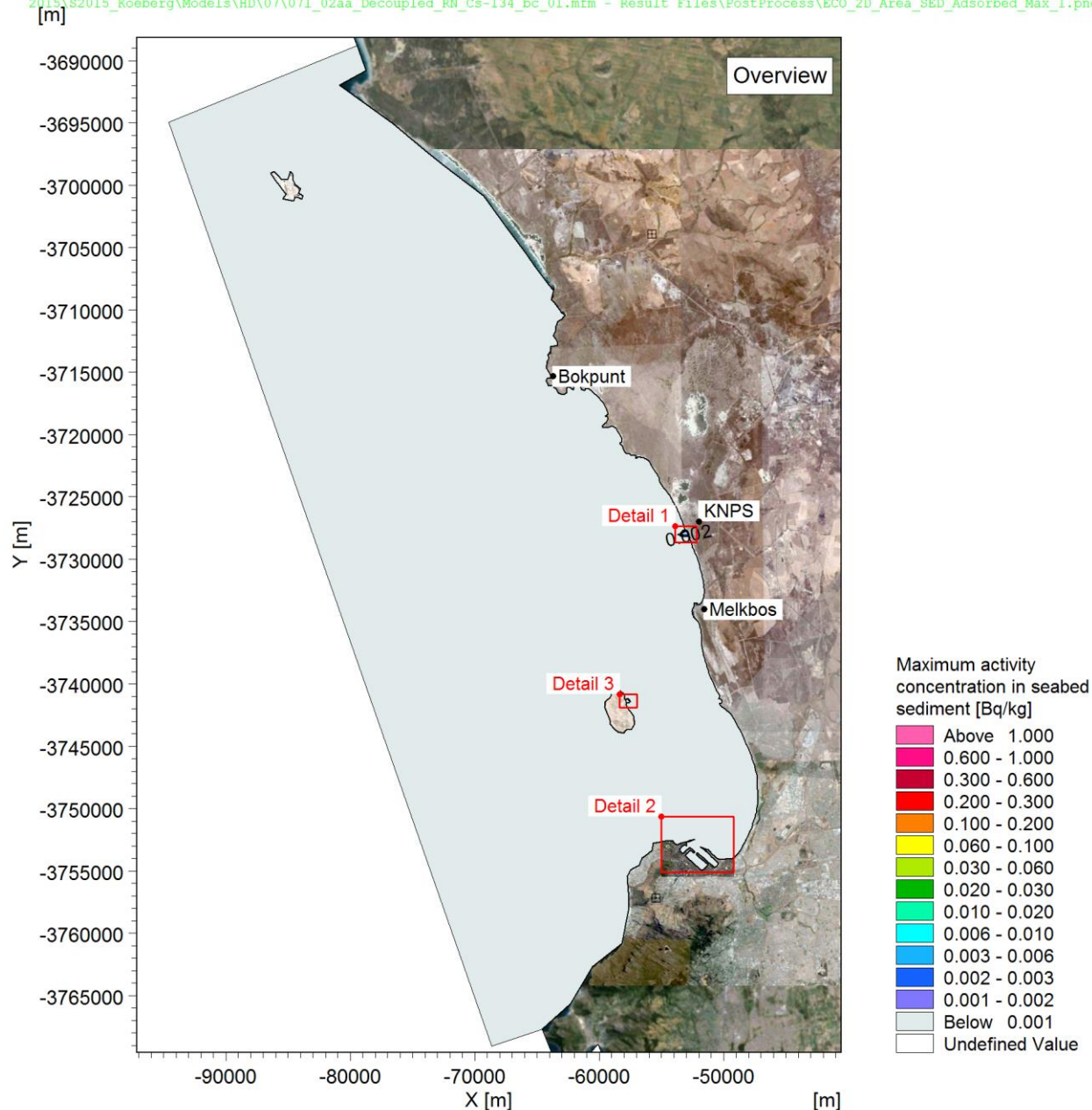


Figure C-26: Maximum concentration of Cs-134 activity in seabed sediment in one modelled year: overview.

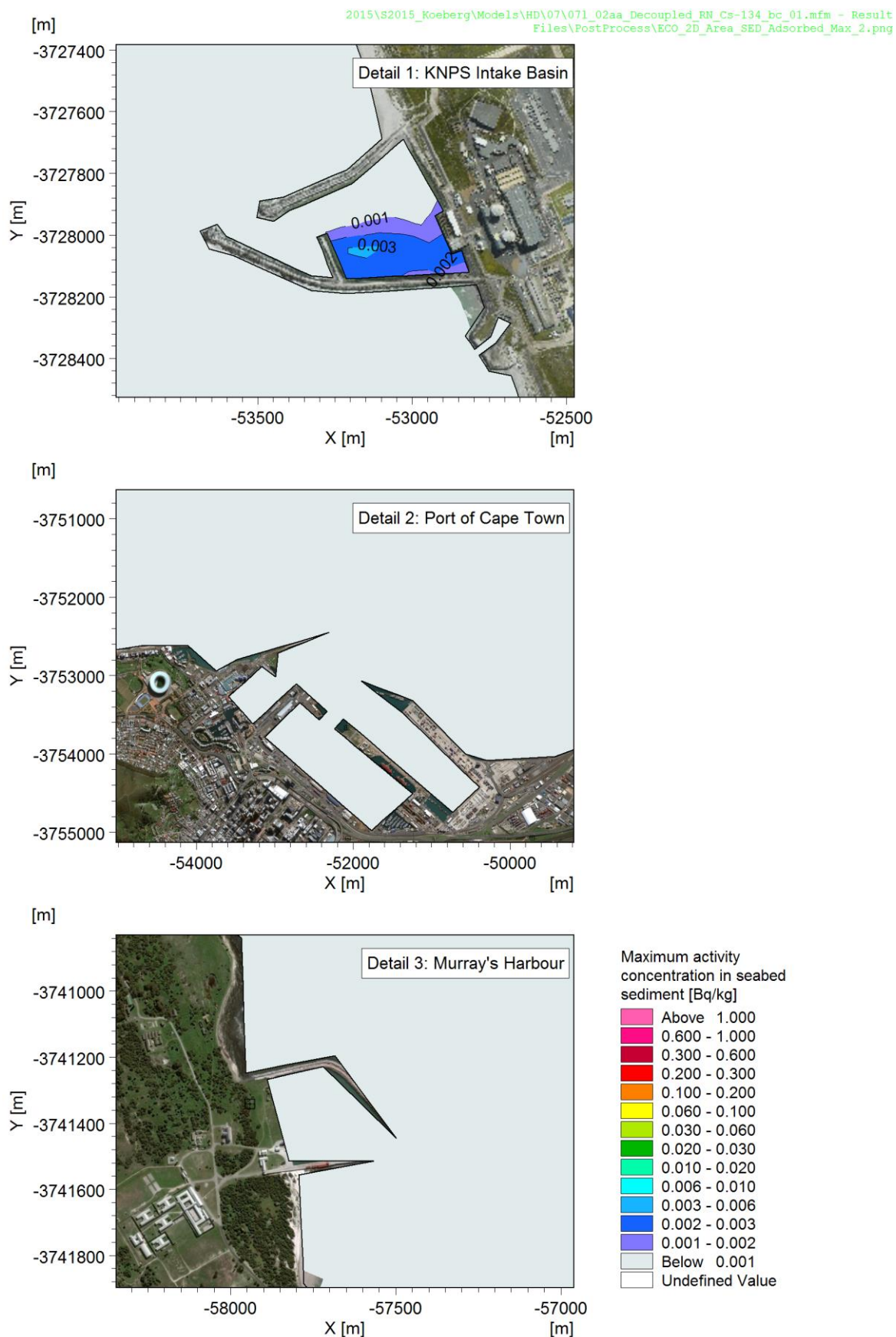
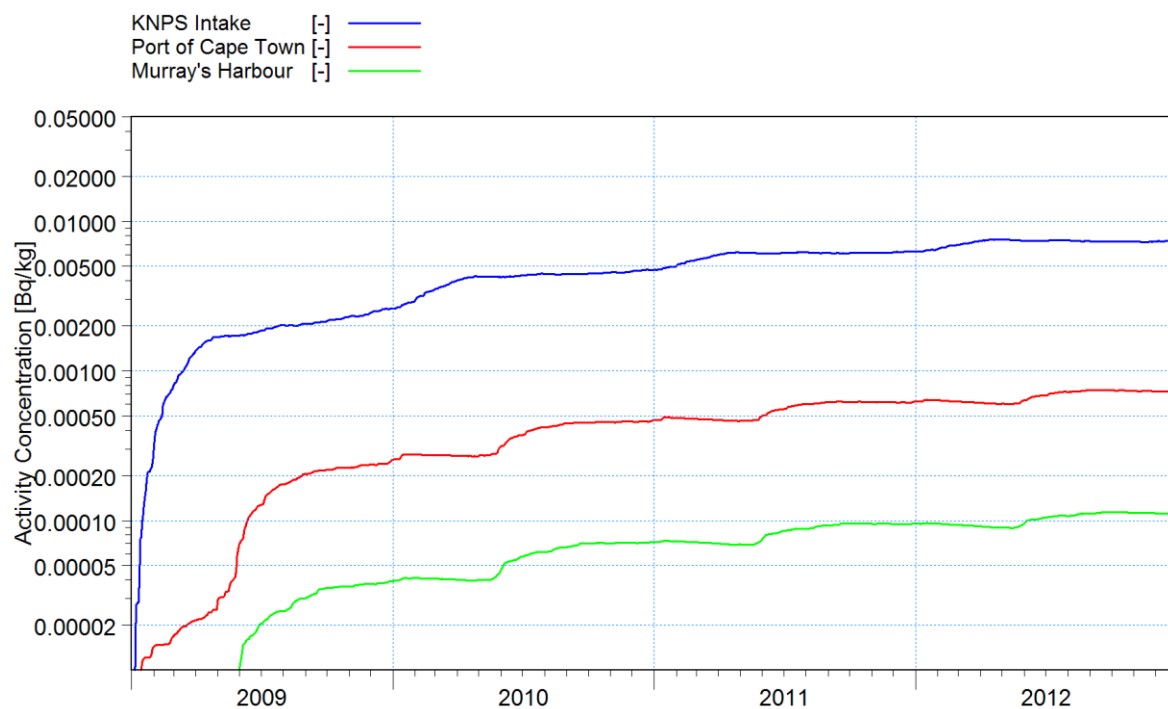


Figure C-27: Maximum concentration of Cs-134 activity in seabed sediment in one modelled year: detail of depo-centres.



2015\S2015_Koeberg\Models\HD\07\071_02aa_Decoupled_RN\TS-Cs-134.png

Figure C-28: Time series of concentration of Cs-134 activity in the seabed sediment at the three depocentres. For comparative purposes, the concentration is plotted on a logarithmic scale.

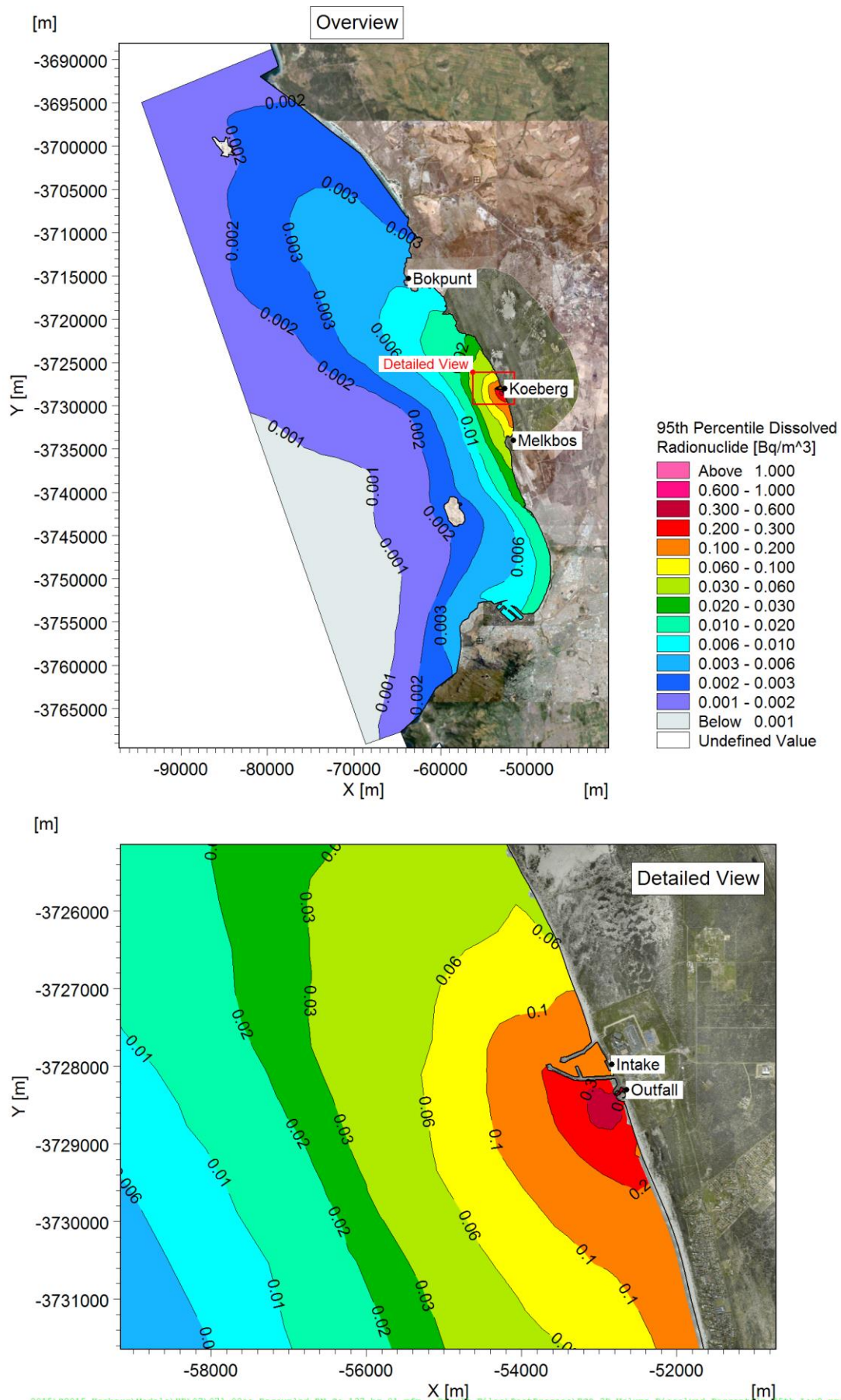


Figure C-29: 95th percentile concentration of dissolved Cs-137 activity in the water column: near-surface.

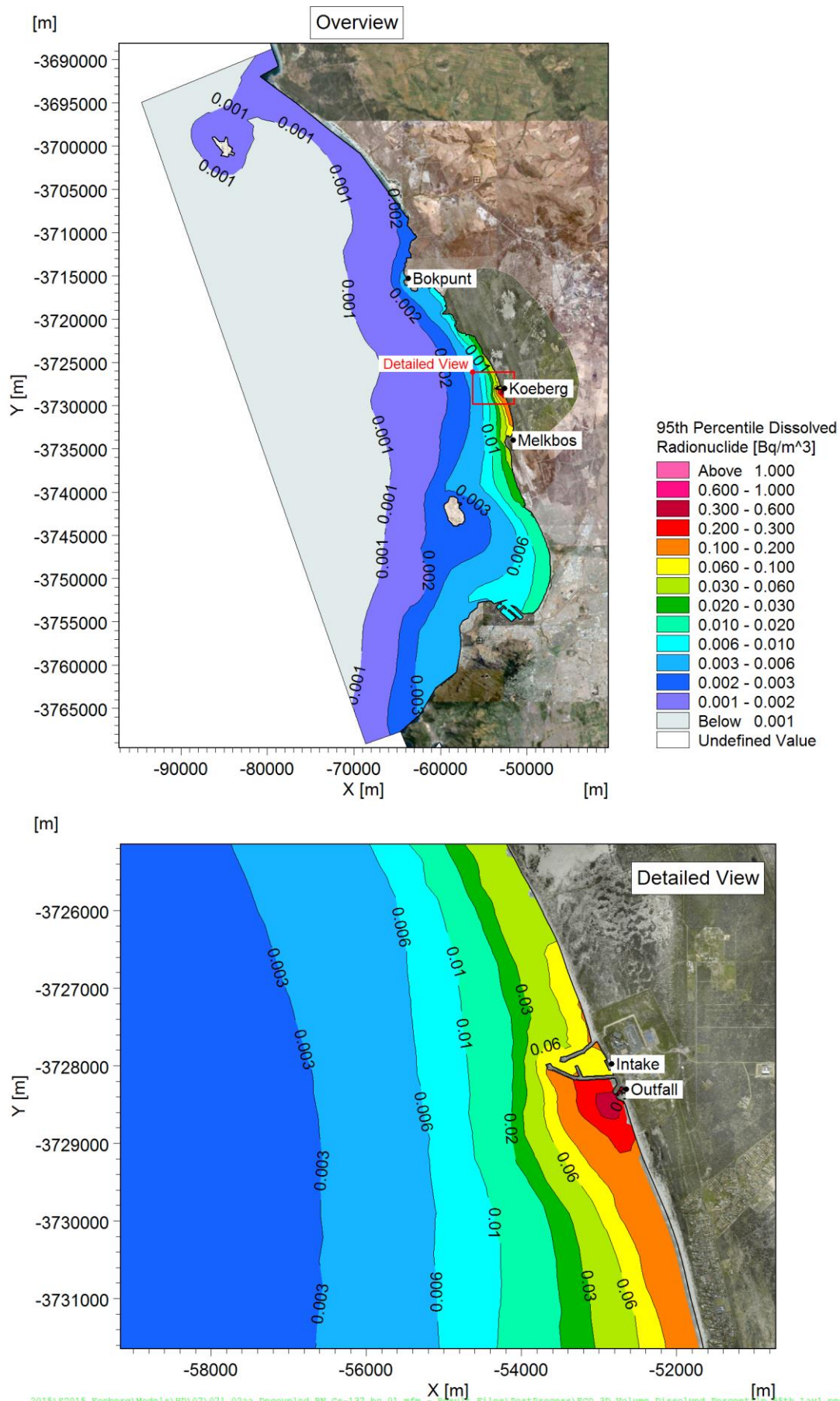


Figure C-30: 95th percentile concentration of dissolved Cs-137 activity in the water column: near-seabed.

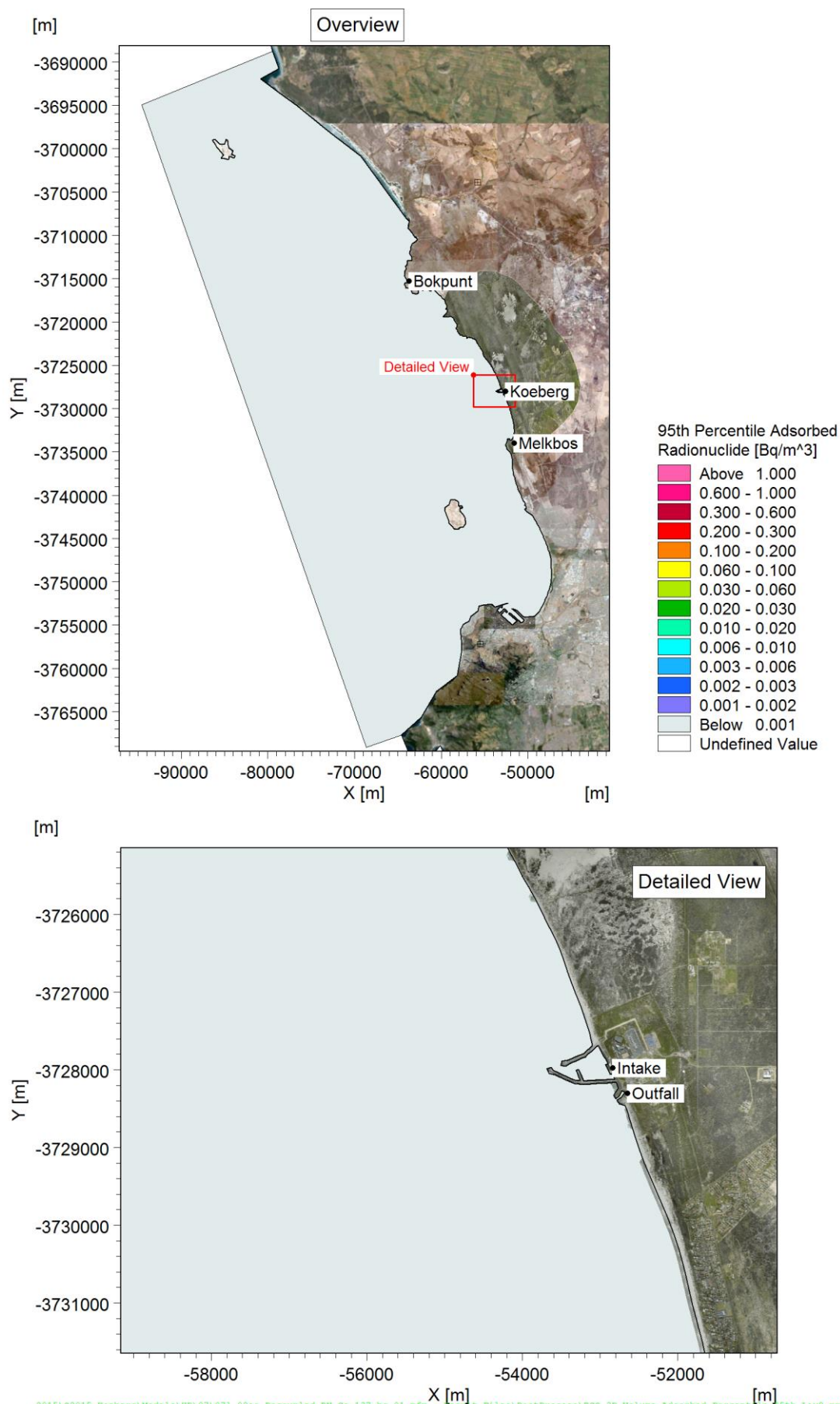


Figure C-31: 95th percentile concentration of adsorbed Cs-137 activity in the water column: near-surface.

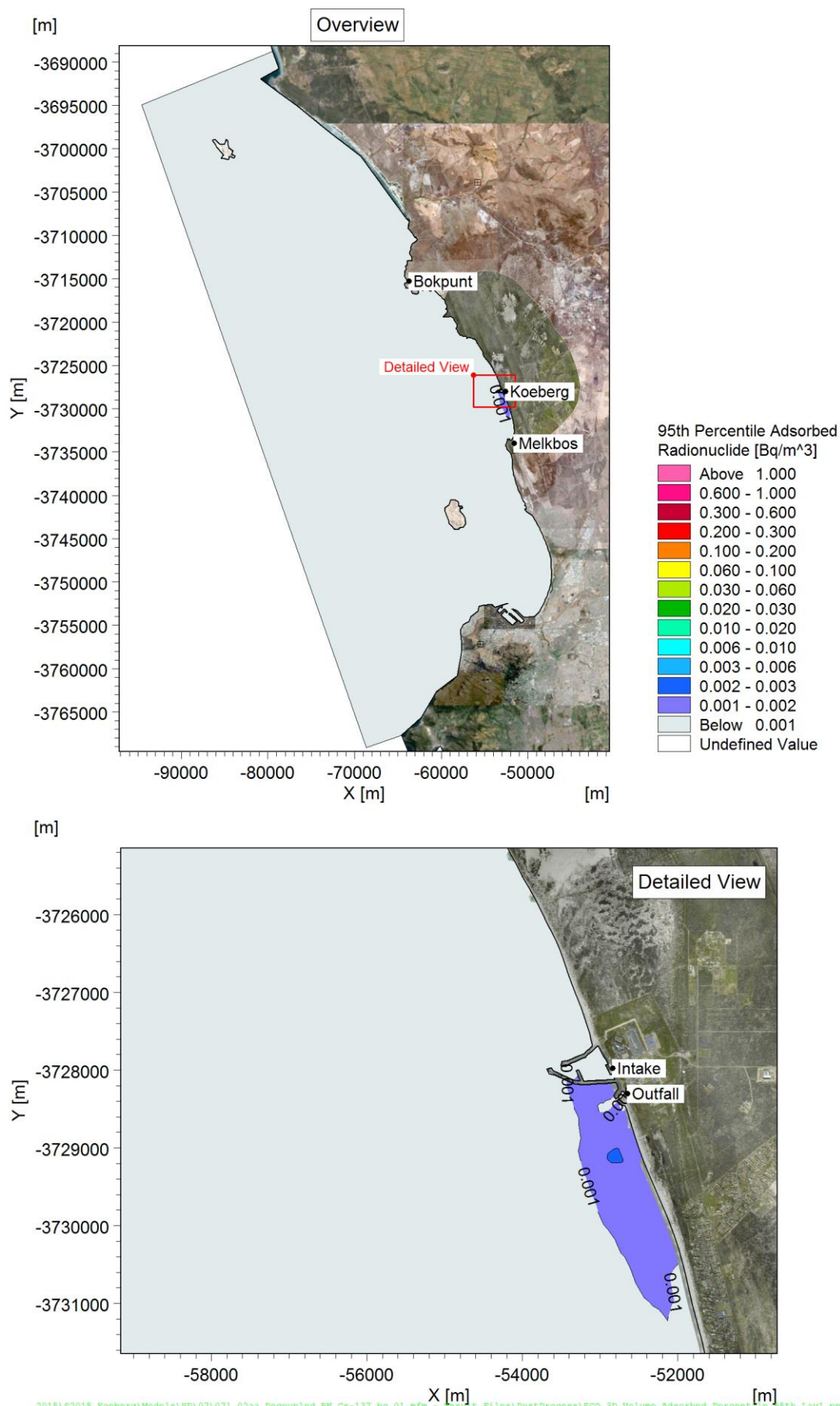


Figure C-32: 95th percentile concentration of adsorbed Cs-137 activity in the water column: near-seabed.

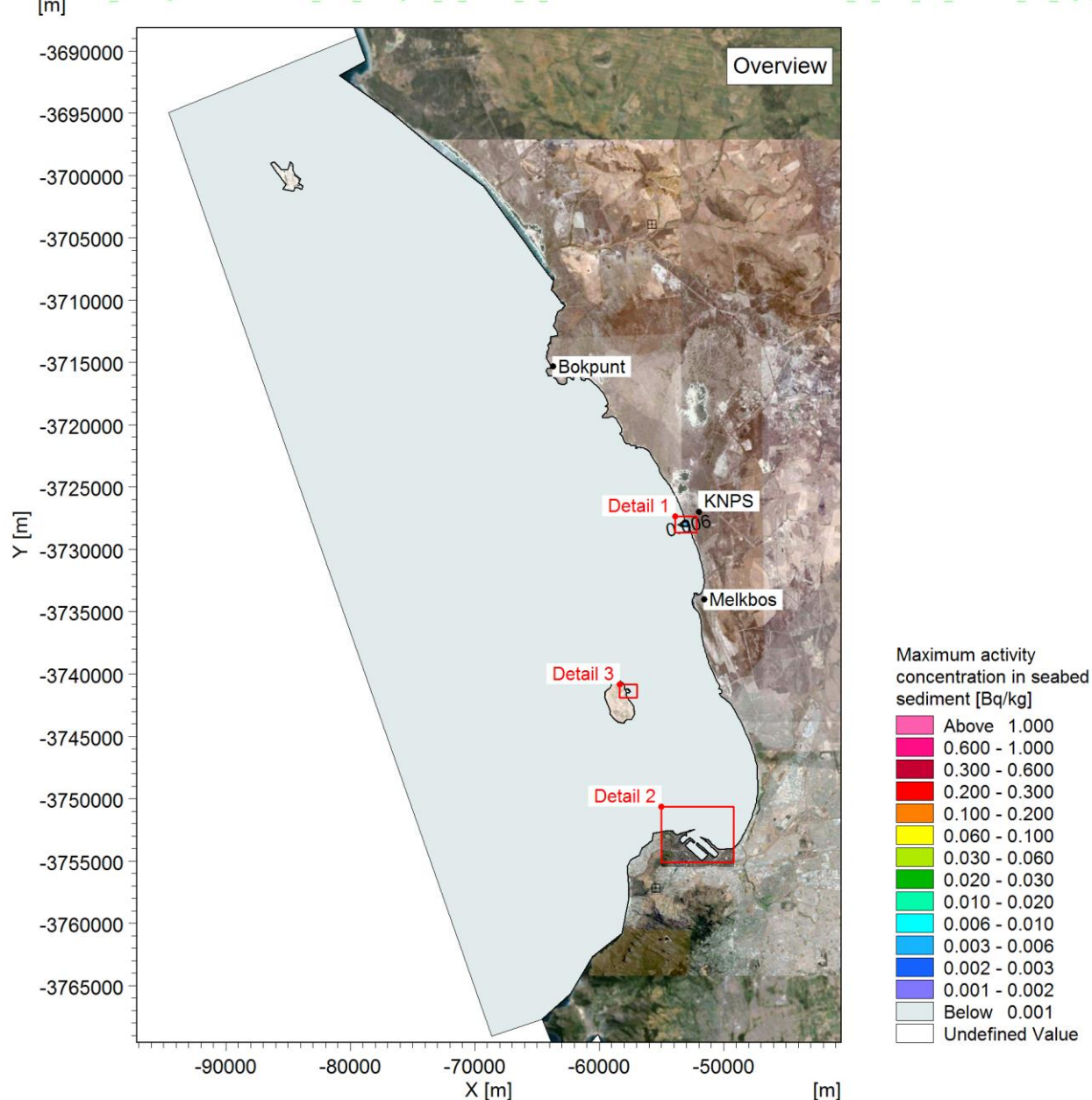


Figure C-33: Maximum concentration of Cs-137 activity in seabed sediment in one modelled year: overview.

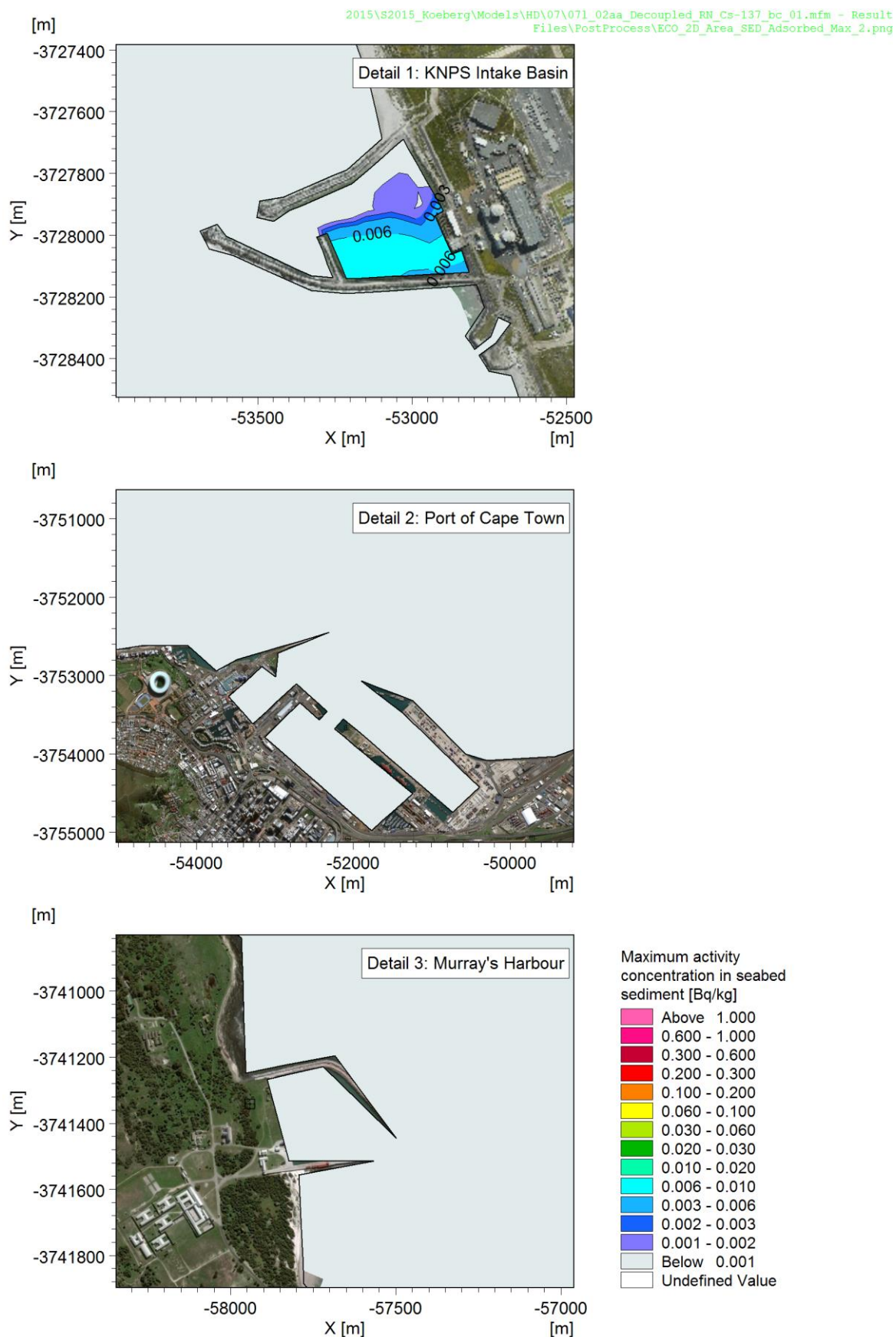
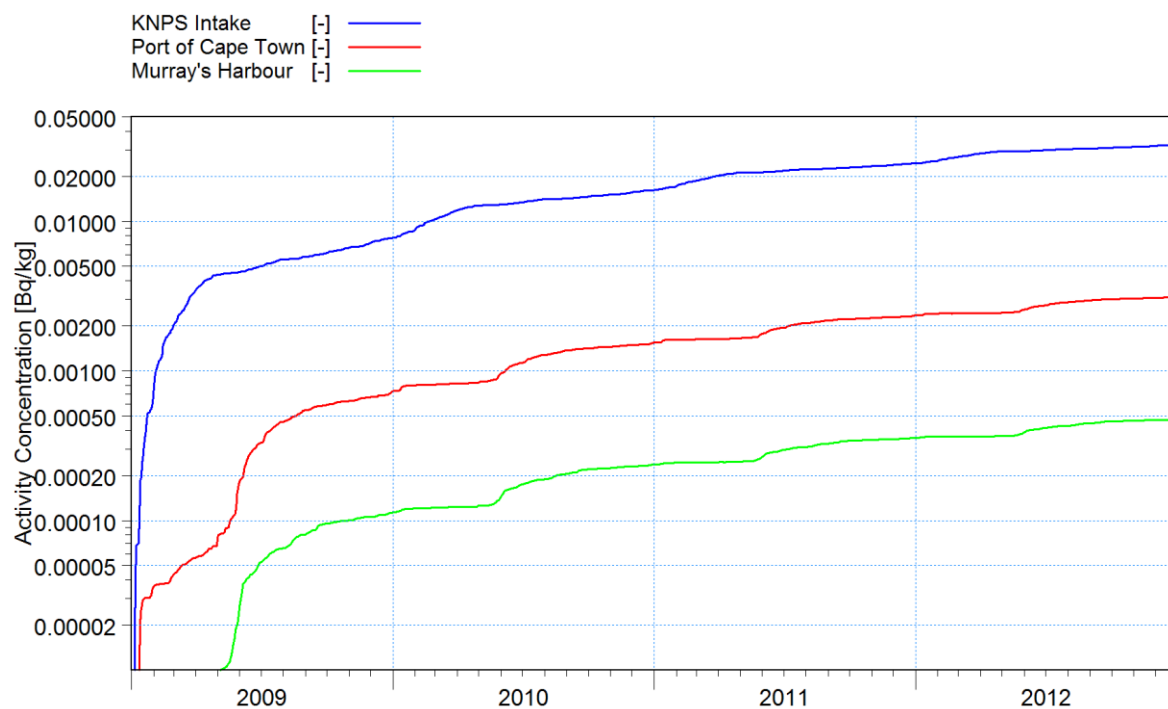


Figure C-34: Maximum concentration of Cs-137 activity in seabed sediment in one modelled year: detail of depo-centres.



2015\S2015_Koeberg\Models\HD\07\071_02aa_Decoupled_RN\TS-Cs-137.png

Figure C-35: Time series of concentration of Cs-137 activity in the seabed sediment at the three depositories. For comparative purposes, the concentration is plotted on a logarithmic scale.

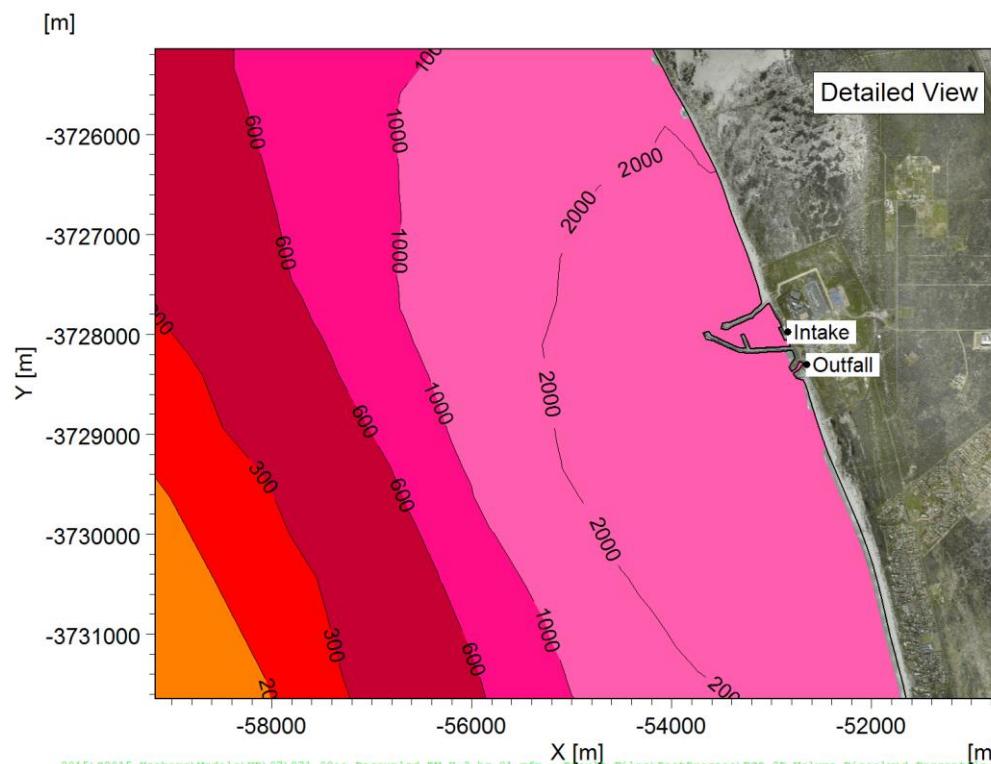
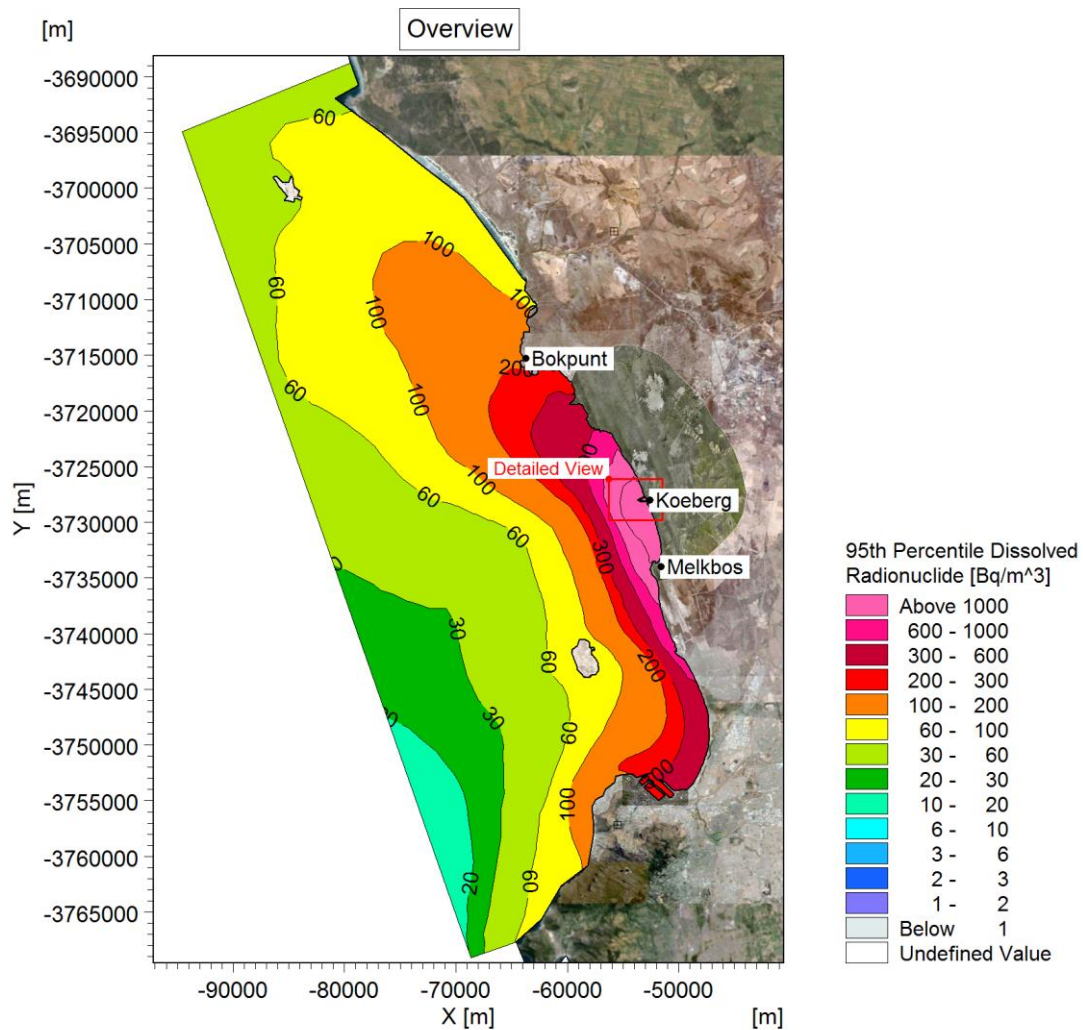


Figure C-36: 95th percentile concentration of dissolved H-3 activity in the water column: near-surface.

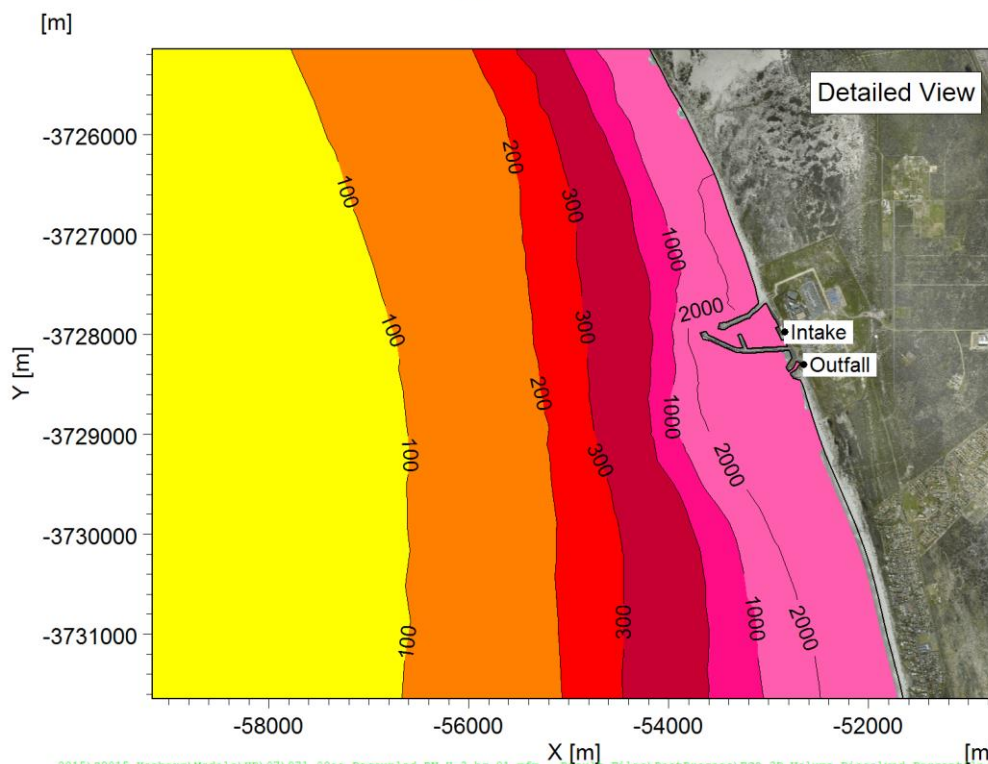
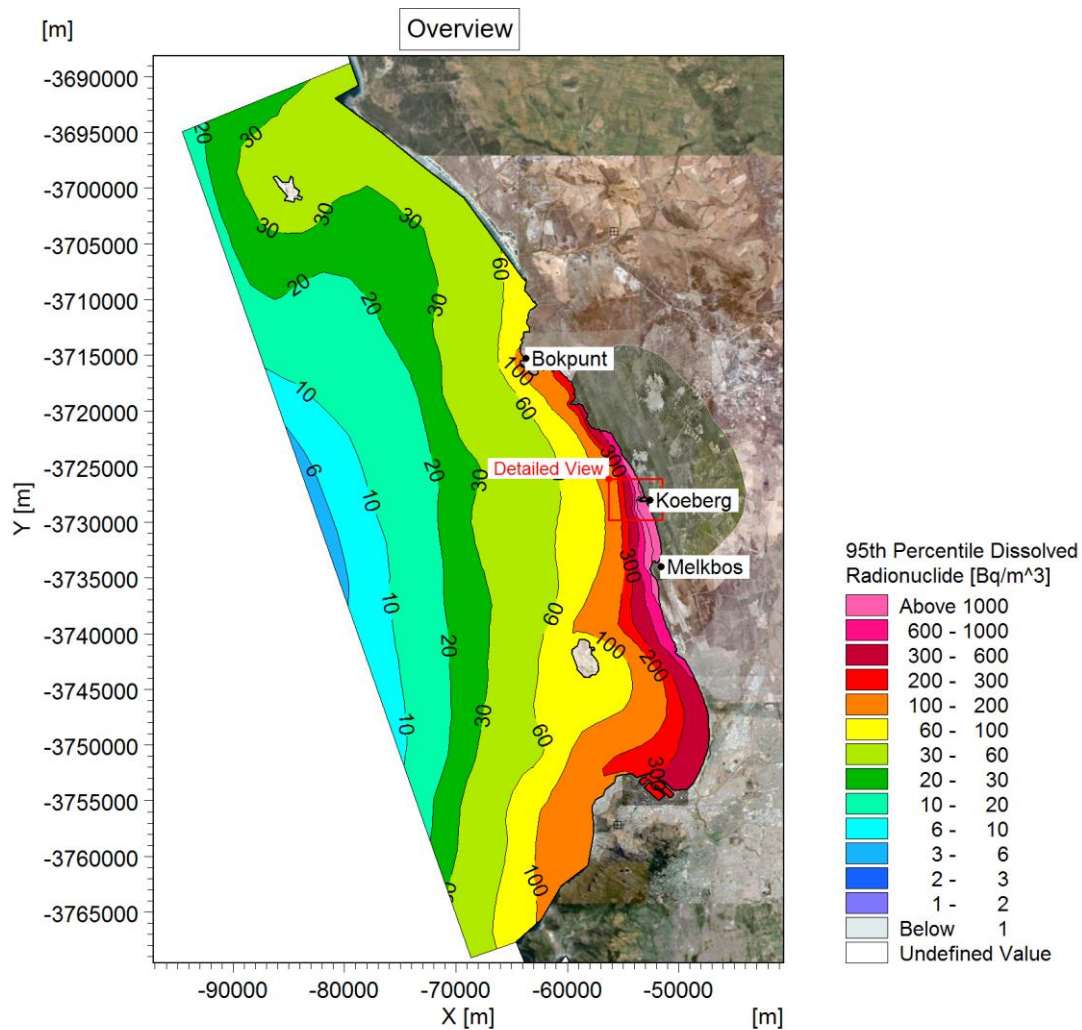


Figure C-37: 95th percentile concentration of dissolved H-3 activity in the water column: near-seabed.

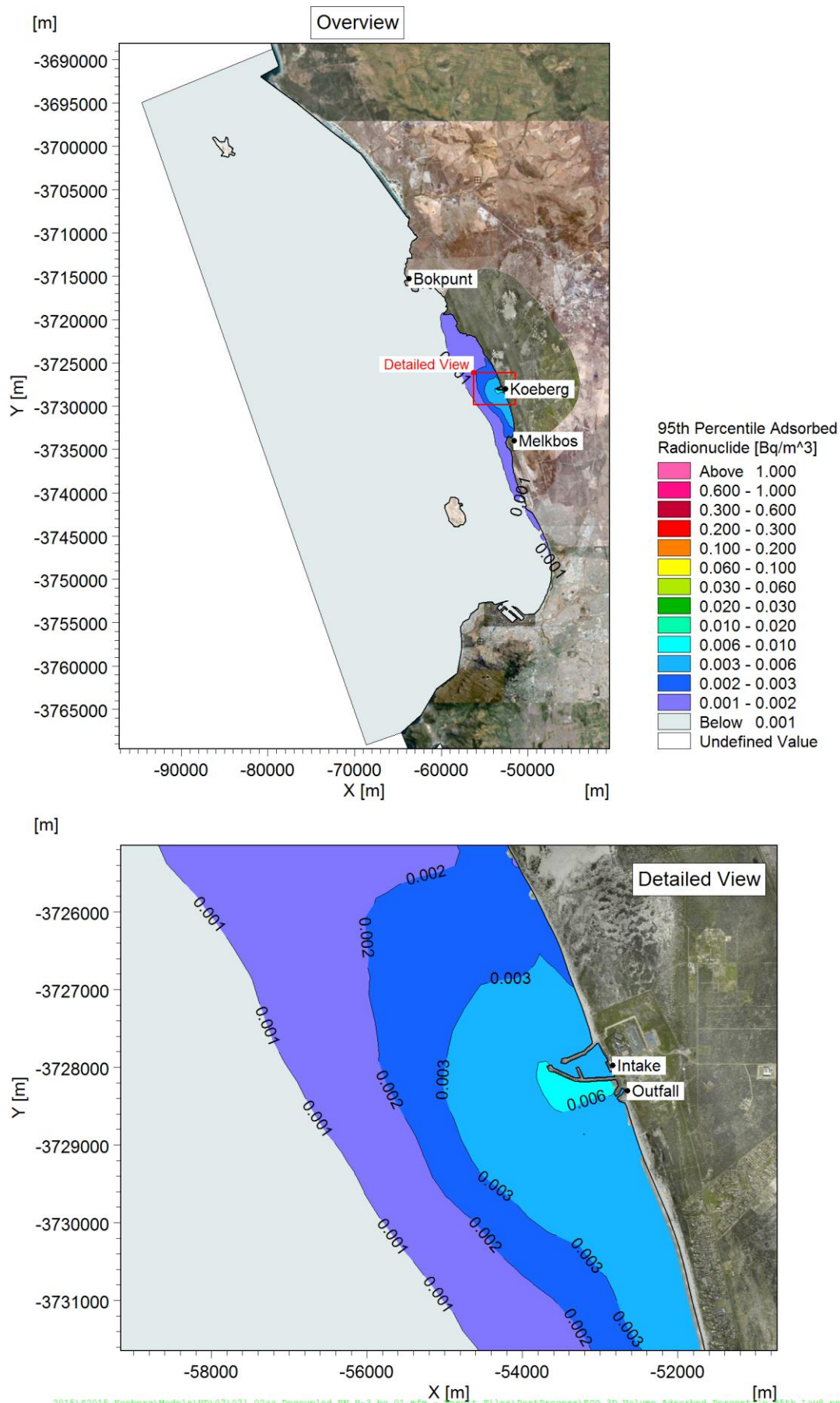


Figure C-38: 95th percentile concentration of adsorbed H-3 activity in the water column: near-surface.

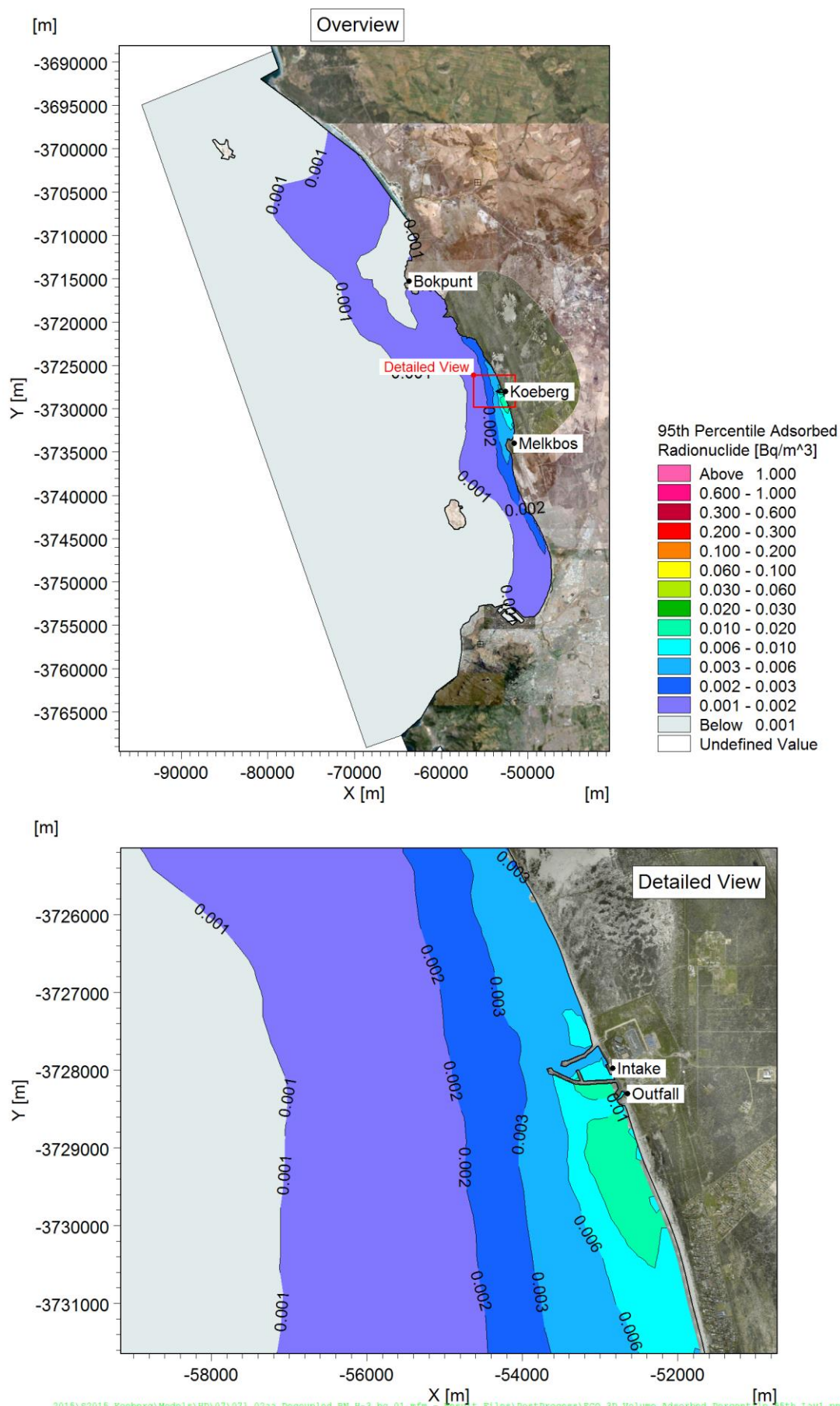


Figure C-39: 95th percentile concentration of adsorbed H-3 activity in the water column: near-seabed.

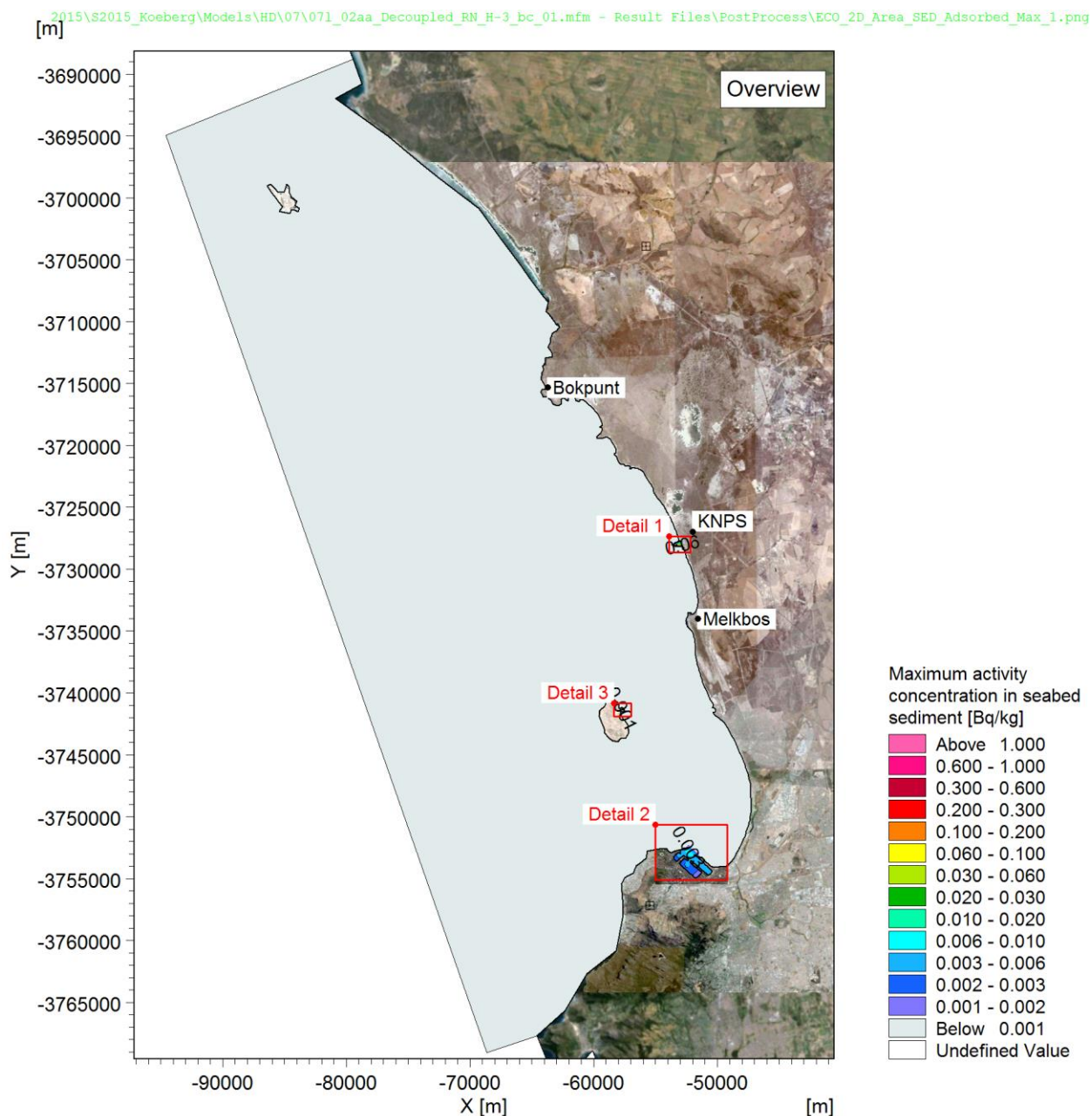


Figure C-40: Maximum concentration of H-3 activity in seabed sediment in one modelled year: overview.

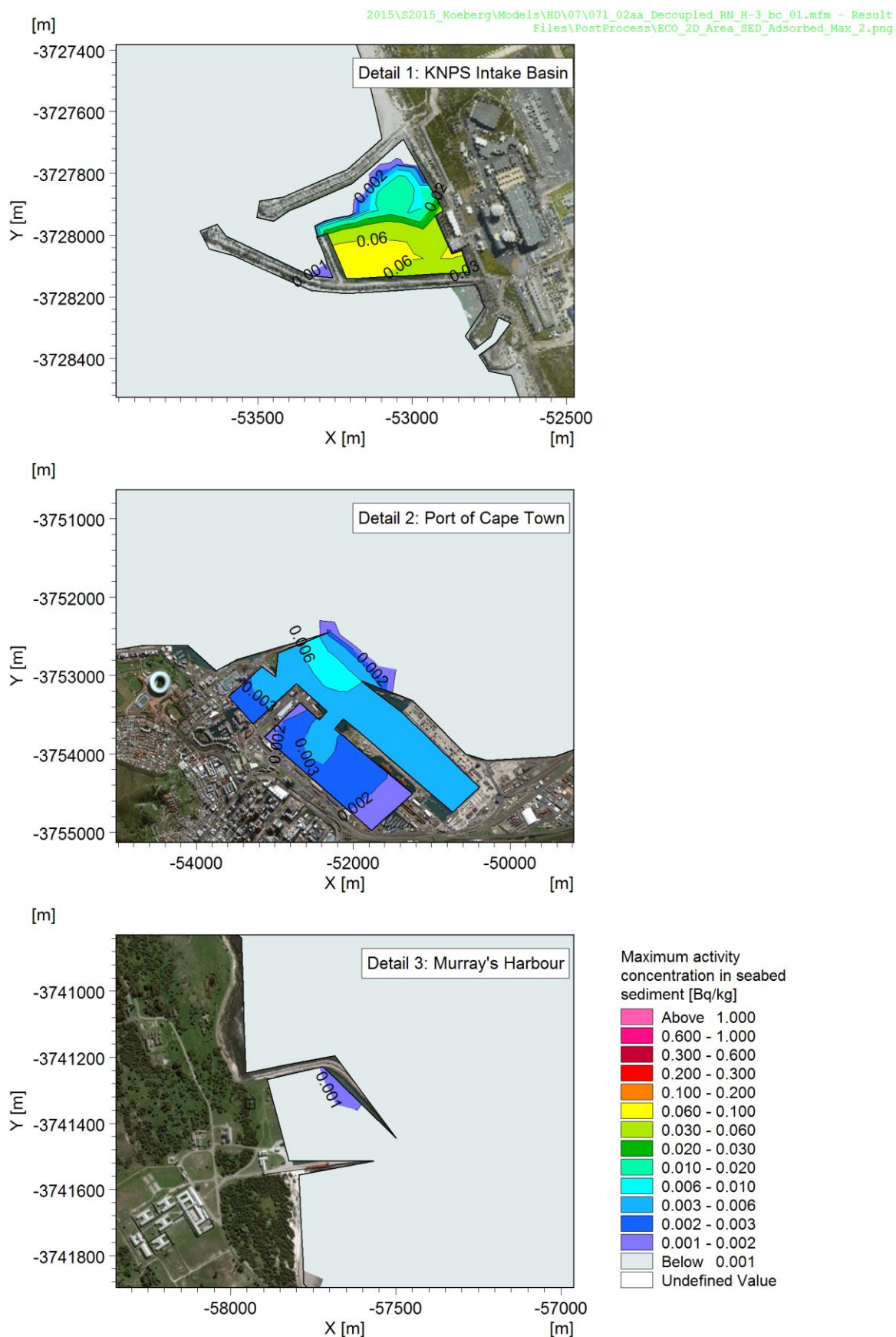


Figure C-41: Maximum concentration of H-3 activity in seabed sediment in one modelled year: detail of depo-centres.

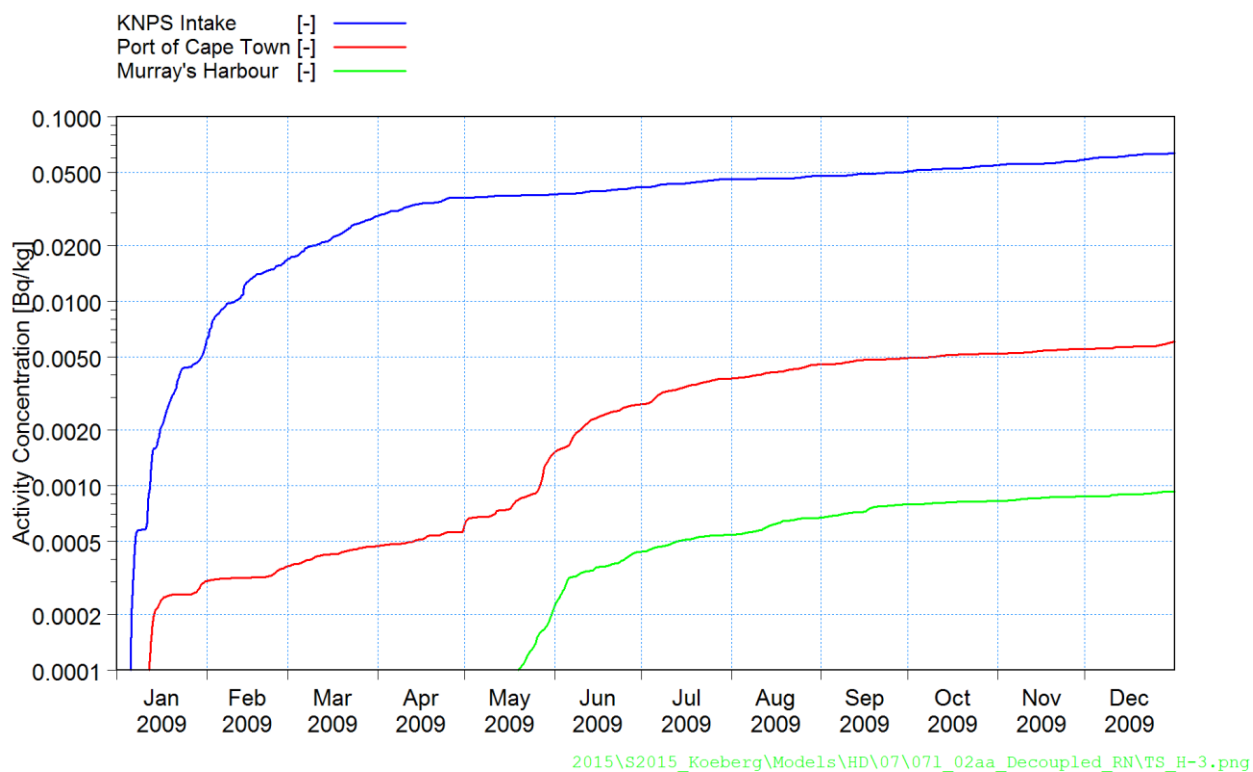


Figure C-42: Time series of concentration of H-3 activity in the seabed sediment at the three depo-centres. For comparative purposes, the concentration is plotted on a logarithmic scale.

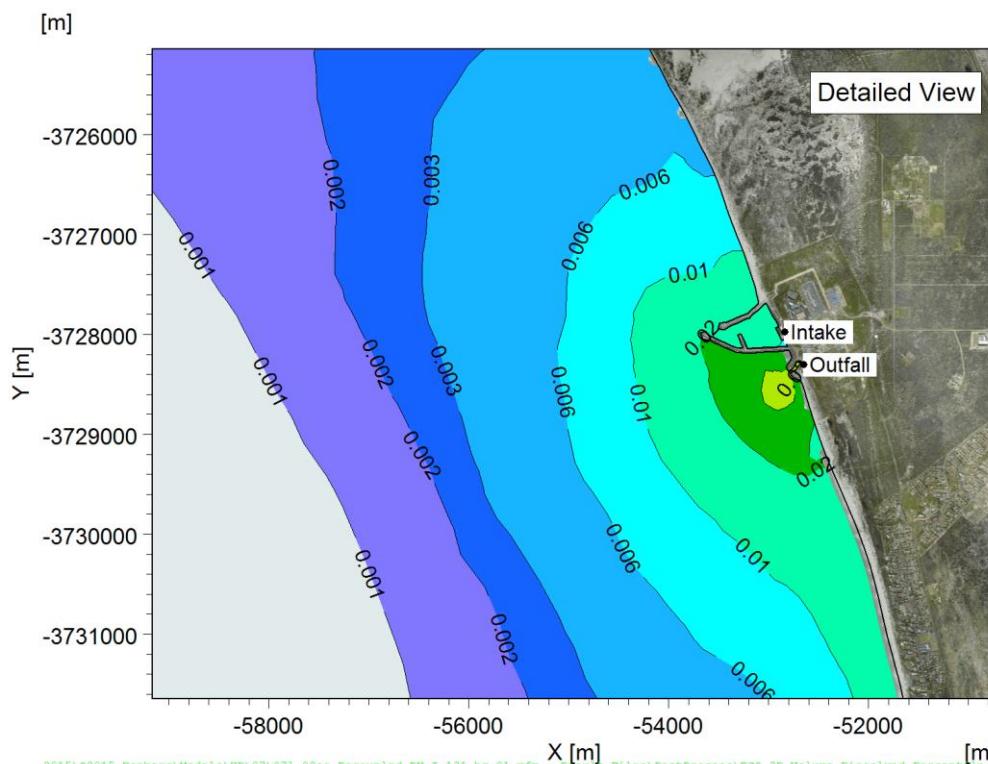
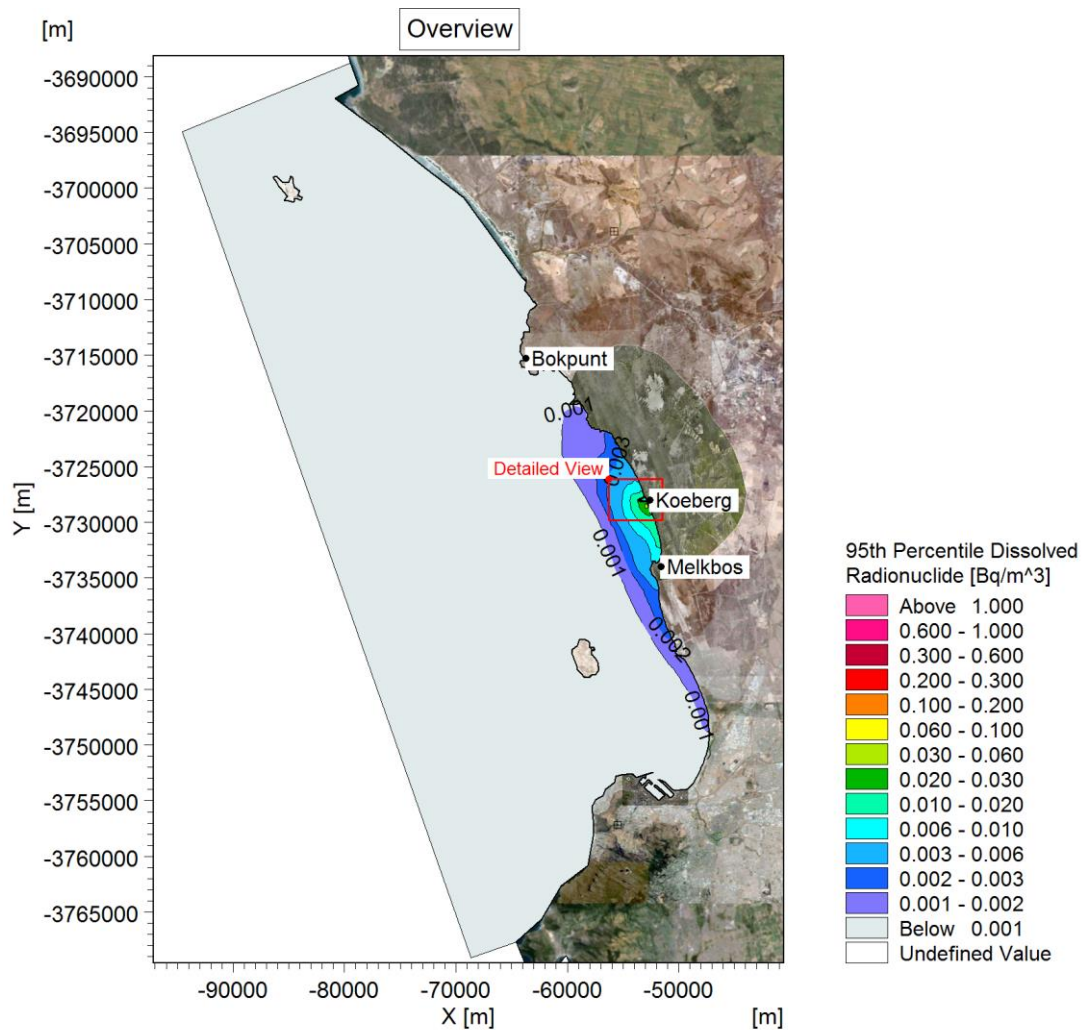


Figure C-43: 95th percentile concentration of dissolved I-131 activity in the water column: near-surface.

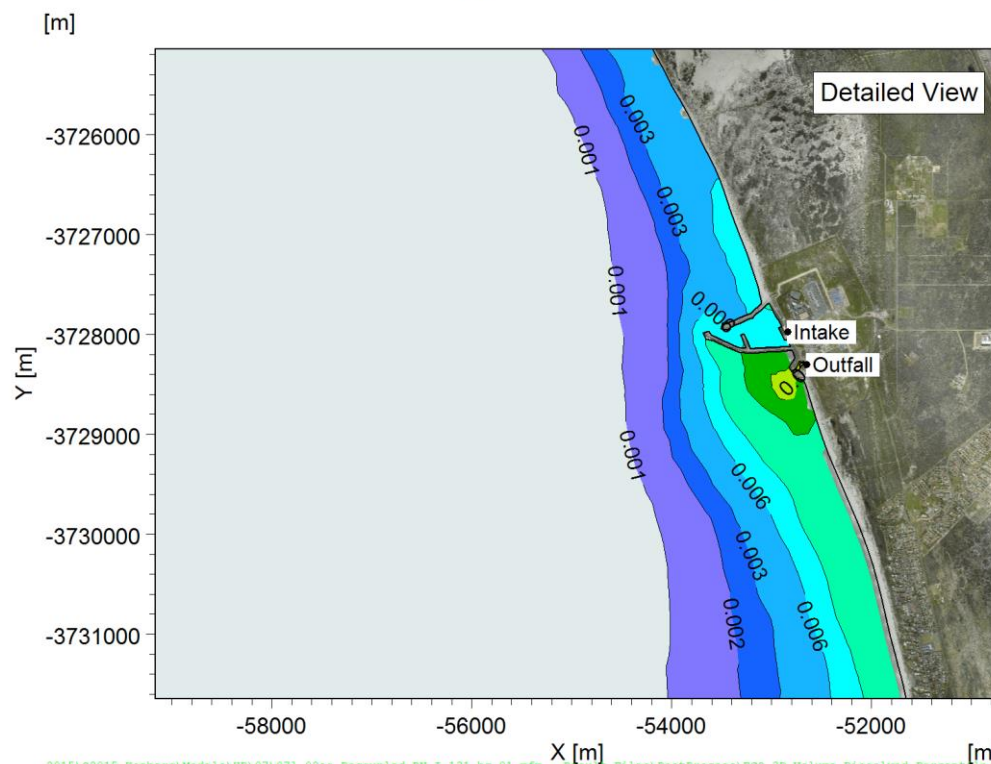
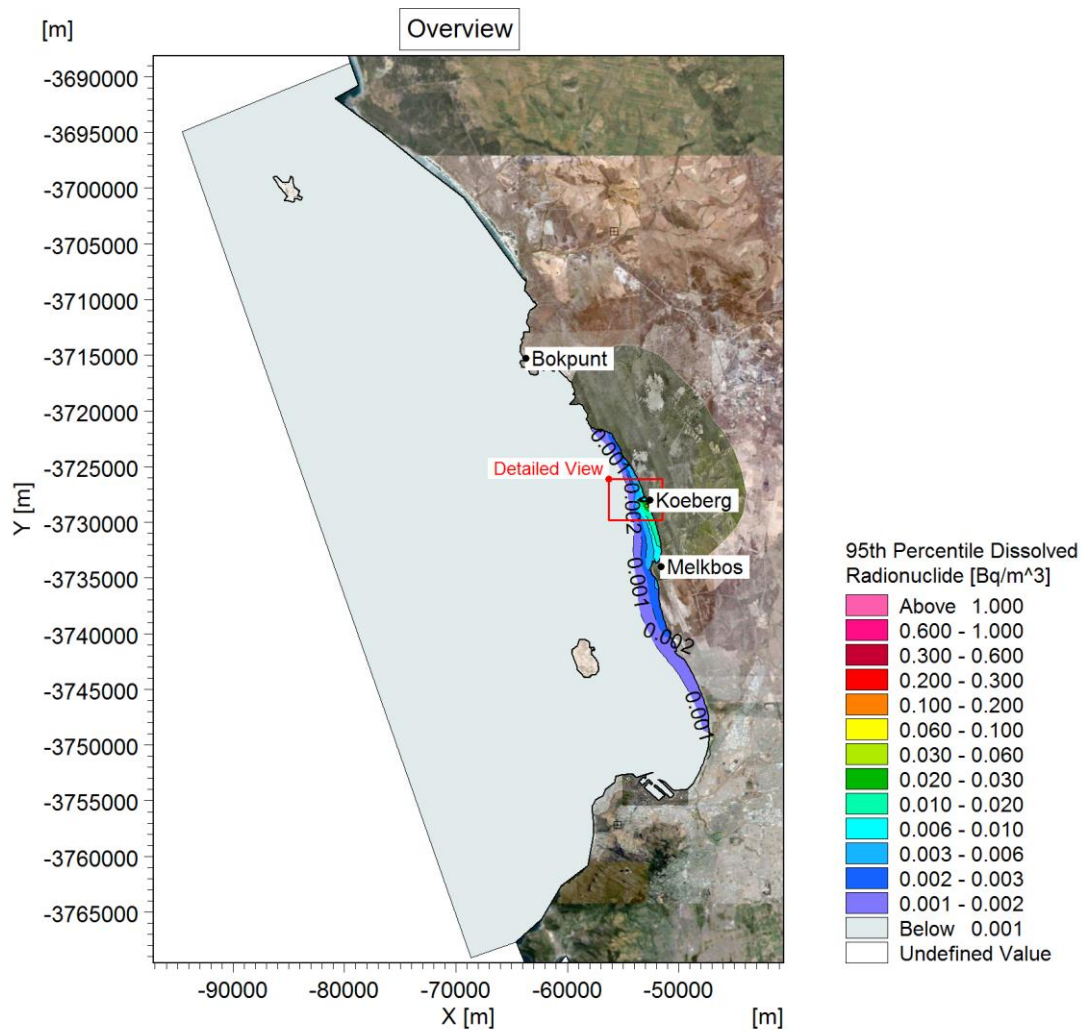


Figure C-44: 95th percentile concentration of dissolved I-131 activity in the water column: near-seabed.

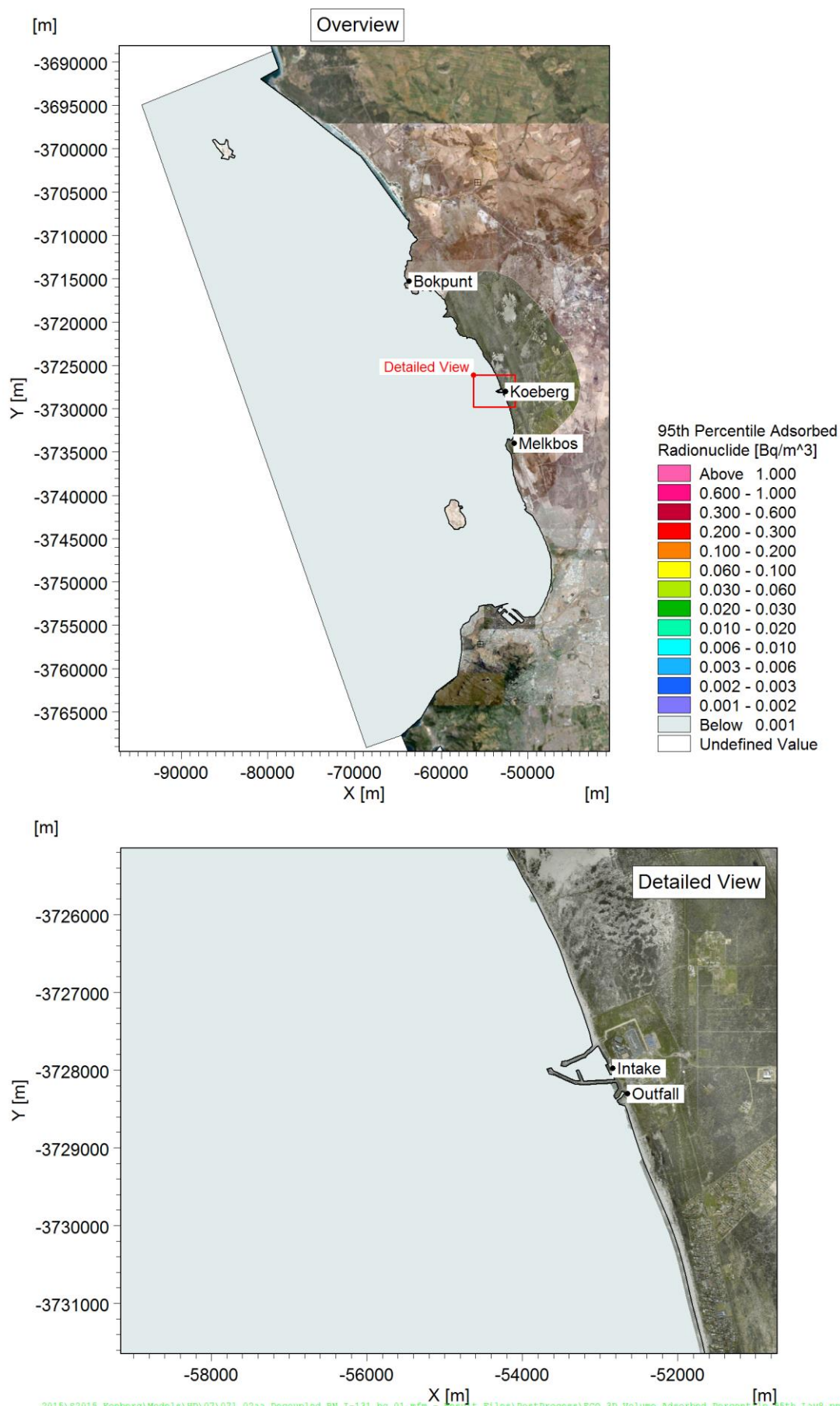


Figure C-45: 95th percentile concentration of adsorbed I-131 activity in the water column: near-surface.

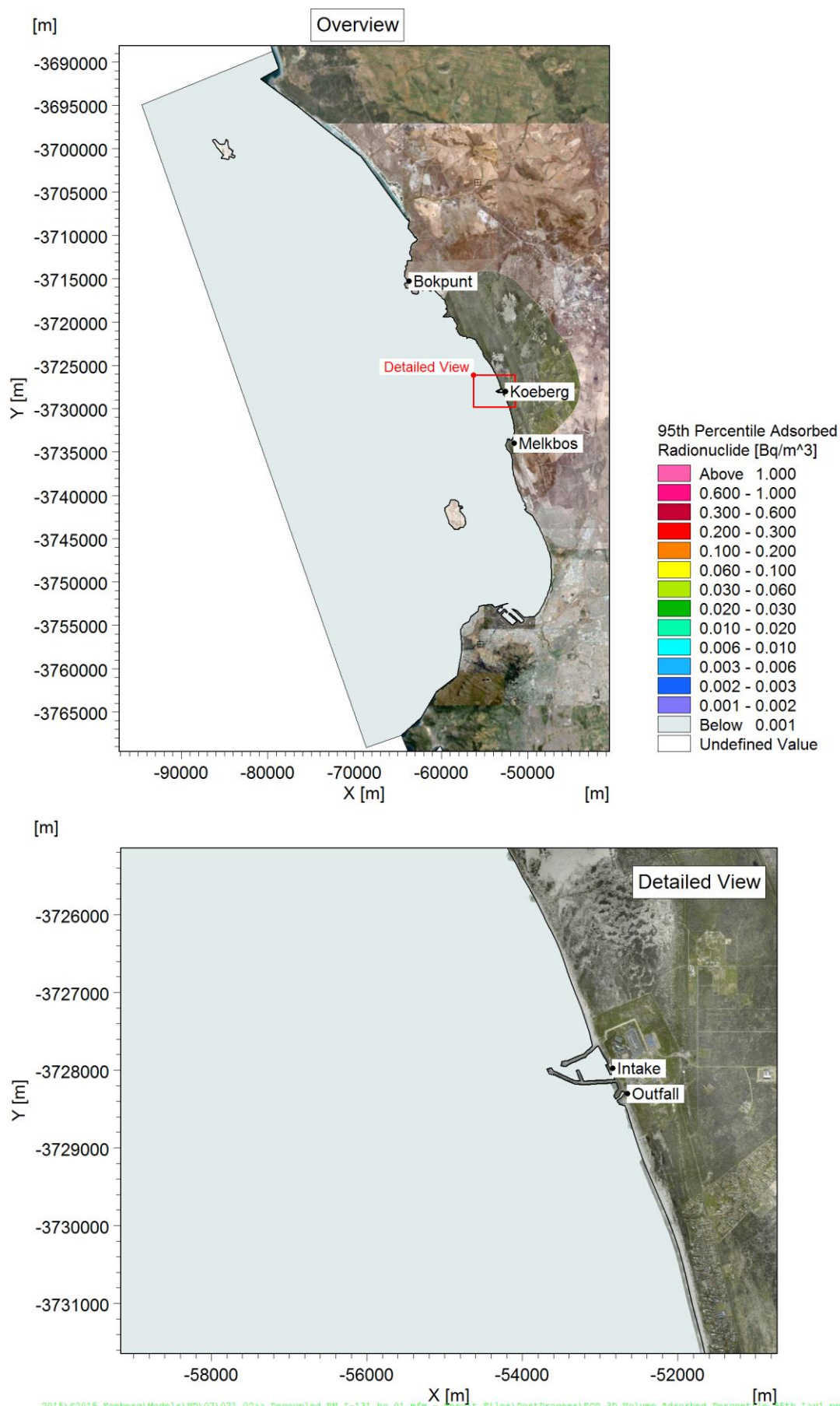


Figure C-46: 95th percentile concentration of adsorbed I-131 activity in the water column: near-seabed.

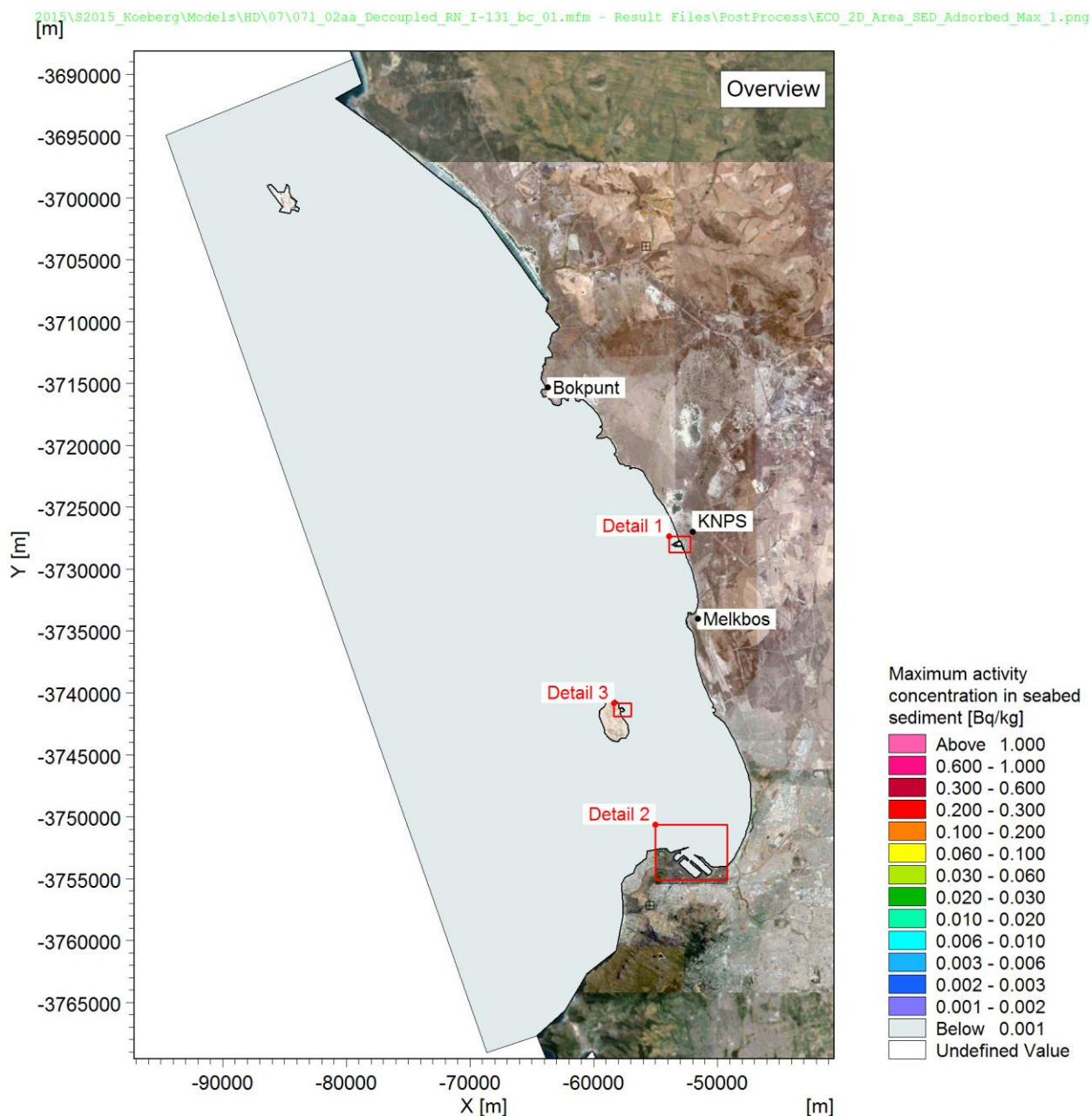


Figure C-47: Maximum concentration of I-131 activity in seabed sediment in one modelled year: overview.

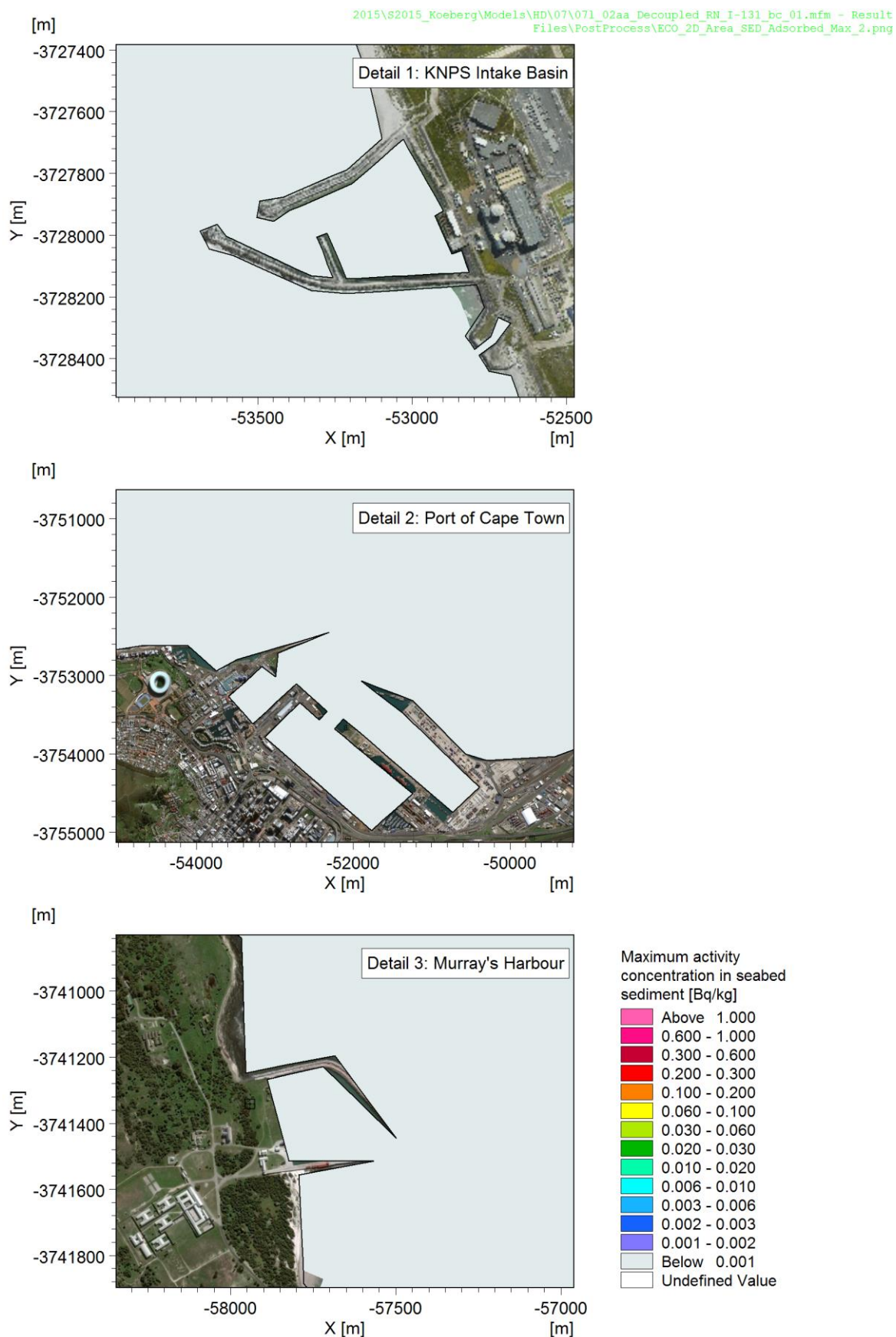


Figure C-48: Maximum concentration of I-131 activity in seabed sediment in one modelled year: detail of depo-centres.

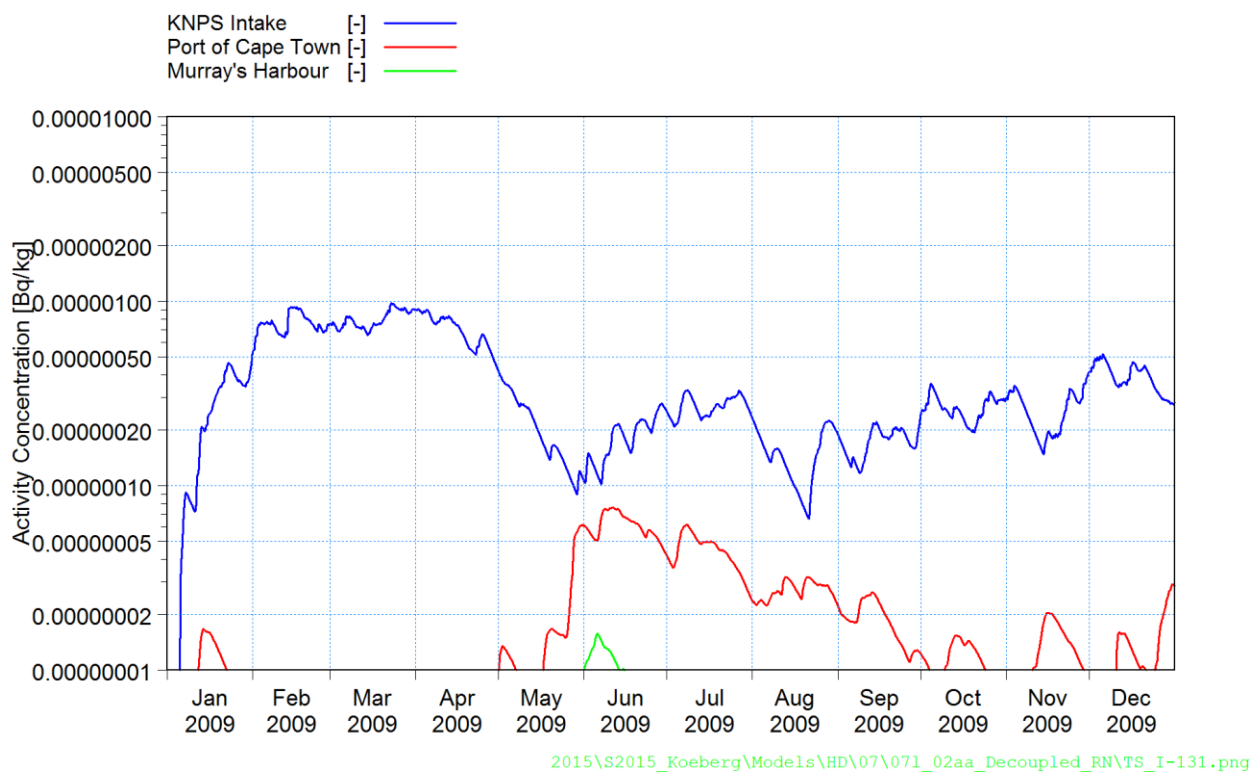


Figure C-49: Time series of concentration of I-131 activity in the seabed sediment at the three depocentres. For comparative purposes, the concentration is plotted on a logarithmic scale.

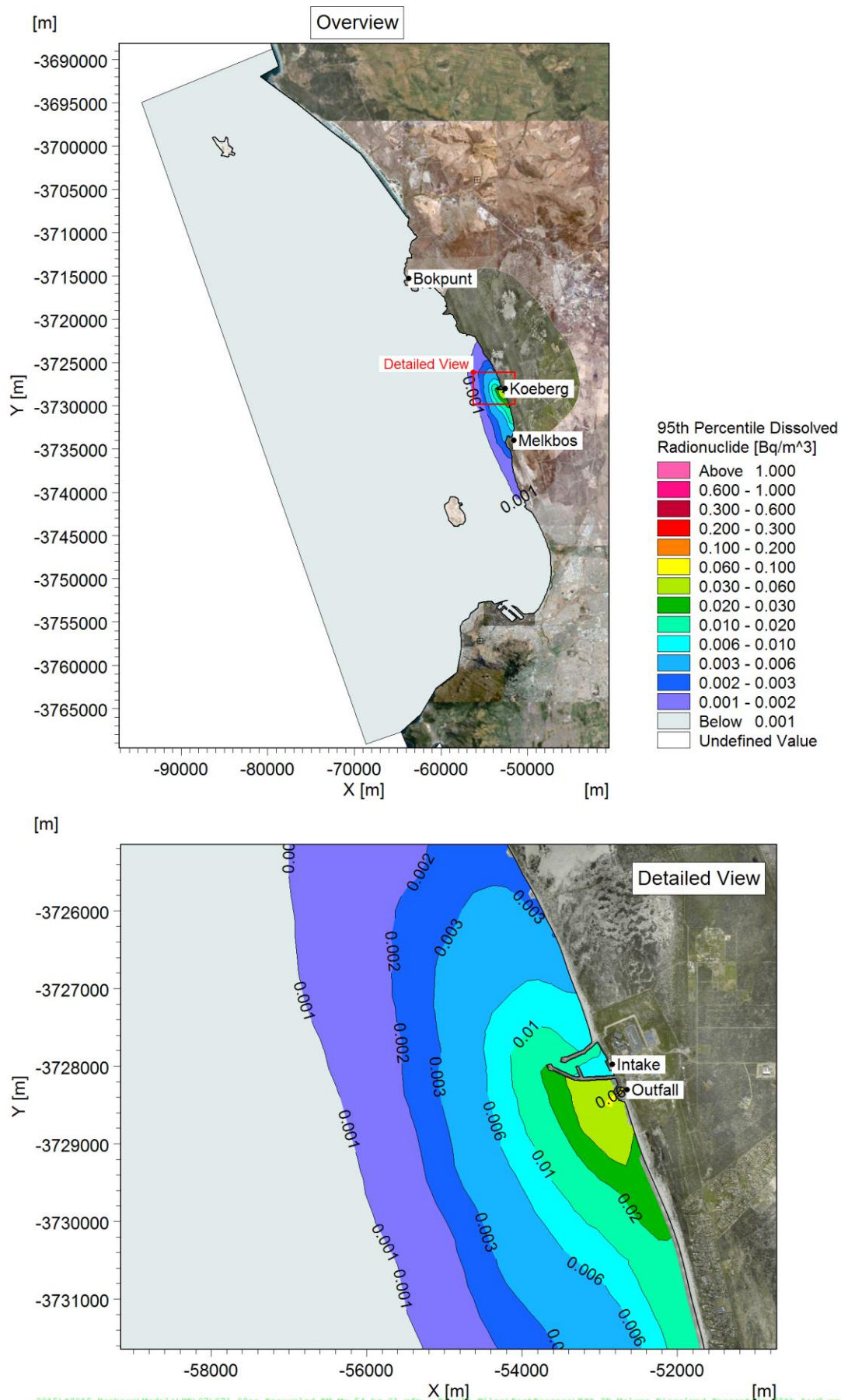


Figure C-50: 95th percentile concentration of dissolved Mn-54 activity in the water column: near-surface.

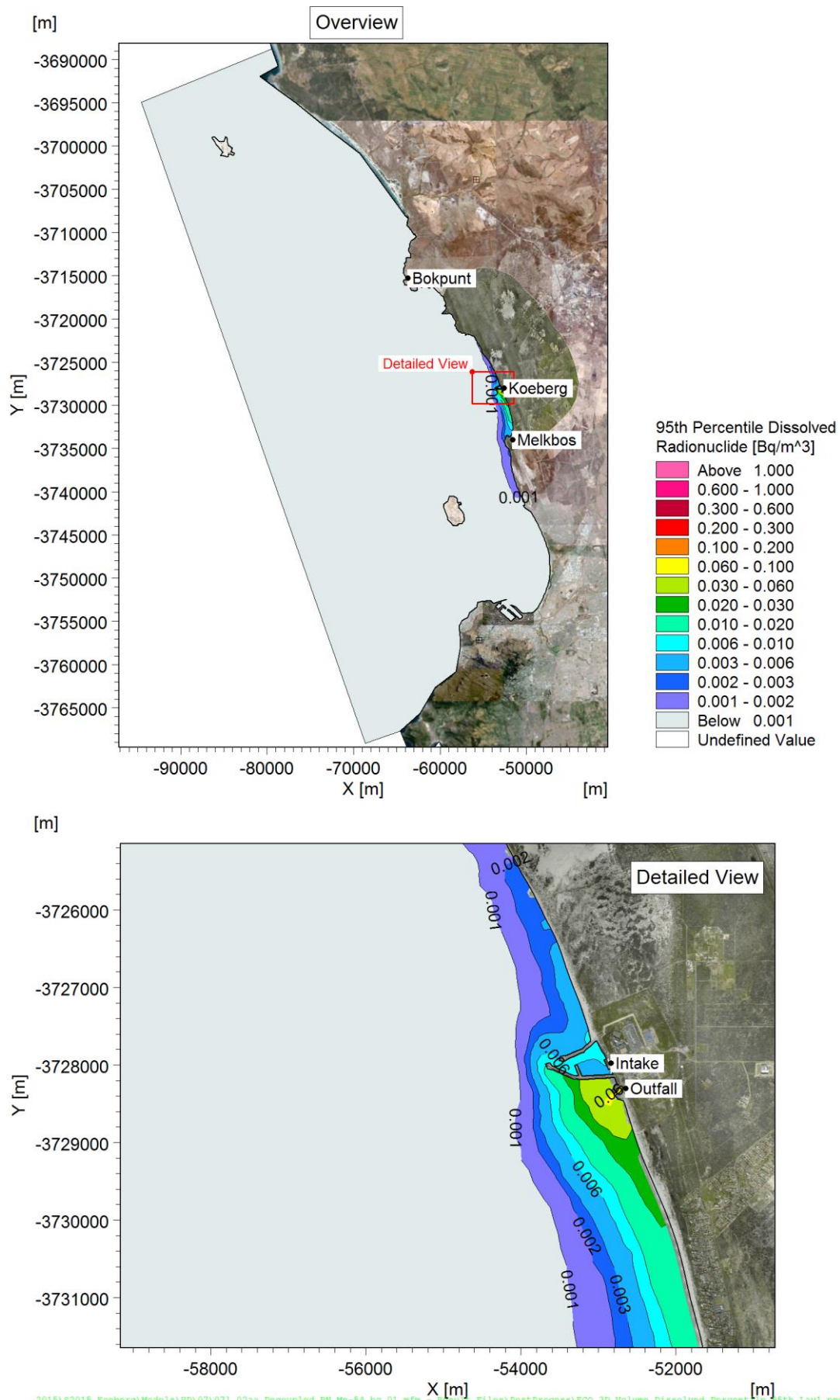


Figure C-51: 95th percentile concentration of dissolved Mn-54 activity in the water column: near-seabed.

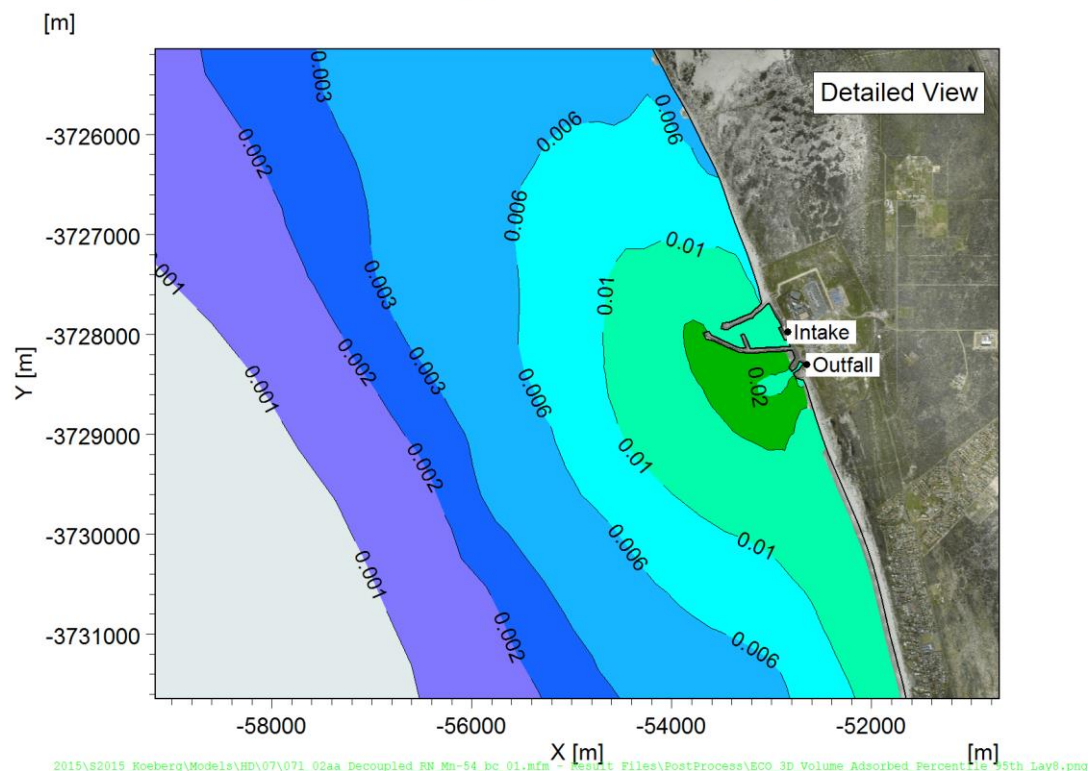
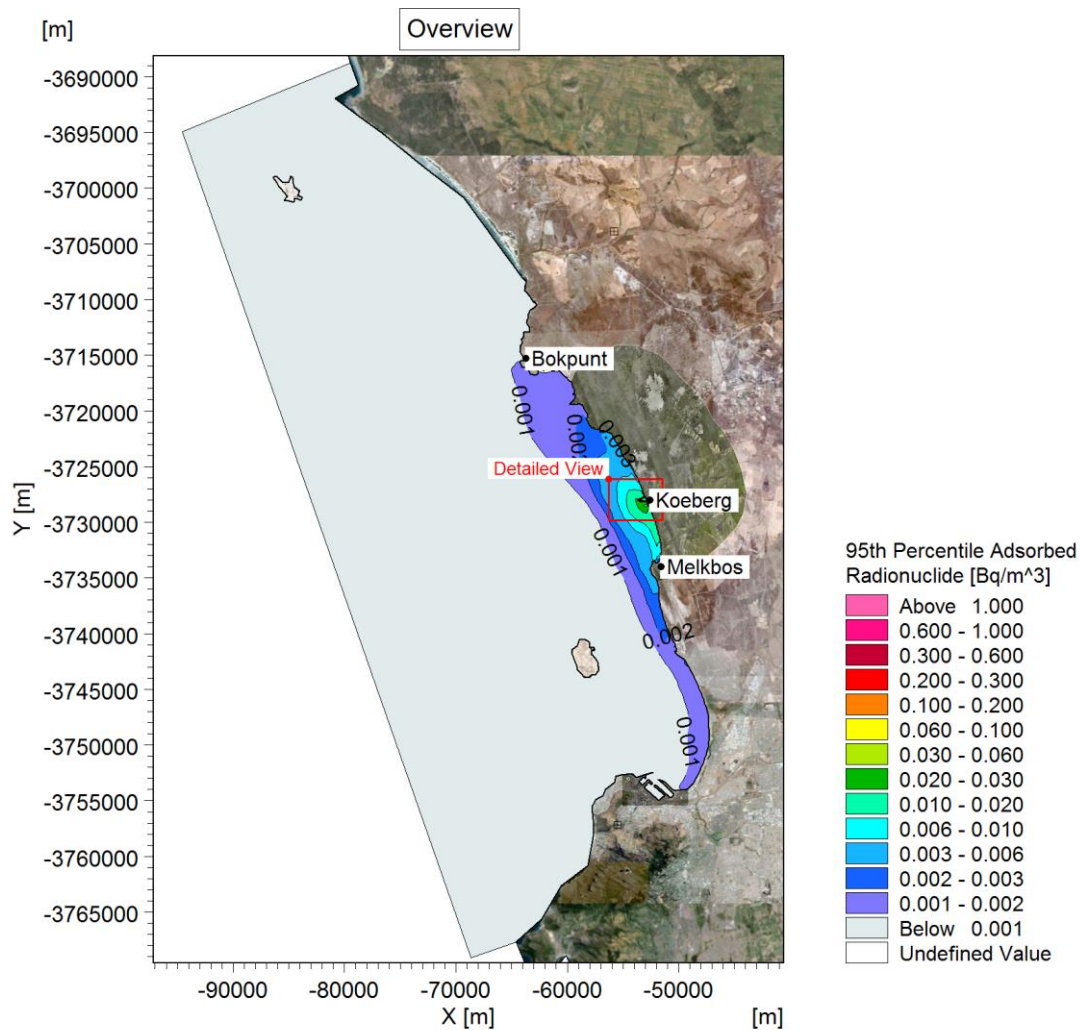


Figure C-52: 95th percentile concentration of adsorbed Mn-54 activity in the water column: near-surface.

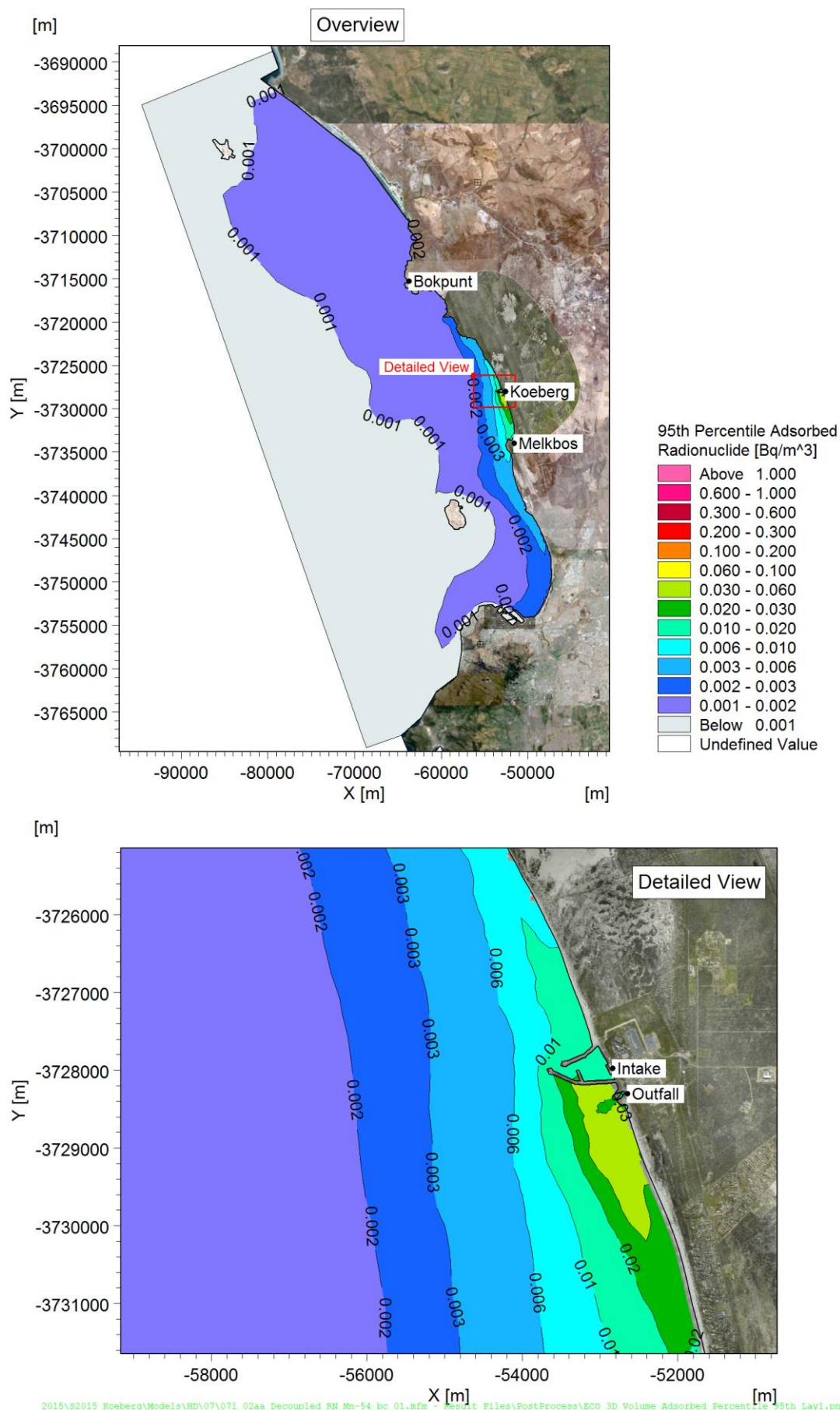


Figure C-53: 95th percentile concentration of adsorbed Mn-54 activity in the water column: near-seabed.

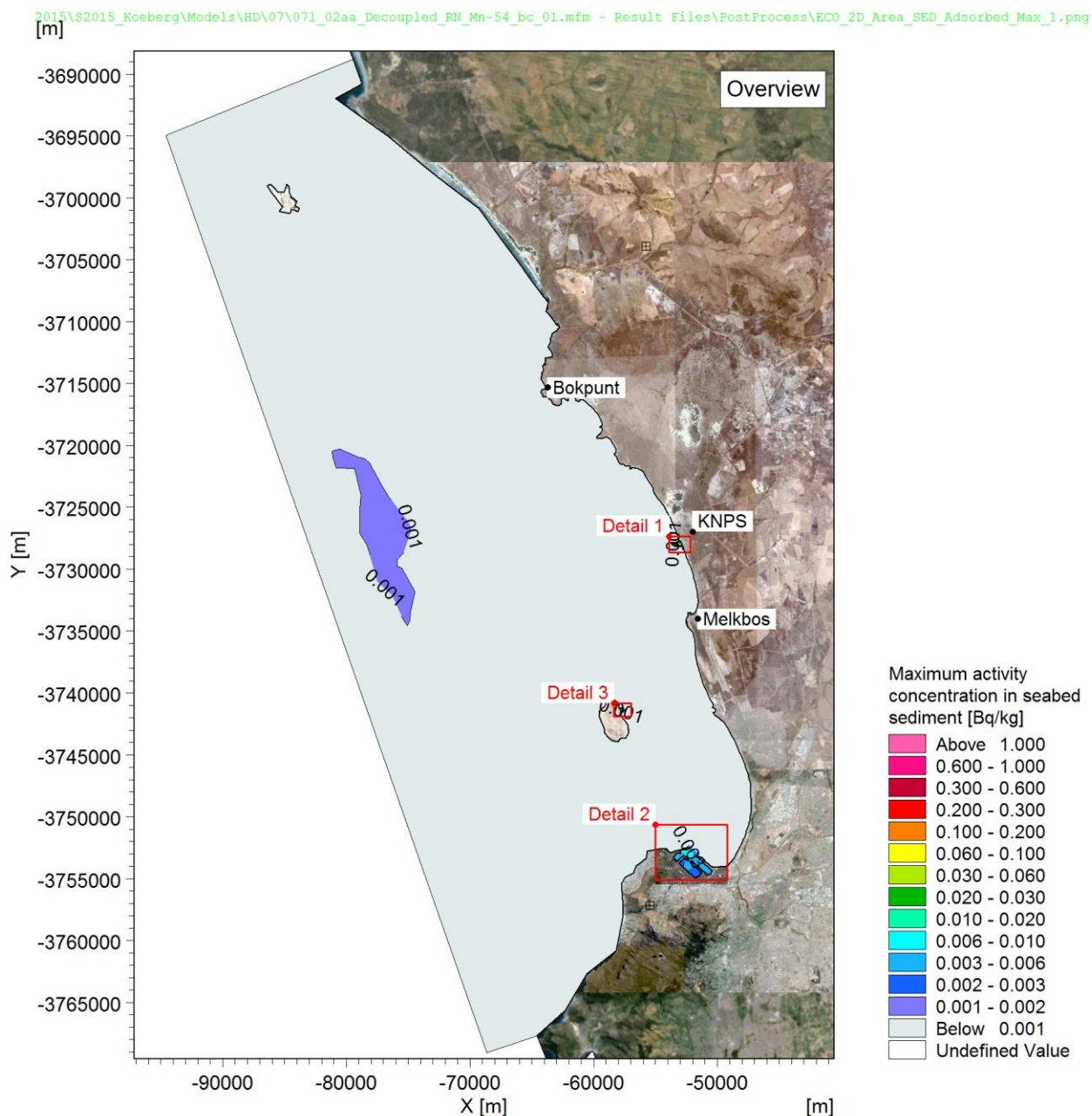


Figure C-54: Maximum concentration of Mn-54 activity in seabed sediment in one modelled year: overview.

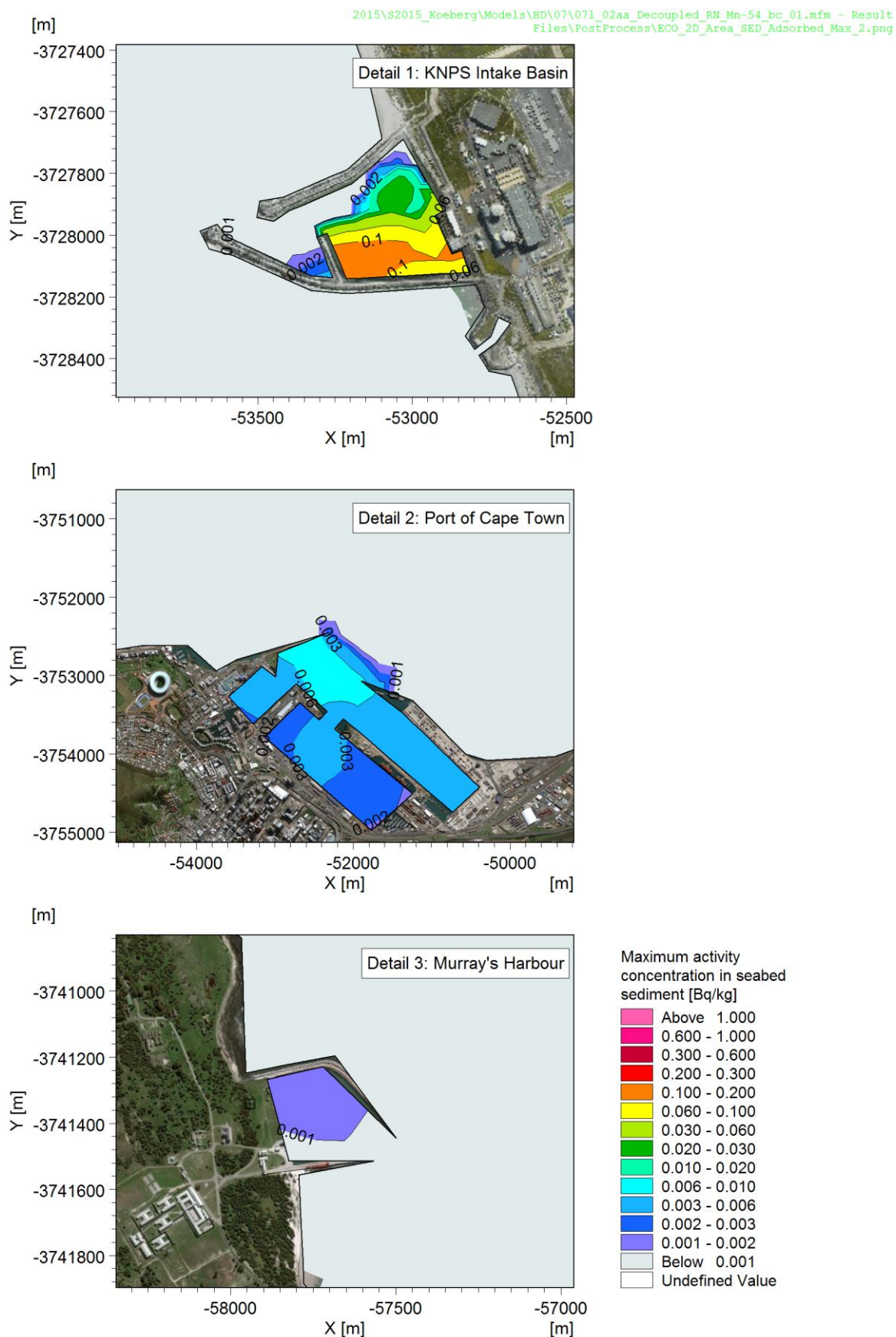
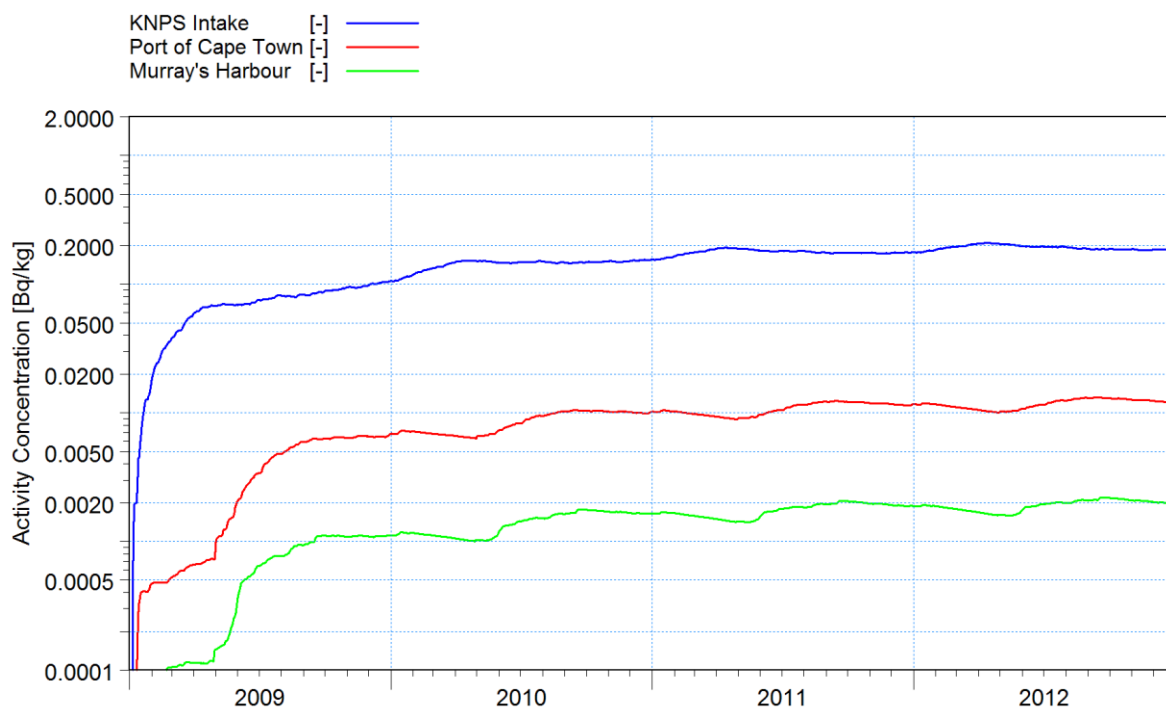


Figure C-55: Maximum concentration of Mn-54 activity in seabed sediment in one modelled year: detail of depo-centres.



2015\S2015_Koeberg\Models\HD\07\071_02aa_Decoupled_RN\TS_Mn-54.png

Figure C-56: Time series of concentration of Mn-54 activity in the seabed sediment at the three depocentres. For comparative purposes, the concentration is plotted on a logarithmic scale.